

Department of Civil and Environmental Engineering

University of Strathclyde

Chemical profiling and environmental modelling
of waste from clandestine
methamphetamine laboratories

A Thesis presented for the Degree of Doctor of Philosophy

by

Lisa Natasha Kates

October 2013

This thesis is the result of the author's original research. It has been composed by the author and has not been previously submitted for examination which has led to the award of a degree.

The copyright of this thesis belongs to the author under the terms of the United Kingdom Copyright Acts as qualified by University of Strathclyde Regulation 3.50. Due acknowledgement must always be made of the use of any material contained in, or derived from, this thesis.

Signed:

A handwritten signature in black ink, appearing to be 'J. A. D.', written in a cursive style.

Date: 4 October, 2013

Acknowledgements

I would like to sincerely thank my supervisor, Dr. Helen Keenan, for her kindness, guidance, and advice. Thank you so much for your incredible support, without which I could not have finished this thesis - you were my saving grace. Thank you for taking a chance on me.

Thank you to Prof. Niamh Nic Daéid for the opportunity to undertake this PhD project. Thank you for your advice and support, especially for saying all the things I needed to hear. I also wish to express my gratitude to Dr. Charles Knapp for his input, support, and advice. Thanks are also extended to Mara Knapp for all her help and assistance with the HPLC!

To my fellow students, in particular Dr. Saravana Jayaram for providing me with sample material that made this project possible. To Seánín, Aoife, and Siriporn, thanks for the great times together, your friendship and support, and to Andy for being such a calming influence. An additional thanks to Aoife and Andy for your help with the soil methods. It is a pleasure to thank Dr. Emma Bell for her feedback, support, friendship, and great chats over coffee.

I wish to acknowledge the Faculty of Engineering and the Department of Civil and Environmental Engineering for funding this project, particularly Dr. Philip Sayer and Prof. Rebecca Lunn for their support.

Thank you to my brother, friends, and family, both near and far, for their support and encouragement.

Words cannot express the role my mom filled in bringing this all together. Thank you for your love, support, understanding, and encouragement - and for putting up with phone calls at all hours of the day. My success would not have been possible without your continued support.

Publications

Kates, L. N., Gauchotte-Lindsay, C., Nic Daéid, N., Kalin, R. M., Knapp, C., and Keenan, H. E. Prediction of the environmental fate of methylamphetamine waste. In: Morrison, R. and O'Sullivan, G. eds. *Environmental Forensics: Proceedings of the 2011 INEF Annual Conference*. Royal Society of Chemistry Press. 2012.

Kates, L. N. Conference report: 20th International Symposium on the Forensic Sciences. *Mass Matters: Official Publication of the British Mass Spectrometry Society*. Edition 63, November 2010.

Conference Proceedings

Kates, L., Nic Daéid, N., and Keenan, H. Environmental modelling of waste products from clandestine methylamphetamine laboratories. Oral Presentation. Presented at *Fourth Scottish Postgraduate Symposium on Environmental Analytical Chemistry*. Glasgow, United Kingdom. December, 2011.

Kates, L. N., Gauchotte-Lindsay, C., Nic Daéid, N., Kalin, R. M., Knapp, C., and Keenan, H. E. Environmental modelling of methylamphetamine waste. Oral Presentation. *Presented at 19th International Association of Forensic Sciences Triennial Meeting*. Funchal, Portugal. September, 2011.

Kates, L. N., Gauchotte-Lindsay, C., Nic Daéid, N., Kalin, R. M., Knapp, C., and Keenan, H. E. Prediction of the environmental fate of methylamphetamine waste. Oral Presentation. Presented at *2nd Biennial International Network of Environmental Forensics Conference*. Cambridge, United Kingdom. July, 2011.

Kates, L., Knapp, C., and Keenan, H. Who dumped the meth lab in the river? Poster Presentation. Presented at *University of Strathclyde Research Presentation Day*. Glasgow, United Kingdom. June, 2011.

Kates, L. and Keenan, H. Environmental impact of clandestine methylamphetamine laboratories. Poster Presentation. Presented at *Glasgow Research Partners in Engineering, Annual Review*. Glasgow, United Kingdom. June, 2011.

Kates, L. N., Gauchotte, C., Nic Daéid, N., and Kalin, R. M. Biodegradation of methamphetamine, its waste products and precursors in the aqueous environment. Oral Presentation.

Presented at *University of Strathclyde Faculty of Engineering Research Presentation Day*. Glasgow, United Kingdom. January 2011.

Kates, L. N., Gauchotte, C., Knapp, C. W., Nic Daéid, N., and Kalin, R. M. Toxicity and chemical profiling of methamphetamine waste. Poster Presentation. Presented at *Australia New Zealand Forensic Science Society: 20th International Symposium on the Forensic Sciences*. Sydney, Australia. September, 2010.

Kates, L. N., Gauchotte, C., Nic Daéid, N., and Kalin, R. M. Methamphetamine and its waste products in the aqueous environment: chemical profiling and biodegradation. Poster Presentation. Presented at *Glasgow Research Partners in Engineering, Annual Review*. Glasgow, United Kingdom. June, 2010.

Kates, L. N. Microbial degradation of methamphetamine, its waste products and precursors in the aqueous environment. Oral Presentation. Presented at *University of Strathclyde Department of Civil Engineering PhD Conference*. Glasgow, United Kingdom. November, 2009.

Kates, L. N., McGregor, L. A., Gauchotte, C., Assal, A., Kalin, R. M., and Nic Daéid, N. Comprehensive two-dimensional gas chromatography time of flight mass spectrometry for environmental forensics applications: Fingerprinting of dense non-aqueous phase liquids. Poster Presentation. Presented at *5th European Academy of Forensic Sciences Conference*. Glasgow, United Kingdom. September, 2009.

Kates, L. N., McGregor, L. A., Gauchotte, C., Assal, A., Kalin, R. M., and Nic Daéid, N. Comprehensive two-dimensional gas chromatography time of flight mass spectrometry: Investigating degradation trends of dense non-aqueous phase liquids. Poster Presentation. Presented at *1st Biennial International Network of Environmental Forensics Conference*. Calgary, Canada. August, 2009.

Assal, A., Gauchotte, C., **Kates, L. N.**, McGregor, L. A., Kalin, R. M., Nic Daéid, N., Thomas, R., and Daly, P. A new holistic approach to environmental forensics: Case study of dense non-aqueous phase liquids from a former manufactured gas plant. Poster Presentation. Presented at *1st Biennial International Network of Environmental Forensics Conference*. Calgary, Canada. August, 2009.

Abstract

Methylamphetamine (MA) is an illicit drug abused by millions of people worldwide. MA can be manufactured easily using a variety of household chemicals and several different methods. The illicit manufacture of MA produces large amounts of waste: one kilogram of MA produces five to seven kilograms of toxic waste, which is illegally disposed of in a number of different ways, creating a source of pollution. MA waste contains many harmful components, however it has never been characterised.

In this work, MA was synthesised following three different synthetic routes. The waste were collected and subject to chemical profiling using gas chromatography-mass spectrometry. Key marker compounds of the waste were identified which may aid in the detection and prosecution of an illicit dumpsite. Those key marker compounds include MA, 1-phenyl-2-propanone, *N*-formylmethylamphetamine, and 2,6-di-*tert*-butylphenol.

Environmental partition coefficients were measured experimentally for several of the identified waste components. The octanol-water partition coefficient (K_{OW}) and the organic carbon partition coefficient (K_{OC}) were measured following standard methods. The K_{OW} values were found to be in accordance with computer estimated values produced from the environmental modelling programme, EPI Suite™, while the K_{OC} values were calculated as a function of organic carbon content from collected sediment samples.

Using the measured K_{OW} values and calculated K_{OC} values, a fugacity model of the waste was generated using EPI Suite™ to predict the distribution of the waste once it enters the

environment. It was determined that the majority of the waste components will partition predominantly into the water compartment.

This study encompasses the first research on waste generated from the illicit manufacture of MA, with the aim to provide information to law enforcement personnel and environment agencies to allow clandestine manufacturers to be prosecuted under environmental legislation in addition to drugs legislation.

Contents

1	Introduction	1
1.1	Scope of Thesis	1
1.2	Background	1
1.2.1	Legislation	3
1.2.1.1	Drugs Legislation	3
1.2.1.2	Precursor Legislation	4
1.2.1.3	Environmental Legislation	4
1.2.2	Profile of Methylamphetamine	5
1.2.2.1	History of Methylamphetamine	5
1.2.2.2	Abuse and Pharmacology of Methylamphetamine	6
1.2.3	Manufacture of Methylamphetamine	7
1.2.3.1	Chemicals	8
1.2.3.2	Routes	9
1.2.3.3	Precipitation: Salting Out	14
1.2.3.4	Crystal Methylamphetamine	15
1.2.3.5	Methylamphetamine Waste	16
1.2.4	Environmental Assessment	16
1.3	Research Aim and Objectives	17
1.4	Thesis outline	18

2	Literature Review	19
2.1	Introduction	19
2.2	Pharmaceutical and Personal Care Products	22
2.3	Impurity Profiling of Illicit Drugs	26
2.4	Clandestine Methylamphetamine Laboratories	35
2.4.1	Remediation of Clandestine Methylamphetamine Laboratories	37
2.4.2	Clandestine Methylamphetamine Laboratories and the Environment	40
2.5	Environmental Modelling	47
2.5.1	Quantitative Structure-Activity Relationships	49
2.5.2	Fugacity Modelling	51
2.5.3	EPI Suite™	55
3	Chemical Profiling of Methylamphetamine Waste	59
3.1	Introduction	59
3.2	Methodology	60
3.2.1	Synthesis of Methylamphetamine Waste	60
3.2.1.1	Leuckart Route	60
3.2.1.2	Moscow Route	63
3.2.1.3	Hypophosphorous Route	65
3.2.2	Extraction of Waste Impurities	67
3.2.2.1	Preliminary Extraction Study	67
3.2.2.2	Acetate Buffer	67
3.2.2.3	Phosphate Buffer	68
3.2.2.4	Tris Buffer	68
3.2.2.5	Extraction Efficiency	68

3.2.3	Solid Phase Extraction of Water-Diluted Waste	69
3.2.4	Extraction of Waste from Sediment	73
3.2.5	Instrumental Analysis of Waste Extracts	73
3.2.5.1	Mass Spectra Library Matching	74
3.3	Results and Discussion	75
3.3.1	Preliminary Extraction Study	75
3.3.2	Extraction Efficiency	84
3.3.3	Profiling of Methylamphetamine Waste	85
3.3.4	Route and Batch Variation	92
3.3.5	Chromatographic Theory and Relevance to MA Waste Analysis	96
3.3.6	Route Specific Waste Components	98
3.3.7	Solid Phase Extraction of Water-Diluted Waste	103
3.3.8	Extraction of Methylamphetamine Waste from Sediment	118
3.4	Conclusions	127
4	Measurement of Environmental Partition Coefficients	129
4.1	Introduction	129
4.2	Methodology	130
4.2.1	Octanol-Water Partition Coefficient, K_{OW}	131
4.2.2	Interactions Between Chemicals and Sediments	132
4.2.2.1	Sample Collection	132
4.2.2.2	Measurement of Total Organic Carbon	135
4.2.2.3	Trace Elemental Metal Analysis: X-Ray Fluorescence	136
4.2.2.4	Crystal Lattice Analysis: X-Ray Diffraction	136
4.2.3	Sediment-Water Partition Coefficient, K_d	136

4.2.4	Organic Carbon Partition Coefficient, K_{OC}	137
4.2.5	K_d and K_{OC} Revisited	138
4.2.5.1	Artificial Soils	138
4.2.5.2	Particle Size Distribution	139
4.2.6	Revised K_d	141
4.3	Results and Discussion	142
4.3.1	Octanol-Water Partition Coefficient	142
4.3.2	Characterisation of Sediment	153
4.3.2.1	Sample Site Characteristics	153
4.3.2.2	Sediment Properties	154
4.3.2.3	Elemental Analysis of Soil Using XRF	154
4.3.2.4	Crystal Lattice Analysis Using XRD	158
4.3.2.5	Lattice Spacing and Adsorption	162
4.3.2.6	Particle Size Distribution of Artificial Soils	163
4.3.3	Sorption of MA Waste onto Sediment: Part 1	165
4.3.4	Sorption of MA Waste onto Sediment: Part 2	176
4.3.4.1	K_d and K_{OC} Calculations	187
4.3.5	Forces of Adsorption	189
4.3.6	Adsorption and Physicochemical Properties	190
4.3.7	Correlation between K_{OW} and K_{OC}	192
4.4	Conclusions	195
5	Environmental Modelling of Methylamphetamine Waste	197
5.1	Introduction	197
5.2	Methodology	199

5.2.1	Estimation of Environmental Fate: Computer Modelling	199
5.2.2	User-Changed Parameters	200
5.2.2.1	Log K_{OW} Values	200
5.2.2.2	Emission Values	201
5.2.2.3	K_{OC} Values	202
5.2.3	Running the Fugacity Model	204
5.2.4	Bioconcentration and Bioaccumulation	205
5.2.5	Ecological Structure Activity Relationships (ECOSAR)	206
5.2.6	Estimation of Acute Environmental Impact: COD	207
5.3	Results and Discussion	207
5.3.1	Environmental Partitioning of MA Waste	207
5.3.1.1	Water Discharge Scenario	209
5.3.1.2	Soil Discharge Scenario	215
5.3.2	Effects of K_{OW} Measurements	220
5.3.3	Assumptions and Limitations of the EPI Suite™ Fugacity Model	221
5.3.4	Accumulation of MA Waste in Biota	223
5.3.5	Estimation of Ecotoxicity	228
5.3.6	Acute Environmental Impact of MA Waste	233
5.4	Conclusions	239
6	Conclusions and Recommendations	242
6.1	Summary Conclusions	242
6.2	Recommendations for future work	248
	References	250

Appendix A	262
A.1 Calculation of d5-MA extraction efficiency for LLE	263
A.2 Calculation of LOD for MA determined by GC-MS	264
A.3 Tables of compounds identified from LLE of crude MA waste	265
A.4 Calculation of d5-MA extraction efficiency for sediment extraction	276
 Appendix B	 277
B.1 X-Ray Diffraction Spectra	278
B.2 Calculation of LOD from HPLC Analysis	283
 Appendix C	 288
C.1 Fugacity models of additional MA waste components	289
C.1.1 Water Emissions Scenario	289
C.1.2 Soil Emissions Scenario	291
 Appendix D: Peer-Reviewed Conference Paper	 293

List of Figures

1.1	Chemical structure of methylamphetamine	2
1.2	Enantiomers of methylamphetamine	7
1.3	Methylamphetamine synthesis from 1-phenyl-2-propanone (from Kunalan et al. 2009)	10
1.4	Methylamphetamine synthesis from ephedrine or pseudoephedrine (Remberg and Stead, 1999; Makino et al., 2005)	11
1.5	Cyclic generation of hydriodic acid by iodine and phosphorus in aqueous solution (Reproduced from Skinner, 1990).	13
1.6	Precipitating methylamphetamine hydrochloride salt	15
2.1	Simplified diagram displaying points of entry of chemicals into surface waters. (Adapted from Wise et al., 2011)	21
2.2	Molecular structures of the target compounds in the Pal et al., 2011 study. (MA: methylamphetamine; MDMA: 3,4-methylenedioxyamphetamine ("ecstasy"); PSE: pseudoephedrine; FMA: N-formylmethylamphetamine; BMN: 1-benzyl-3-methylnaphthalene)	43
2.3	Molecular structure of 1-(1',4'-cyclohexadienyl)-2-methylaminopropane (CMP)	46
2.4	Relationship between fugacity (f), fugacity capacities (Z) and partition coefficients (K). (Adapted from Samiullah, 1990.)	52
2.5	Interactions between five environmental compartments, where each coloured line represents a different partition coefficient.	53

3.1	MA synthesis using the Leuckart route (aqueous waste collected).	62
3.2	MA synthesis using the Moscow route (organic waste collected).	64
3.3	MA synthesis using the Hypophosphorous route (organic waste collected).	66
3.4	Chemical structure of d5-methylamphetamine (MW = 154.20)	69
3.5	Overlay gas chromatogram of three buffer extractions of Leuckart synthesised MA waste	76
3.6	Overlay gas chromatogram of three buffer extractions of Moscow synthesised MA waste	80
3.7	Chemical structure of Tris	84
3.8	GC-MS TIC of MA waste synthesised using the Leuckart route. See Table 3.9 on page 87 for peak identification.	86
3.9	GC-MS TIC of MA waste synthesised using the Moscow route. See Table 3.10 on page 90 for peak identification.	89
3.10	GC-MS TIC of MA waste synthesised using the Hypophosphorous route. See Table 3.11 on page 92 for peak identification.	91
3.11	Van Deemter plot for open tubular columns as sum of three terms: B and C [as Sum of C_m (mobile phase) and C_s (stationary phase)] with $A = 0$. (From Robinson et al., 2004.)	97
3.12	Mechanism of the reduction of pseudoephedrine to MA using HI/red P (modified from Skinner, 1990).	99
3.13	Summary schematic of SPE steps (from Kealey and Haines, 2002)	104
3.14	GC-MS TIC of Leuckart waste (1 mL) diluted in 500 mL water extracted following the SPE protocol of Zuccato et al. (2005), using Oasis MCX cartridges at pH 2. Peak identification table in 3.15 on page 107	106
3.15	GC-MS TIC of Leuckart waste (1 mL) diluted in 500 mL water extracted following the SPE protocol of Boles and Wells (2010), using Oasis HLB cartridges at pH 8.5. Peak identification table in 3.16 on page 110	109

3.16	Overlay GC-MS TIC of Leuckart waste (1 mL) diluted in 500 mL water using different SPE methods. Descriptions of method found in Table 3.2.	111
3.17	GC-MS chromatogram of Leuckart waste (0.5 mL) diluted in 250 mL water using MIP. Peak identification in Table 3.22.	115
3.18	GC-MS chromatogram of sediment blank extraction. See Table 3.24 on page 120 for peak identifications.	119
3.19	GC-MS chromatogram of the sediment extraction of Leuckart waste. See Table 3.25 on page 122 for peak identifications.	121
3.20	GC-MS chromatogram of the sediment extraction of Moscow waste. See Table 3.26 on page 124 for peak identifications.	123
3.21	GC-MS chromatogram of the sediment extraction of Hypophosphorous waste. See Table 3.27 on page 126 for peak identifications.	125
4.1	Map of the sampling locations in the vicinity of Glasgow, United Kingdom . . .	134
4.2	Calibration graph of HPLC log k values versus log K_{OW} standard values	147
4.3	HPLC chromatogram of benzaldehyde at 220 nm.	149
4.4	Molecular structure of a single silica tetrahedron (top) and silica tetrahedron sheet (bottom) (reproduced from Tan, 1998).	159
4.5	Aluminium oxide octahedron (reproduced from Tan, 1998).	159
4.6	Schematic of kaolinite (reproduced from Tan, 1998).	160
4.7	Illustration of x-ray beam diffracting from crystal planes following Braag's law (reproduced from Tan, 1998)	161
4.8	XRD spectra of humus component of artificial soils	161
4.9	Overlay HPLC chromatogram of sediment blank samples at 208 nm.	166
4.10	HPLC calibration sample (0.05 mg/mL) of MA, <i>N</i> -methylacetamide, P2P, and the internal standard, BPA.	167
4.11	Equilibrium graph of P2P adsorption onto Bothwell Bridge sediment at three different water:sediment ratios	169

4.12	Equilibrium graph of P2P adsorption onto Bowling Harbour sediment at three different water:sediment ratios	169
4.13	Equilibrium graph of P2P adsorption onto Renfrew Ferry sediment at three different water:sediment ratios	170
4.14	Equilibrium graph of P2P adsorption onto Port Dundas sediment at three different water:sediment ratios	170
4.15	Equilibrium graph of <i>N</i> -methylacetamide adsorption onto Bothwell Bridge sediment at three different water:sediment ratios	172
4.16	Equilibrium graph of <i>N</i> -methylacetamide adsorption onto Bowling Harbour sediment at three different water:sediment ratios	172
4.17	Equilibrium graph of <i>N</i> -methylacetamide adsorption onto Renfrew Ferry sediment at three different water:sediment ratios	173
4.18	Equilibrium graph of <i>N</i> -methylacetamide adsorption onto Port Dundas sediment at three different water:sediment ratios	173
4.19	HPLC chromatogram of water exposed to sand component	176
4.20	HPLC chromatogram of water exposed to silt component	176
4.21	HPLC chromatogram of water exposed to clay component	177
4.22	HPLC chromatogram of water exposed to humus component	177
4.23	Freundlich isotherms for <i>N</i> -methylacetamide, P2P, phenol, and benzaldehyde, oxime	179
4.24	Equilibrium graph of <i>N</i> -methylacetamide adsorption onto artificial soil #1 at three different water:sediment ratios	180
4.25	Equilibrium graph of <i>N</i> -methylacetamide adsorption onto artificial soil #2 at three different water:sediment ratios	180
4.26	Equilibrium graph of <i>N</i> -methylacetamide adsorption onto artificial soil #3 at three different water:sediment ratios	181
4.27	Equilibrium graph of P2P adsorption onto artificial soil #1 at three different water:sediment ratios	182

4.28	Equilibrium graph of P2P adsorption onto artificial soil #2 at three different water:sediment ratios	182
4.29	Equilibrium graph of P2P adsorption onto artificial soil #3 at three different water:sediment ratios	183
4.30	Equilibrium graph of phenol adsorption onto artificial soil #1 at three different water:sediment ratios	184
4.31	Equilibrium graph of phenol adsorption onto artificial soil #2 at three different water:sediment ratios	184
4.32	Equilibrium graph of phenol adsorption onto artificial soil #3 at three different water:sediment ratios	185
4.33	Equilibrium graph of benzaldehyde, oxime adsorption onto artificial soil #1 at three different water:sediment ratios	186
4.34	Equilibrium graph of benzaldehyde, oxime adsorption onto artificial soil #2 at three different water:sediment ratios	186
4.35	Equilibrium graph of benzaldehyde, oxime adsorption onto artificial soil #3 at three different water:sediment ratios	187
4.36	Correlation between $\log K_{OW}$ and $\log K_{OC}$	193
5.1	EPI Suite™ Homepage (USEPA, 2012b)	199
5.2	EPI Suite™ Log K_{OW} entry box	200
5.3	EPI Suite™ Fugacity model emissions scenario	202
5.4	EPI Suite™ soil K_{OC} value entry box	203
5.5	ECOSAR Homepage (USEPA, 2012b)	206
5.6	Water discharge scenario fugacity model of 2,6-DTBP, from EPI Suite™. (X-axis = model scenario corresponding to Table 5.2 on page 205)	209
5.7	Water discharge scenario fugacity model of <i>N</i> -methylacetamide, from EPI Suite™. (X-axis = model scenario corresponding to Table 5.2 on page 205)	211

5.8	Water discharge scenario fugacity model of MA, from EPI Suite™. (X-axis = model scenario corresponding to Table 5.2 on page 205)	212
5.9	Water discharge scenario fugacity model of P2P, from EPI Suite™. (X-axis = model scenario corresponding to Table 5.2 on page 205)	212
5.10	Water discharge scenario fugacity model of <i>N</i> -formylmethamphetamine, from EPI Suite™. (X-axis = model scenario corresponding to Table 5.2 on page 205)	213
5.11	Soil discharge scenario fugacity model of 2,6-DTBP, from EPI Suite™. (X-axis = model scenario corresponding to Table 5.2 on page 205)	215
5.12	Soil discharge scenario fugacity model of <i>N</i> -methylacetamide, from EPI Suite™. (X-axis = model scenario corresponding to Table 5.2 on page 205)	216
5.13	Soil discharge scenario fugacity model of MA, from EPI Suite™. (X-axis = model scenario corresponding to Table 5.2 on page 205)	217
5.14	Soil discharge scenario fugacity model of P2P, from EPI Suite™. (X-axis = model scenario corresponding to Table 5.2 on page 205)	218
5.15	Soil discharge scenario fugacity model of <i>N</i> -formylmethamphetamine, from EPI Suite™. (X-axis = model scenario corresponding to Table 5.2 on page 205)	218
5.16	Required DO concentrations (mg/L) of different saltwater species (Reproduced from USEPA, 2003.)	236
B.1	XRD spectra of Port Dundas sediment sample	278
B.2	XRD spectra of Bothwell Bridge sediment sample	279
B.3	XRD spectra of Bowling Harbour sediment sample	279
B.4	XRD spectra of Soil #1	280
B.5	XRD spectra of Soil #2	280
B.6	XRD spectra of Soil #3	281
B.7	XRD spectra of sand component of artificial soils	281
B.8	XRD spectra of silt component of artificial soils	282

B.9	XRD spectra of clay component of artificial soils	282
B.10	HPLC calibration curves	283
C.1	Water discharge scenario fugacity model of of 1-phenyl-1,2-propanedione, from EPI Suite™. (X-axis = model scenario corresponding to Table 5.2 on page 205)	289
C.2	Water discharge scenario fugacity model of benzaldehyde oxime, from EPI Suite™. (X-axis = model scenario corresponding to Table 5.2)	289
C.3	Water discharge scenario fugacity model of benzyl alcohol, from EPI Suite™. (X- axis = model scenario corresponding to Table 5.2)	290
C.4	Water discharge scenario fugacity model of phenol, from EPI Suite™. (X-axis = model scenario corresponding to Table 5.2)	290
C.5	Soil discharge scenario fugacity model of of 1-phenyl-1,2-propanedione, from EPI Suite™. (X-axis = model scenario corresponding to Table 5.2 on page 205)	291
C.6	Soil discharge scenario fugacity model of benzaldehyde oxime, from EPI Suite™. (X-axis = model scenario corresponding to Table 5.2)	291
C.7	Soil discharge scenario fugacity model of benzyl alcohol, from EPI Suite™. (X-axis = model scenario corresponding to Table 5.2)	292
C.8	Soil discharge scenario fugacity model of phenol, from EPI Suite™. (X-axis = model scenario corresponding to Table 5.2)	292

List of Tables

2.1	24 target compounds for MA impurity profiling as determined by Dujourdy et al., 2008	32
2.2	Route specific methylamphetamine impurities identified by Kunalan (2010) . . .	34
2.3	Measured and referenced exposure levels for chemicals evaluated from clandestine MA laboratories in Martyny et al., 2007	37
2.4	Remediation guidelines for key chemicals associated with clandestine MA laboratories (New Zealand Ministry of Health, 2010).	39
3.1	Summary of MA waste synthesised for this study	65
3.2	Summary of SPE methods	72
3.3	List of compounds identified in MA Leuckart waste extracted with a pH 10.5 phosphate buffer	77
3.4	List of compounds identified in MA Leuckart waste extracted with a pH 8.1 Tris buffer	77
3.5	List of compounds identified in MA Leuckart waste extracted with a pH 6.0 acetate buffer	78
3.6	List of compounds identified in MA Moscow waste extracted with a pH 10.5 phosphate buffer	81
3.7	List of compounds identified in MA Moscow waste extracted with a pH 8.1 Tris buffer	82

3.8	List of compounds identified in MA Moscow waste extracted with a pH 6.0 acetate buffer	83
3.9	List of compounds identified in the waste extract of MA synthesised from the Leuckart route	87
3.10	List of compounds identified in the waste extract of MA synthesised from the Moscow route	90
3.11	List of compounds identified in the waste extract of MA synthesised from the Hypophosphorous route	92
3.12	MA waste compounds identified by GC-MS using pH 10 phosphate buffer LLE. The presence of the identified chemical in each batch is indicated by a ‘✓’. Route abbreviations: L = Leuckart; M = Moscow; Hypo = Hypophosphorous	93
3.13	Summary of chemicals in common across the three MA synthetic routes studied .	95
3.14	MA waste impurities identified in this study compared to MA impurities identified in Kunalan (2010).	100
3.15	List of compounds identified in Leuckart waste SPE using Oasis MCX cartridges at pH 2. In bold: compounds identified in both the raw waste LLE and spiked water SPE.	107
3.16	List of compounds identified in Leuckart waste SPE using Oasis HLB cartridges at pH 8.5. In bold: compounds identified in both the raw waste extract and spiked water extract.	110
3.17	List of compounds identified in Leuckart waste SPE 1 using Oasis MCX cartridges at pH 2. In bold: compounds identified in both the raw waste extract and spiked water extract.	112
3.18	List of compounds identified in Leuckart waste SPE 2 using Oasis MCX cartridges at pH 2. In bold: compounds identified in both the raw waste extract and spiked water extract.	112
3.19	List of compounds identified in Leuckart waste SPE 3 using Oasis MCX cartridges at pH 2. In bold: compounds identified in both the raw waste extract and spiked water extract.	113

3.20	List of compounds identified in Leuckart waste SPE 4 using Oasis MCX cartridges at pH 2. In bold: compounds identified in both the raw waste extract and spiked water extract.	113
3.21	List of compounds identified in Leuckart waste SPE 5 using Oasis HLB cartridges at pH 8.5. In bold: compounds identified in both the raw waste extract and spiked water extract.	113
3.22	List of compounds identified in Leuckart waste SPE using MIP cartridges at pH 8. In bold: compounds identified in both the raw waste extract and spiked water extract.	116
3.23	MA SPE concentration factors of water diluted Leuckart waste	117
3.24	List of compounds identified in sediment blank extraction	120
3.25	List of compounds identified in Leuckart waste sediment extraction. In bold: compounds identified in both the raw waste extract and spiked sediment extract. In italics: compounds identified in the sediment blank extract.	122
3.26	List of compounds identified in Moscow waste sediment extraction. In bold: compounds identified in both the raw waste LLE and spiked sediment extract. In italics: compounds identified in the sediment blank extract.	124
3.27	List of compounds identified in Hypophosphorous waste sediment extraction. In bold: compounds identified in both the raw waste extract and spiked sediment extract. In italics: compounds identified in the sediment blank extract.	126
4.1	GPS coordinates of sampling locations.	134
4.2	Particle size of sand, silt, and clay according to British Standard BS 3882:2007 (British Standards, 2007)	139
4.3	Percentage of soil components in each artificial soil	139
4.4	λ max and chemical structures of reference compounds (190 nm to 400 nm scan).	144
4.5	λ max and chemical structures of selected MA waste compounds (190 nm to 400 nm scan).	145

4.6	HPLC dead times and retention times of K_{OW} reference materials	146
4.7	HPLC dead times and retention times of MA waste components	146
4.8	Log K_{OW} values determined using OECD standard method 117 compared against EPI Suite™ estimated values.	148
4.9	Computer estimated pKa values of MA waste components using chemicalize.org (ChemAxon, 2013)	151
4.10	Sampling site data and sediment properties.	153
4.11	Sediment properties of collected sediments and artificial soils.	154
4.12	Elemental composition of collected sediment samples using XRF (+/- refers to instrument margin of error in ppm)	155
4.13	Elemental composition of artificial soil samples using XRF (+/- refers to instru- ment margin of error in ppm)	156
4.14	Elemental composition of artificial soil sample components using XRF (+/- refers to instrument margin of error in ppm)	157
4.15	Minerals identified in soil and sediment samples from XRD analysis	162
4.16	d-spacing of common clay lattice structures detected in XRD analysis of sample soils and sediments (from Tan, 1998)	162
4.17	Molecular size of MA waste components (from ChemAxon, 2013)	163
4.18	Percent particle size distribution of components of artificial soils	164
4.19	Sedimentation test of silt (average of three replicates)	164
4.20	Calculated ln K_{OC} values of selected MA waste impurities based on Equation 4.5 on page 136	165
4.21	Measured K_{OC} values for P2P and <i>N</i> -methylacetamide	175
4.22	LOD and LOQ values for HPLC K_{OC} method ($\mu\text{g/mL}$)	178
4.23	Experimentally determined log K_{OC} values for MA waste components	188
4.24	K_{OC} values calculated using experimental K_{OW} values in Equation 4.19	194

4.25	Estimated K_{OC} values of MA waste impurities from K_d part 2 based on Equation 4.5 on page 136	194
5.1	Name, CAS number and SMILES notation of MA waste components used for entry into EPI Suite™	205
5.2	Summary of EPI Suite™ fugacity model scenarios	205
5.3	K_{OC} values calculated using different parameters	208
5.4	EPI Suite™ estimated half life values, in hours, of MA waste in the environment .	214
5.5	Set and variable parameters of the EPI Suite™ fugacity model	222
5.6	Estimated bioaccumulation and bioconcentration factor based on default and experimental log K_{OW} values.	225
5.7	Estimated biotransformation half lives of fish based on default and experimental K_{OW} values.	227
5.8	ECOSAR predicted acute ecotoxicity using default log K_{OW} values (mg/L) . . .	230
5.9	ECOSAR predicted chronic ecotoxicity using default log K_{OW} values (mg/L) . .	230
5.10	ECOSAR predicted acute ecotoxicity using experimental log K_{OW} values (mg/L)	231
5.11	ECOSAR predicted chronic ecotoxicity using experimental log K_{OW} values (mg/L)	231
5.12	COD of individual MA waste chemicals (mg/L COD; n = 2)	234
5.13	COD of five MA waste chemicals in a mixture (mg/L COD; n = 2)	234
5.14	EC ₁₀ and EC ₅₀ values for the dehydrogenase activity of 3 test soils. (Reproduced from Pal et al., 2008)	238
A.1	Calculation data of extraction efficiency for d5-MA from phosphate buffer LLE of Moscow waste #1, six replicate extractions	263
A.2	Average d5-MA percent recoveries from phosphate buffer LLE of each synthetic route	263
A.3	Calculation data of LOD for MA determined by GC-MS	264

A.4 Complete list of compounds identified in the waste extract of MA synthesised from the Leuckart route (#1)	265
A.5 Complete list of compounds identified in the waste extract of MA synthesised from the Leuckart route (#2)	267
A.6 Complete list of compounds identified in the waste extract of MA synthesised from the Leuckart route (#3)	269
A.7 Complete list of compounds identified in the waste extract of MA synthesised from the Leuckart route (#4)	271
A.8 Complete list of compounds identified in the waste extract of MA synthesised from the Leuckart route (#5)	272
A.9 Complete list of compounds identified in the waste extract of MA synthesised from the Moscow route (#2)	273
A.10 Complete list of compounds identified in the waste extract of MA synthesised from the Moscow route (#3)	275
A.11 Average d5-MA percent recoveries from sediment extraction of each synthetic route	276
B.1 Calculation data of LOD for P2P determined by HPLC	284
B.2 Calculation data of LOD for <i>N</i> -methylacetamide determined by HPLC	285
B.3 Calculation data of LOD for phenol determined by HPLC	286
B.4 Calculation data of LOD for benzaldehyde, oxime determined by HPLC	287

List of Abbreviations

2,6-DTBP	2,6-ditertbutylphenol
ACN	Acetonitrile
ADD	Attention deficit disorder
AMP	Amphetamine
ASTM	American Society for Testing and Materials
ATS	Amphetamine Type Stimulants
BAF	Bioaccumulation factor
BCF	Bioconcentration factor
BMK	Benzyl methyl ketone
BMN	1-benzyl-3-methylnaphthalene
CAS	Chemical Abstract Service
CHAMP	Collaborative Harmonisation of Methods for Profiling of Amphetamine Type Stimulants
CMP	1-(1',4'-cyclohexadienyl)-2-methylaminopropane
COD	Chemical oxygen demand
DCM	Dichloromethane
DDT	Dichlorodiphenyltrichloroethane

DO	Dissolved oxygen
EC50	Median effective concentration
ECOSAR	Ecological Structure Activity Relationships
EDDP	2-ethylidene-1,5-dimethyl-3,3-diphenylpyrrolidine
EE2	17- α -ethinyl estradiol
EPI Suite	Estimation Program Interface Suite
FMA	N-formylmethamphetamine
GC	Gas chromatography
GC-MS	Gas chromatography-mass spectrometry
HI	Hydriodic acid
HPLC	High performance liquid chromatography
HPLC-MS	High Performance Liquid Chromatography-Mass Spectrometry
i.d.	Internal diameter
ICPMS	Inductively coupled plasma mass spectrometry
IRMS	Isotope ratio mass spectrometry
Kd	Sediment-water partition coefficient
Koc	Organic carbon partition coefficient
Kow	Octanol-water partition coefficient
LC50	Median lethal concentration
LLE	Liquid-liquid extraction
LOD	Limit of detection
LOEC	Lowest observed effect concentration
LSD	Lysergic acid diethylamide

MA	Methylamphetamine
MAS	Methylamphetamine sulphate
MA·HCl	Methylamphetamine hydrochloride
MCI	Molecular connectivity index
MDA	3,4-methylenedioxyamphetamine
MDMA	3,4-methylenedioxyamphetamine
MIP	Molecular imprinted polymers
NIST	National Institute of Standards and Technology
NOEC	No observed effect concentration
OECD	Organisation for Economic Co-operation and Development
P2P	1-phenyl-2-propanone
PAH	Polyaromatic hydrocarbon
PCB	Polychlorinated biphenyl
PPCP	Pharmaceutical and Personal Care Products
PSE	Pseudoephedrine
QSAR	Quantitative structural-activity relationships
red P	Red phosphorous
RPHPLC	reversed phase high performance liquid chromatography
RRF	Relative response factors
RSD	Relative standard deviation
SMILES	Simplified Molecular Input Line Entry System
SPE	Solid phase extraction
TBT	Tributyltin

THC-COOH	11-nor-9-carboxy-delta9-tetrahydrocannabinol
TIC	Total ion chromatogram
TOC	Total organic carbon
Tris	Tris(hydroxymethyl)aminomethane
UNODC	United Nations Office on Drugs and Crime
US EPA	United States Environmental Protection Agency
WWTP	Wastewater treatment plant
XRD	X-Ray Diffraction
XRF	X-Ray Fluorescence

Chapter 1

Introduction

1.1 Scope of Thesis

This thesis is focused on the waste produced from the clandestine manufacture of the illicit drug methylamphetamine (MA). MA is a central nervous system stimulant that is synthesised in clandestine laboratories all over the world. Clandestine laboratories can be found in a wide variety of locations, in both rural and urban settings. For each kilogram of MA produced, five to seven kilograms of waste is generated. This waste is being disposed of through illegal dumping into the environment and the effects of those actions are largely unknown. Research into MA has largely focused on two areas: impurity profiling of MA and the detection of MA in rivers, lakes, and wastewater treatment plants in order to estimate drug consumption of the catchment area. An emerging area of MA research has investigated the degradation of MA and several of its precursors and by-products in soil. While there is research relating MA to the environment, no research has investigated the waste produced from the manufacturing process, nor the environmental impact the waste may cause. In this work, the composition of the waste will be determined and its environmental fate estimated using laboratory experimentation and computer modelling.

1.2 Background

The abuse of illicit drugs is cause for concern throughout the world. The United Nations Office on Drugs and Crime (UNODC) estimates that 5% of the world population aged 15 - 64 (230

million people) consumed illicit drugs in 2010 (UNODC, 2012). The most widely abused drug globally is cannabis, followed by amphetamine-type stimulants (ATS). ATSs are synthetic drugs first synthesised in the late 1800s and early 1900s to treat asthma and for use as decongestants (UNODC, 2012; ACMD, 2005). The synthetic nature of these drugs means they can be manufactured anywhere. Unlike crop-dependent drugs such as cocaine and heroin, ATSs are not confined to any particular region of the globe. In 2010, a total of 14,742 illicit ATS laboratories were reported the UNODC (2012). Throughout the years, illicit ATS manufacture has been detected in over 60 countries (UNODC, 2012).

Methylamphetamine (also known as methamphetamine or metamfetamine, Figure 1.1) is the most commonly produced ATS worldwide (White, 2004). MA is typically manufactured in clandestine laboratories close to the consumer; inter-region trafficking is uncommon (UNODC, 2012). The illicit manufacture of MA produces a large amount of harmful waste that is often dumped illegally, creating a potential source of pollution. One kilogram of MA produces five to seven kilograms of waste that includes many volatile, flammable, and corrosive chemicals, as well as heavy metals (White, 2004). Common routes of disposal include: poured down indoor plumbing; dumped directly into ditches, rivers, canals; dumped into burn pits; and/or dumped into burial pits (USEPA, 2005). Illicit drug manufacturers are often not prosecuted for crimes relating to polluting the environment, due to the costs associated with prosecuting the charges and lack of research in this area to support a case of environmental harm. If a person is caught manufacturing MA, a number of charges may be laid under manufacturing, possession, and supply laws. It would be desirable to also be able to charge that person with polluting the environment, where sufficient evidence exists.

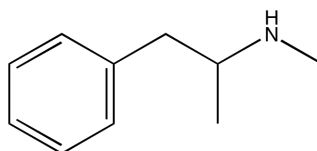


Figure 1.1: Chemical structure of methylamphetamine

1.2.1 Legislation

1.2.1.1 Drugs Legislation

In the United Kingdom, there are two pieces of legislation that control the use and distribution of illicit drugs. They are the Misuse of Drugs Act 1971 and the Misuse of Drugs Regulations 2001. The Misuse of Drugs Act (the Act) defines which substances are controlled, as well as the penalties for possession, supply, manufacture, etc. of a particular drug. The Act is divided into three Classes based on a drug's perceived harmfulness, with Class A being the most harmful and Class C being the least harmful. The Misuse of Drugs Regulations (the Regulations) dictates who may have legitimate access to controlled substances and under what circumstances. The Regulations is divided into five Schedules that consider a drug's value as a medicine versus its hazard as a drug. For example, Schedule 1 drugs (e.g. 3,4-methylenedioxy-N-methylamphetamine (MDMA), and lysergic acid diethylamide (LSD)) may not be prescribed, but they may be licensed for scientific research. At the other end of the scale, Schedule 5 drugs may be readily available in the form of a medicinal product and do not carry any penalties (e.g. "low dose" codeine) (King, 2009).

When the Act was first introduced in 1971, MA was a Class B drug. Subsequent to a review in 2006, the classification of MA was changed: MA is now a Class A, Schedule 2 substance. In an effort to combat so-called "designer drugs", the Act includes restrictions on all salts, esters, ethers, or stereoisomers of MA, as well as any preparations containing methylamphetamine. Designer drugs were created in order to circumnavigate the Act. By including salts, esters, ethers and stereoisomers, there is no need to name every single substance that comes under control (King, 2009).

In the United Kingdom, the maximum penalties for a Class A drug are as follows (ACMD, 2005):

- Supply: Life imprisonment and/or unlimited fine
- Production: Life imprisonment and/or unlimited fine
- Possession: 7 years imprisonment and/or unlimited fine

It is also an offense under the Act to permit the use of drugs in a dwelling (e.g. flat or house) or other building (e.g. office) (King, 2009).

1.2.1.2 Precursor Legislation

The chemicals used to manufacture illicit drugs, known as precursors, are also controlled substances in many countries. These chemicals can be broken down into three categories: precursors, reagents, and general-purpose chemicals (White, 2004). Precursors are the vital chemicals that form the backbone of the final product. White (2004) refers to these chemicals as “building blocks”, and it is these chemicals that determine the route of MA synthesis. The precursor chemicals for the manufacture of MA include 1-phenyl-2-propanone (P2P), also known as benzyl methyl ketone, BMK), ephedrine, and pseudoephedrine. All three are controlled in the UK under Article 12 of the United Nations Vienna Convention 1988, Section 13 of the Criminal Justice International Cooperation Act 1990 and Modification Order 1992. P2P, ephedrine, and pseudoephedrine fall under Table 1, Category 1, meaning that in the UK the Home Office must license a premises in order for them be able to possess, manufacture, be supplied to or supply those chemicals (Home Office, 2011).

1.2.1.3 Environmental Legislation

The health of the environment is of growing interest to many governments and as well as the general public. While the awareness and understanding of the effects of pollution is increasing, so is environmental crime. Interpol defines environmental crime as follows: “Environmental crime is a breach of national or international law or treaty that exists to ensure the conservation and sustainability of the world’s environment, biodiversity or natural resources” (Interpol, 2009). Environmental crime is perceived by criminals as low risk, high profit crime due to low detection and prosecution rates. Those involved in environmental crime are often engaged in other illegal activities, such as murder, bribery, fraud, and drug smuggling (Interpol, 2009). This broad range of illegal activities has lead Interpol to encourage the cooperation of different branches of law enforcement. This would also require the collaboration of different branches of scientists to advise law enforcement personnel.

In 2004, the European Commission put into place an environmental liability directive aimed at punishing polluters financially. This directive came into force by member states in 2007 and promotes the “polluters pay” principle (European Parliament, 2004). In Scotland, this Directive was implemented by the The Environmental Liability (Scotland) Regulations 2009, which came into force on 24 June, 2009.

1.2.2 Profile of Methylamphetamine

MA is an ATS, and is the most widely abused drug in the amphetamines-group. The amphetamines-group includes amphetamine as well as less common drugs, such as methcathinone UNODC (2012). As of 2010 (the most recent year for which data is available), there are an estimated 14 - 52.5 million amphetamine-group users worldwide (0.3 - 1.2% of the population aged 15 - 64), making amphetamine-group substances more widely abused than cocaine and heroin combined, and second only to cannabis. The 2012 World Drug Report (UNODC, 2012) estimated that MA users account for 54 - 59% of all amphetamine-group users. MA use is most prevalent in North America, Central America, and Oceania, with use on the rise in East and South-East Asia, Central Asia and Transcaucasia. Crystalline MA (described in Section 1.2.3.4 on page 15) is now the most commonly used drug in Brunei Darussalam, Japan, Philippines, and the Republic of Korea. In Europe, users have historically primarily consumed amphetamine and ecstasy, with the exception of the Czech Republic and Slovakia where MA use is more prevalent. Recently, MA consumption has been increasing in Finland, Latvia, Norway, Sweden, and Germany where it is hypothesized to be replacing amphetamine (UNODC, 2012).

1.2.2.1 History of Methylamphetamine

Naturally occurring amphetamine products have been used for many years in traditional Chinese medicine. A plant derivative called Ma Haung (*Ephedra*) was used for many years as a bronchial dilator to treat respiratory ailments, such as asthma. The active ingredient derived from *Ephedra* is ephedrine. As natural sources of ephedrine began to become scarce, pharmaceutical companies began investigating cheaper and more sustainable alternatives (ACMD, 2005). Amphetamine emerged as a cheaper alternative to ephedrine in 1927, even though it was first synthesised many years earlier in Germany by Leuckart in 1887. Another alternative to ephedrine, MA,

was synthesised in Japan in 1919. Therapeutic uses for amphetamines included: treatment of narcolepsy, depression, obesity and attention deficit disorder (ADD). Amphetamines and amphetamine-related drugs are currently still in use for the treatment of ADD and in asthma inhalers.(ACMD, 2005; Hunt et al., 2005).

During World War II, amphetamines were widely distributed to troops, particularly pilots, in order to relieve fatigue and increase alertness (ACMD, 2005; Hunt et al., 2005). It is estimated that 200 million tablets of amphetamine or MA were distributed to American troops, and another 72 million supplied to British troops. Due to its highly addictive nature, after the war there was a demand for amphetamines from troops who had been using it during the war. Abuse soon followed, as did drug controls. As the legitimate sources of amphetamines began to decline, a rise in amphetamine trafficking and illicit synthesis began to appear (ACMD, 2005).

1.2.2.2 Abuse and Pharmacology of Methylamphetamine

MA is a central nervous system stimulant that mimics the neurotransmitter dopamine and acts on the brain's reward pathway, making it a highly addictive substance (Cruickshank and Dyer, 2009). The short-term effects are: increased pulse and breathing, decreased appetite, and increased alertness. Long-term side effects include: addiction, paranoia, hallucinations, delusions, violent behaviour, insomnia, weight loss, severe tooth decay, and brain damage (Cruickshank and Dyer, 2009; White, 2004). The paranoid hallucinations caused by long term MA use are often indistinguishable from acute paranoid schizophrenia. MA-induced hallucinations are often auditory, visual and tactile. Tactile hallucinations such as formication, the sensation of something crawling under the skin, is often associated with skin-picking, can lead to further complications, such as bacterial infections (Cruickshank and Dyer, 2009).

MA is most often found as a hydrochloride salt. The solid form makes it more practical and easier to distribute. In this form, MA can be taken orally, snorted, injected or smoked. Powder forms have a typical purity of 10% MA salt, whereas the crystalline form is typically >80% pure. MA hydrochloride is sufficiently volatile that it may be smoked, however, the more pure crystalline form, "Crystal Meth" or "Ice", is more suitable for smoking because it vaporises without pyrolysis and avoids the pyrolysis of any cutting agents. This smokeable form of MA has an

increased incidence of dependence compared to the lower purity forms. This increased incidence of addiction is due to the increased speed at which MA vapours reach the brain compared to other routes of administration (Cruickshank and Dyer, 2009; King, 2009). Typical doses of MA range from 5 - 30 mg, however fatal overdoses have been observed from doses of 20 mg and survival has been recorded at a dose of 640 mg (Cruickshank and Dyer, 2009).

MA has one chiral carbon and two enantiomers (Figure 1.2). MA is found as a racemic mixture of the *R* and *S* enantiomers, or as pure *S*-MA. The *R* enantiomer is not found on its own and this is due to the synthetic processes used to manufacture MA (see Section 1.2.3). The *S* enantiomer is two to three times more biologically active than the *R,S* racemic mixture, and five times more potent than the *R* enantiomer (Marnell, 2001).

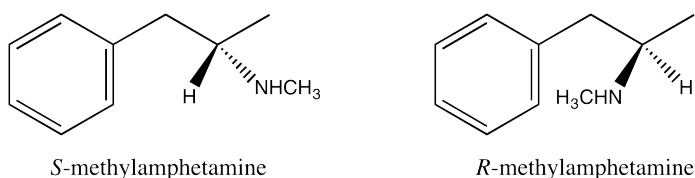


Figure 1.2: Enantiomers of methylamphetamine

1.2.3 Manufacture of Methylamphetamine

The illicit manufacture of MA has been detected in over 60 countries worldwide, with manufacture primarily concentrated in East and South-East Asia, Oceania, and North America (also the regions with highest MA usage) (UNODC, 2012). In 2009, manufacture of ATs was estimated to be between 197 and 624 metric tons (UNODC, 2011). While manufacture estimates were not provided in the 2012 World Drug Report, seizures of MA in 2010 totalled 45 tons, which is a 44% increase on seizures from 2008. In 2010, the total number of seized MA laboratories reported to the UNODC was 13,607 – a 25% increase from 2009, yet far below the high of 18,778 in 2004. MA labs are the most numerous synthetic drug labs seized, accounting for 92.3% of all ATs laboratories seized in 2010 (UNODC, 2012).

The manufacture of MA can take place in a variety of settings from small, rudimentary laboratories to large, highly sophisticated laboratories. These laboratories can be located in residential

dwellings, hotel and motel rooms, flats, boats, vehicles, campgrounds, or commercial premises. Although they are called “laboratories”, illicit drug manufacturing sites rarely resemble legitimate chemistry laboratories (New Zealand Ministry of Health, 2010). Clandestine labs are hazardous sites, erected with little regard for safety and may be “booby trapped” against law enforcement personnel. Historically, MA has most often been manufactured in small, kitchen-sized labs, commonly referred to as “mom and pop” labs. These labs are not meant for large-scale production, but are sufficient to support the habit of one or two users, producing a few grams per production cycle. However, recently, large “super labs”, with production capacity of 10 Kg or more per production cycle, have become increasingly common for the manufacture of MA. Previously, these large labs were typically found manufacturing amphetamine or ecstasy, as they require more sophisticated chemical knowledge and equipment. The small labs are more likely to pose health and safety hazards due to the inexperience of the manufacturers. Less than 10% of persons arrested for the synthesis of MA have a background in chemistry (Hargreaves, 2000).

MA can be manufactured easily using a variety of common household chemicals and several different methods, or routes. Information on how to synthesise MA is readily available on the Internet, publicly accessible scientific journals, chemical patents, and published books (Shulgin and Shulgin, 1991; Uncle Fester, 2009; White, 2004). The ease in obtaining such information and the simplicity of the process itself has dictated the trends in MA manufacture.

1.2.3.1 Chemicals

The route used to manufacture MA is often dictated by the availability of chemicals, the complexity of the method, and the skill level of the manufacturer. These chemicals are broken down into three categories: precursors, reagents and general-purpose chemicals (White, 2004).

The availability of common precursors, i.e. the “building blocks”, is restricted by legislation. It is these chemicals that determine the route of MA synthesis. As mentioned earlier, the precursor chemicals for the manufacture of MA include P2P, ephedrine, and pseudoephedrine. which are all controlled chemicals in the UK as well as many other countries.

As a result, clandestine chemists find alternative sources for precursor materials. P2P is often found on the black market, or can be synthesised from a variety of other chemicals that are not controlled (Uncle Fester, 2009; White, 2004). Meanwhile, ephedrine and pseudoephedrine (pseudo/ephedrine) are found in over the counter cold medicines, such as Sudafed®. While restrictions are in place to prevent the sale of large quantities of such products, it has become common for clandestine chemists to visit multiple pharmacies in order to obtain a large enough supply. This has been termed “smurfing” (UNODC, 2009). The pseudo/ephedrine found in over the counter tablets can be easily extracted using a few simple steps. To combat this issue, the pharmaceutical industry has started adding fillers and other compounds to hinder and prevent the extraction of the active ingredients. However, as soon as a new formula comes on the market, it is not long before someone determines how to circumvent it (Uncle Fester, 2009). Other sources of pseudo/ephedrine are available, though are rarely encountered. It is possible to synthesise pseudoephedrine (Uncle Fester, 2009) and ephedrine can be found in alternative medicines, such as the plant product *Ephedra*. The alternative medicine industry is largely unregulated, thus making *Ephedra* relatively easy to obtain (Uncle Fester, 2009).

Reagents and general-purpose chemicals are much easier to acquire. Examples of reagents include lithium and iodine. Lithium can be extracted from everyday batteries (Uncle Fester, 2009; White, 2004) and iodine can be extracted from antiseptic tinctures found at local pharmacies (Uncle Fester, 2009). General-purpose chemicals include solvents and acids to enable the reaction, and to wash and extract the final product. Examples of general-purpose chemicals include ammonia, found in bleach and window cleaner; toluene, found in paint thinner; hexane, found in camper fuel; and hydrochloric acid, found in cleaning solutions (Man et al., 2009).

1.2.3.2 Routes

As the choice of route depends primarily on the availability of the precursor chemicals, several different clandestine methods exist and they are continuously evolving. Novel methods are discovered by law enforcement on a regular basis and are often reported in scientific journals.

Synthetic routes can be broken down into two categories: those that use P2P as a precursor (Figure 1.3) and those that use pseudo/ephedrine as a precursor (Figure 1.4) (Remberg and

Stead, 1999). Routes that use P2P as a precursor result in a racemic mixture of *S,R*-MA and pseudo/ephedrine routes result in racemically pure *S*-MA. The most common routes employed during the past 10-15 years are those that call for the reduction of pseudo/ephedrine (Scott and Dedel, 2006), however the use of P2P-based routes are on the rise as pseudo/ephedrine has become more difficult to obtain. Route preferences vary by geographic region, with P2P-based routes currently the most popular in the United States, and pseudo/ephedrine routes currently most common in Oceania.

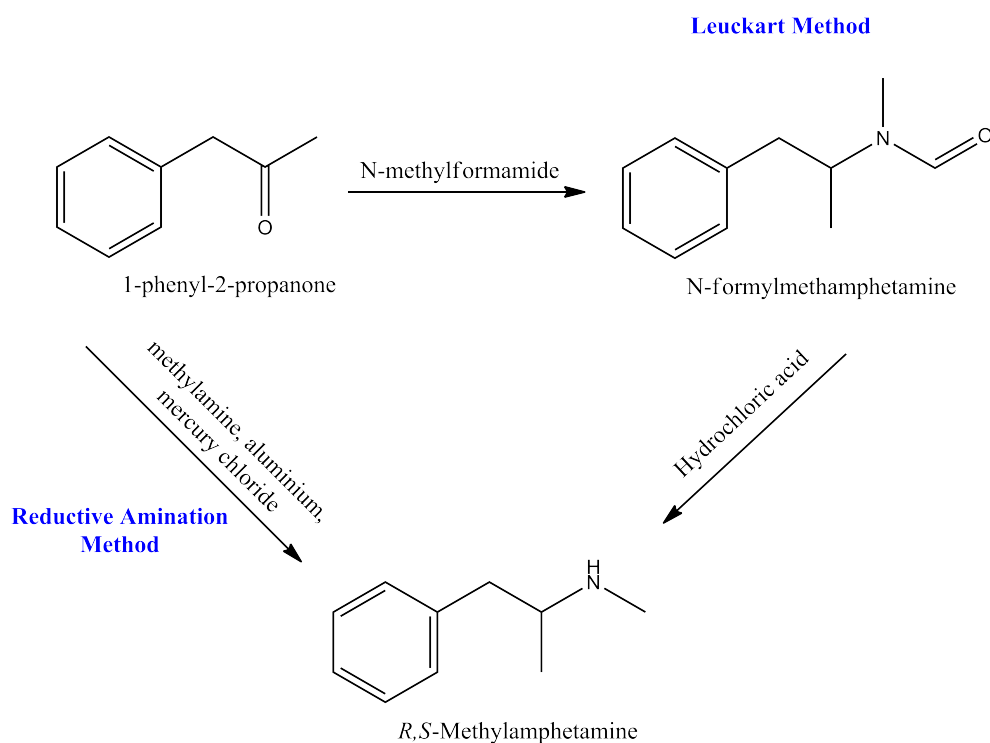


Figure 1.3: Methylamphetamine synthesis from 1-phenyl-2-propanone (from Kunalan et al. 2009)

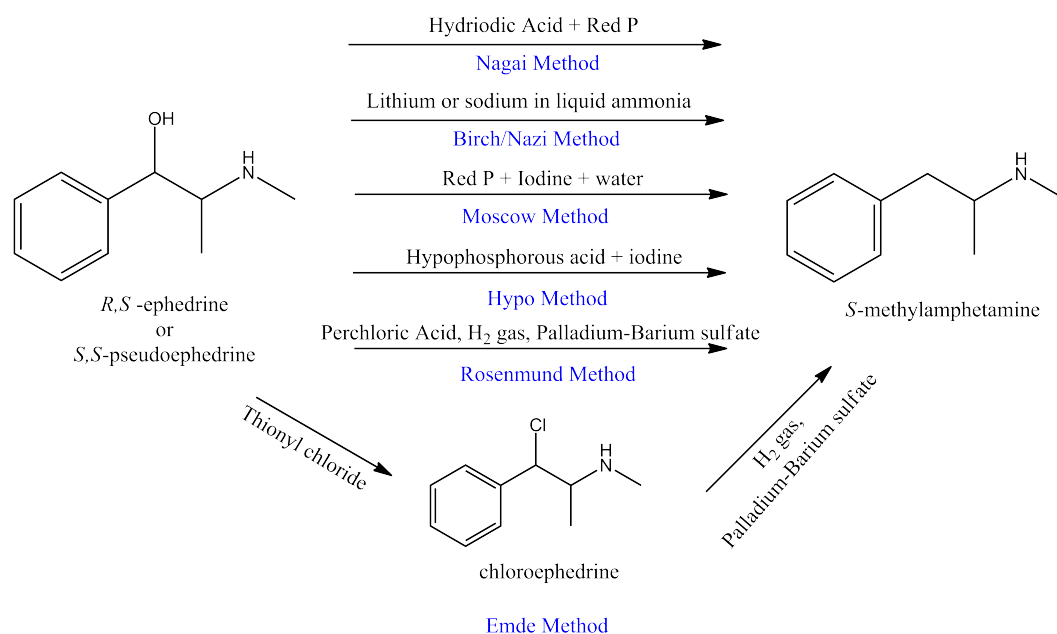


Figure 1.4: Methylamphetamine synthesis from ephedrine or pseudoephedrine (Remberg and Stead, 1999; Makino et al., 2005)

Leuckart Route

The Leuckart reaction is primarily used for the synthesis of amphetamine, however if a few reagents are changed, *R,S*-MA will be the final product. The Leuckart reaction is more labour intensive and time consuming compared to most other methods (White, 2004). Due to the many steps involved, the Leuckart route produces large quantities of waste. When MA labs first started appearing en masse in the 1980s, the most common route was the Leuckart method, which utilises P2P as precursor material. Once P2P became controlled, clandestine manufacturers switched to methods that utilise pseudo/ephedrine (Maxwell and Rutkowski, 2008).

Reductive Amination Synthesis

Another method that uses P2P as a precursor is reductive amination. Aluminium foil is used to produce activated aluminium, which acts as a reducing agent to form MA from P2P and methylamine (Kunalan et al., 2009; White, 2004).

It is also possible to manufacture MA through the reduction of pseudo/ephedrine using several different routes. *R,S*-ephedrine or *S,S*-pseudoephedrine are used to produce the more psychologically active *S* isomer of MA. *S,S*-pseudoephedrine is more commonly found than *R,S*-ephedrine and is the main ingredient in many over-the-counter decongestant medicines.

Birch/Nazi Route

The Birch or Nazi method uses lithium, sodium, and anhydrous liquid ammonia and is most often produced in smaller quantities due to the hazardous nature of those reagents (White, 2004). Lithium can be found in batteries, while sodium hydroxide and anhydrous liquid ammonia can be found from agricultural sources and cleaning products (Man et al., 2009; White, 2004).

Moscow Route

The Moscow route and the hypophosphorous route use different sources of phosphorous, which combines with iodine to produce hydriodic acid (HI) in situ. HI is a powerful reducing agent that can be used to manufacture MA when combined with red phosphorous (the Nagai Route). Once HI became tightly regulated in the 1980s, routes such as the Moscow route and the hypophosphorous route emerged as alternatives. The reaction of phosphorous and iodine works in a cyclic manner to regenerate HI and iodine as the reaction takes place, as shown in Figure 1.5 (Skinner, 1990).

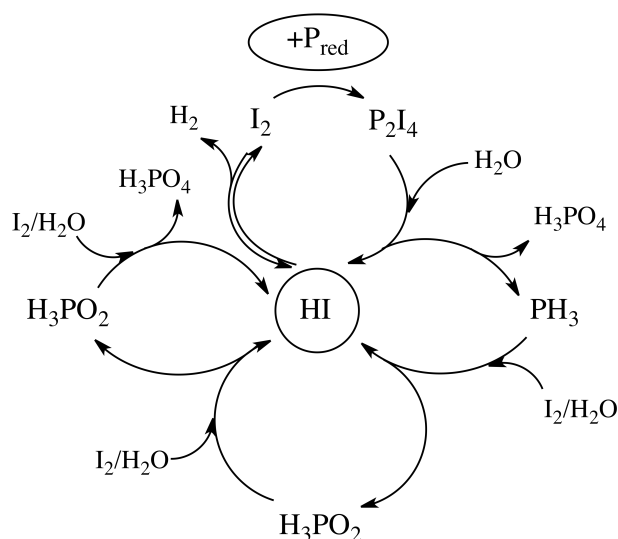


Figure 1.5: Cyclic generation of hydriodic acid by iodine and phosphorus in aqueous solution (Reproduced from Skinner, 1990).

The Moscow route uses red phosphorous (red P) and iodine to generate HI in situ. Red P can be found on the strike pads of matchbooks and in road flares. Iodine is a controlled chemical in many countries, but it can easily be extracted from antiseptic solutions, usually 2-7% iodine, found at most pharmacies and veterinary suppliers (Uncle Fester, 2009).

Hypophosphorous Acid

The hypophosphorous route works in a similar manner as the Moscow route, except it uses hypophosphorous acid instead of red phosphorous. Hypophosphorous acid is also tightly controlled and has few legitimate uses in industry. However, it can be synthesised following a variety of different methods (Uncle Fester, 2009).

Both the Moscow route and the hypophosphorous route run the danger of producing phosphine gas. A by-product of both those routes is phosphorous acid. If phosphorous acid is overheated, it breaks down to produce phosphine gas, which is highly toxic and can ignite spontaneously. Phosphine gas can also form from the break down of hypophosphorous acid, which occurs at a lower temperature than for phosphorous acid (White, 2004).

Rosenmund

The Rosenmund reduction is based on a German article published in 1942 by Rosenmund and Karg (Rosenmund and Karg, 1942). Pseudo/ephedrine is reduced using perchloric acid in the presence of a palladium barium sulphate catalyst.

Emde

The Emde route is similar to the Rosenmund reduction but is a two step reaction. Pseudo/ephedrine is first transformed to a chloroephedrine intermediate using thionylchloride. The hydroxyl group on pseudo/ephedrine gets replaced with a chlorine group, which is subsequently reduced through the addition of palladium barium sulphate.

1.2.3.3 Precipitation: Salting Out

The final product of the above reactions is an oily liquid, containing MA base. The liquid base is slightly volatile and difficult to administer and distribute, thus MA is converted into a solid salt. The MA is precipitated to form either a sulphate salt or hydrochloride salt – a process called “salting out”. MA is most often found as the hydrochloride salt as opposed to the sulphate salt. While the salt form is water soluble, the base form is not (White, 2004).

The salting out procedure (Figure 1.6) is the same regardless of which route was used to manufacture MA. The procedure is again, simple, yet highly dangerous and messy. Two acids are required for this step: 37% hydrochloric acid (HCl) and concentrated sulphuric acid (H₂SO₄), as well as sodium chloride. The concentrated H₂SO₄ is added drop-wise to a mixture of 37% HCl and NaCl, which causes the formation of HCl gas. This gas is allowed to pass from the reaction vessel into the MA mixture. MA precipitates out as MA·HCl, a white solid that can be washed with solvent (usually acetone or toluene) and dried (Buchanan, 2009).

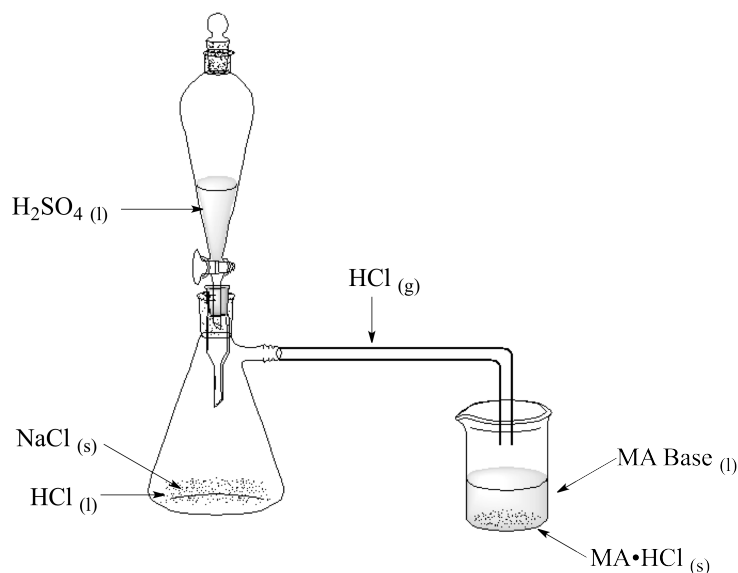


Figure 1.6: Precipitating methylamphetamine hydrochloride salt

1.2.3.4 Crystal Methylamphetamine

In order to produce crystal meth, one further step is required after the salting out phase. The MA·HCl is dissolved in a small amount of acetone or alcohol and left to stand. As the solvent evaporates, large MA·HCl crystals will begin to form, which may take several weeks (Uncle Fester, 2009; White, 2004).

Crystal MA, also called “crystal meth” or “ice”, is the smokeable form of MA (White, 2004). The oil base is also smokeable, but is more difficult to sell than a solid (Uncle Fester, 2009). Crystal meth is often found in purities upwards of 80% and is thus recognised by users as a pure form of the drug. However, within the past decade crystal MA has been found in lower purities. In an effort to achieve maximum price and in order to circumvent the tougher penalties from this highly pure form, crystal MA has been diluted, or “cut”, with bulking and cutting agents more commonly associated with the powder or tablet form of the drug (White, 2004). Examples of bulking agents include ingredients such as sugar and talc powder, while cutting agents have physiological effects, such as paracetamol or another illicit drug.

1.2.3.5 Methylamphetamine Waste

The environmental impact of clandestine MA laboratories is largely unknown and is a growing concern in many countries. As the drug is being manufactured illicitly, it is likely that waste is also being disposed of by illegal means. The illicit manufacture of MA produces a large amount of waste: one kilogram of MA produces five to seven kilograms of toxic waste (White, 2004). As the amount of MA seized is increasing (UNODC, 2012), it follows that the amount of waste being produced is also increasing. While much work has been completed investigating the reaction impurities of clandestine MA manufacture (Kunalan et al., 2009; Lee et al., 2006; Qi et al., 2007; Remberg and Stead, 1999), no research has been published that investigates MA waste. There are no published studies to date that have investigated the profile or environmental impact of MA waste.

1.2.4 Environmental Assessment

In order to be able to assess the impact of MA waste in the environment, it is important to understand what happens to the waste once it is released into the environment. The fate of contaminants entering the environment is dependent on their physicochemical properties, such as hydrophobicity, vapour pressure, and stability (Walker et al., 1996). Therefore, to aid in the detection and prosecution of an illicit dumpsite, an understanding of the chemical behaviour of the waste components is essential. As such, environmental modelling of organic chemicals is useful in predicting the behaviour of the chemicals once released into the environment. This behaviour can be estimated using environmental modelling.

The use of mathematical models to estimate the behaviour of chemicals in the environment has increased rapidly in the past 10 - 20 years with the advancement of computer technology (Draber and Fujita, 1992). Mathematical models that require lengthy and complicated equations are readily accessible to the general public thanks to various computer programmes. While many different environmental models exist, the fugacity model was chosen for this work due to its relative simplicity and widespread availability.

A fugacity model calculates the tendency of a compound to partition into each environmental compartment. The model uses partition coefficients and mass balance equations to predict the movement of a contaminant across environmental compartments (Mackay, 1979). An easy to use and freely available fugacity model can be found in the United States Environmental Protection Agency's (US EPA) computer modelling programme EPI (Estimation Programs Interface) Suite™ (USEPA, 2012b). EPI Suite™ uses a Level III fugacity model, meaning it assumes all compartments (air, water, soil, and sediment) are homogeneous. A Level III model also assumes steady-state conditions, but not equilibrium. According to Mackay (2001), steady-state implies consistency with time, while equilibrium implies that once equilibrium is reached, concentrations have no tendency for net transfer. An advantage of using the EPI Suite™ model is the ability to create a site-specific environmental model by easily changing multiple variables. This feature allows the user to enter specific data relating to a sampling location as well as chemical and physical properties of the compounds of interest.

It is important to determine the chemical composition of the waste in order to identify potential markers of a MA dumpsite. To facilitate the prosecution of clandestine drug chemists for polluting the environment, it is equally important to understand what happens to the waste once it enters the environment. The environmental partitioning and persistence of MA and its waste can be predicted using environmental modelling.

1.3 Research Aim and Objectives

The aim of this project is to assess the environmental fate and impact of waste produced from the clandestine manufacture of MA. In order to achieve this aim, the following objectives will be targeted:

- Manufacture MA to produce and identify waste.
- Establish a chemical profile of MA waste. This includes validating an extraction method and an instrumental analysis method.
- Determine the environmental partition coefficients of the compounds identified in the waste, such as the octanol-water partition coefficient and the sediment-water partition

coefficient following standard methods.

- Computer modelling of the fate of the waste components based on the measured partition coefficients, and comparison with the computer default model.
- Assess the suitability of using environmental pollution legislation to prosecute clandestine drug manufacturers.

1.4 Thesis outline

The research question this thesis aims to answer is what are the environmental impacts of illicit MA laboratories? In order to avoid detection of a clandestine drug lab, the waste that is released by these synthetic processes is most often dumped haphazardly without concern for the environment. The long term and short term effects of MA waste need to be understood in order to protect the ecosystem and human health for those in contact with a dumpsite. An understanding of these effects will allow a targeted remediation of the contaminated site. It would be ideal to be able to provide the scientific community with information what will allow it to determine whether or not a particular MA lab or final product can be linked to a specific dumpsite, thus allowing criminal charges to be laid. The aim of this research is to provide the appropriate tools and information to forensic chemists and law enforcement personnel to allow clandestine drug producers to be prosecuted to the fullest extent of the law.

Chapter 2

Literature Review

2.1 Introduction

The field of Environmental Forensics is a relatively new discipline that combines environmental and analytical chemistry with traditional forensic science. The aim of environmental forensics investigations is most often source apportionment of a chemical dumpsite. The field gained much exposure following the Exxon Valdez oil tanker spill in Alaska, USA, in 1989. Scientists investigating the spill had to differentiate between the crude oil carried in the oil tanker Exxon Valdez from historic sources of contamination. Using chemical markers, analysis of marker ratios, and stable isotope analysis, investigators were able to apportion blame for the current spill while eliminating contamination from other sources, such as smaller and older spills. Subsequently the field of environmental forensics emerged with prominence (Morrison, 2000; Wang and Stout, 2007).

Environmental forensics has benefitted greatly from the advancement of analytical instrumentation, such as advances in gas chromatography, liquid chromatography, and mass spectrometry. Where environmental forensics differs from traditional forensics is the lack of established protocols and uniformity across the profession. Since traditional forensic science has spent many years going through the criminal justice system, several guidelines and standards have been drafted for the scientific community to adhere to. In the United States, this comes in the form

of the Daubert inquiry which states very clearly the standards of scientific evidence that are permissible in court, for example peer reviewed techniques and known error rates (United States Supreme Court, 1993). In the United Kingdom, a House of Commons review on forensic science has recommended the development of regulations based on the Daubert criteria (House of Commons, 2005). In many cases, environmental forensics has yet to be bound by Daubert criteria. Without those restrictions, environmental forensics has more flexibility in applying and researching less conventional, novel techniques.

Another difference between the two disciplines is the type of compounds of interest. In traditional forensic chemistry, the focus is most often on illicit drugs, flammable liquids, paints, waxes, and inks. Whereas environmental forensics primarily investigates polyaromatic hydrocarbons (PAH), polychlorinated biphenyls (PCB), and dioxins in complicated matrices. In the past five to ten years, pharmaceuticals and personal care products (PPCP) have been identified as important ‘emerging pollutants’ (Heberer, 2002), creating collaborative opportunities between the two fields. As wastewater treatment plants (WWTP) do not remove all of PPCPs excreted by humans, those products are discharged into the environment and cause unknown consequences. Figure 2.1 on the following page, adapted from Wise et al. (2011), shows the main routes chemicals may enter into surface waters. Thanks to advancements in analytical instrumentation, lower and lower limits of detection are available - down to ng/L and µg/L. However, just because a chemical is detectable in the environment, it may not necessarily cause negative effects. It is the responsibility of environmental scientists to investigate the actual harmfulness of chemicals, which may be accomplished by using environmental modelling and toxicity testing.

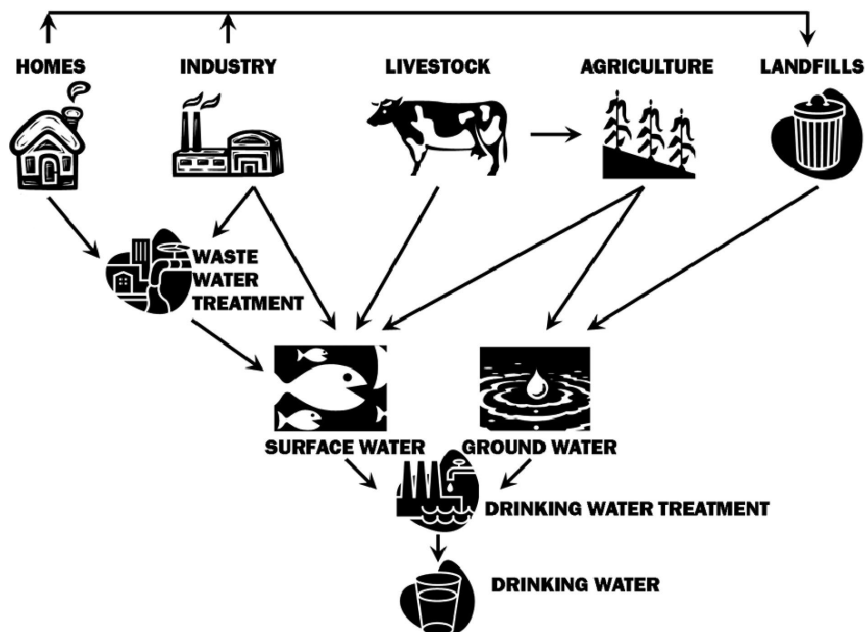


Figure 2.1: Simplified diagram displaying points of entry of chemicals into surface waters. (Adapted from Wise et al., 2011)

Walker et al. (1996) differentiate between a “pollutant” and a “contaminant”. The term “pollutant” indicates that the chemical of interest causes actual environmental harm, whereas the term “contaminant” implies the chemical is not harmful. Given the general toxicological principle that toxicity is related to dose, the same chemical may be considered a pollutant in one instance, but a contaminant in another. Many factors may influence the toxicity of a chemical once released into the environment, primarily uptake of the chemical by organisms. Factors influencing uptake include environmental conditions, such as pH, temperature, and water oxygen content. The route of uptake is also a factor that depends on the physicochemical properties of the compound and the organism of interest. For example, hydrophobic compounds will adsorb to bottom sediments and pose a greater harm to bottom-dwelling organisms who may ingest sediment along with their food. Hydrophilic compounds may prove to be more harmful when the major route of uptake is through water, such as passing through fish gills.

One well established consequence of low levels of pollutants harming the environment is the feminization of male aquatic organisms, such as fish and frogs, caused by the discharge of endocrine disruption chemicals, such as bisphenol A, synthetic estrogens, PCBs, and the herbicide

atrazine (Sumpter and Johnson, 2005; Hayes et al., 2011; Wise et al., 2011). A review into the levels of oral contraceptives, primarily the synthetic hormone 17- α -ethinyl estradiol (EE2), in drinking water by Wise et al. (2011) notes that 40% of a 26 $\mu\text{g}/\text{day}$ dose of EE2 ends up in WWTPs in its active form. The removal efficiency of EE2 from WWTPs can range from 80% to 98% depending on the process and conditions. Despite the removal of the majority of EE2 during the treatment process, EE2 has still been detected in surface waters at levels ranging from <0.1 to 5.1 ng/L. Wise et al. conclude that while there is insufficient evidence to suggest environmental discharges of oral contraceptives have an impact on human reproductive health, they have been shown to pose problems to the reproductive health of fish and other aquatic species. Even though relatively small levels of endocrine disrupting chemicals, and other pollutants, are discharged into surface waters, this discharge occurs daily which may lead to the accumulation of potentially persistent xenobiotics in the environment.

When pharmaceuticals began to be detected in WWTP effluent, several research groups began to investigate the occurrence of illicit drugs in WWTP influent and effluent, as well as in surface waters (Huerta-Fontela et al., 2008; Kasprzyk-Hordern et al., 2009; Zuccato et al., 2005, 2008). By measuring the discharged amount of illicit drugs and their metabolites, it was possible to calculate the drug usage of the surrounding population. The area of research that this project aims to fill is tying together emerging pollutants with conventional forensic science.

2.2 Pharmaceutical and Personal Care Products

A popular research area emerging in the late 1990s and early 2000s was the detection of pharmaceuticals and illicit drugs in wastewater, rivers, and lakes. Experiments conducted in many different countries across three different continents yielded similar results. More than 80 pharmaceutically active compounds and their metabolites have been detected in water samples (Heberer, 2002). These compounds have been found in concentrations from ng/L to $\mu\text{g}/\text{L}$, which may or may not be significant to the environment but are well below therapeutic dosage levels. However, even at low levels, pharmaceutically active compounds can negatively impact aquatic species. For example, the concentration of substances such as hormones are high enough to cause endocrine disrupting effects in localised areas.

When monitoring surface water and wastewater for drugs of human consumption, it is important to consider the ratio of un-metabolised drug to the ratio excreted as the metabolite(s). If this ratio were to vary significantly, it would indicate that the drug itself is being disposed of directly into the water (Kasprzyk-Hordern et al., 2009; Zuccato et al., 2005).

Zuccato et al. (2005) detected an abundance of cocaine in numerous water samples. Samples were collected from the River Po, Italy's longest river, and from wastewater treatment plants from four medium-sized Italian cities. By quantifying levels of cocaine and its main metabolite, benzoylecgonine, the study found that the River Po was carrying approximately 4 Kg of cocaine per day. Given the catchment area where the samples were taken from, this equals approximately seven 100 mg doses per day per 1000 people, or 27 100 mg doses per day per 1000 people in the young adult category (15-35), the main users of cocaine (UNODC, 2009). Analysis of influent from wastewater treatment plants had similar findings, albeit a slightly lower abundance of the drug (9-17 doses per 1000 for the young adult population).

A similar study from the same group (Zuccato et al., 2008) examined water samples from Italy and the UK for the presence of multiple illicit drugs and their metabolites. The drugs of interest were (metabolites in italics): cocaine, *benzoylecgonine*, *norbenzoylecgonine*, *norcocaine*, *co-caethylene*, amphetamine (AMP), methylamphetamine (MA), 3,4-methylenedioxyamphetamine (MDA), 3,4-methylenedioxyamphetamine (MDMA), morphine, *6-acetylmorphine* (a metabolite of heroin, or diamorphine), 11-nor-9-carboxy-delta9-tetrahydrocannabinol (THC-COOH, metabolite of the active ingredient of cannabis), codeine, *6-acetylcodeine*, and methadone, 2-ethylidene-1,5-dimethyl-3,3-diphenylpyrrolidine (EDDP).

Samples by the group were taken once again from the River Po, two additional Italian rivers, three Italian lakes, and the River Thames in England. When sampling from the River Thames, samples were taken from both rural and urban (also tidal) areas of the river.

Throughout the study, all of the drugs and metabolites tested for were found in at least one river water sample, but three compounds were not detected in the lake water samples. Those were amphetamine, 6-acetylmorphine, and 6-acetylcodeine. Cocaine and benzoylecgonine were the most abundant illicit drugs present in the water samples. For the River Thames samples,

benzoylecgonine was quantified in samples from all five sampling points (two rural locations and three from the London area), and morphine was found in four of the five locations. Amphetamine and MA were not detected in the River Thames. Levels of benzoylecgonine and morphine were many times higher in the London area than rural areas. However, it must be taken into account that London is the point in the river where it widens and becomes tidal. Thus the amount of a drug found has been subjected to a large dilution factor. Therefore it is difficult to compare usage between the urban areas of the Thames with the rural areas.

In addition to the measurement of illicit drugs in surface water and wastewater, the Zuccato group was able to establish and implement an effective method for the extraction of drugs from wastewater samples (Castiglioni et al., 2006; Pomati et al., 2006; Zuccato et al., 2005, 2008). This method has been successfully repeated by others (Huerta-Fontela et al., 2008; Kasprzyk-Hordern et al., 2009). The acceptance and adoption of a successful analytical method by several research groups is an important factor in establishing legally acceptable scientific criteria for criminal prosecutions. The standardisation of methods is an important step in advancing the field of environmental forensics.

As stated in the literature (Glassmeyer et al., 2005; Huerta-Fontela et al., 2008; Kasprzyk-Hordern et al., 2009; Zuccato et al., 2008), illicit drugs, personal care, and pharmaceutical products are ubiquitous in river water, surface water, and wastewater. As drug usage increases, more of these products are going to be found in the aqueous environment. Given the potent pharmacological action these products have on the human body, research is lacking on the effects of those products in the environment, even in such small quantities.

There are two studies of note which have examined the toxicity effects of illicitly produced drugs and illicit drugs at low, environmental levels (Finnon et al., 2001; Pomati et al., 2006). However, neither of them examined the potentially adverse effects on environmentally related organisms.

The first study (Finnon et al., 2001) was an investigation into the toxicity levels of impurities found in the illicit manufacture of AMP. It was found that the levels of reaction impurities that were toxic to the cells studied were much higher than the levels of reaction impurities that would be found in a typical dose of street AMP. AMP synthesised in-house was found to be more toxic

than the chemical standard purchased from Sigma Aldrich, suggesting that the manufacturing by-products are more harmful than the parent drug. A major drawback of this report was it did not specify what types of cells were used in this investigation: whether they were human-related cells or environmentally related cells.

The second study (Pomati et al., 2006) investigated the toxicity of a mixture of 13 pharmaceuticals at concentrations typically found in environmental samples (ng/L). The paper also investigated additive effects the pharmaceuticals had on each other. The types of cells used for this study were human embryonic cells, which the authors acknowledge is a sensitive cell line.

When the cells received a fresh dose of the pharmaceutical mixture each day, cell proliferation decreased by 30-40% when compared to negative controls. Cell growth was not as affected when the cells received a single dose of the mixture and monitored over time. The reduction in proliferation of those cells was approximately 10%, indicating that the mixture accumulated when added daily and became more toxic with repeated exposure. This shows the cell community did not develop an immunity for the mixture.

In order to assess whether or not the toxicity of the mixture was the result of additive effects or due to one chemotherapy drug (cyclophosphamide), the toxicity of cyclophosphamide was assessed individually and compared to the drug mixture. When initially exposed to environmental levels of cyclophosphamide, the embryonic cells actually experienced an increase in growth of approximately 10%. When the cells were exposed to same levels of the drug mixture, there was a decrease of approximately 30% growth compared to the negative controls. A decrease in cell growth (20%) only began to appear when cyclophosphamide was added in concentrations 100 times above that which is normally found in the environment. Therefore, the interaction of various pharmacologically active compounds with each other can produce additive toxicological effects that are greater than the toxicity of an individual drug.

While it has been shown that levels of pharmacologically active compounds as found in the environment can be toxic to human cells, little is known of their toxicity to the environment. And while most human waste goes through WWTPs, these plants are variable in the range of

efficiency in terms of proportion of drug removed, and is dependent on the design of the WWTP and other non controllable factors, such as rainfall.

Returning to the detection of controlled drugs in the environment, Huerta-Fontela et al. (2008) sampled 42 WWTPs in north-eastern Spain. Of the amphetamine type stimulants, AMP, MA, and MDMA were found in the influent of 22, 17 and 32 WWTP, respectively. Worryingly, those drugs were also found in the effluent of 10, 12 and 18 WWTP, respectively. The removal efficiency of MA had a wide range, from 44% to >99%. No drug in this study was removed >99% in all 42 WWTP studied.

Due to the relative ease at which MA can be manufactured, it is often made locally in small, domestic labs (UNODC, 2011). Therefore, if MA is being detected in waters of a particular region, it is most likely being manufactured in close proximity. The manufacture of MA produces a significant amount of chemical waste (White, 2004) that will also end up in the environment. Persons engaged in the illicit manufacture of MA are not likely to be overly concerned with properly disposing their waste. Thus the waste is likely to be disposed of illegally.

In summary, illicit drugs and other pharmacologically active compounds have been detected in wastewater, river water, and surface water in various countries around the world. While the threat that these drugs pose to humans at environmental levels is beginning to receive attention, the threat posed to the aqueous environment itself remains unstudied.

2.3 Impurity Profiling of Illicit Drugs

Environmental forensics and traditional forensics have both utilised chemical profiling since the 1970s. While both fields work with extremely different matrixes (sediment, soil, and water versus drugs of abuse), they have a common goal to determine the origin of a sample.

Environmental forensics has utilised chemical fingerprinting since the 1970s as a tool to determine the source of a chemical discharge into the environment (Wang and Stout, 2007), using gas chromatography (GC) with a packed column. In recent years the term “fingerprint” has fallen

out of favour for the term “profile”. This is because a fingerprint will not change over time while a profile will, which is in accordance with weathering and mixing of the chemical once it is in the environment. The advancements of GC detector and column technology over the years has kept GC as the preferred analytical method for the chemical profiling of oil spills. The use of gas chromatography-mass spectrometry (GC-MS), in particular, enables a high level of specificity to distinguish between different oils by using target compounds, such as PAHs and biomarkers (triterpene and sterane compounds) (Wang and Stout, 2007).

Forensic chemists can produce a drug “fingerprint”, known as an impurity profile, by performing a detailed chemical analysis of seized drug. Since illicit drugs that are manufactured clandestinely are rarely found in the pure form, impurity profiling provides valuable intelligence that may ultimately lead investigators to a source of origin. Information that comprises the impurity profile includes information regarding the route of manufacture and the composition of additives. As illicit drugs are mixtures of cutting agents, adulterants, by-products, and impurities from the manufacturing process, each sample produces a unique profile (White, 2004).

The chemical profiling of illicit drugs has been employed for several decades. As far back as 1975, Strömberg used GC to profile amphetamine sulphate (Strömberg, 1975 as cited by Andersson et al., 2007a). Illicit drug profiling is, in essence, an intelligence-gathering tool used by law enforcement agencies to assist with criminal investigations. While much data can be attained from a drug seizure, the usefulness of this information depends on how it is applied. The physical and chemical information gathered from drug profiling can help to identify relationships between drug seizures, sources, and trafficking routes, which may ultimately assist in identifying and disrupting drug trafficking organisations (Dujourdy et al., 2008; Collins et al., 2007).

The clandestine manufacture of illicit synthetic drugs is most often carried out by persons with little knowledge of organic chemistry. As such, the quality of the final product varies immensely and impurities from the synthetic method can be found in the final product. The profiling of synthetic drugs can determine the synthetic route and precursor chemicals used. This intelligence can provide law enforcement personnel with information to help control the attempted purchase, importation, or diversion of industrial chemicals that may otherwise have legitimate uses (Collins et al., 2007).

The routine profiling of MA is not currently carried out in the UK, due to the associated costs and low frequency of MA abuse in the UK. However, impurities may be identified during routine MA analysis using GC-MS. Other countries where MA is more prevalent, such as Japan, Thailand, Australia, and the United States, have developed impurity profiling methods for MA (White, 2004). In Europe, where AMP is more widely abused than MA, the focus has been on developing profiling methods for AMP.

In the early 2000s, the European Commission funded a project for the impurity profiling of illicit AMP. The aims were to harmonise profiling methods across Europe and to create a common database for seized drug impurities. The project was called Collaborative Harmonisation of Methods for Profiling of Amphetamine Type Stimulants (CHAMP) and produced six publications detailing optimised laboratory methods for AMP profiling (Aalberg et al., 2005b,a; Andersson et al., 2007a,b,c; Lock et al., 2007). The six papers covered the following topics:

1. Synthesis of organic standards commonly found in AMP seizures
2. Stability of the impurities in various organic solvents
3. Optimisation of the gas chromatographic method
4. Optimisation of the sample preparation (extraction) method
5. Determination of the variability of the optimised method
6. Statistical evaluation methods for comparison of AMP samples

The CHAMP method, developed by researchers in seven different countries, started with the synthesis of 21 different AMP impurities that had previously been identified in the literature (Aalberg et al., 2005b). Like MA, AMP can be synthesised following several different routes. There are three primary routes used to synthesise AMP: Leuckart, nitrostyrene, and reductive amination of P2P. As mentioned in Section 1.2.3, MA can also be manufactured from the Leuckart and reductive amination routes. The difference is the use of catalysts with the extra methyl group to produce MA. The compounds synthesised in this first step were used throughout the study to evaluate the entire method.

The first variable to be investigated was the choice of extraction solvent (Aalberg et al., 2005a). Six different solvents were evaluated for their suitability as extraction solvents, and for the stability of the impurities in the solvent. Those solvents were: isooctane, toluene, ethanol, dichloromethane (DCM), ethyl acetate, and diethyl ether. In this portion of the study, the extraction efficiency was not measured, rather the focus was on the stability of the impurities in the solvent. The variable that was measured was the peak size from GC-MS analysis, quantified by the percent relative standard deviation (RSD) of the relative response factors (RRFs). RRFs were calculated by dividing the peak area of each target compound by the peak area of the internal standard. It was found that several of the impurities were unstable regardless of the solvent, and the authors cautioned against using those impurities as profiling markers. Toluene and isooctane were found to provide the most inert conditions, having mean RSD values of 1.8% and 1.7%, respectively.

High performance liquid chromatography (HPLC) and GC have both been used for the profiling of AMP (Andersson et al., 2007a). In the CHAMP study, GC was chosen because it has higher resolving powers, better stability, is user friendly, and has traditionally been used for the profiling of AMP for many years. Many variables were investigated, such as the injection port temperature, column phase, oven temperature programme, and injection volume. RSDs of RRFs of the 21 target compounds were again used to determine the optimum method.

The subsequent paper (Andersson et al., 2007b) studied the most effective extraction procedure to remove the impurities from AMP samples. AMP was synthesised in-house using three different methods: the Leuckart, nitrostyrene, and reductive amination. Previous works have used both solid phase extraction (SPE) and liquid-liquid extraction (LLE) for profiling AMP impurities. This report found SPE and LLE to be comparable in terms of extraction efficiency, however LLE was selected as the preferred method due to the lack of information regarding the long term stability of SPE cartridges. Using LLE as the preferred method, three different buffers were examined: citrate (pH 6.20), phosphate (pH 7.0), and tris(hydroxymethyl)aminomethane (Tris, pH 7.90). Toluene, isooctane, ethyl acetate, and DCM were trialled as extraction solvents. Other variables considered were volume of the buffer, volume of the solvent, and amount of AMP.

In general, it was found the recovery of target analytes was more influenced by the choice of solvent than by the choice of buffer. Isooctane and toluene were once again the best performing solvents. The problem with using ethyl acetate as a solvent is its high solubility with water, thus a larger volume was required to enable adequate separation of the two phases which resulted in a lower peak response from GC analysis. DCM was eliminated based on two reasons. Firstly, DCM does not dissolve caffeine, which is a common adulterant of illicit drugs, and secondly, it is denser than water which made transfer of the organic layer to GC autosampler vials more difficult. Recovery of the target analytes was greater in buffers with basic or neutral pH (Tris/phosphate), which favoured the extraction of basic analytes.

The meticulous research conducted for the CHAMP programme highlights the high level of standard required by forensic chemists in the court of law. Protocols developed from the CHAMP project have been applied further afield in the Special Testing and Research Laboratory of the United States Drug Enforcement Administration, and by the Australian Illicit Drug Intelligence Program (Collins et al., 2007). By having an internationally harmonised method, the collection and exchange of data can be easily compared across laboratories and borders.

Many papers have been published on the profiling of illicit MA (such as Inoue et al., 2003; Lee et al., 2006; Ko et al., 2007; Qi et al., 2007; Kunalan et al., 2009). However, each study presents different extraction and analysis methods - there is no continuity. Despite the focus on AMP, the methods developed through the CHAMP project were successfully applied to illicit MA by Dujourdy et al. (2008). Four different laboratories were involved in the Dujourdy et al. study, applying the CHAMP method without any modifications. The study used both control samples (n=27) distributed by the partner laboratory in Finland, and street samples (n=151) seized in Finland, Estonia, Norway, Denmark, and the Czech Republic.

The authors found that the CHAMP method was excellent for the extraction and separation of MA impurities, with results based on peak RRFs and RSDs of target compounds. Starting with a list of 43 compounds of interest found in the control samples, a final list of 24 target compounds was determined. The selection of a peak was determined based on RSD values: the impurity was considered acceptable when the RSD was below 15%, and considered significant when the RSD was above 15%. For example, if a compound was rarely present but had a high

variability between samples, it was considered discriminant.

Correlation of variables was assessed using normalised data (peak area of target analyte divided by sum of all target peak areas), modified Pearson (Equation 2.1) and Squared cosine (Equation 2.2). The final selection of target analytes was a combination of stability, correlation, and integration criteria. The 24 target compounds proposed by Dujourdy et al. (2008) for the profiling of MA are listed in Table 2.1 on the following page.

$$\textit{Modified Pearson} = \frac{1 - R}{2} \times 100 \quad (2.1)$$

$$\textit{Squared cosine} = 100 - (100 \times \cos^2\theta) \quad (2.2)$$

Table 2.1: 24 target compounds for MA impurity profiling as determined by Dujourdy et al., 2008

Name
<i>cis</i> -1,2-Dimethyl-3-phenyl-aziridine
Ephedrone
Ephedrine
Pseudoephedrine
<i>para</i> - <i>t</i> -Butylmethylanphetamine
<i>N</i> -Formylmethylanphetamine
<i>N</i> -Acetylmethylanphetamine
1,3-Diphenyl-2-propylmethylanamine
DPIA1
DPIA2
Alpha-methyldiphenethylamine
<i>cis</i> -3,4-Diphenyl-3-buten-2-one
DPIMA1
DPIMA2
Unknown-58d
1-Benzyl-3-methyl-naphtalene
Methylanphetamine dimer
1,3-Dimethyl-2-phenyl-naphtalene
Benzoylmethylanphetamine
2,6-Di-Me-3,5-diphenylpyridine
Pyridines 7 and 14
<i>N</i> -Methyl- <i>N</i> -(1-methyl-2-phenylethyl)-2-phenylacetamide
Unknown 58-190
<i>cis</i> -Cinnamoyl-methylanphetamine

DPIA = *N,N*-di(beta-phenyl-isopropyl)amphetamine

DPIMA = *N,N*-di(beta-phenyl-isopropyl)methylanphetamine

Using additional statistical analysis, Dujourdy et al. were able to further discriminate between samples based on the route of manufacture. First, a Plus Least Squares-Discriminant Analysis (PLS-DA) model was calculated to show the difference between samples based on which precursor was utilised, P2P or pseudoephedrine. From the scores plot, two distinct groupings were evident which clearly separated MA synthesised using P2P from MA samples synthesised using pseudoephedrine. The pseudoephedrine group showed a wide spread of results that were further clustered into several smaller groups, though less distinction within the pseudoephedrine group

was seen. Using dendrogram analysis on 90 of the street samples, the pseudoephedrine group was separated into six clusters based on the most prevalent impurity. Dujourdy et al. have shown that it is possible to use the CHAMP method for the profiling of illicit MA and to be able to differentiate between different routes of manufacture.

Perhaps the most comprehensive study on the profiling of illicit MA was conducted by Vanitha Kunalan as a PhD dissertation at the University of Strathclyde, Centre for Forensic Science (Kunalan, 2010). The research gap Kunalan's work aimed to fill was that samples used in most profiling studies have used MA from seized samples, meaning the route of synthesis is unknown. While it may be possible to statistically differentiate between synthetic routes, it cannot be determined for certain which route was used if the provenance is unknown. However, this is where additional police intelligence, such as chemicals found at a clandestine laboratory, may be factored into the analysis.

Kunalan synthesised a total of 149 MA samples using seven different routes that are most commonly used by clandestine drug manufacturers. Those seven routes included two P2P based routes, the Leuckart, reductive amination (Figure 1.3); and five pseudoephedrine based routes: Nagai, Rosenmund, Birch, Moscow, and Emde (Figure 1.4). Impurity profiling was achieved using a several analytical and statistical tools, including GC-MS, bulk isotope ratio mass spectrometry (IRMS), and inductively coupled plasma mass spectrometry (ICPMS). Samples were extracted using a LLE extraction at two different pH levels: an acetate buffer at pH 6.0 and a phosphate buffer at pH 10.5. Ethyl acetate was the extracting solvent. Despite the many tiers of analysis, Kunalan found that GC-MS analysis on a DB-1 column was able to differentiate between all seven routes based on route specific impurity compounds identified in the study. Of two different extractions used, the extraction at pH 10.5 removed the most number of compounds, but several key route specific impurities were removed using the pH 6.0 buffer. Route specific impurities identified in the extracts for the seven synthetic routes is shown in Table 2.2 on the next page.

Table 2.2: Route specific methylamphetamine impurities identified by Kunalan (2010)

Route	Compound	Peak m/z	Extraction pH
Leuckart	α,α -dimethyldiphenethylamine	91, 162, 119, 65, 44	6 & 10.5
	N,α,α -trimethyldiphenethylamine	176, 91, 58, 119	10.5
Reductive amination	1-phenyl-2-propanol	92, 91, 65, 45, 77	6
Nagai	Dimethylphenylnaphthalene	232, 217, 202, 77	6 & 10.5
	Benzylmethnaphthalene	232, 217, 202, 58	6 & 10.5
	N -methyl- N -(α -methylphenethyl)-amino-1-phenyl-2-propanone	238, 91, 105, 190, 120	10.5
	(Z)- N -methyl- N -(α -methylphenethyl)-3-phenylpropenamide	131, 91, 58, 103, 188	10.5
	N -methyl- N -(α -methylphenethyl)-amino-1-phenyl-2-propanone	238, 91, 105, 190, 120	6
Rosenmund	Ethylamphetamine	72, 44, 58, 91	10.5
	N -acetylamphetamine	44, 86, 118, 91, 65	6 & 10.5
	Unknown 1	58, 91, 118, 239	10.5
	Unknown 2	58, 263, 248	10.5
Birch	Unknown 3	58, 77	10.5
Emde	<i>cis</i> -1,2-dimethyl-3-phenylaziridine	146, 105,132, 91	6 & 10.5
	Unknown 4	120, 42, 77, 91	10.5
	Methamphetamine dimer	238, 91, 120,148	10.5
	<i>trans</i> -1,2-dimethyl-3-phenylaziridine	146, 105,132, 91	6
	Unknown 4	120, 42, 77, 91	6
	Chloroephedrine	58, 77, 91, 146, 166	6
Moscow	Unknown 5	43, 125, 89, 168, 105	6 & 10.5
	Unknown 6	91, 145, 262	10.5
	Dimethylphenylnaphthalene	232, 217, 202, 77	6 & 10.5
	Benzylmethnaphthalene	232, 217, 202, 58	6 & 10.5
	N -methyl- N -(α -methylphenethyl)-amino-1-phenyl-2-propanone	238, 91, 105, 190, 120	6 & 10.5

The importance of the Kunalan's work is that it is one of the most comprehensive studies to date on the profiling of MA impurities. Using Kunalan's work as a reference, it is possible to compare impurities from MA waste against route specific impurities from seven different routes, as shown in Chapter 3.

2.4 Clandestine Methylamphetamine Laboratories

A clandestine laboratory is defined by the Australian/New Zealand Standard for the Handling and Destruction of Drugs (Australian/New Zealand Standard, 2002 as cited by New Zealand Ministry of Health, 2010) as: “an illicit operation consisting of apparatus and/or chemicals that either have been or could be used in the manufacture or synthesis of drugs. This includes premises and/or sites.” Examples of premises include, but are not limited to, houses, hotel rooms, mobile homes, vehicles, commercial premises, and campgrounds. Clandestine drug laboratories are inherently dangerous sites that may be contaminated with harmful chemicals, explosion hazards and “booby traps” (Martyny et al., 2007; Hargreaves, 2000). The inherent problem with clandestine MA laboratories is that manufacturers have little or no chemistry training to properly and safely synthesise the drug. Additionally, they often use inappropriate, make-shift equipment. In the United States, one in five MA laboratories is discovered due to an explosion, creating a burn risk to those in the vicinity (New Zealand Ministry of Health, 2010). The synthesis itself most often occurs in closed quarters with little to no ventilation. As such, contamination of the manufacturing site is inevitable and ubiquitous (Abdullah and Miskelly, 2010; New Zealand Ministry of Health, 2010).

Existing literature on the effects of contamination from MA laboratories most often relates to the indoor environment, or the “cooking” environment. Martyny et al. (2007) investigated the levels of harmful and toxic fumes and residues that are released during the cooking process. The study focused on by-products from the most common synthetic routes in the United States at the time of the study. Those three routes were pseudoephedrine-based routes: red phosphorous, hypophosphorous, and anhydrous ammonia (Birch). The compounds sampled for at clandestine laboratories included: phosphine gas, hydrogen chloride, iodine, ammonia, and MA. The aim of their study was to assess the risks encountered by law enforcement personnel and first responders investigating a clandestine MA laboratory. They were also interested in determining which phase of the manufacturing process posed the greatest risk to first responders, children, and other adults present at the clandestine laboratory.

The study was divided into two sections. In the first section, air samples and surface wipes were collected from seized clandestine MA labs. Samples were collected concurrently with the seizure

of the site by law enforcement personnel. The sites were inactive, that is MA manufacture had not taken place recently, except for one. In the second section, MA was synthesised (commonly referred to as “cooking”) under controlled conditions in buildings designated for demolition (several houses and one hotel). Various air monitors were placed throughout the cooking room or house, including detectors attached to the chemist. The monitors measured the levels of various gases in real time as the cook progressed. Additionally, surfaces were swabbed for MA contamination. The levels of vapours and surface contamination were compared to multiple workplace exposure limits set by various organisations in the United States.

The first part of the study affirmed that exposure to inactive clandestine MA labs pose a health risk to first responders and those in contact with the site. Surface wipes of walls, ceilings, counters, and floors found that traces of MA were ubiquitous throughout the structure. It is hypothesised that this is due to the formation of a MA aerosol throughout the manufacture process. Levels of MA on the surface wipes ranged from below detection limits to 16,000 µg/sample (mean = 511 µg/sample; median = 28 µg/sample). Airborne levels of phosphine, hydrogen chloride, and iodine were either not detected or found at low levels. At several sites, iodine stains were visible, however airborne contamination of iodine was not detected. It is interesting to note that the study did not collect surface swabs for iodine.

Quantification of vapours of the toxic gas phosphine were found to be unreliable due to high readings of the field blanks. Although it is known phosphine gas is produced during the manufacture of MA using a source of phosphorous, it is not surprising that the researchers were unable to detect the gas at an inactive site. While phosphine gas is extremely toxic and can cause death, it is also highly reactive. Phosphine has a high vapour pressure (4186 kPa at 20°C) and does not persist for long periods of time if there is any moisture in the air (New Zealand Ministry of Health, 2010). In this first section of the Martyny study, all of the levels of tested chemicals were well below workplace exposure limits, with the exception of MA, which does not have a workplace exposure limit.

In the second part of the study, MA was synthesised using four different synthetic routes: anhydrous ammonia, red phosphorous, hypophosphorous, and phosphorous flakes. The gases

emitted from the cooking process were dependent on the route of manufacture. High levels of ammonia were detected during cooks following the anhydrous ammonia route, levels that well exceeded workplace exposure limits and also exceeded levels immediately dangerous to life and health. For all methods, high levels of MA and hydrogen chloride gas were detected. In this part of the study, the levels of chemicals measured were well above or slightly below workplace exposure limits. See Table 2.3 for a comparison of inactive and active clandestine MA sites to occupational exposure levels in the United States.

Table 2.3: Measured and referenced exposure levels for chemicals evaluated from clandestine MA laboratories in Martyny et al., 2007

Chemical	Inactive Site (ppm)	Active Site (ppm)	NIOSH REL (ppm)	NIOSH IDLH (ppm)
Ammonia	NT	130-3348	25	300
Hydrogen chloride	0.005-0.13	0.03-20	5	50
Iodine	0.0008-0.002	0.001-0.15	0.1	2
Phosphine	NQ	0.1-13	0.3	50
MA - surface	1.0-16,000 ¹	0.1-860 ¹	None	None
MA - airborne	NT	2.6-5500 ²	None	None

¹ Units are $\mu\text{g}/100\text{ cm}^2$

² Units are $\mu\text{g}/\text{m}^3$

NIOSH: National Institute of Occupational Safety & Health; REL: Recommended Exposure Limit; IDLH: Immediately Dangerous to Life and Health; NT: not tested; NQ: not quantified

The Martyny et al. (2007) study demonstrates that the vapours and gases emitted during MA manufacture do not persist for extended periods of time once a cook has been completed. While ammonia vapours, phosphine gas, and hydrogen chloride gas are known to be harmful to humans, once the vapours reach the outdoor air, the dilution factor will be so large as to make those vapours very difficult to impossible to detect. Even if those vapours were detected through general screening, it would be difficult to determine whether the vapours were due to legitimate or illegitimate activity.

2.4.1 Remediation of Clandestine Methamphetamine Laboratories

Once a clandestine drug laboratory has been discovered and seized by law enforcement personnel, it is possible to remediate the site for re-occupation. Australia (Australian Government, 2011),

New Zealand (New Zealand Ministry of Health, 2010), and the United States (USEPA, 2009b; USDEA, 2005) appear to be the only countries with remediation guidelines for clandestine drug laboratories (New Zealand Ministry of Health, 2010). It is important to highlight that these are guidelines only and do not form part of any legislation. The Australian and New Zealand guidelines are based heavily on the guidelines developed in the United States, which were published in 1990 (USDEA, 2005). Although the guidelines from the United States have been provided at the federal government level, 22 states also have their own remediation guidelines.

In each country, it is the responsibility of the property owner to carry out remediation of the property. Law enforcement and government personnel are responsible for dismantling the laboratory, removing bulk chemicals, equipment, and waste. The decision to remediate the property may be dependent on costs, as the costs of remediating a clandestine MA laboratory have been estimated to range from \$5,000 to \$150,000 (US dollars). Costs are dependent on the size and accessibility of the site, level of contamination, and laboratory and contractor fees (USEPA, 2009b). For sites such as mobile homes, the cost of remediation may far outweigh the value of the property. The main purpose of remediation guidelines is to provide contractors and property owners with information on how to proceed with the remediation of a contaminated site.

Once the site is rendered safe by the authorities, pre-remediation sampling should be conducted. If contamination is detected, decontamination will ideally follow. After all areas of contamination have been thoroughly cleaned, post-remediation sampling is to be conducted, followed by further remediation and sampling as required until sufficiently low levels of contamination are attained. The guidelines provide greater details, suggesting how to collect samples, which analytical methods to use, which cleaning solutions to use, and how to clean specified surfaces - everything from porous and non-porous surfaces to children's toys.

It is recommended that any areas of obvious staining from iodine or red phosphorous be removed, along with porous objects, such as upholstered furniture, and appliances that may have been used during the manufacturing process. Plumbing should also be inspected to ensure any corrosive chemicals that may have been poured down drains have not damaged the pipes. Attention should be paid to sites which have heating, ventilation, and air conditioning systems,

as those systems may have collected contaminants and may distribute them throughout the property.

Levels of chemical residues have been suggested for various clandestine MA lab-associated chemicals. It is not practical or cost effective to sample for every type of contaminant, therefore sampling primarily for MA and signs of obvious iodine or red phosphorous staining are recommended. It is assumed that if MA and heavy metals have been decreased to acceptable levels, other chemicals without guideline values will have been sufficiently removed as well. A summary of remediation guidelines for key chemicals from the New Zealand remediation guide is shown in Table 2.4.

Table 2.4: Remediation guidelines for key chemicals associated with clandestine MA laboratories (New Zealand Ministry of Health, 2010).

Chemical	Indoor criteria		Outdoor soil (mg/Kg)	Potable water (mg/L)
	Surface ($\mu\text{g}/100\text{cm}^2$)	Air (mg/m^3)		
Benzene	NE	0.0036	1.1	0.01
Hydrogen chloride	NE	0.009	N/A	N/A
Iodine	20	0.0008	780	N/A
Lead	2	0.0002	N/A	0.01
Mercury (inorganic)	35	0.0033	N/A	0.007
Methylamphetamine	0.5	N/A	5	N/A
Phosphine	NE	0.0004	NE	N/A
Toluene	NE	0.3	68	0.8
Xylenes (total)	NE	0.7	48	0.6

NE = not expected to be found in that compartment

N/A = not available at the time of writing

It is acknowledged that the guideline MA levels are somewhat arbitrary (New Zealand Ministry of Health, 2010; USEPA, 2009b). In the United States, recommended remediated MA levels range from $0.05 \mu\text{g}/100\text{cm}^2$ to $1.5 \mu\text{g}/100\text{cm}^2$. These numbers are not based on health guidelines because the health effects caused by long term exposure to low levels of MA have not been studied. The recommended levels were selected based on what can be scientifically measured, which are believed to be conservatively set so as to be health protective (USEPA, 2009b).

These guidelines focus solely on remediating the indoor environment to make it suitable for re-occupation. There are no guidelines on how to remediate land contaminated from clandestine MA laboratories. Each country (Australian Government, 2011; New Zealand Ministry of Health, 2010; USDEA, 2005; USEPA, 2009b) refers to their respective environmental legislation regarding contaminated land. The clean-up of MA contaminated land is expected to be remediated as any other contaminated site would be: with attention being paid to disposal of debris to ensure more pollution is not caused (i.e. not incinerated) or taken to proper landfill sites.

2.4.2 Clandestine Methylamphetamine Laboratories and the Environment

There is currently one research group studying the persistence of MA, its precursors, and manufacturing by-products in the environment. This Australian research group has published three articles (Janusz et al., 2003; Pal et al., 2011, 2012) studying the microbial degradation of MA and associated chemicals in soil.

The aim of their first study (Janusz et al., 2003) was to identify chemicals associated with the clandestine manufacture of MA which may be persistent in the environment. The anticipation is that forensic drug chemists may be able to use those chemicals to determine the route of MA manufacture from discarded residues. Once persistent chemicals are identified, the environmental assessment of clandestine MA laboratories may begin. As part of their report, the authors identified several gaps and many unknowns in the literature concerning the impact of clandestine MA laboratories on the environment. Such unknowns include the metabolites of degraded organic chemicals used for MA synthesis, the persistence, and the toxicity of those chemicals to soil and water borne microorganisms.

In the Janusz et al. (2003) study, methylamphetamine sulphate (MAS) and P2P were added to soil samples. Although MA is more commonly found as the hydrochloride salt as opposed to the sulphate salt (White, 2004), MAS was used in this study because the standard was readily available (Kirkbride, 2010). The persistence of those two chemicals was investigated using urban and agricultural soils collected in South Australia. Microbial cultures were enriched with P2P in order to study the metabolic products of microbial degradation of P2P.

In order to study the persistence of MAS and P2P in the soil, soil samples were spiked with either P2P or MAS and left to incubate at room temperature. P2P was spiked into four different soils: two from agricultural regions (total carbon = 2.6%, 0.8%) and two from urban regions (total carbon = 3%, 5%). MAS was only spiked into one soil type, an agricultural soil with an organic carbon content of 2.6%. One soil sample was removed each day in order to extract the chemicals and profile the product using GC-MS.

The results indicated that P2P degraded very rapidly, while MAS persisted at high levels for the duration of the study. For the one agricultural soil type in which it was examined, MAS was still present after six weeks at two thirds of its original concentration. Conversely, the concentration of P2P was halved within four to eight days, and was not detected at all after 14-20 days. P2P degraded equally rapidly in all four soils.

Chemical profiling using GC-MS of the P2P soil extract identified six different P2P metabolites. They included: 1-phenyl-2-propanol, 1-phenyl-1,2-propanedione, 1-hydroxy-1-phenyl-2-propanone, 2-hydroxy-1-phenyl-1-propanone, and *syn*- and *anti*-1-phenyl-1,2-propanediol. Metabolites began to appear after two days, with a maximum concentration at six days before decreasing. No compounds were found to accumulate, suggesting the metabolites were a result of microbial degradation and not oxidation reactions.

Additional experiments were conducted using P2P enriched media to examine the soil bacteria's ability to degrade P2P in liquid media. One sample each of agricultural soil and urban soil at 70-80% water holding capacity were spiked with 500 mg/mL of P2P and incubated for two weeks in order for the P2P to degrade. An additional spike of 500 mg/mL of P2P was added and left for seven days. The P2P enriched soil samples were added to a mineral salts medium, from which aliquots were used to inoculate a liquid media for culture experiments. Thus the bacteria within those inoculums were able to grow in the presence of P2P. The nutrients added to the liquid media were varied, creating four different growth conditions. One was a mineral salts medium, another had yeast extract added to the mineral salts medium, the third was comprised of a 1% Tryptone Soy Broth (TSB), and the fourth added glucose to the mineral salts medium. The concentration of P2P and its main metabolite 1-phenyl-2-propanol were measured, along with the optical density (600 nm) of the soil liquid medium.

In the first medium, the only source of carbon available to the bacteria was P2P. Under those conditions, the bacteria were able to grow, using P2P and its metabolites as their carbon source. The optical density saw a sharp increase, indicating the bacteria were growing well. Over the eight days of the experiment, P2P and 1-phenyl-2-propanol were completely utilised within a few days. Results were similar for the medium with an added carbon source (glucose), however 1-phenyl-2-propanol was present in higher concentrations and persisted for a longer period of time. The purpose of the yeast media was to create an abiotic environment to assess whether or not P2P would be degraded under abiotic conditions. In the abiotic trials, there was no change in optical density, meaning no growth was taking place. Additionally, the concentration of P2P did not decrease, indicating that the degradation of P2P is dependent on the presence of microorganisms.

When comparisons were made between the liquid cultures prepared from urban soils to those prepared from agricultural soils, the degradation rates of P2P were noticeably different. Differences were even apparent between the two different urban soil samples. In general, P2P degraded faster in the urban derived cultures compared to the agriculturally derived cultures. The differences observed between the two different urban soils were related to the availability of carbon. For the first soil type, when glucose was added to the media the rate of degradation of P2P decreased. This suggests that the bacteria first consume the readily available source of carbon (the glucose) before attacking the P2P molecules. In the second urban soil sample, the rate of P2P degradation was slightly higher when glucose was present. The bacteria were therefore utilising each carbon source equally, and as the bacterial population increased, so did their consumption of carbon. The liquid culture experiments indicate that the degradation of P2P and the chemical profile created will vary depending on soil type and the amount of available carbon.

It is often a great asset to a police investigation to be able to determine the route of MA manufacture. The results of the Janusz et al. study indicate this will be a difficult task when analysing samples discarded in the environment. The speed at which P2P degrades in soil has significant implications for route determination. Not only is P2P a precursor for synthesis using the Leuckart reaction, but it is also a by-product of MA synthesis following the reduction of

pseudoephedrine using red phosphorous and hydriodic acid. The chemical profile is thus very different if it has been subjected to microbial degradation. The new chemical profile may not be recognisable as a product of MA synthesis. Therefore further research is required to determine new profiles based on degradation products and metabolites.

To further understand the degradation patterns of chemicals associated with Amphetamine Type Stimulants (ATS), the Australian research group followed up their 2003 article in 2011 (Pal et al., 2011). The aim of the second article was to investigate the influence of soil physicochemical properties on five ATS associated chemicals. Those five chemicals (Figure 2.2) were MA, MDMA ("ecstasy"), the MA precursor pseudoephedrine (PSE), and two MA by-products: *N*-formylmethylamphetamine (FMA) from the Leuckart route, and 1-benzyl-3-methylnaphthalene (BMN) from the Nagai route (reduction of PSE using hydriodic acid and red phosphorous, Figure 1.4). The authors once again highlighted the lack of understanding of the impact clandestine laboratory chemicals have on the environment.

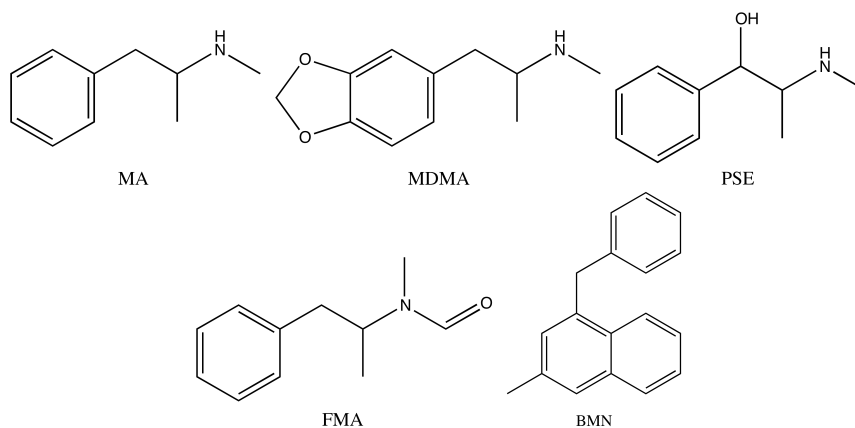


Figure 2.2: Molecular structures of the target compounds in the Pal et al., 2011 study. (MA: methylamphetamine; MDMA: 3,4-methylenedioxyamphetamine ("ecstasy"); PSE: pseudoephedrine; FMA: *N*-formylmethylamphetamine; BMN: 1-benzyl-3-methylnaphthalene)

In this study (Pal et al., 2011), the degradation of the above five chemicals was investigated over a one year period in three different South Australian soils. The soils were adjusted to 50% water holding capacity and either used as is or autoclaved to produce sterilised soil. The sterile soil was used to assess the degradation of compounds due to abiotic factors, such as oxidation and hydrolysis. Each of the three soils had slightly different physicochemical properties. The

authors measured pH (1:2.5 H₂O), electrical conductivity, cation exchange capacity, organic carbon content, dissolved organic carbon, and the particle size distribution.

The non-sterile, biotic, soil experiments corroborated findings from the Janusz et al. study on MA. MA was unable to completely degrade over the course of the one year study period, showing losses of $45.8\% \pm 1.24\%$, $68.4\% \pm 1.27\%$, and $89.6\% \pm 0.59\%$ in each of the three soils. The degradation of MA is in clear contrast to the degradation of the precursor PSE which was completely degraded in two soils within four weeks, and within four months in the third soil. The behaviour of FMA was somewhat between MA and PSE. Its concentration was relatively constant after four weeks, however the concentration subsequently declined rapidly, approaching zero after nine months. The authors cite a study by Hiromatsu et al. (2000) which may explain that the delayed degradation may be due to the presence of a tertiary amine group, which Hiromatsu et al. reported inhibits biodegradation. MDMA exhibited a similar degradation pattern to PSE, degrading rapidly within four months. The Nagai-route by-product BMN degraded slowly, as MA did, persisting in all three soils for the duration of the study. BMN contains a benzyl group at the α -naphthalene position which may cause steric hinderance, slowing degradation.

Assuming first order kinetics, the authors calculated half life values and degradation rate constants. Each value was calculated for each soil, thus three different rate constants and half lives were calculated for each of the five chemicals. Half life values were calculated using the best fit lines of the logarithm of residual concentrations versus time elapsed. Based on those calculations, half life values for MA ranged from 131 to 502 days; for PSE 3.70 to 30.1 days; for FMA 35.0 to 57.9; for MDMA 15.4 to 59.0 days; and for BMN 151 to 10,034 days. The degradation rate constant (k^{-1} : degradation of target compound over time) was taken as the negative slope of the regression line of concentration versus time. Calculated k values are as follows: MA 0.0006 to 0.0023; PSE 0.0100 to 0.0814; FMA 0.0052 to 0.0086; MDMA 0.0051 to 0.0195; and BMN 0.00003 to 0.0020. Interestingly, the degradation rate of the parent drug MA was much lower than the degradation potential of its precursor, PSE. The only structural difference between the two chemicals is the presence of an OH group at the 1-propane position (see Figure 2.2 on the preceding page). The presence of the OH functional group has been

reported to enhance biodegradability (Hiromatsu et al., 2000 as cited by Pal et al., 2011).

The degradation potential in each soil type was different for each chemical. For example, PSE and FMA degraded most rapidly in the soil with highest pH (8.91), the highest cation exchange capacity ($19.24 \text{ cmol(p+)} \text{ Kg}^{-1}$), and the lowest organic carbon (1.11%). The other three chemicals, MA, MDMA and BMN, had the highest degradation potential in the soil with the median pH value (5.98), lowest cation exchange capacity ($6.30 \text{ cmol(p+)} \text{ kg}^{-1}$), and highest organic carbon content (2.88%).

For the abiotic trials, focus was on the two least stable compounds, PSE and MDMA, over 60 days. Degradation did occur in the absence of bacteria, however it was much slower. Degradation rate constants ranged from 0.0006 to 0.0021 for PSE, and 0.0028 to 0.0040 for MDMA. Both chemicals exhibited abiotic degradation that varied slightly according to soil type. Small variations were present, but were not as great as during the biotic trials. For example, PSE degraded rapidly in two of the three soils, and moderately in the third soil during the biotic trials. During the abiotic trials, all three soils exhibited similar speeds of degradation.

While each chemical degraded to a different extent in each soil, the authors did not speculate as to which physicochemical property was most likely responsible for the differences. Another factor which would affect biodegradation is microbial activity, however, the microbial activity in each soil was not characterised in this study. While degradation is primarily dependent on biotic, abiotic, and physicochemical soil properties, other factors such as chemical reactivity and chemical structure also influence degradation patterns.

The third article published by the same Australian research group (Pal et al., 2012) follows the same methodology as the previous article (Pal et al., 2011). The authors used the same three soils to study the sorption-desorption, degradation, and metabolism pattern of a sixth ATS associated chemical: 1-(1',4'-cyclohexadienyl)-2-methylaminopropane (CMP, Figure 2.3 on the next page). CMP is the major by-product from the clandestine manufacture of MA following the reduction of PSE using ammonia and excess lithium, the Birch/Nazi method.

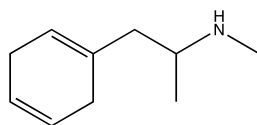


Figure 2.3: Molecular structure of 1-(1',4'-cyclohexadienyl)-2-methylaminopropane (CMP)

For the sorption study, CMP was added to 5 g of soil and shaken for 24 hours. Five different concentrations were used: 5, 10, 20, 50, and 100 $\mu\text{g}/\text{mL}$ in 0.01 M CaCl_2 . After centrifugation, CMP was quantified in the supernatant using High Performance Liquid Chromatography-Mass Spectrometry (HPLC-MS). The amount sorbed was calculated based on the mass balance of the initial and final CMP concentrations. The experiment was conducted for each of the three South Australian soil types. The sorption of CMP was determined to be dependent on the initial concentration, following a Freundlich isotherm, which describes an empirical relationship between sorption of the solute and solid surface area. The sorption coefficient (K_d) was calculated for CMP, as was the organic carbon partition coefficient (K_{OC}) which normalises K_d for the amount of organic carbon in the soil.

Both the K_d and K_{OC} values of CMP varied greatly across the concentration range of 5-100 $\mu\text{g}/\text{mL}$. The authors hypothesised that this was due to a large range of organic carbon content in their three soil types. However, a range of 1.11% to 2.88% organic carbon is not very broad. It is interesting to note that the standard method E1195-01 for the measurement of K_{OC} determined by the American Society for Testing of Materials International (ASTM, 2008) focuses on examining different soil-water ratios rather than different chemical concentrations. This article does not state which, if any, standard method they followed for their sorption study. According to the ASTM method, one concentration is typically employed as the levels of the chemical found in the environment are typically very low. At these low levels, sorption approaches linearity and the effects of different solid to water ratios are greater than concentration effects. The authors did not state at what levels CMP is expected to be found in the environment, nor did they state at what levels CMP is typically found in illicit MA.

Desorption of CMP from soil following the sorption of 20 $\mu\text{g}/\text{mL}$ was also quite variable, from 41.4% to 5.1%. The corresponding organic carbon content of those soils was 1.11% and 2.88%, respectively. The 5.1% desorption assumes the remainder is irreversibly sorbed by soil organic

carbon and clay. Those results are in accordance with the theory that organic molecules will bind tightly to organic carbon.

The degradation of CMP was found to be relatively unstable in both sterile and non-sterile soil, persisting for one to four weeks. In the three non-sterile soils, CMP exhibited half life values from 0.8 to 8.3 days. For the sterilised soils, the half life of CMP ranged from 2.60 to 5.64 days. The parallel degradation pattern of CMP under non-sterile and sterile conditions indicates that abiotic factors have a greater effect on the degradation of CMP.

What was most interesting from this study was the unexpected transformation of CMP to MA. After time zero, MA began to appear in the soil samples, reaching its maximum concentration within four weeks. As with the previous study (Pal et al., 2011), MA then persisted for the duration of the trial. Soil samples were spiked with an initial concentration of 100 mg/Kg of only CMP. Within four weeks, the concentration of MA was measured at ~60 to 80 mg/Kg in non-sterile soil and ~30 to 60 mg/Kg in sterile soil. These results suggest the CMP is not degrading into smaller compounds, but is transforming into MA. Therefore, CMP can be dangerous to the environment by transforming into the much more persistent MA.

The progress of research into the environmental impacts of clandestine MA laboratories has been encouraging in the past few years, mostly due to the Australian research group. However, no research has been conducted into the environmental impact of waste from clandestine MA laboratories. As it is the waste that is produced in the largest quantities, it is likely the waste that will have the largest impact on the environment.

2.5 Environmental Modelling

The American Chemical Society maintains a database of registered chemicals called the Chemical Abstract Service (CAS). There are currently more than 60 million substances registered in the CAS database (Chemical Abstract Service, 2012). Of those 60 million substances, more than 49 million are commercially available, however only 300,000 (0.65%) are inventoried or regulated. It is inevitable that a certain portion of those 49 million substances will ultimately end up in

the environment. Although the amount of compounds that end up in the environment may be considered too low to have an impact, the continuous discharge of persistent foreign chemicals into the environment will result in their accumulation over time, possibly causing unknown harm (Drillia et al., 2005).

Historically, rigorous environmental assessments of new chemicals were not standard practice. Before a chemical becomes commercially available, an environmental risk assessment is now required. Such an assessment provides an understanding of the likely environmental behaviour and effects of the chemical under review. Current assessments aim to prevent toxic chemicals from being released into the environment, preventing the marketing of future PCBs and dichlorodiphenyltrichloroethane (DDT) (Mackay, 1979). Once hailed as a scientific achievement and its creator awarded a Nobel prize, DDT is no longer manufactured due to its detrimental effects on the environment (Newman and Unger, 2003).

Currently, there are stricter laws and guidelines that must be followed during the development of novel chemicals. In the United States, new chemicals must conform to Section 5 of the Toxic Substances Control Act, which is enforced by the US EPA under the New Chemicals Program. The New Chemicals Program aims to act as a “gatekeeper” to prevent harmful chemicals from entering into production (USEPA, 2012c). As part of the New Chemicals Program, an exposure assessment must be conducted for each new chemical. The exposure assessment includes health testing, environmental toxicity testing, and environmental fate testing (USEPA, 2010).

With over 700,000 compounds being reported each year (Hansch et al., 1995), conducting an environmental assessment on each one is a daunting task. Hansch et al. (1995) ask “how many of those chemicals would need to be tested so that the activity of the rest could be estimated?” Fortunately, with the advancements of environmental modelling, conducting chemical assessments need not be an overly complicated or expensive process. Mathematical modelling facilitates an understanding and a prediction of how organic compounds will react within the environment (i.e. soil, air, water, and sediment) and with various biological systems (i.e. enzymes, organelles, membranes) (Hansch et al., 1995; Mackay, 1979).

When chemicals are released into the environment, it can be very difficult to remove them. In order to hold polluters legally responsible for harming the environment, an understanding of the chemical behaviour of the pollutants is essential. As such, environmental modelling of organic chemicals is useful in predicting the behaviour of a chemical once released into the environment.

2.5.1 Quantitative Structure-Activity Relationships

The development of environmental modelling began with quantitative structural-activity relationships (QSAR), which have their origins in medicinal chemistry and drug discovery. QSARs have been used to relate a chemical's physicochemical properties to its biological activity. According to basic chemical and physical theories, it is evident that the biological activity of a chemical will depend on its molecular structure (Jensen, 2007). While each part or functional group of the compound will have a different level of biological activity, predicting the combined effects of each molecular part can be very difficult (Patrick, 2005). Equations to quantify biological activity have been developed which take into account physical, structural, and chemical properties. The most commonly used properties are hydrophobicity, electronic, and steric properties as those are quantifiable (Patrick, 2005). Other popular factors include acid/base dissociation constants (pK_a and pK_b), molecular weight, dipole moments, and infrared frequencies (Jensen, 2007). An important characteristic of most organic chemicals is that their properties vary consistently, and changes in molecular structure are predictable (Mackay, 2001).

QSAR studies are multiple regression analyses that search for statistically significant correlations between a biological response, such as median lethal dose, and chemical properties, such as lipid solubility. A general multiple regression QSAR equation is as follows (Draber and Fujita, 1992):

$$\log A = a_0 + \sum a_i x_i + \sum b_i x_i^2 \quad (2.3)$$

Where:

A = biological response variable

x_i = molecular of substituent parameters for each molecule

a_i, b_i = coefficients that relate the physicochemical parameters to the response

Lipophilicity is perhaps the most important property of biologically active compounds. Early on in drug discovery, in the early 1900s, it was accepted that medicines were required to cross cell membranes in order to be biologically active. As cell membranes are comprised of lipids, drugs needed to be lipid soluble, or hydrophobic. The first experiment to select for lipid soluble compounds was to observe partitioning of the compound into olive oil (Draber and Fujita, 1992). In general, as the hydrophobicity of a substance increases, so does its biological activity. Drug receptor sites and enzymes are often hydrophobic, thus hydrophobic compounds that are able to cross hydrophobic barriers are more likely to reach their target (Patrick, 2005). An excellent measurement of a compound's hydrophobicity, related to its polarity, is the octanol-water partition coefficient (K_{OW} , Equation 2.4). This is a measure of the distribution of the compound between two phases, octanol and water, at equilibrium. Octanol is an excellent substitute for organic matter, both in humans and other organic structures, such as fats and plant waxes. This is because octanol has a similar carbon : hydrogen : oxygen ratio as lipids (Mackay, 2001) and mimics the membrane barrier. Since K_{OW} values can range from 10^{-3} to 10^7 , they are often reported in log form as $\log K_{OW}$.

$$K_{OW} = \frac{[\textit{chemical concentration in octanol}]}{[\textit{chemical concentration in water}]} \quad (2.4)$$

Just as the biological activity of drugs depends on their physical properties, so does the environmental fate of organic compounds. Lipophilicity is an important factor, along with chemical stability and vapour pressure. While many drugs are designed for optimum biological activity in humans, they will at some point enter into the environment during their life cycle. Those same mechanisms that make them effective in humans may cause deleterious effects in aquatic organisms. The high lipophilicity content that permits compounds to enter cell membranes is also linked to bioconcentration of organic substances in aquatic organisms. High bioconcentration factors are associated with high K_{OW} values as most pollutants are taken up by aquatic organisms through passive diffusion, as measured by bioconcentration factor (BCF, Equation 2.5).

$$BCF = \frac{[\textit{chemical concentration in biota}]}{[\textit{chemical concentration in water}]} \quad (2.5)$$

BCF is related to K_{OW} via the equation of the line, as shown in Equation 2.6:

$$\log BCF = a \log K_{OW} + b \quad (2.6)$$

While hydrophobic properties are important in determining the fate of organic chemicals in the environment, they are not the only factors which must be considered. QSARs may be useful to predict the biological activity of a compound of interest, however, they are limited in predicting the fate of a chemical in a model as complex as the environment. If a chemical is going to be released into the environment, it is beneficial to know how long the chemical will survive and what causes its removal (Mackay, 2001). The fate of a chemical in the environment is determined by two main factors: 1) the inherent properties of the chemical (i.e. water solubility, vapour pressure, chemical reactivity) and 2) the properties of the environment to which the chemical is discharged (temperature, flows of air, water, and solids) (Mackay et al., 1992). A popular method to predict the fate of organic chemicals in the environment is fugacity modelling.

2.5.2 Fugacity Modelling

The concept of fugacity was introduced by G. N. Lewis in 1901 (Mackay, 2001), but not applied to environmental modelling until Mackay in the 1970s (Mackay, 1979; Walker et al., 1996). Lewis introduced fugacity as a way to explain chemical potential, which was possible since it has been shown that a chemical's partitioning behaviour is equal to the chemical potential of the substance in each phase (Mackay, 1979).

“Fugacity” is taken from the Latin root *fugere*, which means to flee or escape. Thus fugacity can be described as the escaping tendency of a compound from a pure phase. When the escaping tendency is equal between two phases, the phases are said to be at equilibrium. Fugacity has units of pressure and is equal to partial pressure in ideal gases. At low concentrations (most concentrations of environmental interest), fugacity is linearly proportional to concentration. Fugacity models use partition coefficients and mass balance equations to predict the movement of contaminants across environmental compartments (Mackay, 1979, 2001). Figure 2.4 on the following page shows the comprehensive relationship between fugacity constants and partition coefficients. A simpler model that shows the interactions between the five environmental com-

partments is shown in Figure 2.5 on page 53.

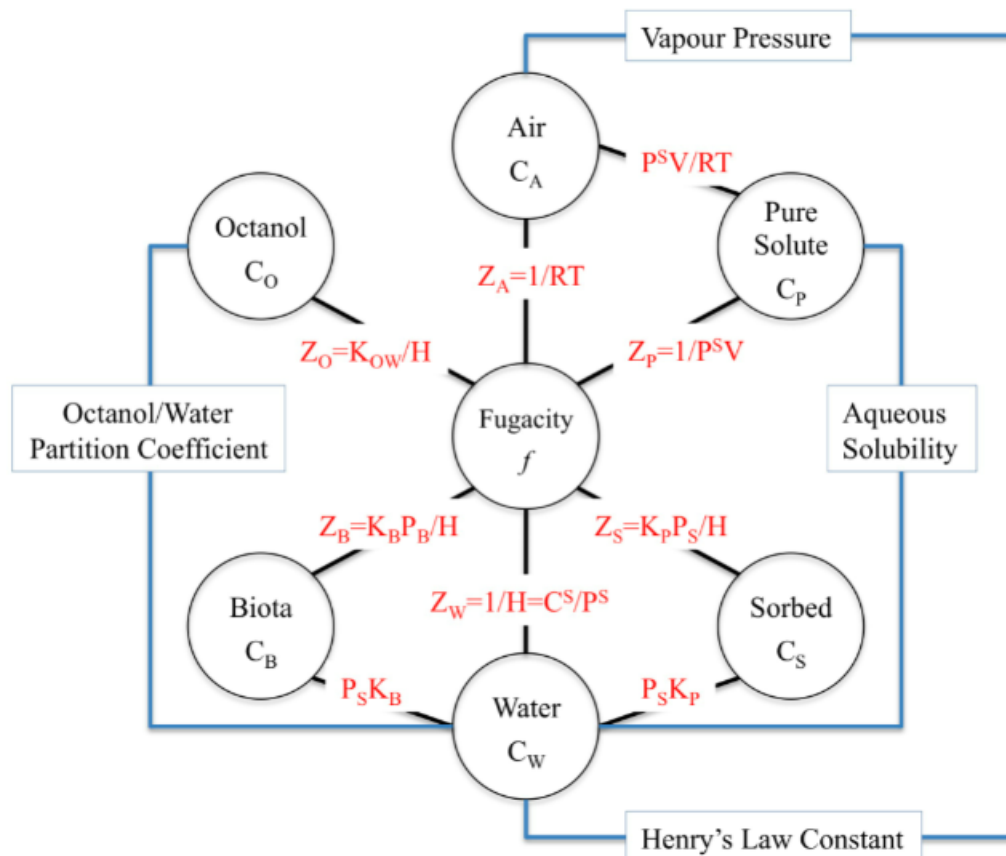


Figure 2.4: Relationship between fugacity (f), fugacity capacities (Z) and partition coefficients (K). (Adapted from Samiullah, 1990.)

Where:

Compartment	Definition of Z ($\text{mol m}^{-3} \text{ Pa}$)	Definition of Terms
Air	$Z_A = 1/RT$	$R = 8.314 \text{ Pa m}^3/\text{mol K}$ $T = \text{Temp (}^\circ\text{K)}$ $K_{AW} = \text{air/water partition coefficient}$
Water	$Z_W = 1/H \text{ or } C^S/P^S$	$H = \text{Henry's law constant (Pa m}^3/\text{mol)}$ $C^S = \text{aqueous solubility (mol/m)}$ $P^S = \text{vapour pressure (Pa)}$
Soil sorbent	$Z_S = K_{sw} P_s/H$	$K_{sw} = \text{soil/water partition coefficient}$ $P_s = \text{phase density (Kg/L)}$
Biota	$Z_B = P_S K_B/H$	$K_B = \text{Bioconcentration factor}$
Pure solute	$Z_P = 1/P^S V$	$V = \text{solute molar volume (m}^3/\text{mol)}$
Octanol	$Z_{OW} = K_{OW}/H$	$K_{OW} = \text{octanol/water partition coefficient}$

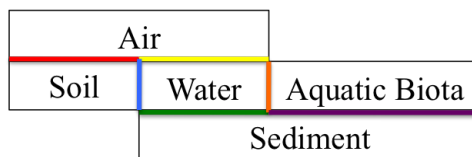


Figure 2.5: Interactions between five environmental compartments, where each coloured line represents a different partition coefficient.

Environmental modelling is based on the simple mass balance principle, that mass can neither be created or destroyed. Fugacity models, and all other chemical environmental fate models, simplify the mathematical equations that are able to account for the reactivity and physical transport of chemicals through the environment (Schnoor, 1996). Schnoor (1996) lists four key elements in a mass balance equation:

1. A clearly defined control volume.
2. A knowledge of inputs and outputs that cross the boundary of the control volume.
3. A knowledge of the transport characteristics within the control volume and across its boundaries.
4. A knowledge of the reaction kinetics within the control volume.

Calculating mass balance is an accounting exercise that takes into account mass inputs, outputs, reactions, and accumulation. Mass balance can be described by the following equation, where mass inputs and mass outflows thus equal transport:

$$\text{Accumulation within control volume} = \text{mass inputs} - \text{mass outputs} \pm \text{reactions} \quad (2.7)$$

Only a few criteria are required in order to run such a simple model: field data on chemical concentrations and mass discharge inputs; rate constants and equilibrium coefficients for the mathematical model; and some performance criteria with which to judge the model (Schnoor, 1996).

Due to the high complexity of predicting environmental variables, i.e. wind speed and temperature, fugacity models have limited usefulness as predictive models. They are rather considered

evaluative models which describe the distribution of pollutants under defined conditions. When the distribution of pollutants between adjoining environmental compartments reaches equilibrium, the fugacity is the same in each compartment, as shown in Equations 2.8 and 2.9 (Walker et al., 1996).

$$f = \frac{C}{Z} \quad (2.8)$$

Where:

f = fugacity

C = concentration of chemical in compartment

Z = fugacity capacity

Therefore in a two-compartment system, $f_1 = f_2$, and:

$$\frac{C_1}{Z_1} = \frac{C_2}{Z_2} = k_{1,2} \quad (2.9)$$

Where:

$k_{1,2}$ = the partition coefficient between compartment one and compartment two.

It is assumed that each compartment is homogeneous and at equilibrium. Although these assumptions are generally invalid in real life due to inflows and outflows, they tend to remain valid for very persistent chemicals that are of greatest environmental concern (Mackay, 1979). Under these assumptions, thermodynamics can be used to describe the partitioning behaviour. While the environmental properties will change, the chemical properties will remain constant. Rather than research chemical behaviour through field observations, it is possible to calculate their behaviour using a generic, evaluative model environment. In subsequent stages, a site-specific model could be simulated by inputting region-specific characteristics.

There are four levels of fugacity models that range in complexity. The Level III model is the most commonly used and recommended model. A Level III fugacity model requires physical chemical property data (i.e. molecular weight, melting point, vapour pressure, solubility, K_{OW}), degrading reaction half lives, and information on the media of discharge. With this information, the Level III model uses transport velocity parameters to develop equations for intermedia

transport. Such equations provide insight into the chemical fate of discharges into the four main compartments (air, soil, water, and sediment, omitting aquatic biota from Figure 2.5). Only those four compartments are considered in order to simplify the calculations. Additionally, the air compartment includes aerosols; the water compartment includes suspended particles and fish; the soil compartment includes solids, air, and water; and the sediment compartment includes solids and pore water. Each compartment in the four phase model is considered a “bulk phase” rather than a “pure phase”. Furthermore, the Level III model assumes that direct discharges into the sediment compartment do not occur (Mackay et al., 1992). A final assumption of the Level III model is steady-state conditions, but not equilibrium. According to Mackay (2001), steady-state implies consistency with time, while equilibrium implies that once equilibrium is reached, concentrations have no tendency for net transfer.

Most chemicals do not behave in the same manner under all circumstances. Often their behaviour will depend on how they entered the environment. For example, were they discharged into the air, soil, or water? Discharges into different compartments results in different concentrations, and thus a chemical’s harmfulness to organisms in each compartment will vary. Level III fugacity calculations allow a maximum amount of predictive data to be elucidated without the need for extensive chemical specific data (Mackay et al., 1992).

Over the past several decades, Mackay has developed extensive computer-based fugacity models. His work forms the basis of the fugacity model in the computer modelling programme EPI Suite™, (USEPA, 2012b) which is produced by the United States Environmental Protection Agency (US EPA).

2.5.3 EPI Suite™

EPI (Estimation Program Interface) Suite™ is a computer-based environmental modelling programme developed by the US EPA and Syracuse Research Corporation and is maintained and distributed by the US EPA. EPI Suite™, which is freely available over the Internet, is capable of estimating a wide range of properties that influence the fate and behaviour of a chemical discharged into the environment. EPI Suite™ as a whole is comprised of 17 individual programmes

which calculates physical and chemical properties, together with the estimation of environmental fate. Those programmes include, but are not limited to (USEPA, 2012b):

KOWWINTM Estimates the log octanol-water partition coefficient, $\log K_{OW}$.

$$\log K_{OW} = \sum (f_i n_i) + \sum (c_j n_j) + 0.229 \quad (2.10)$$

Where:

f_i = coefficient for each atom/fragment

n_i = the number of times the atom/fragment occurs in the structure

c_j = coefficient for each correction factor

n_j = the number of times the correction factor occurs in the molecule

AOPWINTM Estimates the gas-phase reaction rate for the reaction between the most prevalent atmospheric oxidant, hydroxyl radicals, and a chemical.

$$t_{1/2} = 0.693/k_{OH}[OH] \quad (2.11)$$

Where:

$t_{1/2}$ = half-life in the troposphere

k_{OH} = hydroxyl radical rate constant ($\text{cm}^3/\text{molecule}\cdot\text{sec}$)

$[OH]$ = hydroxyl radical concentration in units of molecules (or radicals) per cm^3

HENRYWINTM Calculates the Henry's Law constant (air/water partition coefficient).

MPBPWINTM Estimates melting point, boiling point, and vapour pressure.

$$Tb = 198.2 + \sum (n_i \times g_i) \quad (2.12)$$

Where:

Tb = boiling point ($^{\circ}\text{K}$)

g_i = a group increment value

n_i = number of times the group occurs in the compound

$$Tm = 0.5839 \times Tb \quad (2.13)$$

Where:

Tm = melting point ($^{\circ}\text{K}$)

BIOWIN™ Estimates aerobic and anaerobic biodegradability of organic chemicals.

BioHCWin: Estimates biodegradation half-life values for hydrocarbons.

KOCWIN™ Estimates the organic carbon-normalised sorption coefficient for soil and sediment,

K_{OC}

$$K_{OC} = \frac{(\mu\text{g adsorbed/g organic carbon})}{(\mu\text{g/mL solution})} \quad (2.14)$$

$$\log K_{OC} = 0.5213MCI + 0.60 \quad (2.15)$$

Where:

MCI = Molecular Connectivity Index

WATERNT™ Estimates water solubility.

$$\log WatSol (moles/L) = \sum (f_i + n_i) + \sum (c_j + n_j) + 0.24922 \quad (2.16)$$

Where:

f_i = coefficient for each atom/fragment

n_i = number of times the atom/fragment occurs in the structure

c_j = coefficient for each correction factor

n_j = number of times the correction factor is applied in the molecule

BCFWIN™ Estimates fish bioconcentration factor (BCF).

$$\log BCF = 0.6598 \times \log K_{OW} - 0.333 + \sum \text{correction factors} \quad (2.17)$$

WVOLWIN™ Estimates the rate of volatilisation of a chemical from rivers and lakes.

STPWIN™ Predicts the removal of a chemical in a typical activated sludge-based sewage treatment plant.

LEV3EPI™ Level III fugacity model that predicts the partition of chemicals into air, soil, sediment, and water.

Several of the programmes within the EPI Suite™ package calculate values based on the other programmes. EPI Suite™ also contains a large database of organic chemicals, and experimentally elucidated physical properties may be entered if known. An advantage of using the EPI Suite™ model is the ability to create a site-specific environmental model by easily changing multiple variables. This feature allows the user to enter specific data relating to a sampling location as well as chemical and physical properties of the compounds of interest. For example, it is possible to specify air and water flows, water depth, and wind velocity. In the fugacity model programme, it is possible to alter the amount of chemical being discharged into each compartment, as well as K_{OC} values.

Keenan et al., 2008 and Bangkedphol et al., 2009 used EPI Suite™ as a comparative tool against laboratory experimentation. Both papers experimentally determined the K_{OC} and K_{OW} values of oestrogens (Keenan et al., 2008) and tributyltin (Bangkedphol et al., 2009), and subsequently used those values in the EPI Suite™ model to estimate fate, persistence, and toxicity. By comparing the default model with models input with experimentally determined parameters, they discovered that the EPI Suite™ model has a tendency to underestimate the K_{OC} values. Thus the default model predicts that a higher concentration of the pollutants will be found in the aqueous phase than the solids compartments. However, the experimentally determined K_{OC} values indicate this would not be the case, and more care should be taken in the handling of contaminated solids. Both papers conclude that while EPI Suite™ is a good tool, it should not be substituted for laboratory experimentation.

EPI Suite™ can be used for estimating the environmental fate of organic chemicals when limited experimental data is available. In the literature, most researchers use EPI Suite™ solely for the estimation of physical chemical properties, such as Henry's Law constant and K_{OW} . Its purpose as an environmental estimation programme appears to be greatly overlooked. This project will incorporate laboratory experimentation with EPI Suite™ modelling in order to estimate as accurately as possible the environmental fate of waste from clandestine MA laboratories.

Chapter 3

Chemical Profiling of Methylamphetamine Waste

3.1 Introduction

There are many different pathways used to synthesise MA, and methods are readily available on the Internet, in publicly accessible journal articles, and in published books (ACMD, 2005). MA synthesis is relatively simple and requires an assortment of household chemicals. As such, it is no surprise that over 90% of those arrested for clandestine MA manufacture are not trained chemists (Hargreaves, 2000). Ultimately, the synthetic route chosen by the clandestine manufacturer is selected according to the availability of precursor materials and the skill level of the producer (White, 2004).

The illicit manufacture of MA produces five times more waste than final product. The illegal disposal of MA waste can have a negative impact on the environment which has not yet been assessed. As such, illicit drug manufacturers are often not prosecuted for crimes relating to polluting the environment due to the costs associated with prosecution and lack of research to support successful prosecution.

Before a suspected clandestine dumpsite can be investigated, it is important to determine the chemical composition of the waste in order to identify potential markers of a MA dumpsite. As of yet, no research has been published regarding the composition and chemical profile of MA waste. The bulk of the waste is comprised mostly of large volumes of solvents and acids, however it is the marker compounds present in small quantities that would indicate a clandestine dumpsite. Solvents and acids have many legitimate uses in industry, and their discovery in the environment may indicate an illegal dumping of chemical waste. However, the presence of solvents and acids alone would not be indicative of an illicit MA dumpsite. In order to identify an illicit MA waste dumpsite, it is necessary to identify what chemicals are in the waste.

In this chapter, MA was synthesised following three different methods and the waste collected for further analysis. Through the chemical profiling of MA waste, it is anticipated that several key impurities will be identified that can be used as markers of a MA dumpsite.

3.2 Methodology

3.2.1 Synthesis of Methylamphetamine Waste

MA was synthesised using three different routes and two different precursors, and the waste collected. All reagents were purchased from Sigma Aldrich (UK) and all solvents from Fisher Scientific (UK), except where noted.

3.2.1.1 Leuckart Route

MA was synthesised five times using P2P as a precursor following the Leuckart route. The synthesis was accomplished following the method of Kunalan et al. (2009).

In a round bottom flask set up for reflux, 5.4 mL of P2P and 13.4 mL of *N*-methylformamide were added. Boiling chips were added to reduce the veracity of the reaction and prevent splatter. The flask was placed over a heating mantle, with the gap between the flask and heating mantle insulated using aluminium foil. The temperature was increased slowly to 165-170°C and allowed to reflux for 24-36 hours. The reaction mixture was cooled to room temperature, at which point

24 mL of 10 M sodium hydroxide was added. The mixture was refluxed for a further two hours and cooled to room temperature. Two layers were apparent: a red organic layer containing MA base oil, and a yellow, clear aqueous layer. Using a separatory funnel, the two layers were separated and the aqueous layer collected as waste for further analysis. The waste, 15 mL to 20 mL, was stored in glass Schott bottles in the dark at 4°C.

In order to produce MA·HCl, several additional steps would be required. However, as the compound of interest was the waste, the reaction was halted at this stage. Figure 3.1 on the next page illustrates the complete Leuckart reaction, the steps where waste is produced, the step where waste was collected, and the point where the reaction was stopped. An organic waste is generated from the precipitation of the final MA·Cl salt, however only the aqueous waste was collected from the Leuckart route because the reaction was not continued to the final precipitation stage. The collected aqueous waste has a basic pH, while the salt precipitation waste has an acidic pH. The collection of a basic aqueous waste from the Leuckart route provides a wider range of matrixes for analysis because the other wastes collected from the Moscow and Hypophosphorous routes are acidic organics.

Leuckart synthesis was carried out a total of five times, yielding five separate batches of aqueous waste.

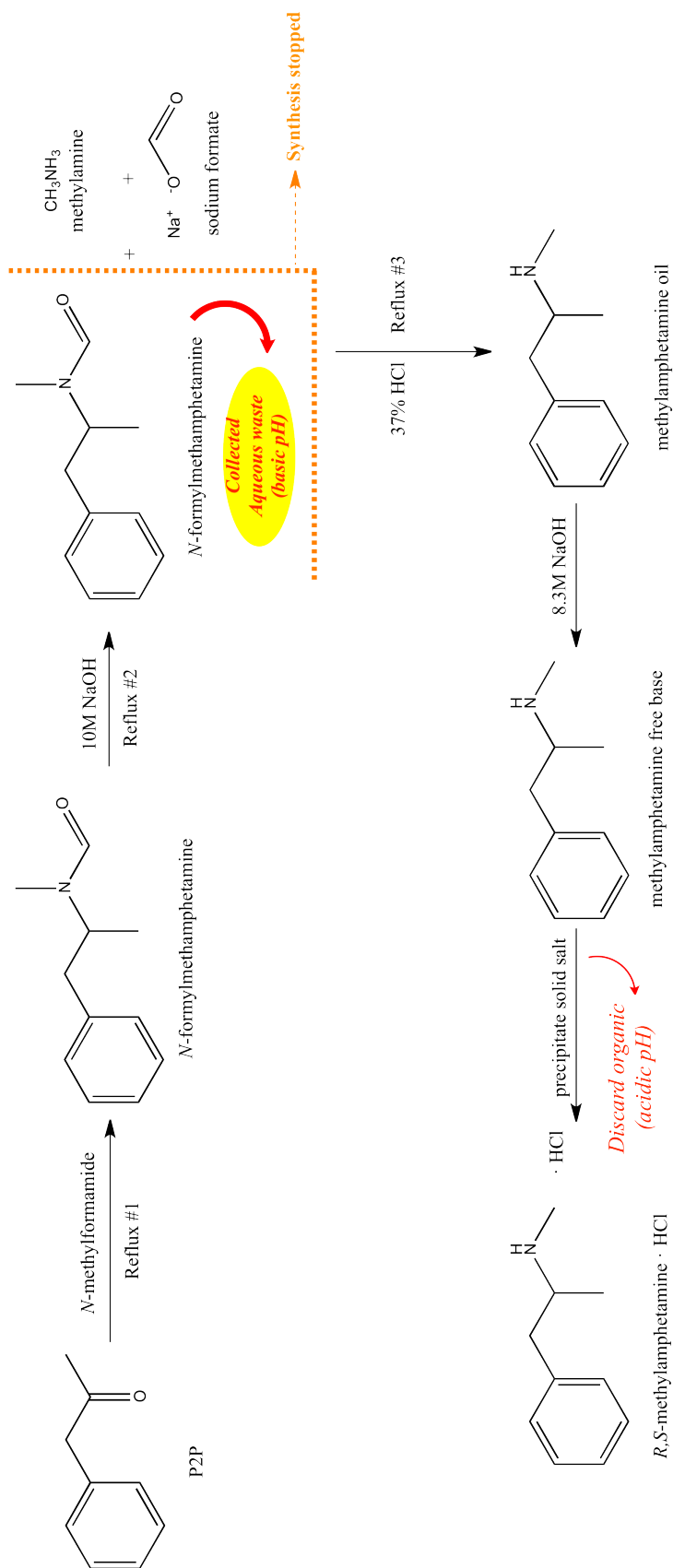


Figure 3.1: MA synthesis using the Leuckart route (aqueous waste collected).

3.2.1.2 Moscow Route

MA was synthesised three times using pseudoephedrine (PSE) as a precursor following the Moscow route. The synthesis for this route was carried by Dr. Saravana Jayaram in the Centre for Forensic Science, University of Strathclyde as part of his PhD research (Jayaram, 2012). Jayaram used synthetic methods following Uncle Fester (2005) to produce MA using clandestine methods and materials as closely as possible. The PSE Jayaram used was extracted from cold medicine tablets (also following Uncle Fester, 2005), rather than commercial grade pseudoephedrine. Jayaram's research was focused on the final MA product, with no interest in the waste. Therefore waste was collected from his syntheses for this study. Figure 3.2 on the following page illustrates the Moscow reaction, and the step where waste is produced and was collected. This is a much simpler process than the Leuckart method and produces less waste. The only waste produced is during the precipitation step.

A total of four batches of Moscow waste were received. Two waste samples represented a mixture of toluene-based waste collected from multiple MA syntheses (approximately two litres each). The other two waste samples received represented one MA batch each (approximately 50 mL each). Samples were stored in glass Schott bottles in the dark at 4°C.

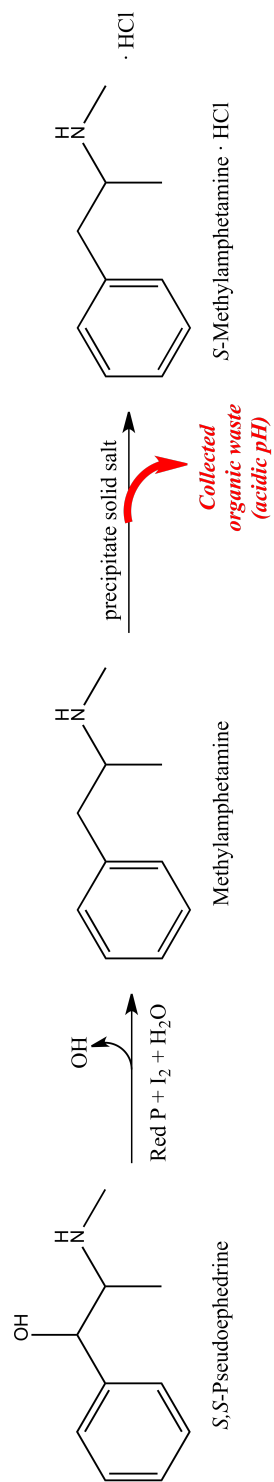


Figure 3.2: MA synthesis using the Moscow route (organic waste collected).

3.2.1.3 Hypophosphorous Route

The second PSE-based route that was used to synthesise MA was the Hypophosphorous route. The synthesis for this route was also carried out by Dr. Saravana Jayaram, following Uncle Fester (2005) and using PSE extracted from cold medicine tablets. Figure 3.3 on the next page illustrates the Hypophosphorous reaction, and the step where waste is produced and was collected. As with the Moscow route, this is a one-step reaction that is a much simpler reaction than the Leuckart method and produces less waste. The only waste produced is during the precipitation step.

One sample of MA waste from the hypophosphorous route was received (approximately 500 mL), representing one batch of MA. This was a toluene-based waste from the precipitation step. The sample was stored in a glass Schott bottle in the dark at 4°C.

A summary of the waste synthesised for this study is shown in Table 3.1.

Table 3.1: Summary of MA waste synthesised for this study

Route	Type	pH	Quantity	Batches
Leuckart	Aqueous	Basic	15-20 mL	5
Moscow	Organic	Acidic	50 mL	2
Moscow	Organic	Acidic	2000 mL*	1
Hypophorous	Organic	Acidic	500 mL	1
			Total	9

*Mixture of multiple batches

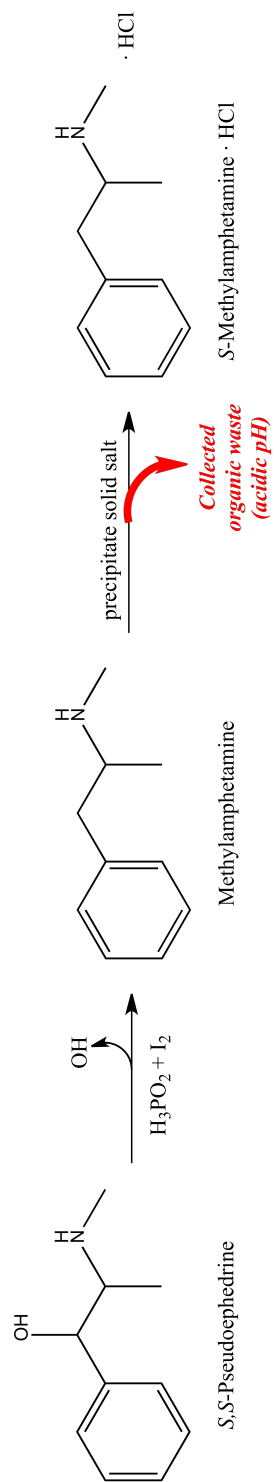


Figure 3.3: MA synthesis using the Hypophosphorous route (organic waste collected).

3.2.2 Extraction of Waste Impurities

In order to extract the waste impurities from the raw waste, three different liquid-liquid extraction (LLE) protocols were trialled following the literature (Andersson et al., 2007b; Kunalan et al., 2009). Three different buffer solutions and two different organic solvents were used as described below. Each type of waste was extracted six times and analysed at minimum in duplicate by GC-MS. One blank sample was created for each buffer. The blank extraction was carried out as described below, however, the addition of 0.5 mL MA waste was omitted.

3.2.2.1 Preliminary Extraction Study

A preliminary study used waste from the Leuckart and Moscow routes to determine the most effective extraction procedure. The most effective extraction procedure was defined as the method which extracted the highest number of impurities from the waste, taking into account any significant chemical markers. Eicosane (C_{20}) was the internal standard, and caffeine was used as a surrogate to measure extraction efficiency. After the preliminary study, it was decided to change internal standards to tetradecane (C_{14}) as its elution time was closer to the analytes. Caffeine was an unsuitable surrogate as its chemical structure varied dramatically from MA and other analytes of interest. Therefore, extraction efficiency was measured using isotopically labelled MA, d5-MA, as described in 3.2.2.5 on the next page.

3.2.2.2 Acetate Buffer

LLE using an acetate buffer, pH 6, was performed following Kunalan et al. (2009).

For 500 mL of pH 8, 0.1 M acetate buffer in deionized water, 4.1 g of sodium acetate was added to the water. The pH was adjusted to 6.0 using glacial acetic acid.

To extract MA waste impurities, 0.5 mL of the waste was added to 2.0 mL of the 0.1 M acetate buffer in a screw-cap test tube. The mixture was sonicated for 5 minutes, followed by 2 minutes of vortex mixing. Ethyl acetate (200 μ L) was added and centrifuged at 4500 RPM for 5 minutes. The organic layer was removed and transferred to 2 mL autosampler vials containing 50 μ L micro-vial inserts. The microvial inserts were first filled with internal standard (10 μ L of 1.0

mg/mL eicosane in ethyl acetate) before being filled by the sample up to the top. The microvial inserts were filled to 50 μ L for all extracts, with a percent relative standard deviation of 3.48% ($n = 10$). Extracts were analysed within 48 hours as per the instrumental parameters detailed in Section 3.2.5 on page 73.

3.2.2.3 Phosphate Buffer

LLE using a phosphate buffer, pH 10.5, was performed following Kunalan et al. (2009).

For 500 mL of pH 7, 0.1 M phosphate buffer in deionized water, 6.8 g of potassium phosphate monobasic ($\text{H}_2\text{KO}_4\text{P}$) and 8.9 g of sodium phosphate dibasic dihydrate ($\text{Na}_2\text{HPO}_4 \cdot 2\text{H}_2\text{O}$) were weighed out. The pH was adjusted to 10.5 using a 10% (w/v) sodium carbonate solution. The extraction method for the phosphate buffer was identical to that of the acetate buffer.

3.2.2.4 Tris Buffer

LLE using a Tris buffer, pH 8.1, was performed following Andersson et al. (2007b).

For 500 mL of 1.0 M Tris(hydroxymethyl)aminomethane (Tris) buffer in deionized water, 60.5 g of Tris was weighed out. The pH was adjusted to 8.1 using 36% HCl.

To extract MA waste impurities, 0.5 mL of the waste was added to 4.0 mL of the 1.0 M Tris buffer in a screw-cap test tube. The test tube was agitated on a horizontal shaker for 10 minutes. 200 μ L of toluene was added, and the test tube shaken for another 10 minutes, followed by centrifugation at 4500 RPM for 5 minutes. The organic layer was removed and transferred to 2 mL autosampler vials containing 50 μ L micro-vial inserts. The microvial inserts were first filled with internal standard (10 μ L of 1.0 mg/mL eicosane in ethyl acetate) before being filled by the sample up to the top. Samples were analysed using GC-MS within 48 hours as per the instrumental parameters detailed in Section 3.2.5.

3.2.2.5 Extraction Efficiency

When the optimal LLE method was determined following the preliminary study, the extraction efficiency was determined by calculating the percent recovery of an isotopically labelled

surrogate. Using six replicates of each of the three MA routes, 25 μL of 1.0 mg/mL d5-MA in methanol (Figure 3.4, Cerilliant, LGC Standards, UK) was added to the test tube prior to extraction of waste impurities.

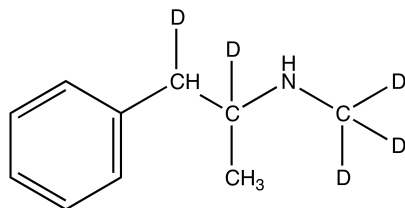


Figure 3.4: Chemical structure of d5-methylamphetamine (MW = 154.20)

3.2.3 Solid Phase Extraction of Water-Diluted Waste

The extraction of MA Leuckart waste from water was trialled using a solid phase extraction (SPE) method developed by Zuccato et al. (2005), and replicated by others (Kasprzyk-Hordern et al., 2007). The SPE cartridges were Oasis MCX reversed-phase cation exchange cartridges (6 mL, 200 mg, Waters UK). Leuckart aqueous waste (1 mL) and 100 μL of 1 mg/mL caffeine (surrogate) were added to 500 mL of Nanopure water (Barnstead Nanopure, ThermoFisher Scientific, UK) and acidified to pH 2 using 36% HCl. The SPE cartridges were conditioned without vacuum using 6 mL of methanol, 3 mL of Nanopure water, and 3 mL of Nanopure water pH 2 (36% HCl). Vacuum was applied to load the sample onto the cartridge and to elute the compounds using 3 mL methanol and 3 mL 2% ammonia in methanol. Extracts were blown down to dryness under nitrogen gas and reconstituted in 1.5 mL methanol with 100 μL of 1.0 mg/mL eicosane in ethyl acetate as internal standard. Samples were analysed using GC-MS within 48 hours as per the instrumental parameters detailed in Section 3.2.5.

A second SPE phase was trialled using Oasis HLB cartridges (6 mL, 200 mg, Waters UK) following the method of Boles and Wells (2010). Leuckart aqueous waste (1 mL) and 50 μL of 1 mg/mL caffeine (surrogate) were added to 500 mL of Nanopure water (Barnstead Nanopure, ThermoFisher Scientific, UK) and acidified to pH 8.5 using 36% HCl. The SPE cartridges were conditioned without vacuum using 5 mL of methanol and 5 mL of Nanopure water. The sample was applied under vacuum, followed by a wash step using 5 mL Nanopure water and dried

under vacuum for 15 minutes. Elution was with 6 mL of methanol. Extracts were blown down to dryness under nitrogen gas and reconstituted with 1.5 mL methanol. Eicosane was added as an internal standard, 50 μL of 1.0 mg/mL in ethyl acetate. Samples were analysed using GC-MS within 48 hours as per the instrumental parameters detailed in Section 3.2.5.

In addition to the Zuccato et al. (2005) and Boles and Wells (2010) methods, SPE using molecular imprinted polymers (MIP) was undertaken using SupelMIP[®] SPE - Amphetamine (3 mL, 25 mg, Sigma-Aldrich UK) cartridges. These cartridges are manufactured for the selective extraction of amphetamine related drugs, such as AMP, MA, and MDMA. This work is the first time this SPE phase has been used to extract, concentrate, and identify MA markers from MA waste.

The experimental method followed the instructions that came with the cartridges. Leuckart aqueous waste (0.5 mL) was added to 250 mL of Nanopure water (Barnstead Nanopure, ThermoFisher Scientific, UK). From the diluted waste, 5 mL was added to 5 mL of 10 mM ammonium acetate buffer, pH 8 (1:1 v/v sample dilution). The pH was to be between 7.5 and 8.5, which did not require further adjustment. The cartridge was conditioned and equilibrated with 1 mL methanol and 1 mL 10 mM ammonium acetate buffer (pH 8). Buffer-diluted sample (1 mL) was loaded onto the cartridge and washed with 2 x 1 mL Nanopure water, followed by 1 mL of 60/40 acetonitrile/Nanopure water. The cartridge was then vacuum-dried for 5-10 minutes, followed by 1 mL of 1% acetic acid in acetonitrile. The compounds were eluted using 2 x 1 mL 1% formic acid in methanol, with a light vacuum between each elution. Extracts were blown down to dryness under nitrogen gas and reconstituted with 1 mL methanol. Tetradecane was added as an internal standard, 50 μL of 1.0 mg/mL in ethyl acetate. Samples were analysed using GC-MS within 48 hours as per the instrumental parameters detailed in Section 3.2.5.

Five additional SPE methods using Oasis HLB and MCX cartridges were also attempted following variations of the Zuccato et al. (2005) and Boles and Wells (2010) methods. Details of each SPE method are shown in Table 3.2 on page 72. SPE 1-4 followed a similar procedure as the Zuccato et al. (2005) method, with changes made to the eluent and reconstitution solvents as detailed in Table 3.2. SPE 5 followed the similar procedure as the Boles and Wells (2010) method, with changes made to the eluent and reconstitution solvents as described in Table 3.2.

For SPE 1-5, 1 mL of Leuckart waste was diluted with 500 mL of Nanopure water. The Leuckart waste was a basic extract, with a pH in the range of 8-10, therefore the acidity was adjusted to the specified pH using 36% HCl. Caffeine was used as a surrogate (100 μ L of 10 mg/mL in ethyl acetate) and tetradecane was added as an internal standard, 50 μ L of 1.0 mg/mL in ethyl acetate. Samples were analysed using GC-MS within 48 hours as per the instrumental parameters detailed in Section 3.2.5. One blank sample was run for each SPE method, whereby the experimental method was followed as described above without the addition of MA waste.

Table 3.2: Summary of SPE methods

Identifier	Cartridge Phase	Sample pH	Condition	Eluent	Reconstitution
Zuccato	Oasis MCX	2	6 mL MeOH	3 mL MeOH	1.5 mL MeOH
			3 mL H ₂ O	3 mL 2% NH ₃ in MeOH	
			3 mL H ₂ O, pH 2		
Boles/Wells	Oasis HLB	8.5	5 mL MeOH	6 mL MeOH	1.5 mL MeOH
			5 mL H ₂ O		
SPE 1	Oasis MCX	2	6 mL MeOH	3 mL EA	1.5 mL EA
			3 mL H ₂ O		
			3 mL H ₂ O, pH 2		
SPE 2	Oasis MCX	2	6 mL MeOH	3 mL 2% NH ₃ in MeOH	1.5 mL EA, 1.5 mL MeOH
			3 mL H ₂ O	3 mL MeOH	
			3 mL H ₂ O, pH 2		
SPE 3	Oasis MCX	2	6 mL MeOH	3 mL EA	1.5 mL EA, 1.5 mL MeOH
			3 mL H ₂ O	3 mL 2% NH ₃ in MeOH	
			3 mL H ₂ O, pH 2		
SPE 4	Oasis MCX	2	6 mL MeOH	6 mL EA	1.5 mL EA
			3 mL H ₂ O		
			3 mL H ₂ O, pH 2		
SPE 5	Oasis HLB	8.5	5 mL EA	2 mL EA	1.5 mL EA
			5 mL acetone	8 mL acetone	
			5 mL H ₂ O		
MIP	MIP	8	1 mL MeOH	2 mL 1% FA in MeOH	1 mL MeOH
			1 mL 10 mM ammonium acetate buffer (pH 8)		

MeOH = methanol
EA = ethyl acetate
FA = formic acid

3.2.4 Extraction of Waste from Sediment

Aliquots of waste from the Leuckart, Moscow, and Hypophosphorous routes were spiked into sediment samples in order to determine if key chemical markers could be extracted. The extraction method used was a variation of the extraction used by Pal et al. (2011) for the extraction of PSE, MA, and MDMA from soil. One sample of each waste type was extracted six times and analysed in duplicate by GC-MS. One soil sample blank was extracted during each batch, whereby the experimental method was followed as described below without the addition of MA waste.

The sediment used was collected from the River Clyde in Glasgow, UK, at a location called Bothwell Bridge. This is a relatively clean point of the river, before it enters the city. The sediment was fully characterised, described in Section 4.2.2 on page 132.

To a glass universal bottle, 1 mL of waste was added to 5 g of oven dried sediment, along with 50 μ L of 1.0 mg/mL of d5-MA in methanol as a surrogate. The mixture was vortexed for approximately 60 seconds to ensure the mixture was evenly distributed throughout the sediment. The extraction solvent mixture was comprised of chloroform:acetonitrile:methanol:acetic acid at a ratio of 80:10:9:1. 10 mL of the solvent mixture was added to the spiked sediment and sonicated for 20 minutes, followed by centrifugation at 4500 RPM for 10 minutes. The supernatant was filtered using nylon filter membranes (Corning, US, 1.0 μ m pore size). This was performed in duplicate and the combined extracts (20 mL) were blown down to dryness under nitrogen gas and reconstituted using 2 mL of methanol. 10 μ L of 1.0 mg/mL tetradecane in ethyl acetate was added as an internal standard. Samples were analysed using GC-MS within 48 hours as per the instrumental parameters detailed in Section 3.2.5.

3.2.5 Instrumental Analysis of Waste Extracts

Instrumental analysis was carried out using gas chromatography-mass spectrometry (GC-MS). Analysis was performed on a Thermo Trace Ultra GC coupled with a DSQII mass spectrometer, fitted with a DB35UI-MS capillary column (30 m x 0.25 mm ID x 0.25 μ m film thickness, J & W Scientific). Initial oven temperature was 50°C, held for 1 minute, increased to 300°C

at 10°C/minute and held for 10 minutes. Helium was the carrier gas at 1 mL/min; inlet temperature 220°C; transfer line 300°C. The injection volume was 1 µL, with a split ratio of 10. Solvent delay on the MS was 3.5 minutes, scanning from 50-400 amu, source temperature at 220°C. Solvent blanks corresponding to the sample matrix were run every two to three samples.

Column phase selection was based on research by the CHAMP project (Andersson et al., 2007a) and Inoue et al. (2003). A column with a larger internal diameter (0.32 mm) was used in the earlier stages of this study, however, the wide interior diameter proved to be problematic reaching sufficiently low vacuum pressure with the mass spectrometer. After the initial LLE method development, subsequent samples were analysed using a column with an interior diameter of 0.25 mm.

3.2.5.1 Mass Spectra Library Matching

The identification of unknown compounds was accomplished primarily using a National Institute of Standards and Technology (NIST) Library search using the MS software. The “Reverse Match” (R. Match) criteria was used to determine the probability of a library match. An R. Match of 999 represents a perfect match, 900 is an excellent match; 800-900, a good match; 700-800, a fair match; and less than 600, a very poor match (NIST, 2008). No names were assigned to unknowns for matches less than 800. Also taken into consideration were other “hits” on the search list, such as the number of compounds on the list with the same name and if isomers or congeners existed on the list. Manual inspection of every match hit was performed, paying attention to key fragmentation patterns and any differences between the unknown and the library match. Knowledge of the compounds of interest, compounds relevant to clandestine MA, was also taken into account when assigning names to unknown compounds.

3.3 Results and Discussion

3.3.1 Preliminary Extraction Study

The preliminary study to determine which buffer extraction method was superior showed few differences between the three buffers examined. Figure 3.5 shows an overlay GC chromatogram of all three liquid-liquid buffer extractions of the Leuckart waste. The phosphate pH 10.5 buffer (Table 3.3) removed more constituents than both the Tris (Table 3.4) and acetate buffer (Table 3.5) extraction methods. Importantly, the phosphate buffer was able to extract the well established Leuckart by-product *N*-formylmethylamphetamine. The CHAMP method (Andersson et al., 2007b) using a Tris buffer was also able to remove this compound, however the Tris buffer only removed two other compounds: MA and phenol.

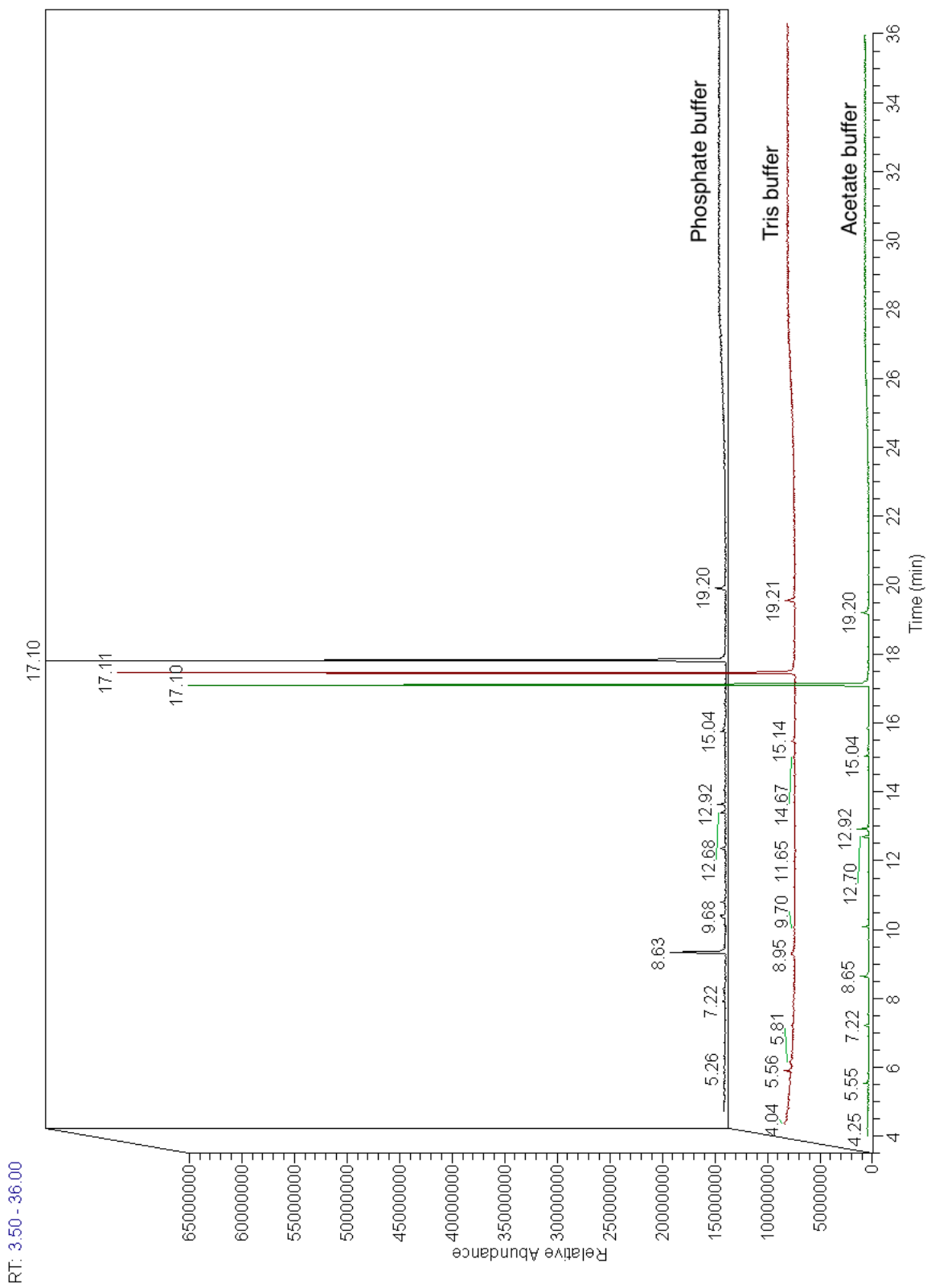


Figure 3.5: Overlay gas chromatogram of three buffer extractions of Leuckart synthesised MA waste

Table 3.3: List of compounds identified in MA Leuckart waste extracted with a pH 10.5 phosphate buffer

No	RT (min)	Compound	Peak m/z	R. Match
1	7.22	Unknown alkane (cyclodecane?)	55, 69, 56, 83	903
2	8.63	Methylamphetamine	58, 91, 56, 65	
3	9.42	Unknown	72, 73, 70, 92	
4	10.09	Unknown long chain alkene or alcohol	55, 70, 97, 83	
5	12.68	Unknown long chain alkene or alcohol	55, 97, 69, 83	
6	12.92	2,6-di-tert-butylphenol	191, 57, 192, 206	883
7	15.04	Unknown long chain alkene or alcohol	55, 57, 83, 70	
8	15.12	N-formylmethylamphetamine	86, 58, 91, 118	942
9	15.86	Benzophenone	105, 77, 182, 51	906
IS	17.10	Eicosane	57, 71, 85, 55, 282	935
SUR	19.20	Caffeine	194, 109, 67, 55	875

Table 3.4: List of compounds identified in MA Leuckart waste extracted with a pH 8.1 Tris buffer

No	RT (min)	Compound	Peak m/z	R. Match
1	5.56	Phenol	94, 66, 65, 55	877
2	8.95	Methylamphetamine	58, 91, 56, 77	730
3	15.14	N-formylmethylamphetamine	86, 58, 91, 118	
IS	17.11	Eicosane	71, 57, 85, 55, 282	944
SUR	19.21	Caffeine	194, 109, 67, 82	875

Table 3.5: List of compounds identified in MA Leuckart waste extracted with a pH 6.0 acetate buffer

No	RT (min)	Compound	Peak m/z	R. Match
1	5.55	Phenol	94, 66, 65, 63	885
2	7.22	Unknown alkane	69, 55, 70, 97	
3	8.65	Methylamphetamine	58, 91, 65, 56	844
4	10.09	Unknown long chain alkene or alcohol	55, 69, 97, 70	
5	12.70	Unknown long chain alkene or alcohol	55, 83, 97, 69	
6	12.92	2,6-di-tert-butylphenol	191, 57, 192, 206	838
7	15.04	Unknown long chain alkene or alcohol	83, 97, 57, 55	
8	15.86	Benzophenone	105, 182, 77, 51	879
IS	17.10	Eicosane	57, 71, 85, 55, 282	952
SUR	19.20	Caffeine	194, 109, 67, 55	873

Comparing the acetate buffer to the phosphate buffer, the acetate buffer was able to extract one compound not found in the phosphate buffer extracts: phenol. Phenol has many uses in industry and its presence in the environment may not necessarily be indicative of a MA dumpsite. However, *N*-formylmethamphetamine is strictly a by-product of MA synthesis, it is not manufactured on a commercial scale and is not used in legitimate industry. Therefore, the presence of *N*-formylmethamphetamine in the environment is much more discriminatory and may indicate a MA dumpsite. Additionally, of the three LLE methods studied, the phosphate buffer removed MA in the largest proportions.

The results from the preliminary extractions of Moscow waste are similar to that of the Leuckart waste. Figure 3.6 is an overlay GC chromatogram of all three buffer extractions of the Moscow waste, with peak identifications found in Table 3.6, Table 3.7, and Table 3.8. There were a lot more unknown peaks in the Moscow waste that could not be identified using the NIST library or a journal search. This could be a result of the different pH of the two wastes. The pH of the Leuckart waste averaged 14, while the average pH of the Moscow waste was three. The pH was not taken after the buffer was added, as a result, the extent of the buffering capacities on the waste is not known. The different buffering capacities of each buffer would have affected the extraction of the analytes and could have caused interferences with the GC column or in the injection port, making identification more difficult.

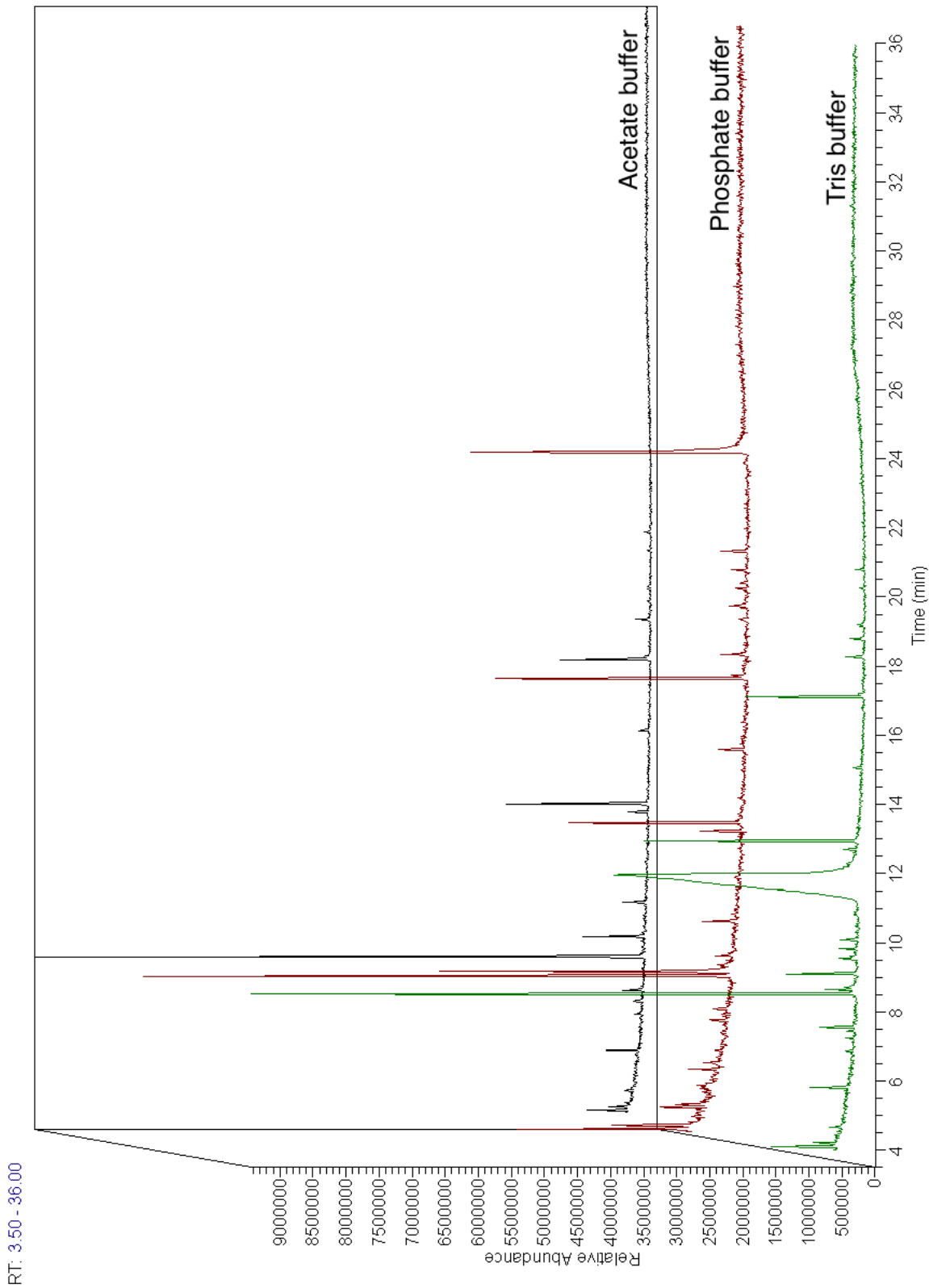


Figure 3.6: Overlay gas chromatogram of three buffer extractions of Moscow synthesised MA waste

Table 3.6: List of compounds identified in MA Moscow waste extracted with a pH 10.5 phosphate buffer

No	RT (min)	Compound	Peak m/z	R. Match
1	4.08	Unknown	56, 55, 83, 98	
2	4.20	Unknown	81, 55, 97, 96	
3	4.73	Unknown	95, 67, 55, 69	
4	4.80	Unknown	95, 91, 195, 68	
5	5.81	Benzaldehyde	77, 51, 105, 106	814
6	6.02	Unknown	99, 92, 81, 53	
7	6.34	Unknown	91, 92, 78, 51	
8	7.24	Unknown	70, 55, 91, 56	
9	7.34	Unknown	92, 91, 70, 90	
10	7.40	Unknown	70, 91, 90, 56	
11	7.57	Unknown	73, 77, 121, 51	
12	8.50	1-Phenyl-2-propanone	91, 65, 92, 63	858
13	8.65	Methylamphetamine	58, 91, 56, 65	856
14	8.83	Unknown	90, 108, 91, 51	
15	9.09	1-Phenyl-1,2-propanedione	77, 105, 51, 63	781
16	10.09	Unknown	55, 70, 69,56	
17	12.70	Long chain alkene or alcohol	55, 97, 69, 57	
18	12.94	2,6-Di-tert-butylphenol	57, 94, 74, 77	680
19	15.06	Long chain alkene or alcohol	55, 69, 92, 57	
IS	17.12	Eicosane	57, 71, 85, 55, 282	874
20	17.20	Unknown	55, 69, 71, 83	
21	17.81	Fatty acid methyl ester	88, 101, 57, 55	
22	19.22	Unknown	67, 55, 109, 82	
23	19.73	Unknown	88, 92, 57, 101	
24	19.87	Unknown	55, 97, 61, 70	
25	20.79	Unknown	108, 91, 101, 51	
26	23.66	Unknown	57, 70, 55, 71	

Table 3.7: List of compounds identified in MA Moscow waste extracted with a pH 8.1 Tris buffer

No	RT (min)	Compound	Peak m/z	R. Match
1	4.10	Unknown	56, 91, 55, 83	
2	4.23	Unknown	55, 81, 91, 97	
3	4.67	Unknown	127, 141, 184, 51	
4	5.81	Benzaldehyde	77, 105, 51, 106	894
5	6.87	Unknown	79, 91, 51, 108	
6	7.24	Unknown	55, 69, 56, 70	
7	7.44	Unknown	88, 75, 89, 91	
8	7.57	Benzaldehyde dimethyl acetal	121, 77, 51, 91	903
9	8.52	1-Phenyl-2-propanone	91, 65, 92, 63	883
10	8.65	Methylamphetamine	58, 56, 65, 91	806
11	8.71	Unknown	91, 70, 83, 100, 54	
12	9.09	1-Phenyl-1,2-propanedione	77, 105, 51, 50	903
13	9.54	Unknown	75, 71, 76, 91	
14	9.83	Unknown	75, 56, 91, 89	
15	10.09	Fatty acid methyl ester	89, 57, 55, 70	
16	11.97	Tromethamine	90, 60, 72, 73	908
17	12.70	Long chain alkene or alcohol	55, 69, 57, 83	
18	12.94	2,6-Di-tert-butylphenol	57, 91, 74, 191	694
19	15.06	Unknown	83, 57, 55, 69	
IS	17.12	Eicosane	57, 71, 85, 55, 282	908
20	18.26	Unknown	57, 55, 59, 128	
21	18.79	Long chain alkene or alcohol	55, 56, 83, 57	
22	19.20	Unknown	67, 55, 109, 82	
23	20.81	Unknown	51, 115, 101, 108	

Table 3.8: List of compounds identified in MA Moscow waste extracted with a pH 6.0 acetate buffer

No	RT (min)	Compound	Peak m/z	R. Match
1	4.06	Unknown	56, 55, 98, 83	
2	4.18	Unknown	81, 96, 55, 67	
3	4.29	Unknown	91, 70, 56, 55	
4	4.63	Unknown iodo compound	127, 184, 91, 141	
5	5.79	Benzaldehyde	77, 51, 105, 106	855
6	6.85	Benzyl alcohol	79, 108, 50, 107	742
7	7.22	Unknown	55, 56, 70, 69	
8	7.55	Benzaldehyde dimethyl acetal	121, 77, 91, 51	854
9	8.50	1-Phenyl-2-propanone	91, 65, 92, 63	870
10	9.09	1-Phenyl-1,2-propanedione	77, 105, 51, 50	863
11	10.09	Unknown	89, 55, 91, 69	
12	12.70	Long chain alkene or alcohol	55, 57, 69, 97	
13	12.92	2,6-Di-tert-butylphenol	57, 91, 191, 74	713
14	15.04	Long chain alkene or alcohol	69, 55, 83, 57	
IS	17.10	Eicosane	57, 71, 85, 55, 282	902

Of the compounds that were identified, each of the three buffer extractions for the Moscow route waste removed many of the same impurities. Those compounds were: benzaldehyde, P2P, and 2,6-di-tert-butylphenol. MA was extracted by the phosphate and Tris buffers, but not by the acetate buffer. The acetate buffer was able to extract two impurities neither of the other two buffers extracted: an iodo-containing compound and benzyl alcohol. The presence of an iodo-containing compound is very interesting as iodine is used in the Moscow route. In the toluene extract from the Tris buffer, Tris (Tris(hydroxymethyl)aminomethane) Figure 3.7, was detected in the GC-MS chromatogram, showing a broad, fronting peak due to its high polarity.

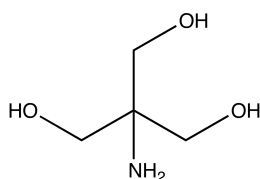


Figure 3.7: Chemical structure of Tris

The ability of the phosphate buffer to extract both MA and P2P, without matrix interferences, was the determining factor in the decision to proceed with using the phosphate buffer for waste LLEs. It is also desirable to be able to use the same method for different types of waste, given that investigators might not know which route was used to produce the waste. The superior performance of the phosphate buffer with the Leuckart waste, combined with average results from the Moscow waste, resulted in the selection of using only the phosphate pH 10.5 buffer LLE method.

3.3.2 Extraction Efficiency

The extraction efficiency of MA was tested using an isotopically labelled surrogate, d5-MA. The percent yields of d5-MA after extraction ranged from 13% to 18% (calculations shown in Appendix A, Table A.1 on page 263). Although the percent yields were quite low, the RSDs were acceptable, from 1.16% to 4.3%. Due to the cost and limited volume of d5-MA, MA was used to quantify d5-MA; known as a semi-quantification where it is assumed the response of the compound of interest is comparable to the compound used. The limit of detection (LOD) of MA was 8 $\mu\text{g}/\text{mL}$ (calculations shown in Appendix A, Table A.2 on page 264).

The CHAMP method (Andersson et al., 2007b) was designed for the profiling of AMP and has been successfully applied to the profiling of MA (Dujourdy et al., 2008). With drug profiling, the analytes of interest are the compounds present in small quantities, compounds which are not necessarily the parent drug. When profiling drug samples, if too much of the parent drug is extracted it would overload the instrumental analysis. Therefore, MA is not the target compound of the extraction method, resulting in low extraction efficiency. A more accurate measurement of the extraction efficiency of impurities would be to use an isotopically labelled impurity. However, many of those compounds are difficult in themselves to obtain; isotopically labelled versions would be extremely rare and prohibitively expensive for this project.

This study marks the first occasion a deuterated surrogate was used to determine the extraction efficiency of the an ATS profiling method. The most important aspect for the CHAMP study was that the extraction protocol be repeatable and reproducible, thus the researchers focused on RSD values rather than extraction efficiencies.

3.3.3 Profiling of Methylamphetamine Waste

A chemical profile of the organic components of MA waste was determined using a phosphate pH 10.5 buffer LLE, followed by instrumental analysis by GC-MS. The compounds were identified using mass spectrometry. Positive identification was accomplished, where possible, using a literature search and a National Institute of Standards and Technology (NIST) library search. Typical total ion chromatograms (TIC) for each route, Leuckart, Moscow, and Hypophosphorous, are shown in Figures 3.8, 3.9, and 3.10, respectively. Corresponding data on the identification of the waste components for the Leuckart, Moscow, and Hypophosphorous synthetic routes is shown in Table 3.9, Table 3.10, and Table 3.11, respectively.

In the Leuckart waste extract, there were many compounds on the gas chromatogram that were unidentifiable. These compounds appear to be large aromatic compounds which elute later in the chromatogram, after 21 minutes. A complete table of the Leuckart peaks, including all unknowns, is shown in Appendix A, Table A.4. Additionally in Appendix A are peak tables for each of the other four Leuckart route waste (Table A.5, Table A.6, Table A.7, and Table A.8) and peak tables for the other two Moscow route waste (Table A.9 and Table A.10).

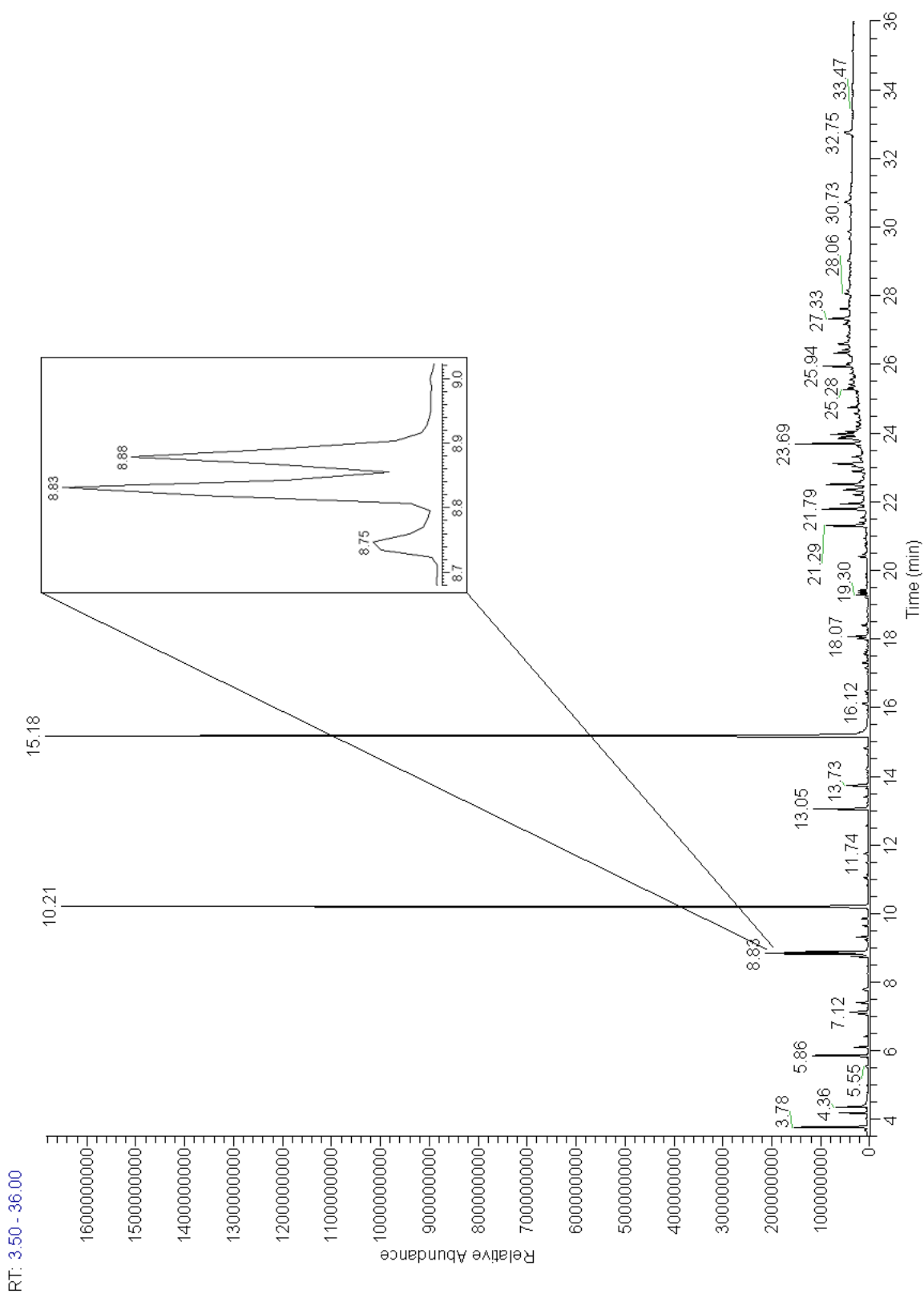


Figure 3.8: GC-MS TIC of MA waste synthesised using the Leuckart route. See Table 3.9 on the next page for peak identification.

Table 3.9: List of compounds identified in the waste extract of MA synthesised from the Leuckart route

Peak No	RT (min)	Compound	Peak m/z	R. Match
1	3.78	<i>p/m</i> -Xylene	91, 106, 105, 77	948
2	4.19	<i>o</i> -Xylene	91, 106, 105, 77	936
3	4.33	Styrene	104, 103, 78, 77	920
4	4.36	Acetamide, <i>N</i> -methyl-	73, 58, 74, 54	909
5	5.01	1-Ethyl-2-methylbenzene	117, 118, 115, 91	874
6	5.86	Phenol	94, 66, 65, 63	955
7	6.11	Benzaldehyde	105, 106, 77, 51	912
8	6.43	Benzene, 2-propenyl	117, 118, 115, 91	949
9	6.63	Benzonitrile	103, 76, 104, 75	913
10	7.07	Benzylidenemethylamine	118, 119, 77, 107	882
11	7.12	Benzyl alcohol	108, 107, 79, 77	922
12	7.41	Phenol, 4-methyl-	107, 108, 77, 79	923
13	7.80	Acetophenone	105, 77, 120, 51	868
14	7.94	Benzoic acid, methyl ester	105, 77, 136, 51	907
15	8.25	Amphetamine	91, 65, 92, 63	920
16	8.47	1-Phenyl-2-propanol	92, 91, 65, 93	894
17	8.75	1-Phenyl-2-propanone	88, 58, 91, 134	
SUR	8.83	d5-Methylamphetamine	62, 92, 63, 66	N/A
18	8.88	Methylamphetamine	58, 91, 56, 65	931
19	9.00	1-Methylbutylbenzene	105, 103, 104, 77	809
20	9.24	Benzaldehyde, oxime	103, 121, 104, 77	907
21	9.32	1-Phenyl-1,2-propanedione	105, 77, 51, 106	886
22	9.64	Dimethylamphetamine	72, 91, 70, 73	875
23	10.14	3-Buten-2-one, 3-phenyl-	103, 146, 77, 104	857
IS	10.21	Tetradecane	71, 57, 85, 70	940
24	10.82	Acetophenone, oxime	135, 77, 104, 103	874
25	11.04	2-Propanone, 1-phenyl-, oxime	149, 91, 116, 65	940
26	11.12	3-Methylbenzyl cyanide	91, 131, 116, 130	740
27	11.48	Pentadecane	71, 57, 85, 70, 212	901
28	12.55	Benzamide	105, 77, 121, 51	892
29	13.04	Benzamide, <i>N</i> -methyl-	105, 77, 134, 135	903
30	13.73	Benzeneacetamide, <i>N</i> -methyl	92, 91, 58, 105	925
31	14.61	<i>N</i> -Formylamphetamine	72, 118, 91, 117, 163	932
32	15.17	<i>N</i> -Formylmethylamphetamine	86, 58, 91, 118, 177	960
33	15.34	<i>N</i> -Acetylmethylamphetamine	68, 58, 100, 91, 191	715
34	17.16	Ethanone, 1,2-diphenyl-	105, 77, 106, 199	918

continued on next page

Peak No	RT (min)	Compound	Peak m/z	R. Match
35	17.61	Benzylamphetamine	148, 91, 149, 65	907
36	21.29	2,6 Di- <i>p</i> -tolylpyridine	259, 258, 260, 115	835
37	21.78	3-Ethyl-2,6-diphenylpyridine	258, 259, 243, 244	874

end

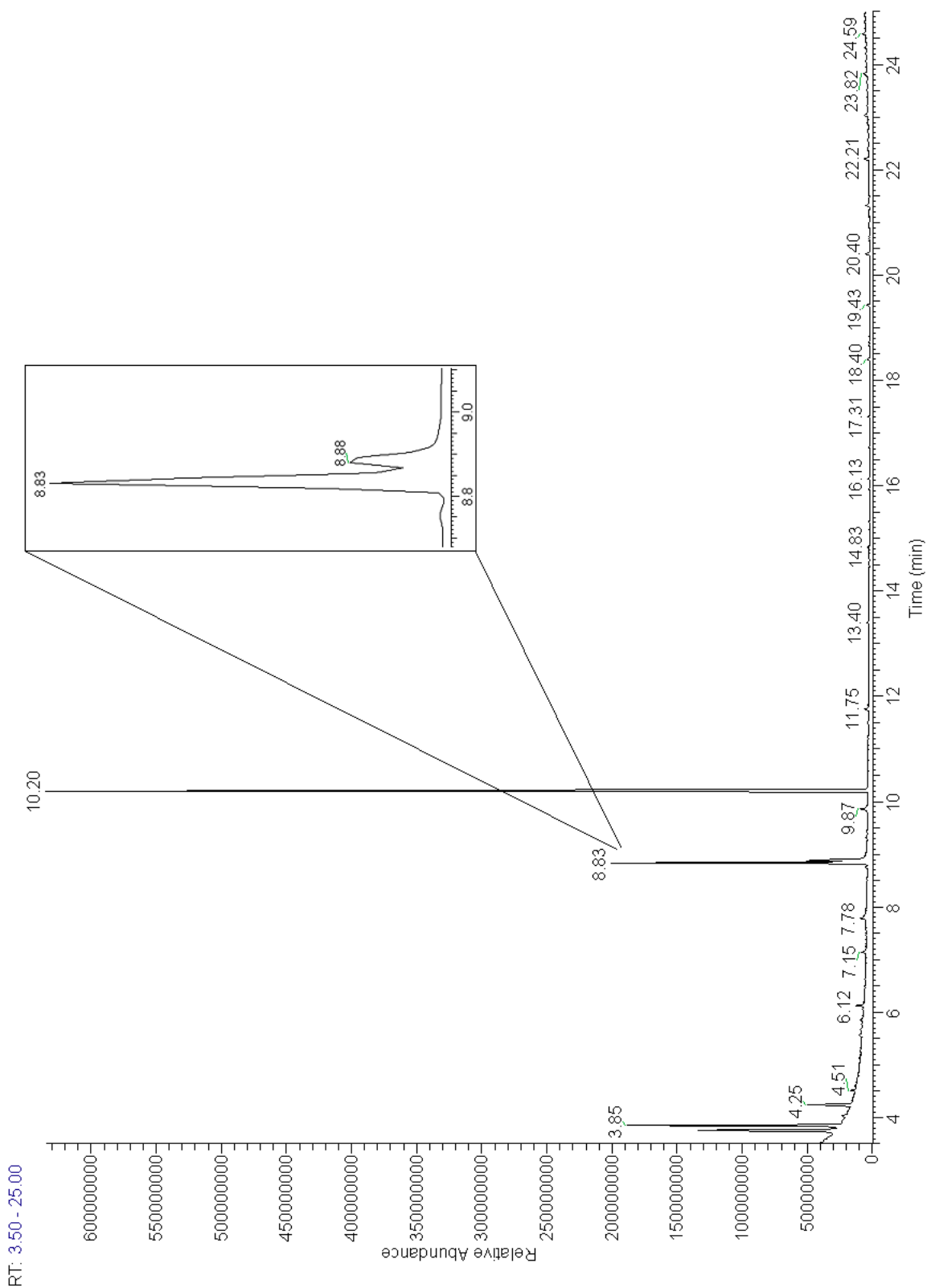


Figure 3.9: GC-MS TIC of MA waste synthesised using the Moscow route. See Table 3.10 on the following page for peak identification.

Table 3.10: List of compounds identified in the waste extract of MA synthesised from the Moscow route

Peak No	RT (min)	Compound	Peak m/z	R. Match
1	3.75	Ethylbenzene	91, 106, 105, 65	940
2	3.85	<i>p/m</i> -Xylene	91, 106, 105, 77	945
3	4.25	<i>o</i> -Xylene	91, 106, 105, 77	937
4	4.51	Unknown	91, 92, 65, 81	
5	5.67	Unknown	105, 71, 120, 57	
6	6.12	Benzaldehyde	105, 106, 77, 51	913
7	7.15	Benzyl Alcohol	108, 107, 79, 77	882
8	8.76	1-Phenyl-2-propanone	91, 134, 92, 65	880
SUR	8.83	d5-Methylamphetamine	62, 92, 63, 59	N/A
9	8.88	Methylamphetamine	58, 91, 56, 65	943
10	9.32	Unknown	105, 77, 91, 92	
IS	10.20	Tetradecane	71, 57, 85, 70, 198	
11	11.50	Pentadecane	71, 57, 85, 70, 212	885
12	15.32	Unknown	104, 62, 91, 61, 207, 66	
13	15.94	Unknown	253, 254, 331, 77	
14	16.74	Unknown long chain alcohol	69, 70, 83, 97	
15	18.67	Unknown	67, 82, 69, 96	
16	18.83	Unknown	149, 150, 223, 205	

end

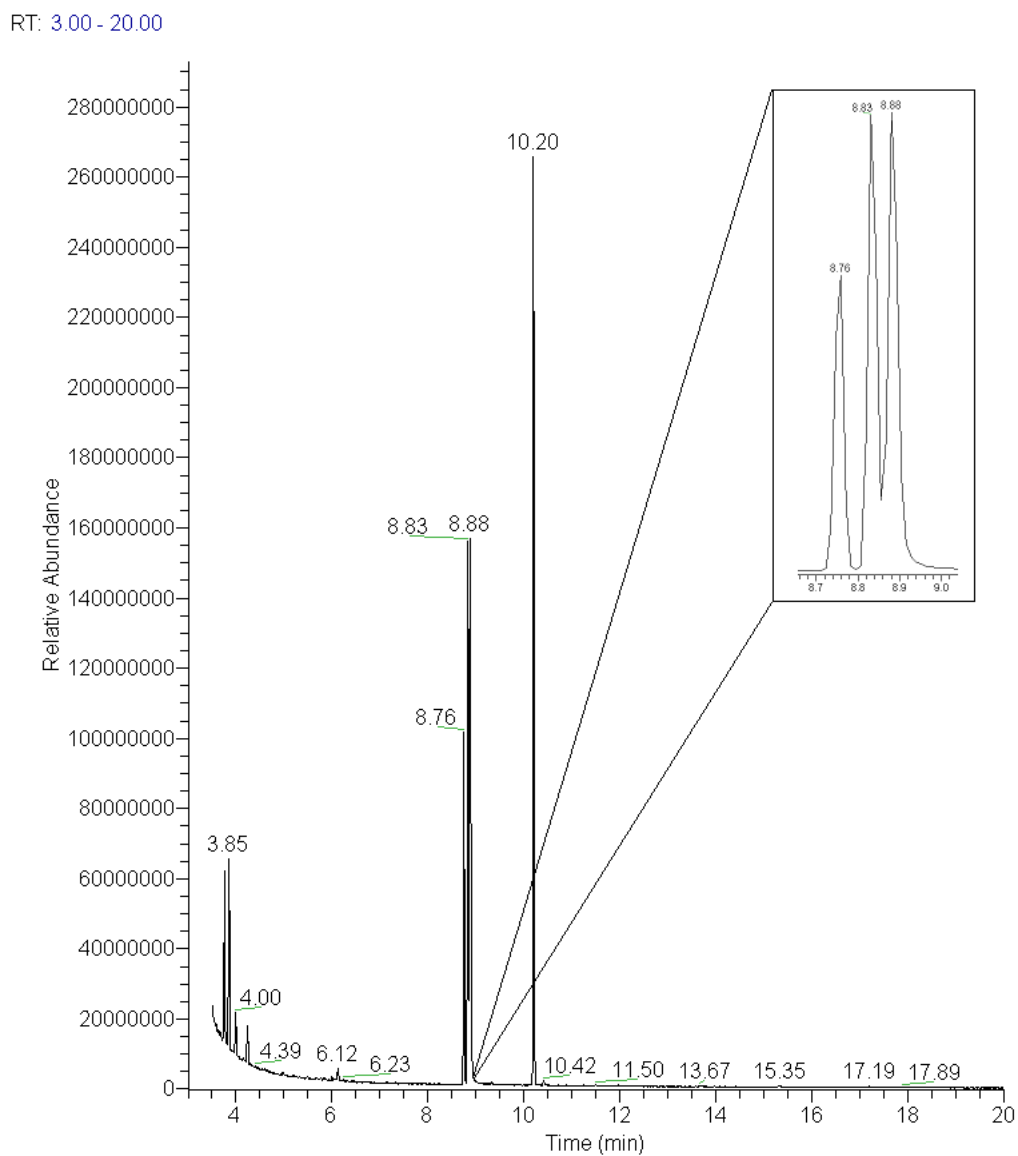


Figure 3.10: GC-MS TIC of MA waste synthesised using the Hypophosphorous route. See Table 3.11 on the next page for peak identification.

Table 3.11: List of compounds identified in the waste extract of MA synthesised from the Hypophosphorous route

Peak No	RT (min)	Compound	Peak m/z	R. Match
1	3.75	Ethylbenzene	91, 106, 105, 65	944
2	3.85	<i>p/m</i> -Xylene	91, 106, 105, 77	949
3	4.00	Cyclopentanone, 2-methyl	98, 69, 55, 70	943
4	4.25	<i>o</i> -Xylene	91, 106, 105, 77	942
5	4.62	Unknown	68, 96, 67, 57	
6	5.23	2-Methyl-2-cyclopentenone	67, 96, 53, 68	911
7	6.00	Cyclohexane, iodo-	83, 55, 67, 69	846
8	6.12	Benzaldehyde	105, 106, 77, 51	877
9	6.41	2-Cyclopenten-1-one, 3-methyl-	96, 67, 53, 81	869
10	7.15	Benzyl alcohol	108, 107, 79, 77	889
11	8.76	1-Phenyl-2-propanone	91, 134, 92, 65	925
SUR	8.83	d5-Methylamphetamine	62, 63, 59, 66	N/A
12	8.88	Methylamphetamine	58, 91, 56, 65	931
13	9.32	Isopropyl phenyl ketone	105, 77, 106, 51	837
IS	10.20	Tetradecane	71, 57, 85, 70, 198	958
14	10.42	Unknown	99, 55, 100, 155	
15	11.49	Pentadecane	71, 57, 85, 70, 212	911
16	13.49	Unknown	107, 150, 149, 178	
17	13.60	Unknown	107, 149, 150, 178	
18	13.67	Unknown	110, 69, 147, 178	
19	13.79	Unknown	177, 162, 192, 161	
20	14.43	Unknown	108, 178, 121, 122	
21	17.19	Unknown aromatic	175, 190, 147, 157	
22	17.47	Unknown aromatic	161, 190, 162, 105	
23	17.88	Unknown aromatic	156, 112, 99, 91	
24	18.67	Unknown	181, 224, 67, 82	
25	18.83	Dibutyl phthalate	149, 150, 205, 223, 104	851

end

3.3.4 Route and Batch Variation

Three different synthetic routes were used to produce a total of nine batches of MA waste for analysis in this study. In comparing the chemicals present or absent in each route and each

batch, it is possible to develop a more comprehensive understanding of the significance of each compound identified. Table 3.12 is a collation of the individual compound tables from each of the nine waste samples and shows the presence or absence of a positively identified chemical for each batch of manufactured MA waste. This provides a comparison of the chemicals identified from each batch across the three different synthetic routes.

Table 3.12: MA waste compounds identified by GC-MS using pH 10 phosphate buffer LLE. The presence of the identified chemical in each batch is indicated by a '✓'. Route abbreviations: L = Leuckart; M = Moscow; Hypo = Hypophosphorous

Compound	L1	L2	L3	L4	L5	M1	M2	M3	Hypo
Ethylbenzene						✓	✓	✓	✓
<i>p/m</i> -Xylene	✓	✓	✓	✓	✓	✓	✓	✓	✓
Cyclopentanone, 2-methyl									✓
<i>o</i> -Xylene	✓	✓				✓	✓		✓
Styrene	✓	✓							
Acetamide, <i>N</i> -methyl-	✓		✓	✓	✓				
4-methoxy-4-methyl-2-pentanone							✓		
1-Ethyl-2-methylbenzene	✓								
Benzene, 1-ethyl-#-methyl-								✓	
Benzene, 1-ethyl-#-methyl-								✓	
2-Methyl-2-cyclopentenone									✓
Benzene, 1-ethyl-#-methyl-								✓	
Benzene, 1-ethyl-#-methyl-								✓	
Phenol	✓	✓	✓	✓	✓				
Cyclohexane, iodo-									✓
Benzaldehyde	✓	✓	✓	✓	✓	✓	✓	✓	✓
Benzene, 2-propenyl	✓	✓		✓	✓				
2-Cyclopenten-1-one, 3-methyl-									✓
Benzyl chloride							✓	✓	
Benzonitrile	✓	✓							
Benzylidenemethylamine	✓		✓	✓	✓				
Benzyl alcohol	✓	✓	✓	✓	✓	✓	✓	✓	✓
Phenol, 4-methyl-	✓	✓		✓	✓				
Acetophenone	✓	✓							
Benzoic acid, methyl ester	✓	✓							
Amphetamine	✓	✓			✓				
1-Phenyl-2-propanol	✓	✓	✓	✓	✓				
1-Phenyl-2-propanone (P2P)	✓	✓				✓	✓	✓	✓

continued on next page

Compound	L1	L2	L3	L4	L5	M1	M2	M3	Hypo
d5-Methylamphetamine	✓					✓			✓
Methylamphetamine (MA)	✓	✓	✓	✓	✓	✓	✓	✓	✓
Benzyl acetate								✓	
1-Methylbutylbenzene	✓	✓							
1-Phenyl-1-propanone		✓					✓		
Benzaldehyde, oxime	✓	✓	✓	✓					
1-Phenyl-1,2-propanedione	✓	✓					✓	✓	
Isopropyl phenyl ketone									✓
Toluene								✓	
Dimethylamphetamine	✓	✓			✓				
3-Buten-2-one, 3-phenyl-	✓	✓							
Tetradecane (Internal Standard)	✓	✓	✓	✓	✓	✓	✓	✓	✓
Acetophenone, oxime	✓	✓							
2-Propanone, 1-phenyl, oxime	✓	✓	✓	✓	✓				
3-Methylbenzyl cyanide	✓	✓							
Pentadecane	✓	✓				✓			✓
Benzamide	✓	✓							
2,6-Di-tert-butylphenol							✓	✓	
Benzamide, <i>N</i> -methyl	✓	✓							
Benzeneacetamide, <i>N</i> -methyl	✓	✓							
<i>N</i> -Formylamphetamine	✓	✓							
<i>N</i> -Formylmethylamphetamine	✓	✓		✓	✓				
<i>N</i> -Acetylmethylamphetamine	✓	✓							
Benzophenone							✓		
Dimethoxynaphthalene								✓	
Phenyl[(1-phenyl-2-propanyl)- -amino]acetonitrile			✓		✓				
Ethanone, 1,2-diphenyl-	✓	✓							
Benzylamphetamine	✓	✓							
Hexadecanoic acid, ethyl ester								✓	
4-Aminophthalimide		✓	✓						
Benzenepropanoic acid, 3,5-bis- -(1,1-dimethylethyl)-4-hydroxy-, -methyl ester							✓		
Dibutyl phthalate								✓	✓
Octadecanoic acid, ethyl ester								✓	
Acetic acid, octadecyl ester								✓	
2,6-Di- <i>p</i> -tolylpyridine	✓	✓							
3-Ethyl-2,6-diphenylpyridine	✓	✓							

end

Several chemicals are present in all synthetic routes studied and in all nine samples. Those four compounds are: *p/m*-xylene; benzaldehyde; benzyl alcohol; and MA. In addition to those four chemicals, three chemicals were detected in all three routes, but not in every batch. Those three chemicals are: *o*-xylene; P2P; and pentadecane. Three chemicals were present in all five of the Leuckart batches, but not in any other routes. Those three chemicals are: phenol; 1-phenyl-2-propanol; and 1-phenyl-2-propanone, oxime. Only two chemicals were present in all three Moscow route batches: ethylbenzene and P2P. However, those two compounds were also present in the single Hypo route sample, therefore they are not definitive indicators of Moscow route waste. The Leuckart and Moscow routes had two chemicals in common that were absent in the Hypo route sample. Those two chemicals are: 1-phenyl-1-propanone and 1-phenyl-1,2-propanedione. Despite the different precursor materials (the Leuckart route uses P2P as a precursor, while both the Moscow and Hypo routes use pseudoephedrine), there is no pattern as to the chemicals in common in the three routes. A summary of the chemicals in common between the three synthetic routes used in this study is presented in Table 3.13.

Table 3.13: Summary of chemicals in common across the three MA synthetic routes studied

Present in all 9 samples	Present in all 3 routes	Leuckart & Moscow only	Moscow & Hypo only
<i>p/m</i> -xylene	<i>p/m</i> -xylene	1-phenyl-1-propanone	ethylbenzene
benzaldehyde	benzaldehyde	1-phenyl-1,2-propanedione	dibutyl phthalate
benzyl alcohol	benzyl alcohol		
MA	MA		
	<i>o</i> -xylene		
	P2P		
	pentadecane		

The Moscow route and Hypo route identified several compounds that were only present in one sample. With the small sample sizes of those two routes ($n=3$, Moscow; $n=1$, Hypo), it is inconclusive as to whether or not those compounds can be used as reliable, definitive markers of route-specific MA waste. The challenge in profiling MA waste is the variability between samples because clandestinely manufactured MA, and subsequently its waste, varies widely from batch to batch. Even the waste considered in this study, manufactured under closely monitored conditions, varied widely. An additional consideration to take into account is the practice of stock-piling waste prior to disposal. This would greatly change the waste profile, especially if more than one synthetic route was used in a single clandestine laboratory.

3.3.5 Chromatographic Theory and Relevance to MA Waste Analysis

In comparing the chromatograms and peak tables from the preliminary study (Tables 3.3 and 3.6) and the regular study (Tables 3.9 and 3.10), it is apparent that there are many more peaks in the regular study. There are two possible reasons for this difference: as the method is repeated, the analyst becomes more proficient at the extraction technique, and secondly extracts were analysed on two different GC columns. In the preliminary study, the column internal diameter (i.d.) was 0.32 mm - not a conventional diameter, considered a mid-bore or wide-bore column. Inoue et al. (2003) used a 0.32 mm i.d. column in their study of profiling seized MA, which found that the wider diameter prevented overloading of the column as there is more stationary phase for the analytes to dissolve in. In this work, the wider column provided adequate results for the initial study, however the wider diameter caused difficulty in obtaining a sufficiently low vacuum pressure on the mass spectrometer. Therefore while moving forward, a column with the conventional 0.25 mm i.d. was chosen.

As the column i.d. is inversely related to the number theoretical plates, by increasing the i.d. Inoue et al. (2003) were in fact decreasing the column's efficiency. By switching from the 0.32 mm i.d. column in the preliminary study to a 0.25 mm i.d. column for the remainder of this study, the resolution power increased, thus another potential cause as to why more peaks were present in the later stages of the study.

GC Column efficiency can be related to plate theory, based on the theory of column distillation (Robinson et al., 2004). While it is a somewhat dated theory, losing favour to kinetic (rate) theory and GC columns have no actual plates, plate theory can still be used to describe the efficiency of GC columns. Each plate is described as a point along the column at which the analytes and stationary phase are at equilibrium. The more plates a column has, the shorter the height equivalent to a theoretical plate, thus the column has greater its efficiency. Plate number and column height are related using Equations 3.1 and 3.2 (Robinson et al., 2004).

$$N = 5.54 \left(\frac{t_r}{w_b} \right)^2 \quad (3.1)$$

$$H = \frac{L}{N} \quad (3.2)$$

Where:

N = number of theoretical plates

t_r = retention time

w_h = peak width at half the peak height

H = height equivalent to a theoretical plate

L = length of column

H is further related to column i.d. via the Van Deemter equation, relating flow rate of the mobile phase, Equation 3.3. The Van Deemter equation describes the flow conditions which will produce the highest resolution. Flow rate of the mobile phase is dependent on column i.d. and temperature. The Van Deemter equation can also be described by the plot in Figure 3.11.

$$H = A + \frac{B}{\mu} + C\mu \quad (3.3)$$

Where:

A = multi-path term

B = longitudinal diffusion term

C = mass transfer term

μ = flow rate

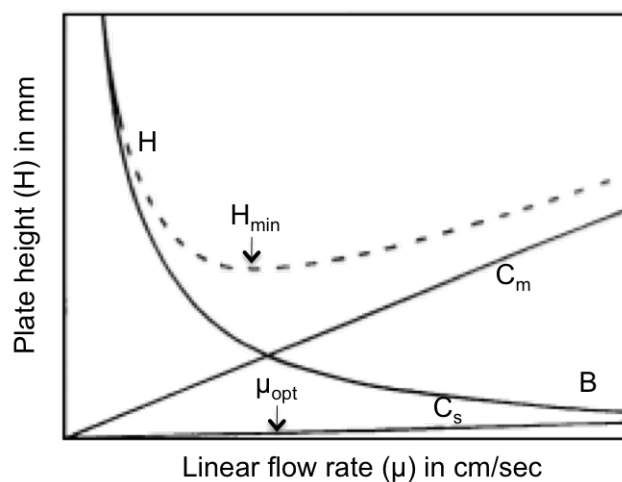


Figure 3.11: Van Deemter plot for open tubular columns as sum of three terms: B and C [as Sum of C_m (mobile phase) and C_s (stationary phase)] with $A = 0$. (From Robinson et al., 2004.)

Chromatographic plate theory explains the discrepancies between the number of peaks between the preliminary and regular study. By switching from a wide bore column (0.32 mm) to a standard 0.25 mm i.d., peak resolution increases, resulting in more peaks being detected. Using Leuckart waste as an example, the number of compounds in Table 3.3 (part of the preliminary study) is nine, compared to 37 in Table 3.9 on page 87 (the regular study), and even more in Table A.4 on page 265, in which every unknown is also accounted for.

There is one additional factor that contributed to the discrepancy in peak numbers. One more difference in the instrumental method between the preliminary study and the remainder of the study was the acquisition delay on the mass spectrometer. Data acquisition on the mass spectrometer is delayed for several minutes in order to allow the solvent peak to pass through without overloading the detector, which may cause damage. In the preliminary study, the solvent delay on the mass spectrometer was four minutes, however frequent column changes shortened the column, resulting in slightly earlier retention times. Therefore, during the remainder of the study, the solvent delay was shortened to 3.5 minutes. This shorter solvent delay revealed the presence of *p/m*-xylene and ethylbenzene, which elute before four minutes and were not observed in the preliminary study.

3.3.6 Route Specific Waste Components

The waste components identified from clandestine MA manufacture contain many aromatic compounds. This is consistent with the structures of both the starting materials and end products. In two of the three synthetic routes examined, there was no precursor material found in the waste. (In the Moscow and Hypophosphorous routes there is no pseudoephedrine present in the waste.) Of the five syntheses carried out following the Leuckart route, only two had any precursor material (P2P) present in the waste. This is an indication of the efficiency of the reaction; in the cases where the precursor was completely consumed, this is an indication that the synthesis went to completion.

Several compounds were present in all three sets of waste. Those compounds were: *o*, *m*, and *p*-xylenes, benzaldehyde, benzyl alcohol, MA, P2P, and pentadecane. The presence of P2P in the waste from the Moscow and Hypo routes was expected, as P2P is a well-known reaction

by-product found in MA synthesised using pseudoephedrine (Skinner, 1990). The mechanism of the reaction, derived by Skinner, is illustrated in Figure 3.12.

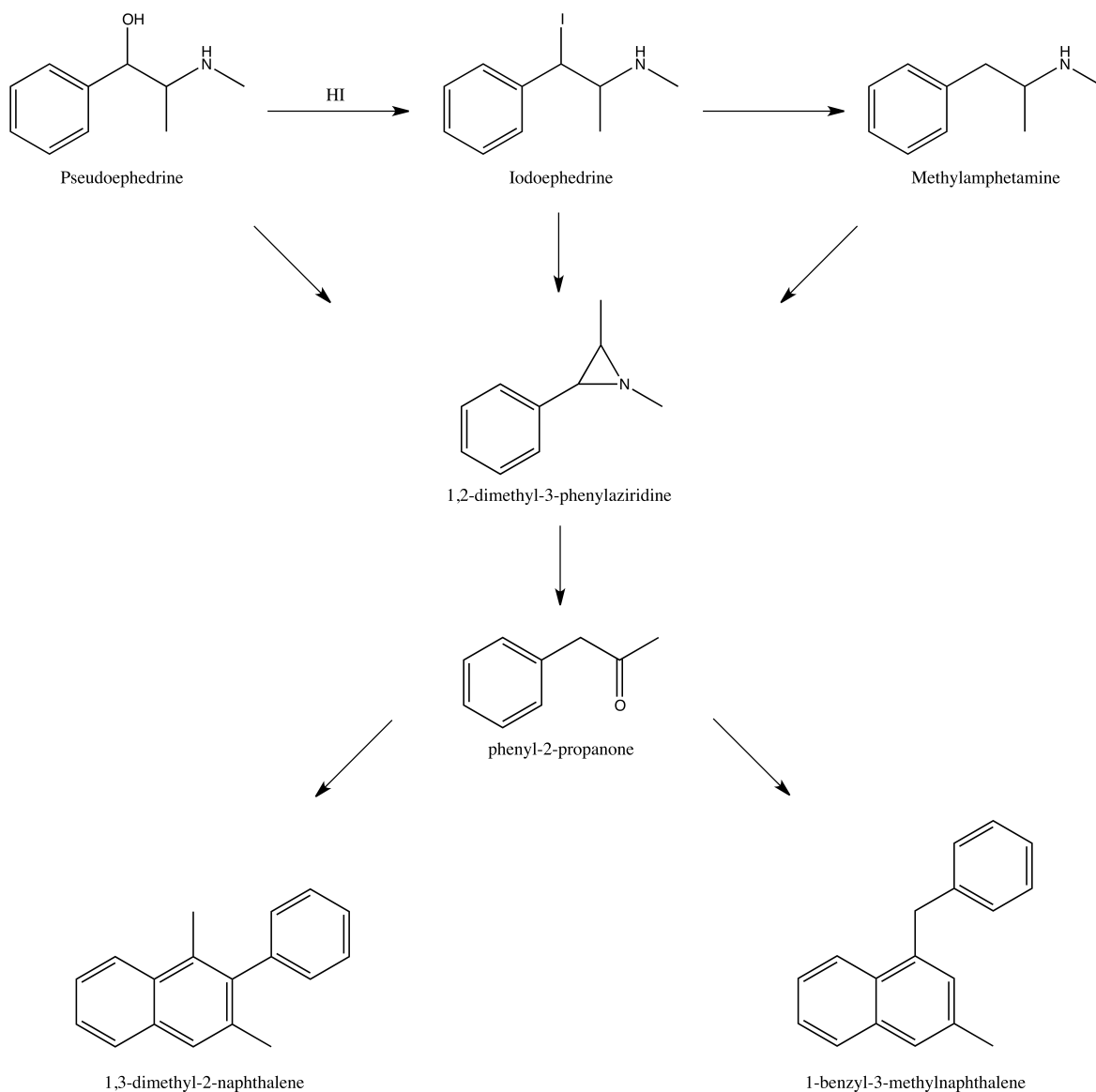


Figure 3.12: Mechanism of the reduction of pseudoephedrine to MA using HI/red P (modified from Skinner, 1990).

Therefore, the presence of P2P in the environment can mean two different things: 1) P2P was used in the clandestine laboratory as a starting material, or 2) P2P was produced as a reaction by-product. Given the difficulty of obtaining P2P on the black market, the disposal of pure P2P seems unlikely unless the clandestine manufacturer was attempting to dispose of evidence. Further research into the ratios of P2P and other waste marker compounds may give an indication as to the origin of P2P at a dumpsite. This would have implications to law enforcement personnel to determine the synthetic route used at a clandestine MA laboratory. Information on synthetic routes is often useful for intelligence purposes and calculations can be performed to determine the manufacturing capacity of a clandestine laboratory.

Of the waste impurities identified, several have been documented by other researchers in relation to clandestine MA. Table 3.14 compares the waste impurities identified in this study with Kunalan's extensive tables of MA impurities. Only four compounds were found to be in common between the two studies: *N*-formylmethylamphetamine, P2P, 1-phenyl-1,2-propanedione, and benzaldehyde. All four of those compounds were identified in several different methods, therefore none can be shown to be route specific. If a suspected MA dumpsite was discovered, those compounds may help to confirm the suspected site as being related to MA manufacture. However, it would not be possible, based on the available data, to determine which route of manufacture was used at the clandestine laboratory.

Table 3.14: MA waste impurities identified in this study compared to MA impurities identified in Kunalan (2010).

Compound	Kates' Routes	Kunalan's Routes
<i>N</i> -formylmethylamphetamine	Leuckart	Leuckart, Reductive amination, Nagai, Rosenmund, Birch, Emde, Moscow
1-phenyl-2-propanone	Leuckart, Moscow, Hypophosphorous	Leuckart, Reductive amination, Nagai, Rosenmund, Birch, Emde, Moscow
1-phenyl-1,2-propanedione	Leuckart, Moscow	Leuckart, Nagai, Birch, Emde, Moscow
Benzaldehyde	Leuckart, Moscow, Hypophosphorous	Rosenmund, Birch, Emde

Several compounds identified in the waste have also been identified by Pal et al. (2011) as metabolites from the biodegradation of P2P in soil. The two compounds in common are 1-

phenyl-2-propanol and 1-phenyl-1,2-propanedione. In the Pal et al. (2011) study, the degradation products began to appear in soil after two days, reaching their maximum concentration after six days, followed by a decrease in concentration until they were no longer detected. At their peak concentrations, the metabolites were only present at 5% of the concentration of P2P. The researchers found that the degradation profiles between P2P and its metabolites was greatly influenced by the soil type, particularly the amount of carbon available. If a carbon source was readily available, P2P would not be degraded as quickly, and vice versa.

While P2P and 1-phenyl-1,2-propanedione have already been identified as MA impurities (Kunanan, 2010), the identification of the P2P metabolite 1-phenyl-2-propanol by Pal et al. (2011) may not necessarily indicate the degradation of P2P. Since 1-phenyl-2-propanol was also identified in waste from the Leuckart route, its detection in the environment could be indicative of a MA dumpsite. The presence of other metabolites identified by Pal et al. (2011) (1-hydroxy-1-phenyl-2-propanone, 1-hydroxy-1-phenyl-2-propanone, and 1-phenylpropylene oxide) should be used in conjunction with the presence of P2P as indications that degradation has taken place, which may aid in dating the dumpsite. Similarly, when using MA waste components as identifiers, a variety of markers should be used, for example *N*-formylmethylamphetamine. *N*-formylmethylamphetamine would be an excellent marker based on its widespread presence across more than one synthetic route, its abundance in the waste, and its limited commercial availability. P2P and MA would also be excellent indicators as they have few legitimate uses. Additionally, as reported by Pal et al. (2011), MA persists for long periods of time in soil which could have two different interpretations. The chances of detecting a waste site would be increased due to the long persistence time. However, due to this long persistence time, determining the age of a site to apportion blame would be quite difficult under current methods. Additionally, the transient nature of clandestine laboratories means that if MA is detected in the environment, the laboratory may no longer be operating.

In Environmental Forensics, when investigating oil spills and other PAH contamination, it is common to use ratios of compounds to aid in dating a site. This is possible because compounds are selected that are commonly present together and whose degradation rates and ratios are known. For example, pristane and phytane, two isoparaffins, are present to the right of C₁₇ and

C₁₈ peaks, respectively, of gas chromatograms of crude oils, middle distillates, and lubricating oils. In fresh samples, C₁₇ and C₁₈ are more abundant than the pristane and phytane peaks. Once released into the environment, bacteria will preferentially biodegrade C₁₇ and C₁₈ over pristane and phytane. Therefore by measuring the ratio of C₁₇/pristane and C₁₈/phytane, an estimation as to the degree of degradation can be calculated (Morrison, 2000).

Using ratios of impurities to estimate the age of a MA dumpsite would be extremely difficult given the illicit nature of the waste. Clandestinely manufactured MA, and subsequently its waste, varies widely from batch to batch. This means that ratios of chemicals in the raw waste or drug vary to such an extent that once they are introduced into the environment it would be next to impossible to say which ratios were caused by degradation and which were due to the manufacture process.

For example, even the waste considered in this study, manufactured under closely monitored conditions, varied widely. Of three samples of toluene-based waste from the Moscow route, P2P was identified in two of the three. Similarly, in five samples of aqueous-based waste from the Leuckart route, P2P was identified in two of the five. Although the presence or absence of individual compounds in the environment is of great value, the presence of those individual compounds as part of a mixture has an even greater value and is more reflective of a real-life example.

Another important consideration regarding clandestine MA waste is the mixing of waste. It is common for clandestine laboratories to combine their wastes before disposal. Therefore, dumpsites may contain waste from one or more manufacturing batch, and from one or more synthetic route. This further variability would compromise any ratio measurements. Furthermore, once the waste is released into the environment, it will become diluted by an unknown factor. Given that most of the impurities are found in small amounts, this dilution factor would increase the difficulty in determining the age of a dumpsite or the route of MA manufacture. The real potential harm from a MA dumpsite would most likely come from the bulk disposal of solvents, such as toluene or acetone, and acids, such as muriatic acid. However, given the volatile nature of most solvents, they may not persist in the environment for a long enough period of time to

be identified as a potential MA waste site. Additionally, solvents alone are not indicative of MA waste as they could have originated from another source of illegal dumping.

One dating method that would warrant further investigation is the use of stable isotopes to measure degradation. Stable isotope analysis works on the principle that certain elements have naturally occurring isotopes with an extra neutron. Carbon exists naturally as 99% ^{12}C with six protons and six neutrons, 1% ^{13}C with six protons and seven neutrons, and the radioactive ^{14}C isotope with six protons and eight neutrons. ^{12}C and ^{13}C are the two most stable Carbon isotopes. The isotopes of hydrogen are ^1H (99.98% abundance) and ^2H , (deuterium, D) which has a natural abundance of 0.02% (Wang and Stout, 2007). The bonds from the heavier isotopes are stronger and once contaminants enter into the environment, the heavier isotopes may preferentially bond during degradation reactions. Thus the heavier isotopes are more resistant to biodegradation. Over time, ^{12}C or ^1H from the contaminant may become substituted by ^{13}C and D, creating an isotopically heavier compound, which is referred to as being enriched. A measurement of the $^{13}\text{C}/^{12}\text{C}$ and/or D/ ^1H ratio may help to date a site of contamination. Stable isotope analysis is best used on small molecules, i.e. smaller than 2-5 ring PAHs (Wang and Stout, 2007), which opens up the possibilities for isotope analysis of MA waste. Given the persistence of MA (as determined by Janusz et al., 2003), MA could be an excellent analyte for isotope analysis to measure natural attenuation and to gauge the age of a dumpsite.

3.3.7 Solid Phase Extraction of Water-Diluted Waste

Solid phase extraction is a sample pre-treatment technique to clean-up “dirty” samples to negate matrix interference effects and concentrate the analytes of interest. SPE uses solid phase sorbents typically made from silica, or chemically-modified silica (Kealey and Haines, 2002).

There are four steps to SPE, summarized below and in Figure 3.13 on the following page:

Condition Flushing the SPE cartridge with sample solvent to wet the sorbent and mimic sample conditions (e.g. pH, solvent composition).

Sample Loading Sample solution is added on top of the cartridge, with the analytes of interest being retained by the sorbent and allowing the matrix to pass through.

Rinsing A solvent is used to remove any compounds not bound to the sorbent.

Elution The analytes are recovered by passing through an appropriate solvent

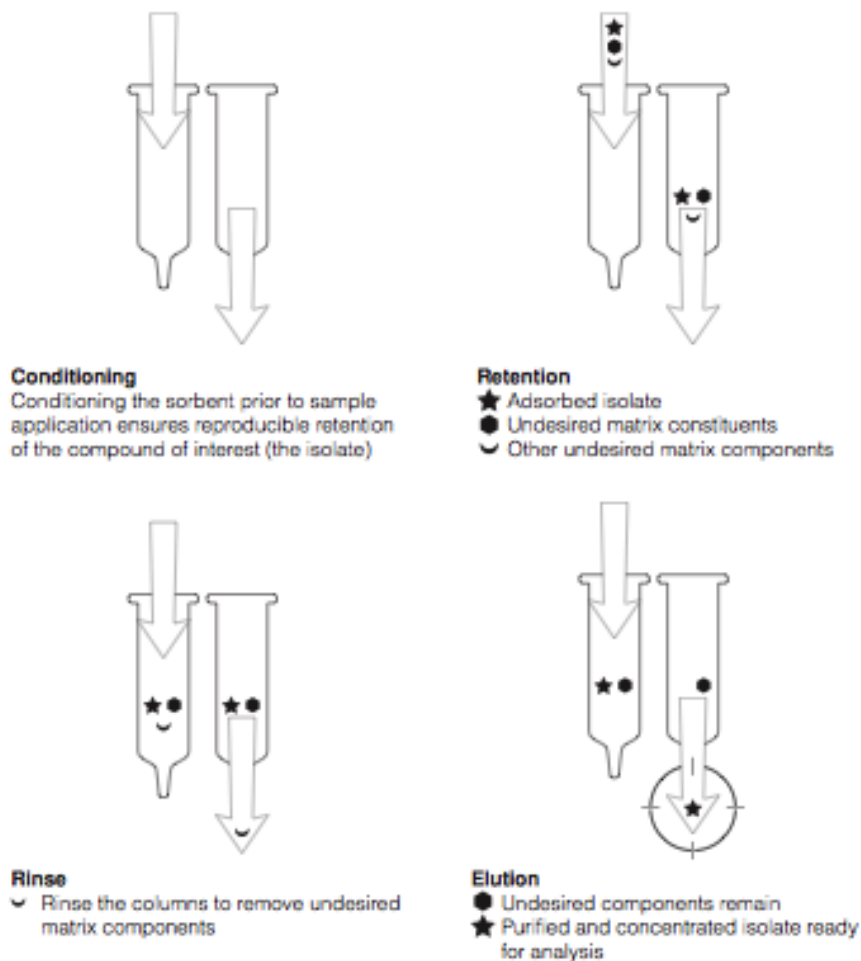


Figure 3.13: Summary schematic of SPE steps (from Kealey and Haines, 2002)

The analytes of interest are separated from the matrix by bonding to the solid phase, typically through van der Waals forces, dipolar interactions, hydrogen bonding, ion-exchange, or size exclusion (steric hindrance effects) (Kealey and Haines, 2002). In this study, two different phases were used: Oasis MCX and Oasis HLB. The MCX cartridges are mixed-mode cation exchange sorbents suitable for compounds with pK_a values from 2-10. The HLB sorbent is a universal reversed phase sorbent suitable for all compounds.

The extraction method used by Zuccato et al.(2005; 2008) to extract a variety of illicit drugs

from surface waters using Oasis MCX cartridges was trialled in this study to extract MA waste from water. A typical gas chromatogram of 1 mL of Leuckart waste diluted in 500 mL of deionized water is shown in Figure 3.14 on the next page, with the corresponding peak identification table in Table 3.15.

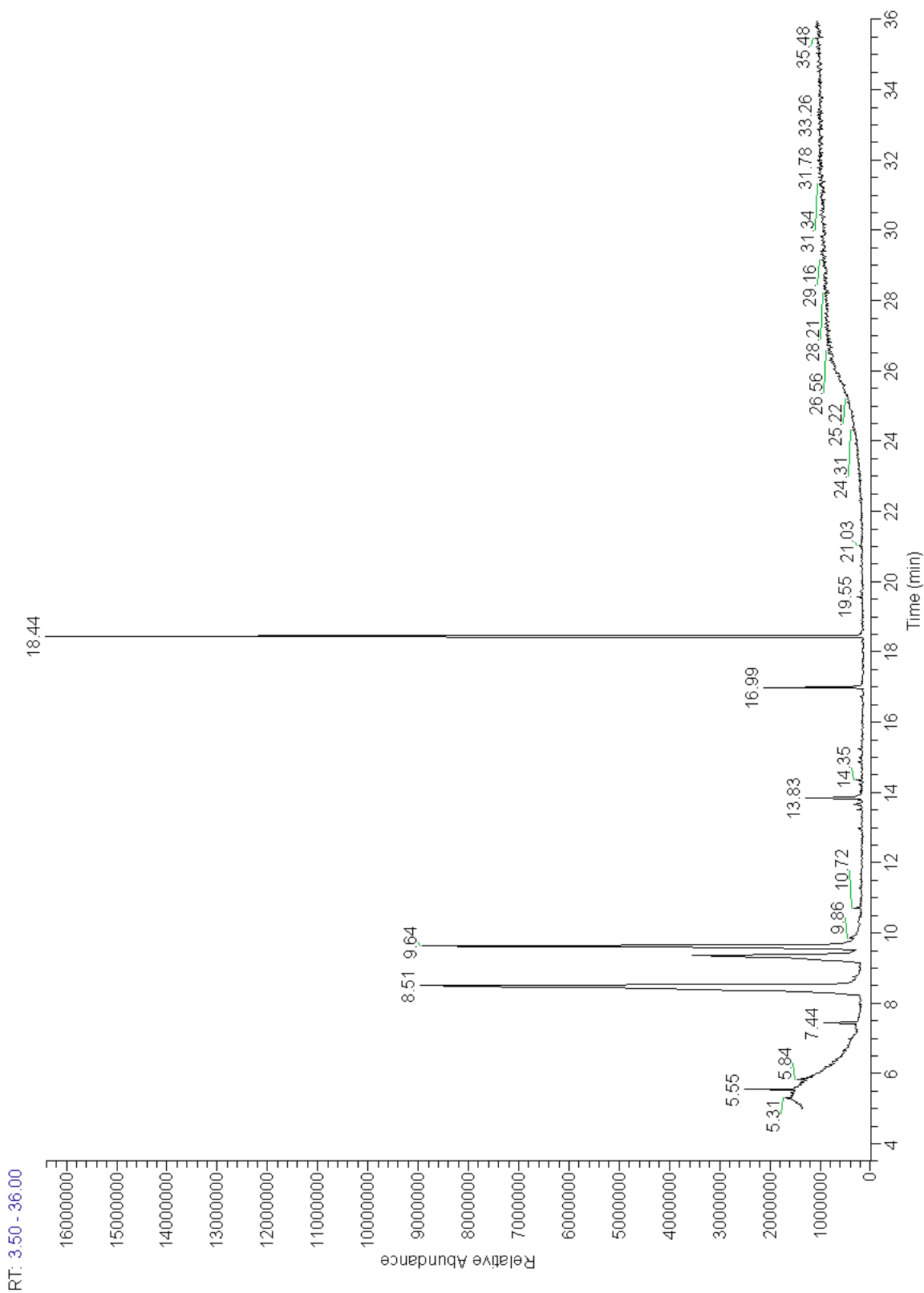


Figure 3.14: GC-MS TIC of Leuckart waste (1 mL) diluted in 500 mL water extracted following the SPE protocol of Zuccato et al. (2005), using Oasis MCX cartridges at pH 2. Peak identification table in 3.15 on the following page

Table 3.15: List of compounds identified in Leuckart waste SPE using Oasis MCX cartridges at pH 2. In bold: compounds identified in both the raw waste LLE and spiked water SPE.

No	RT (min)	Compound	Peak m/z	R. Match
1	5.55	Phenol	94, 66, 65, 95	890
2	7.44	Undecane	57, 71, 85, 56, 156	892
3	8.51	Benzenecarboxylic acid	105, 122, 77, 51	931
4	9.36	Methylamphetamine	58, 91, 56, 65	893
5	9.64	Benzeneacetic acid	91, 136, 92, 65	918
6	11.27	Unknown	105, 133, 104, 91	
7	13.52	Unknown	118, 117, 103, 77	
8	13.66	Unknown	105, 107, 176, 77	
9	13.79	Unknown	107, 105, 77, 176	
10	13.83	<i>N</i>-Formylmethylamphetamine	86, 58, 91, 118	965
11	14.35	Unknown	91, 65, 117, 115	
12	14.86	Unknown	118, 117, 203, 103	
13	15.23	Unknown	91, 92, 89, 117	
14	15.78	Unknown	105, 77, 51, 106	
SUR	16.99	Caffeine	194, 108, 67, 55	905
IS	18.44	Eicosane	57, 71, 85, 55, 282	920
15	19.55	Unknown	178, 250, 176, 179	

The extraction of Leuckart MA waste from water resulted in a profile which was distinctly different from the crude waste. A major difference between the extraction profiles is the ratio of MA to *N*-formylmethylamphetamine. In the LLE, *N*-formylmethylamphetamine was the most abundant compound, whereas in the SPE profile, it is present in much smaller amounts than MA. MA, in contrast, was not a major contributor in the LLE profile. The SPE elution solvent was methanol, compared to ethyl acetate which was used in the LLE of the crude waste, which would have affected the proportions of compounds extracted, as MA is much more soluble in methanol compared to ethyl acetate. The solubility of *N*-formylmethylamphetamine between the two solvents is not known due to the absence of an analytical standard.

The difference in pH levels between the LLE and SPE would also influence the analytes extracted. By acidifying the basic MA waste to pH 2, the degree of ionisation of the analytes would be greatly affected. Extraction at low pH would have extracted mostly acidic compounds. In the LLE method, the use of a pH 10.5 buffer would have extracted the basic analytes.

The SPE cartridges used, Oasis MCX, are mixed-mode cation exchange sorbents suitable for bases with pK_a values of 2-10. Extraction recoveries of MA from wastewater using the Oasis MCX cartridges at pH 2 range from 84% to 103% depending on the wash step and amount of sorbent (Boles and Wells, 2010). An alternative SPE sorbent that has been used for the extraction of MA from wastewater is Oasis HLB, a reversed-phase sorbent but suitable for all compounds. Extraction recoveries of MA from wastewater using the Oasis HLB cartridges at pH 7 range from 18% to 63% depending on the wash step and amount of sorbent, and at pH 3 from 93-99% (Boles and Wells, 2010). Figure 3.15 shows a typical gas chromatogram of 1 mL Leuckart waste diluted in 500 mL of deionized water extracted at pH 8.5 on Oasis HLB cartridges. The corresponding peak identification table in Table 3.16.

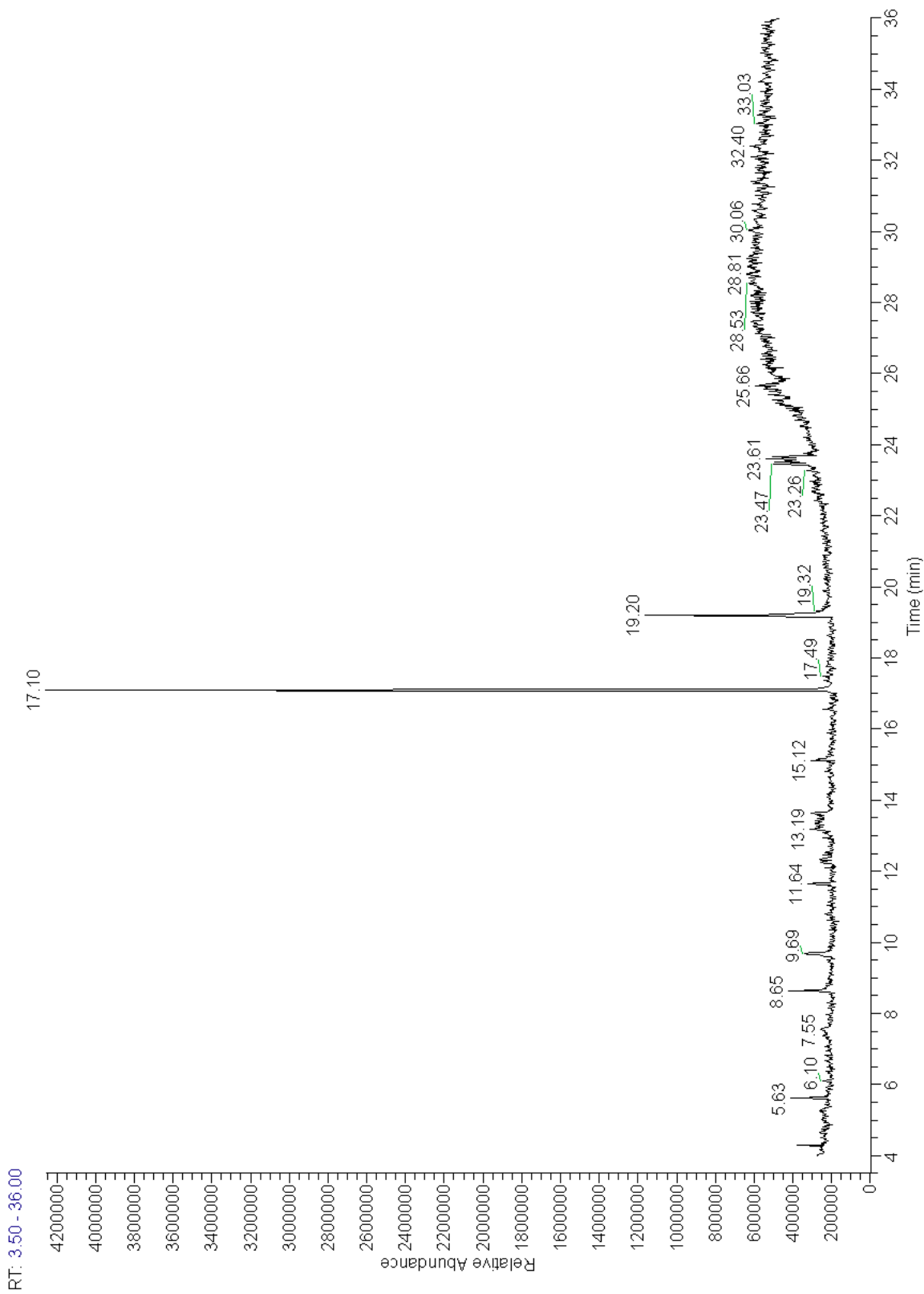


Figure 3.15: GC-MS TIC of Leuckart waste (1 mL) diluted in 500 mL water extracted following the SPE protocol of Boles and Wells (2010), using Oasis HLB cartridges at pH 8.5. Peak identification table in 3.16 on the next page

Table 3.16: List of compounds identified in Leuckart waste SPE using Oasis HLB cartridges at pH 8.5. In bold: compounds identified in both the raw waste extract and spiked water extract.

No	RT (min)	Compound	Peak m/z	R. Match
1	5.63	Undecane	57, 71, 85, 55, 156	822
2	8.65	Methylamphetamine	58, 91, 56, 57	802
3	15.12	N-Formylmethamphetamine	86, 91, 58, 118	
IS	17.10	Eicosane	57, 71, 85, 55, 282	856
SUR	19.20	Caffeine	109, 67, 82, 55	825

Several other combinations of eluent solvents were trialled, however similar results were obtained. An overlay chromatogram of all methods and their peak identification tables are presented in Figure 3.16, and Tables 3.17 to 3.21.

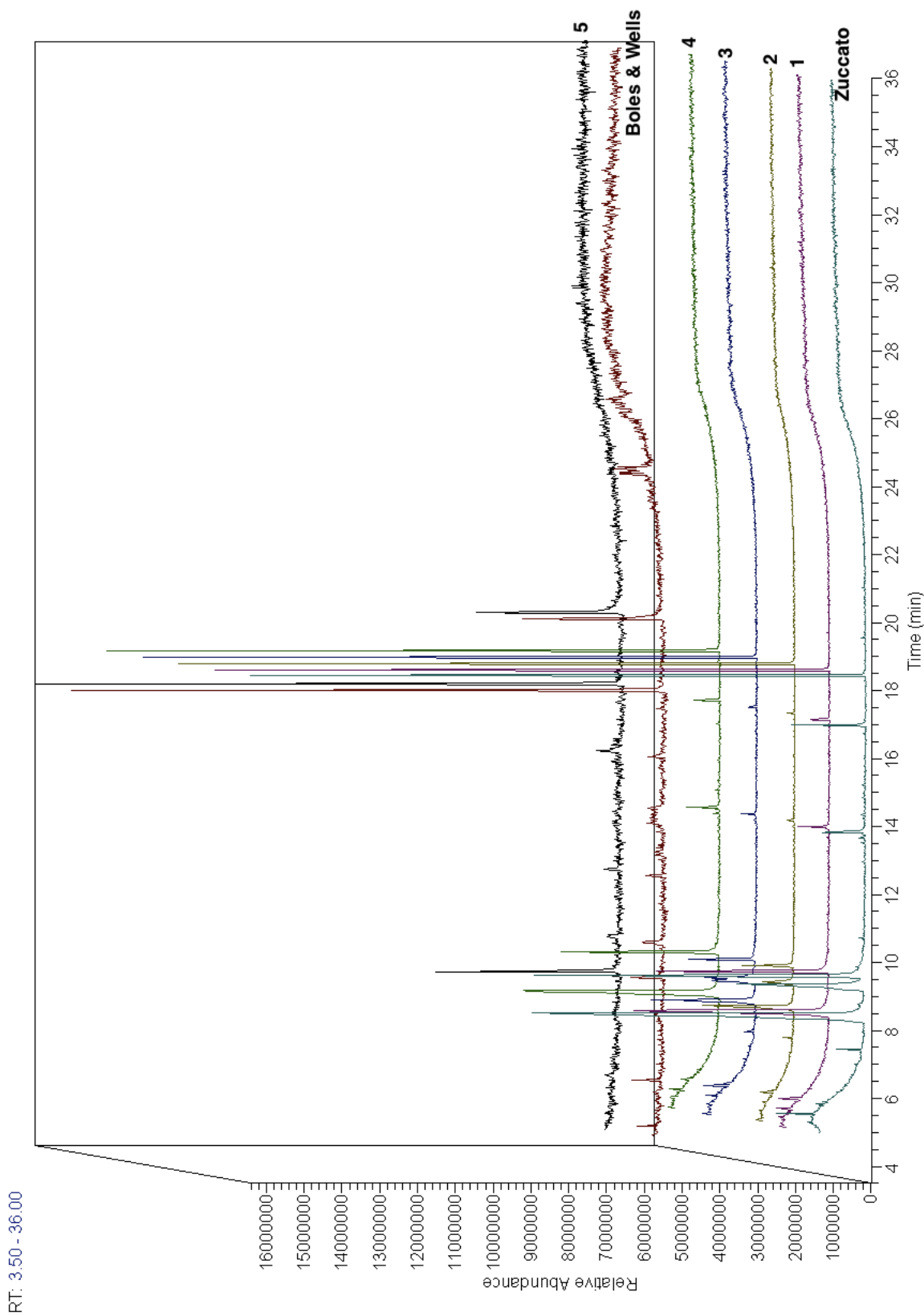


Figure 3.16: Overlay GC-MS TIC of Leucart waste (1 mL) diluted in 500 mL water using different SPE methods. Descriptions of method found in Table 3.2.

Table 3.17: List of compounds identified in Leuckart waste SPE 1 using Oasis MCX cartridges at pH 2. In bold: compounds identified in both the raw waste extract and spiked water extract.

No	RT (min)	Compound	Peak m/z	R. Match
1	5.55	Phenol	94, 65, 65, 95	850
2	8.43	Benzenecarboxylic acid	105, 122, 77, 51	924
3	9.60	Benzeneacetic acid	91, 136, 92, 65	898
4	13.67	Unknown	105, 107, 77, 176	
5	13.83	<i>N</i>-Formylmethylamphetamine	86, 58, 91, 118	929
6	14.24	Unknown	115, 116, 188, 58	
7	14.36	Unknown	91, 65, 117, 51	
SUR	16.99	Caffeine	194, 109, 69, 55	859
IS	18.44	Eicosane	57, 71, 85, 55, 282	923

Table 3.18: List of compounds identified in Leuckart waste SPE 2 using Oasis MCX cartridges at pH 2. In bold: compounds identified in both the raw waste extract and spiked water extract.

No	RT (min)	Compound	Peak m/z	R. Match
1	5.55	Phenol	94, 65, 66, 69	808
2	7.44	Undecane	57, 71, 85, 70, 156	803
3	8.39	Benzenecarboxylic acid	105, 122, 77, 51	915
4	9.08	Methylamphetamine	58, 91, 56, 65	878
5	9.57	Benzeneacetic acid	91, 136, 65, 92	917
6	13.66	Unknown	107, 105, 77, 176	
7	13.84	<i>N</i>-formylmethylamphetamine	86, 58, 91, 118	937
SUR	16.98	Caffeine	194, 109, 67, 55	882
IS	18.45	Eicosane	57, 71, 85, 55, 282	922

Table 3.19: List of compounds identified in Leuckart waste SPE 3 using Oasis MCX cartridges at pH 2. In bold: compounds identified in both the raw waste extract and spiked water extract.

No	RT (min)	Compound	Peak m/z	R. Match
1	5.55	Phenol	94, 66, 65, 55	802
2	7.43	Undecane	57, 71, 85, 56, 156	909
3	8.38	Benzenecarboxylic acid	105, 122, 77, 51	881
4	8.93, 9.03	Methylamphetamine	58, 91, 56, 65	899
5	9.57	Benzeneacetic acid	91, 136, 92, 65	905
6	13.84	N-formylmethylamphetamine	86, 58, 91, 118	913
SUR	16.98	Caffeine	194, 109, 67, 55	859
IS	18.44	Eicosane	57, 71, 85, 55, 282	917

Table 3.20: List of compounds identified in Leuckart waste SPE 4 using Oasis MCX cartridges at pH 2. In bold: compounds identified in both the raw waste extract and spiked water extract.

No	RT (min)	Compound	Peak m/z	R. Match
1	5.56	Phenol	94, 66, 65, 78	820
2	8.45	Benzenecarboxylic acid	105, 122, 77, 51	907
3	9.60	Benzeneacetic acid	91, 136, 92, 65	880
4	13.67	Unknown	105, 107, 106, 77	
5	13.79	Unknown	105, 107, 176, 51	
6	13.83	N-formylmethylamphetamine	86, 58, 91, 118	953
7	14.36	Unknown	91, 117, 65, 103	
8	16.30	Unknown	77, 170, 141, 51	
SUR	16.99	Caffeine	194, 109, 67, 55	851
IS	18.46	Eicosane	57, 71, 85, 55, 282	920

Table 3.21: List of compounds identified in Leuckart waste SPE 5 using Oasis HLB cartridges at pH 8.5. In bold: compounds identified in both the raw waste extract and spiked water extract.

No	RT (min)	Compound	Peak m/z	R. Match
1	8.63	Methylamphetamine	58, 91, 56, 57	802
2	15.12	N-Formylmethamphetamine	86, 91, 58, 118	
IS	17.10	Eicosane	57, 71, 85, 55, 282	856
SUR	19.20	Caffeine	109, 67, 82, 55	825

Additional SPE methods were carried out using molecular imprinted polymers as the cartridge phase. MIPs are designed to extract specific molecules through highly cross-linked polymers to bind one target compound or class of compounds with high selectivity. During the manufacture of MIP polymers, a template molecule is used to create a cavity or imprint that is sterically and chemically selective for the target analyte. Binding of the target analyte(s) occurs through multiple interactions, such as hydrogen bonding, ionic bonding, van der Waals forces, and hydrophobicity. Compared to traditional SPE phases, MIPs exhibit stronger binding forces between the analytes and the polymer, allowing for more rinsing steps, which results in a cleaner extract (Widstrand et al., 2008).

A chromatogram of the MIP extraction is shown in Figure 3.17 on the following page, with peak identification in Table 3.22 on page 116. The results from the MIP method show this method did not work well for MA waste. In this case, MA was detected in the chromatogram, however the chromatogram was so poor, the MA peak was not base-line resolved. Therefore MA could not be quantified from this method. The MIP chromatogram in Figure 3.17 shows lots of column bleed, a sign of column degeneration. While the method used was designed for analysis on HPLC, the extract was reconstituted in methanol which is compatible with GC analysis. Another likely error with this method is the sample was likely diluted too much.

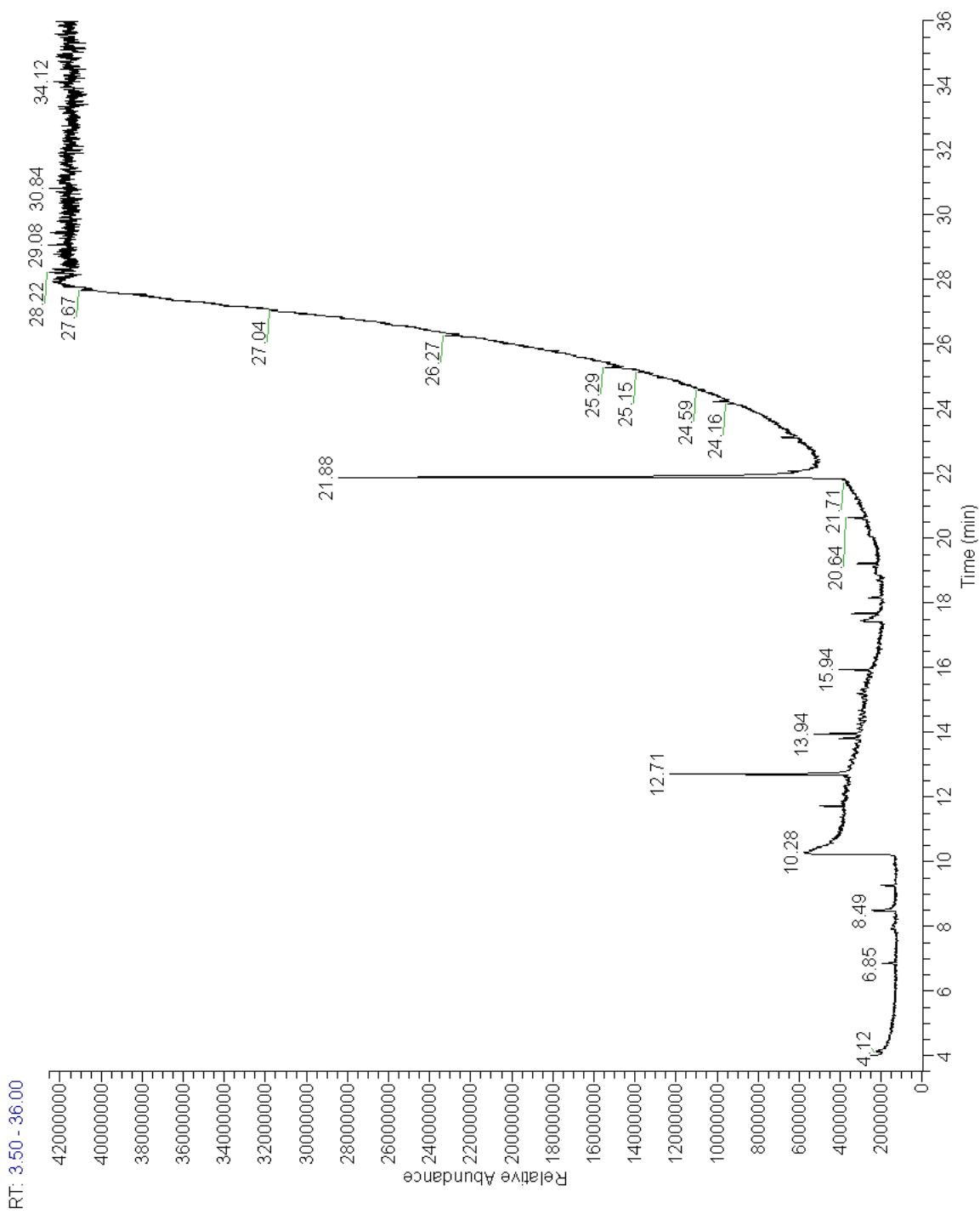


Figure 3.17: GC-MS chromatogram of Leuckart waste (0.5 mL) diluted in 250 mL water using MIP. Peak identification in Table 3.22.

Table 3.22: List of compounds identified in Leuckart waste SPE using MIP cartridges at pH 8. In bold: compounds identified in both the raw waste extract and spiked water extract.

No	RT (min)	Compound	Peak m/z	R. Match
1	4.12-4.17	Column/septum bleed		
2	6.85	Column/septum bleed		
3	8.49	Undecane	57, 71, 85, 56, 156	954
4	9.27	Si-complex		
5	10.28	Methylamphetamine	58, 91, 56, 65	910
6	11.72	Si-complex		
IS	12.71	Tetradecane	57, 71, 85, 55, 198	974
7	13.81	Unknown	16, 203, 175, 91	
8	13.94	Column/septum bleed		
9	15.94	Column/septum bleed		
10	17.42	Benzenesulfonamide, N-butyl-	77, 141, 170, 51	818
11	17.67	Column/septum bleed		
12	18.17	Dibutyl phthalate	149, 57, 56, 104	881
13	19.22	Column/septum bleed		
14	20.64	Column/septum bleed		
15	21.88	1,8-Diazacyclotetradecane-2,7-dione	55, 112, 86, 97	848
16	22.08	Unknown oxygen containing alkane	55, 57, 97, 83	
17	23.12	Column/septum bleed		
18	24.16	Unknown	149, 265, 57, 191	
19	24.24	Column/septum bleed		
20	25.29	Si-complex		

Initial impressions were that the SPE methods were not effective in identifying Leuckart MA waste. The only compounds the SPE methods were able to extract that were identified in the crude waste were phenol, MA, and *N*-formylmethylamphetamine. While the LLE of the crude waste and the SPE of the diluted waste did not result in similar chromatographic profiles, both methods were able to extract the key MA-specific by-product *N*-formylmethylamphetamine. Additionally, the methods were originally developed for the extraction and concentration of MA, not MA waste. As a method for such purposes, the methods worked quite well, as shown by the SPE concentration factors in Table 3.23.

Table 3.23: MA SPE concentration factors of water diluted Leuckart waste

	A		Amount in system (mg)	Water vol. (mL)	System Concentration (mg/mL)	Concentration Factor (A/B)
	[MA] (mg/mL)	Recon. volume (mL)				
Zuccato	0.015	1.5	0.022	500	0.000045	333
Boles & Wells	0.009	1.5	0.014	500	0.000028	333
SPE 1	N/D	-	-	-	-	-
SPE 2	0.011	3	0.032	500	0.000064	166
SPE 3	0.011	3	0.034	-	0.000068	166
SPE 4	N/D	-	-	-	-	-
SPE 5	0.010	1.5	0.015	500	0.000030	333
MIP	N/Q	-	-	-	-	-

N/D = Not Detected
N/Q = Not Quantifiable

In all of the extraction methods, the amount of MA quantified is right on the cusp of the LOD. Further research to optimise SPE methods specifically for MA waste components identified in Table 3.14 (*N*-formylmethamphetamine; P2P; 1-phenyl-1,2-propanedione; and benzaldehyde) and to determine extraction recoveries would be beneficial given that target waste analytes have now been clearly identified.

3.3.8 Extraction of Methylamphetamine Waste from Sediment

Extraction of the target analytes is required in order to separate the compounds of interest from the matrix. In this case, a sediment matrix is especially complex containing many interfering compounds, such as humic acids and other contaminants. The extraction method used in this study serves to isolate and concentrate target analytes in order for analysis to be carried out on analytical instruments without damaging the instrument. It is also necessary in order to distinguish unknown compounds from the matrix background.

The extraction method used by Pal et al. (2011) to extract MA, P2P, and MDMA from soil was trialled in this study to extract MA waste from sediment. The results were somewhat mixed. While the Pal method was able to extract key impurities, such as *N*-formylmethamphetamine, the extraction efficiency was very low and highly variable. The sediment used for the extraction was relatively clean and showed little matrix interferences, as seen in a blank sediment extraction in Figure 3.18. The accompanying peak identification table can be found in Table 3.24.

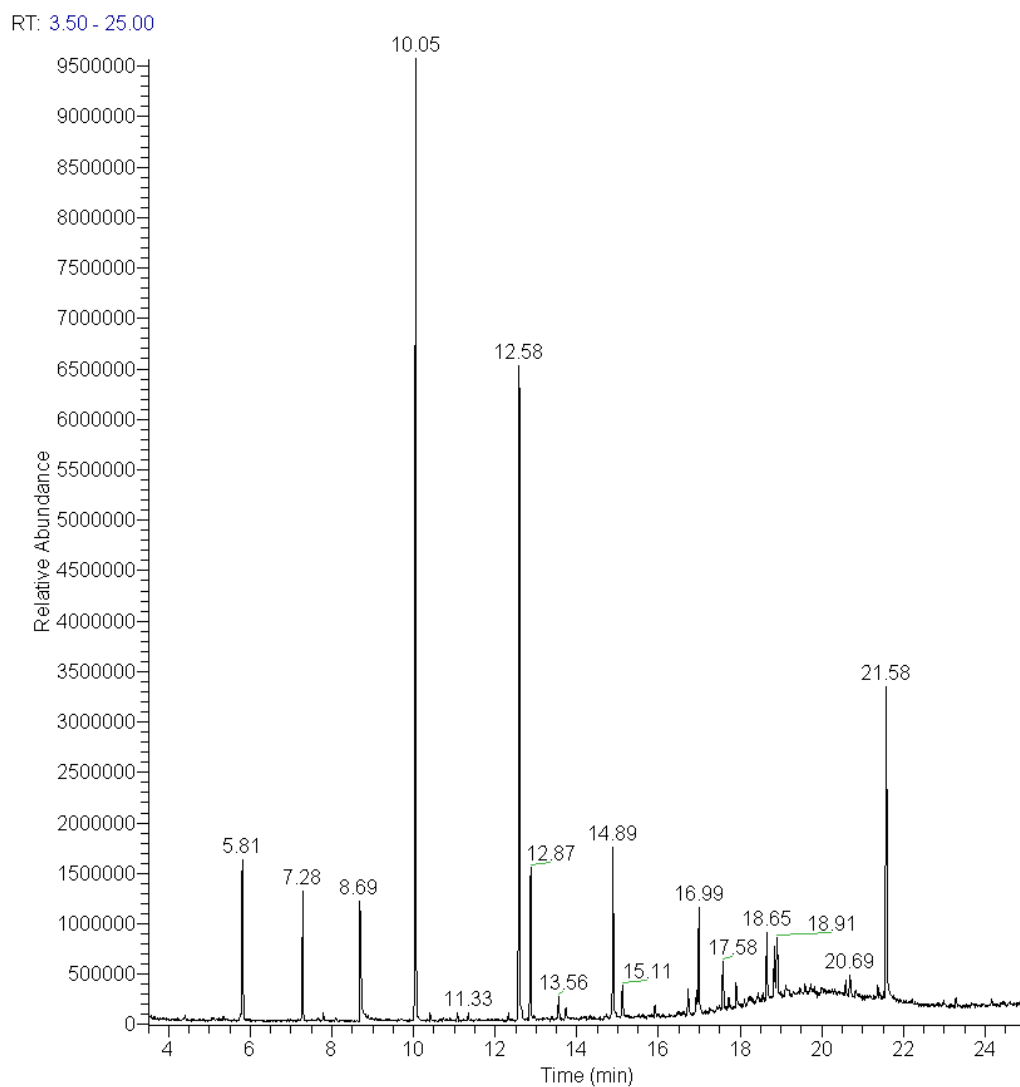


Figure 3.18: GC-MS chromatogram of sediment blank extraction. See Table 3.24 on the following page for peak identifications.

Table 3.24: List of compounds identified in sediment blank extraction

Peak No	RT (min)	Compound	Peak m/z	R. Match
1	5.81	Undecane	51, 71, 85, 156	939
2	7.28	Octanoic acid, methyl ester	74, 87, 115, 127	920
3	7.80	Benzoic acid, methyl ester	105, 77, 136, 76	851
SUR	8.69	d5-Methylamphetamine	62, 92, 59, 63	N/A
IS	10.05	Tetradecane	57, 71, 85, 55, 198	961
4	10.41	Phenol, <i>p/m</i> -tert-butyl	135, 107, 150, 95	
5	11.07	Fatty acid methyl ester	71, 89, 56, 173	
6	11.33	Unknown long chain alkane	57, 71, 85, 56	
7	12.33	Unknown	161, 218, 175, 203	
8	12.58	Dodecanoic acid, methyl ester	74, 87, 171, 143	928
9	12.87	Phenol, 2,4-bis(1,1-dimethylethyl)-	191, 206, 192, 57	834
10	13.55	Unknown	71, 57, 69, 83	
11	14.89	Methyl tetradecanoate	74, 87, 143, 75	888
12	15.11	Hexathiane	64, 192, 128, 194	891
13	16.72	Unknown	55, 73, 83, 69	
14	16.93	Unknown long chain alkane	57, 71, 85, 113	
15	16.99	Hexadecanoic acid, methyl ester	74, 87, 75, 143	879
16	17.58	Unknown	149, 178, 150, 223	
17	17.72	Unknown	170, 77, 141, 158	
18	17.90	Long chain branched alkane	57, 71, 85, 69	
19	18.66	Dibutyl phthalate	149, 150, 223, 76	933
20	18.84	Fatty acid methyl ester	74, 87, 143, 75	
21	18.90	Fatty acid methyl ester	74, 87, 143, 75	
22	20.69	PAH (fluoranthene/pyrene)	202, 200, 201, 101	
23	21.37	PAH (fluoranthene/pyrene)	202, 200, 201, 101	
24	21.58	Unknown	129, 112, 57, 70	

end

The sediment blank contains many methyl esters and fatty acid methyl esters, as well as PAHs and alkanes. Those compounds were also identified in the extraction of the waste from the same sediment. Therefore they are a part of the sediment and were not formed as a result of reactions caused with interaction in the sediment. Additionally, none of the compounds identified in the raw waste extracts were present in the blank sediment extraction.

Chromatograms for Leuckart, Moscow, and Hypophosphorous waste extracted from sediment can be found in Figures 3.19, 3.20, and 3.21, respectively. Corresponding peak tables for Leuckart, Moscow, and Hypophosphorous waste extracted from sediment can be found in Tables 3.25, 3.26, and 3.27, respectively.

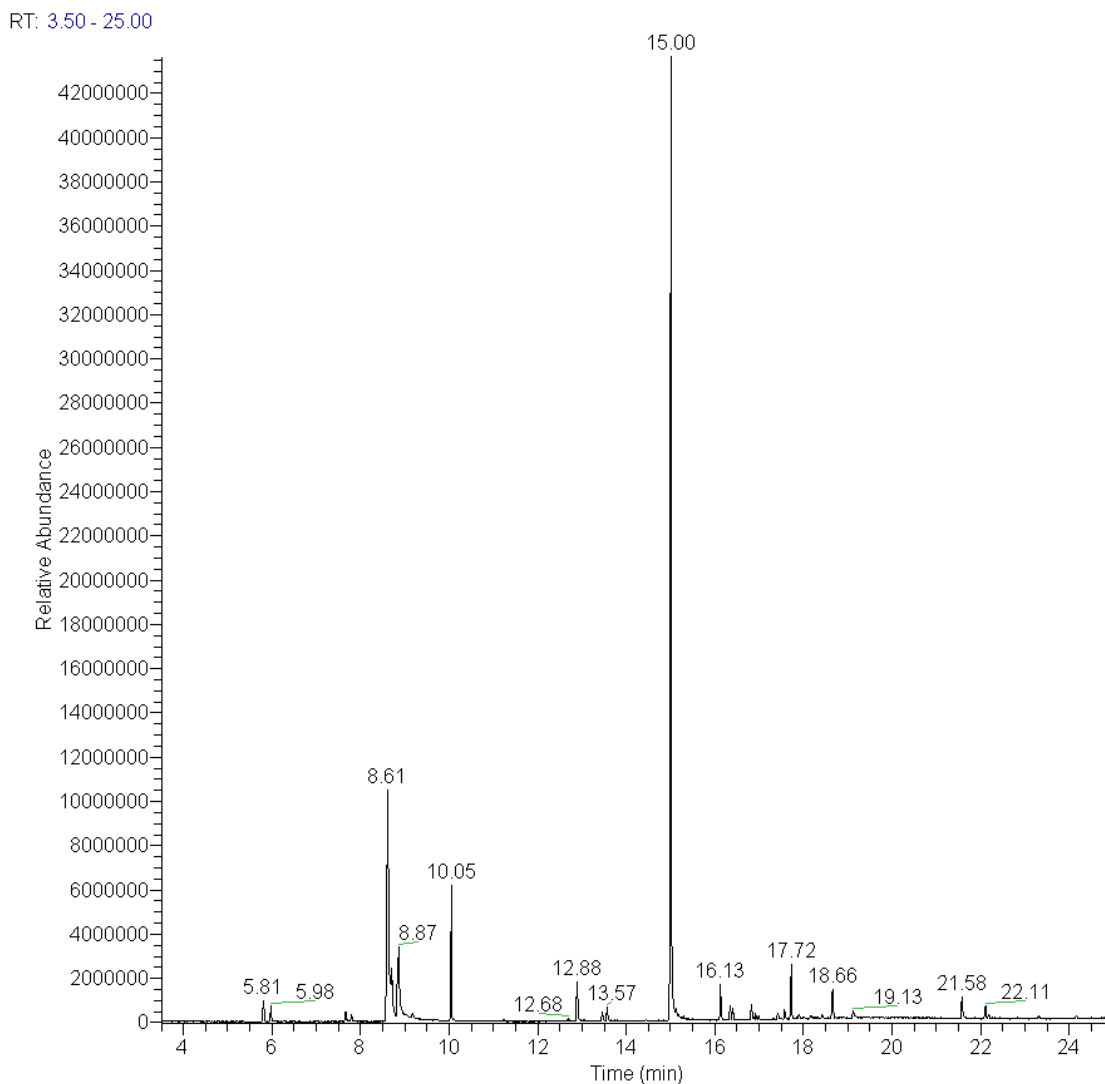


Figure 3.19: GC-MS chromatogram of the sediment extraction of Leuckart waste. See Table 3.25 on the next page for peak identifications.

Table 3.25: List of compounds identified in Leuckart waste sediment extraction. In bold: compounds identified in both the raw waste extract and spiked sediment extract. In italics: compounds identified in the sediment blank extract.

Peak No	RT (min)	Compound	Peak m/z	R. Match
<i>1</i>	<i>5.80</i>	<i>Undecane</i>	<i>51, 71, 85, 56, 156</i>	<i>921</i>
2	5.98	Benzaldehyde	77, 106, 105, 78	925
3	6.50	Benzonitrile	103, 76, 75, 77	841
4	7.65	Acetophenone	105, 77, 120, 121	868
<i>5</i>	<i>7.80</i>	<i>Benzoic acid, methyl ester</i>	<i>105, 77, 136, 76</i>	<i>856</i>
6	8.61-8.70	Urea, <i>N,N'</i> -dimethyl-	88, 58, 59, 89	907
SUR	8.83	d5-Methylamphetamine	62, 92, 63, 66	N/A
7	8.87	Methylamphetamine	58, 91, 65, 56	875
IS	10.05	Tetradecane	57, 71, 85, 55, 198	965
8	11.24	Unknown	105, 77, 51, 95	
9	12.68	Unknown	105, 133, 77, 148	
10	12.88	Benzamide, <i>N</i> -methyl-	105, 77, 134, 135	884
11	13.46	<i>N</i> -Methylphthalimide	161, 76, 104, 117	873
12	13.57	<i>N</i> -Methyl-2-phenylacetamide	92, 91, 58, 105	937
13	15.00	<i>N</i>-Formylmethamphetamine	86, 58, 118, 91	945
14	15.12	Unknown	107, 105, 176, 77	
15	16.13	2,5-Pyrrolidinedione, 1,3-dimethyl-3-phenyl-	118, 117, 203, 77	915
16	16.23	Unknown	102, 187, 76, 103	
17	16.34	2,5-Pyrrolidinedione, 1,3-dimethyl-3-phenyl-	118, 117, 203, 115	829
18	16.40	Unknown	91, 217, 65, 115	
19	16.76	Unknown	116, 115, 201, 117	
20	16.82	2,5-Pyrrolidinedione, 1-methyl-3-phenyl-	104, 189, 103, 78	931
21	17.42	Unknown	91, 203, 117, 118	
<i>22</i>	<i>17.72</i>	<i>Unknown</i>	<i>77, 170, 141, 78</i>	
<i>23</i>	<i>18.66</i>	<i>Dibutyl phthalate</i>	<i>149, 150, 223, 76</i>	<i>911</i>
24	19.13	Unknown	91, 92, 231, 140	
<i>25</i>	<i>21.58</i>	<i>Unknown</i>	<i>129, 112, 57, 70</i>	
26	22.11	Unknown	180, 179, 265, 165	
27	22.18	Unknown	263, 178, 205, 262	

end

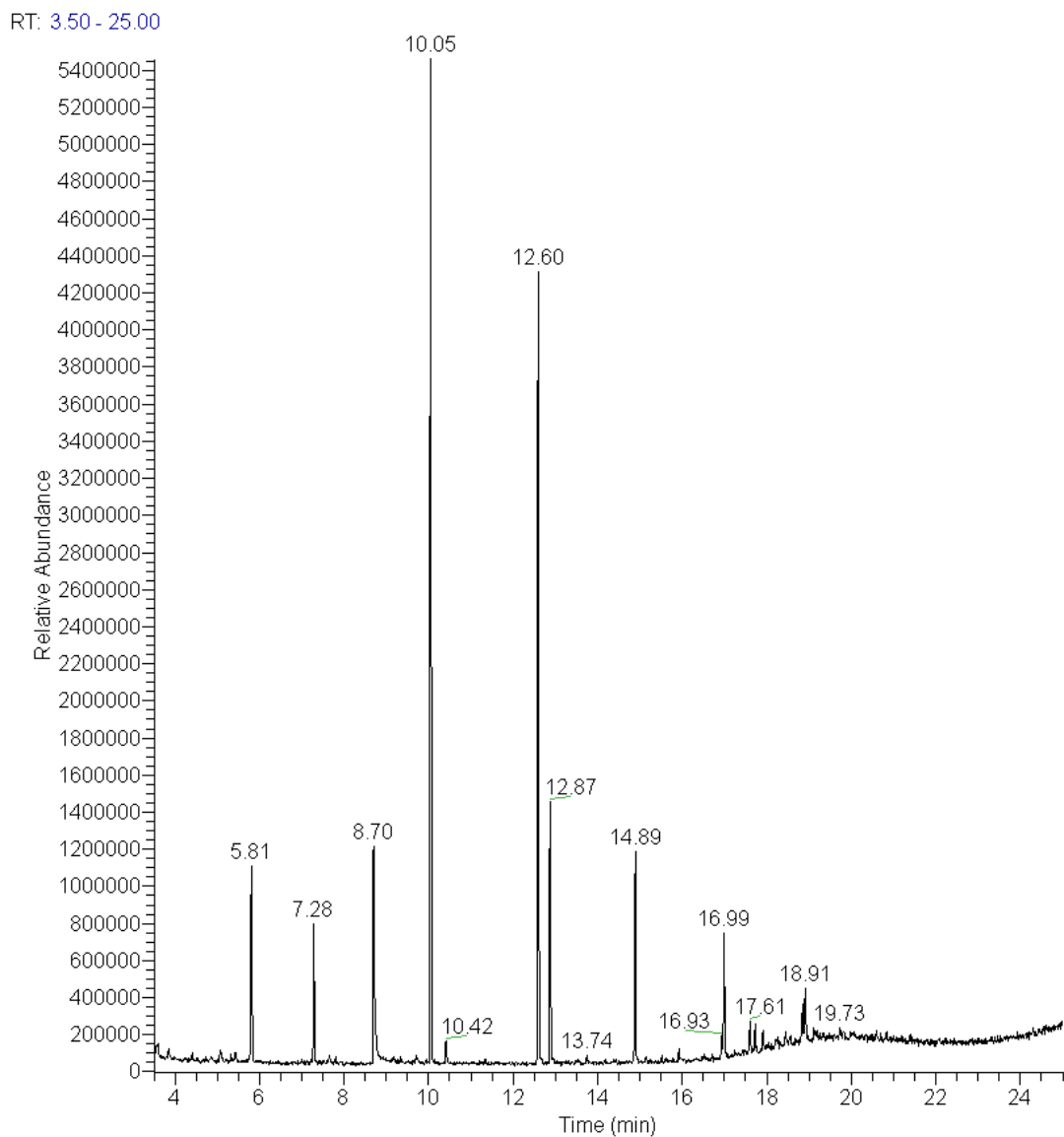


Figure 3.20: GC-MS chromatogram of the sediment extraction of Moscow waste. See Table 3.26 on the following page for peak identifications.

Table 3.26: List of compounds identified in Moscow waste sediment extraction. In bold: compounds identified in both the raw waste LLE and spiked sediment extract. In italics: compounds identified in the sediment blank extract.

Peak No	RT (min)	Compound	Peak m/z	R. Match
<i>1</i>	<i>5.81</i>	<i>Undecane</i>	<i>51, 71, 85, 70, 156</i>	924
<i>2</i>	<i>7.28</i>	<i>Octanoic acid, methyl ester</i>	<i>74, 87, 115, 59</i>	904
SUR	8.70	d5-Methylamphetamine	62, 92, 63, 59	N/A
IS	10.05	Tetradecane	57, 71, 85, 55, 198	960
<i>3</i>	<i>10.42</i>	<i>Phenol, p/m-tert-butyl</i>	<i>135, 107, 150, 77</i>	
<i>4</i>	<i>12.60</i>	<i>Dodecanoic acid, methyl ester</i>	<i>74, 87, 75, 171</i>	911
<i>5</i>	<i>12.87</i>	<i>2,5-di-tertbutylphenol</i>	<i>191, 206, 192, 57</i>	830
<i>6</i>	<i>14.89</i>	<i>Methyl tetradecanoate</i>	<i>74, 87, 143, 75</i>	944
<i>7</i>	<i>16.93</i>	<i>Unknown long chain branched alkane</i>	<i>57, 71, 85, 99</i>	
<i>8</i>	<i>16.99</i>	<i>Hexadecanoic acid, methyl ester</i>	<i>74, 87, 75, 143</i>	867
<i>9</i>	<i>17.61</i>	<i>Unknown</i>	<i>178, 176, 177, 76</i>	
<i>10</i>	<i>17.72</i>	<i>Unknown</i>	<i>77, 170, 141, 158</i>	
<i>11</i>	<i>17.91</i>	<i>Unknown long chain branched alkane</i>	<i>71, 57, 87, 69</i>	
<i>12</i>	<i>18.03</i>	<i>Unknown</i>	<i>277, 82, 292, 83</i>	
<i>13</i>	<i>18.44</i>	<i>Unknown long chain alkane</i>	<i>57, 71, 97, 55</i>	
<i>14</i>	<i>18.55</i>	<i>Unknown long chain alkane</i>	<i>97, 57, 96, 71</i>	
<i>15</i>	<i>18.84</i>	<i>Fatty acid methyl ester</i>	<i>57, 71, 69, 55</i>	
<i>16</i>	<i>18.91</i>	<i>Fatty acid methyl ester</i>	<i>74, 87, 57, 69</i>	
<i>17</i>	<i>20.70</i>	<i>Unknown PAH (fluoranthene/pyrene)</i>	<i>202, 101, 200, 201</i>	
<i>18</i>	<i>21.38</i>	<i>Unknown PAH (fluoranthene/pyrene)</i>	<i>202, 201, 200, 101</i>	

end

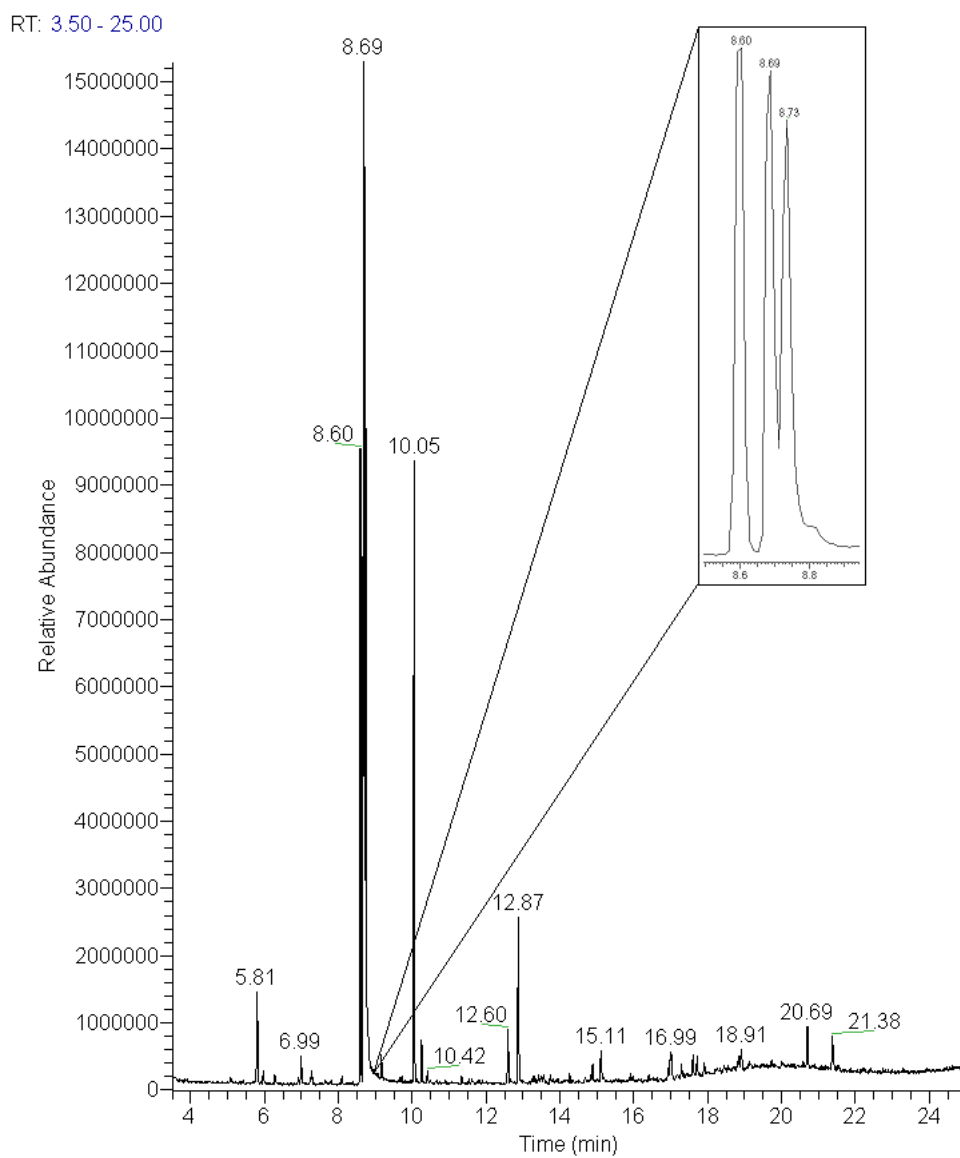


Figure 3.21: GC-MS chromatogram of the sediment extraction of Hypophosphorous waste. See Table 3.27 on the next page for peak identifications.

Table 3.27: List of compounds identified in Hypophosphorous waste sediment extraction. In bold: compounds identified in both the raw waste extract and spiked sediment extract. In italics: compounds identified in the sediment blank extract.

Peak No	RT (min)	Compound	Peak m/z	R. Match
<i>1</i>	<i>5.81</i>	<i>Undecane</i>	<i>51, 71, 85, 70, 156</i>	<i>919</i>
2	6.82	Unknown	96, 67, 81, 95	
3	6.92	Phenol, <i>N</i> -methyl-	108, 107, 77, 78	
4	6.99	Benzyl alcohol	79, 108, 77, 107	878
<i>5</i>	<i>7.28</i>	<i>Octanoic acid, methyl ester</i>	<i>74, 87, 57, 115</i>	<i>865</i>
6	8.10	Unknown long chain alkane	71, 57, 85, 113	
7	8.60	1-Phenyl-2-propanone	91, 134, 92, 65	907
SUR	8.69	d5-Methylamphetamine	62, 59, 63, 92	N/A
8	8.73	Methylamphetamine	58, 91, 65, 56	934
9	9.17	1-Phenyl-1,2-propanedione	105, 77, 51, 106	862
IS	10.05	Tetradecane	57, 71, 85, 55, 198	944
10	10.25	Unknown	99, 55, 100, 128	
<i>11</i>	<i>10.41</i>	<i>Phenol, p/m-tert-butyl</i>	<i>135, 107, 150, 134</i>	
<i>12</i>	<i>11.33</i>	<i>Unknown long chain alkane</i>	<i>57, 71, 85, 56</i>	
13	11.54	Unknown long chain alkane	71, 57, 85, 113	
<i>14</i>	<i>12.58</i>	<i>Dodecanoic acid, methyl ester</i>	<i>74, 87, 75, 143</i>	<i>888</i>
15	12.87	2,6-di-tertbutylphenol	191, 206, 192, 57	834
<i>16</i>	<i>14.89</i>	<i>Methyl tetradecanoate</i>	<i>74, 87, 143, 75</i>	<i>837</i>
<i>17</i>	<i>15.11</i>	<i>Hexathiane</i>	<i>64, 192, 128, 194</i>	<i>910</i>
<i>18</i>	<i>16.95</i>	<i>Unknown long chain branched alkane</i>	<i>57, 71, 55, 69,</i>	
19	17.01	Unknown	175, 190, 77, 147	
20	17.29	Unknown	161, 190, 162, 115	
21	17.60	Unknown aromatic	178, 149, 176, 76	
<i>22</i>	<i>17.71</i>	<i>Unknown</i>	<i>77, 170, 141, 178</i>	
<i>23</i>	<i>17.90</i>	<i>Unknown long chain branched alkane</i>	<i>57, 71, 85, 99</i>	
<i>24</i>	<i>18.84</i>	<i>Fatty acid methyl ester</i>	<i>57, 71, 69, 85</i>	
<i>25</i>	<i>18.90</i>	<i>Fatty acid methyl ester</i>	<i>74, 87, 97, 55</i>	
<i>26</i>	<i>20.70</i>	<i>Unknown PAH (fluoranthene/pyrene)</i>	<i>202, 200, 201, 203</i>	
<i>27</i>	<i>21.38</i>	<i>Unknown PAH (fluoranthene/pyrene)</i>	<i>202, 200, 101, 201</i>	

end

The extraction method was not ideal. Pal et al. (2011) did not report their extraction efficiencies for the method, and this study found that they were both low and highly variable. The percent recovery of d5-MA from the Hypophosphorous waste was 22.83%, with a RSD of 49.08%. Extraction efficiency and RSD from the Leuckart waste was comparable, with a recovery of 21.48% and a RSD of 44.48%. The RSD of d5-MA from the Moscow route was much lower, at only 4.34%, however the extraction efficiency was also much lower at only 12.06%. The extraction efficiencies of d5-MA were comparable to those of d5-MA from the LLE extractions, however the RSDs were much higher. Calculations are shown in Appendix A on page 276.

Not only were the RSDs unacceptable for most of the extractions (using a threshold value of 5%), the extraction of analytes of interest varied as well. For the Moscow waste, P2P was detected in all of the raw waste extracts, however it was only extracted from one of the six replicate sediment extractions. This was also the case with the Leuckart waste where P2P was detected in small amounts in the raw waste, but not at all extracted from the spiked sediment samples. Also with the Leuckart waste, MA was detected in each crude waste sample, but only in five of six replicated sediment extractions.

Overall, the extraction method was impractical, requiring many time consuming steps. For the aqueous Leuckart waste, it took two days and nearly a full bottle of nitrogen gas to blow the extract down to dryness. For practical forensic application where samples must be processed quickly and funding is often limited, this method is not practical in terms of time or money. Additional research into alternative methods, such as pressurised liquid extraction, may provide extraction methods to shorten analysis times and reduce costs.

3.4 Conclusions

The organic chemical profile of waste produced from illicit MA manufacture was successfully determined for three different synthetic routes: Leuckart, Moscow, and Hypophosphorous. Key chemical markers of the waste include MA, P2P, 1-phenyl-2-propanol, 1-phenyl-1,2-propanedione, and *N*-formylmethylamphetamine. Other, less specific, components of the waste include xylene, phenol, and benzaldehyde. It was possible to use previously published methods to extract MA,

P2P, and *N*-formylmethylamphetamine from sediment (Pal et al., 2011) and water (Zuccato et al., 2005), though recoveries were low (13% to 18%) and variabilities were acceptable (1.16 to 4.3 %RSD).

Chemical profiling of the waste was accomplished using well established methods for the profiling of illicit MA. The LLE methods were originally designed for the extraction of powdered illicit drugs, however the methods were able to extract impurities from liquid MA waste. Although the extraction efficiency of d5-MA was low, these methods were designed to extract impurities and by-products, not MA itself. Future work should include measuring the extraction efficiencies of the impurities in order to estimate how much exists in the environment of a suspected dumpsite.

The SPE methods used for the extraction of diluted Leuckart waste were only able to recover three MA waste compounds: phenol, MA, and *N*-formylmethylamphetamine. The absence of a profile corresponding to the crude waste is disappointing, however the methods appear to hold promise based on the extraction of the key MA by-product *N*-formylmethylamphetamine. The SPE concentration factors of MA ranged from 160 to 333. Without an analytical standard of *N*-formylmethylamphetamine, the concentration factor was not determined. The method used for the extraction of MA from sediment had a low recovery rate, from 12-23%, and also had high variability, from 4 to 49 %RSD. The extraction efficiency and %RSD were highly variable between the three synthetic routes. Further research is required to produce a more suitable extraction method for MA waste from sediment.

The benefits of adapting accepted, published, and validated methods provides a reliable starting point for the acceptance of waste profiling methods in a court of law. Additionally, by using methods already familiar to the forensic science community, any additional staff training would be minimal. The difficulty in profiling MA waste is the high variability between samples since clandestinely manufactured MA, and subsequently its waste, varies widely from batch to batch. Even the waste considered in this study, manufactured under closely monitored conditions, varied widely. An additional consideration to take into account is the practice of stock-piling waste prior to disposal. This would greatly change the waste profile, especially if more than one synthetic route was used in a single clandestine laboratory.

Chapter 4

Measurement of Environmental Partition Coefficients

4.1 Introduction

The use of partition coefficients to describe the distribution of organic substances between two different phases began in the early 1900s with biochemical systems, when it was discovered that the activities of narcotic drugs correlated well with their oil-water partition coefficients (Chiou, 2002). By the mid 1960s, octanol replaced oil and the use of the octanol-water partition coefficient was used extensively to describe the behaviour of many different chemical compounds, not just narcotic drugs. In the following decade, the use of partition coefficients to describe the distribution of environmental contaminants in soil/sediment-water systems became increasingly common. While the distribution of a contaminant between water and environmental compartments is more complex than a simple partition coefficient, the distribution of a contaminant in an aquatic system corresponds strongly to the chemical's distribution in the octanol-water system (Chiou, 2002).

The use of partition coefficients, such as K_{OW} and K_{OC} , in environmental modelling of organic chemicals is useful in predicting the behaviour of a contaminant in the environment. In order to facilitate the detection and prosecution of an illicit MA dumpsite, an understanding of the

chemical behaviour of MA waste is essential. However, an environmental model is only as accurate as the information input into the model. Therefore, in order to generate the most accurate model as possible it is essential to gain as much information about the dumpsite and the chemicals as feasible. Information which will aid the accuracy of the model includes the organic carbon content of the dumpsite and partition coefficients of the waste components.

In this chapter, several locations were sampled from along the River Clyde in Glasgow to simulate potential clandestine MA dumpsites. The river sediment collected was characterised to enable a site-specific model to be generated using mathematical modeling. Additionally, K_{OW} and K_{OC} values of the identified MA waste components were experimentally determined for input into an environmental model.

While many different environmental models exist, the fugacity model was used in this work due to its simplicity and universal availability as part of the US EPA's EPI Suite™ computer programme. A fugacity model calculates the tendency of a compound to partition into each environmental compartment. The model uses partition coefficients and mass balance equations to predict the movement of a contaminant across environmental compartments. The data generated in this chapter was used to input into the EPI Suite™ fugacity model in order to generate the most accurate model as possible. Fugacity modelling of the waste components based on the environmental partition coefficients measured in this chapter is detailed in Chapter 5.

4.2 Methodology

The measurement of environmental partition coefficients of MA waste constituents was based on the compounds identified in the initial profiling study. However, not all of the compounds identified by GC-MS were available to purchase as analytical standards. This limited the number of compounds available for partition coefficient testing. The octanol-water partition coefficient, K_{OW} , and the organic carbon partition coefficient, K_{OC} , were experimentally determined following internationally recognised standard methods, as detailed below.

4.2.1 Octanol-Water Partition Coefficient, K_{OW}

The K_{OW} was experimentally determined by reversed phase high performance liquid chromatography (RPHPLC) following the Organisation for Economic Co-operation and Development (OECD) standard method 117 (OECD, 1989). The K_{OW} was determined for nine chemicals identified from the GC-MS analysis of MA waste. Those compounds were: benzaldehyde; benzyl alcohol; P2P; *N*-methylacetamide; phenol; MA; 1-phenyl-1,2-propanedione; benzaldehyde, oxime; and 2,6-di-*tert*-butylphenol (Sigma-Aldrich, UK). The HPLC used was a Dionex UltiMate 3000 with a variable wavelength detector.

The OECD 117 method determines K_{OW} based on RPHPLC retention time using a C₁₈ column (Techsphere5ODS, 25 cm x 4.6 mm) and a mobile phase comprised of 75% methanol (HPLC grade, Fisher Scientific, UK) and 25% water (Barnstead Nanopure, ThermoFisher Scientific, UK). The retention times of the MA impurities were compared against the retention times of reference compounds with known K_{OW} values, as recommended in the standard method. Ten reference compounds were selected to cover the range of predicted K_{OW} values of the MA waste impurities, which were estimated using EPI Suite™ (USEPA, 2012b). The ten reference compounds were: aniline, 4-methoxyphenol, acetophenone, cinnamyl alcohol, 4-chlorophenol, 1-naphthalene, biphenyl, phenanthrene, and triphenylamine. The partition coefficient is calculated using the capacity factor, k , following Equation 4.1:

$$k = \frac{t_R - t_0}{t_0} \quad (4.1)$$

Where:

t_R = retention time of the analyte

t_0 = dead time, i.e. the average time a solvent molecule needs to pass the column

The log k from Equation 4.1 of the reference materials were plotted against the log K_{OW} as specified in the standard method. The equation of the line was then used to determine log K_{OW} of the MA waste impurities. All reference and waste standards were run individually and injected in triplicate.

Prior to HPLC analysis, the maximum wavelength, λ_{max} , was determined for each reference compound and each analyte of interest. This was accomplished by running standard solutions of each compound in a spectrophotometer and conducting a scan from 190 nm to 400 nm (UNICAM UV-Vis spectrophotometer, Vision 4.30 software). The wavelength that gave the highest response is the λ_{max} and was used to set the UV detector on the HPLC.

4.2.2 Interactions Between Chemicals and Sediments

Sediment properties have a great influence over the behaviour of chemicals in the environment. The extent of adsorption of a chemical onto sediment is an important factor in determining the ultimate fate of chemicals in the environment. Adsorption is affected by a number of soil properties, such as organic matter content, type and amount of clay content, and pH. The extent of adsorption is also affected by the physicochemical properties of the compound, such as water solubility and K_{OW} (Drillia et al., 2005).

In order to characterise the sediment, the following tests were carried out.

- | | |
|-----|--|
| TOC | Total Organic Carbon content can greatly influence sorption of organic material. Higher TOC content may result in higher chemical adsorption to soils and sediments. |
| XRF | X-Ray Fluorescence measures trace metals in the sample which can influence binding sites and the type of bonds that may affect adsorption (i.e. form organo-metallic complexes). |
| XRD | X-Ray Diffraction measures the crystal lattice structure to determine the type of clay minerals present in the soil sample. |

4.2.2.1 Sample Collection

In order to get a range of different sediment sample types, sediment samples were collected from the Forth and Clyde Canal and the River Clyde in Glasgow, United Kingdom, for use in adsorption experiments (Section 4.2.3). Four sites were sampled in order to comply with the standard method which suggests that a minimum of four sediments with different organic

contents be used for the study. The sampling locations were selected to represent different potential urban MA dumpsites with varying chemical properties of the sediment.

Sediment samples were collected from four different locations along the Forth and Clyde Canal and the River Clyde in the vicinity of Glasgow, United Kingdom (Figure 4.1). Sample 1 was taken from Bothwell Bridge (55°47'42.99"N, 4°3'29.70"W), to the east of Glasgow before the river enters the city. Sample 2 was taken from the Renfrew Ferry terminal (55°53'9.95"N, 4°22'57.91"W), in the west end of Glasgow after the river has passed through the city centre, two waste water treatment plants, and one hospital. The third sample was collected from Bowling Harbour (55°55'48.57"N, 4°29'1.17"W), to the west of Glasgow, where the Forth and Clyde Canal meets the Clyde River estuary. The fourth sample was collected from Port Dundas, a disused city branch of the Forth and Clyde Canal, a commercial area that is known to be heavily polluted (Bangkedphol et al., 2009). Two sampling trips were required to the Port Dundas site, as once the sediment was oven dried, there was not enough mass remaining to complete the sorption experiments. Upon return for the second trip, the original sampling location was covered with ice that was impenetrable. Therefore, sediment was collected from a different spot along the same canal, as reflected in the GPS coordinates in Table 4.1. GPS coordinates were obtained using Google Earth.

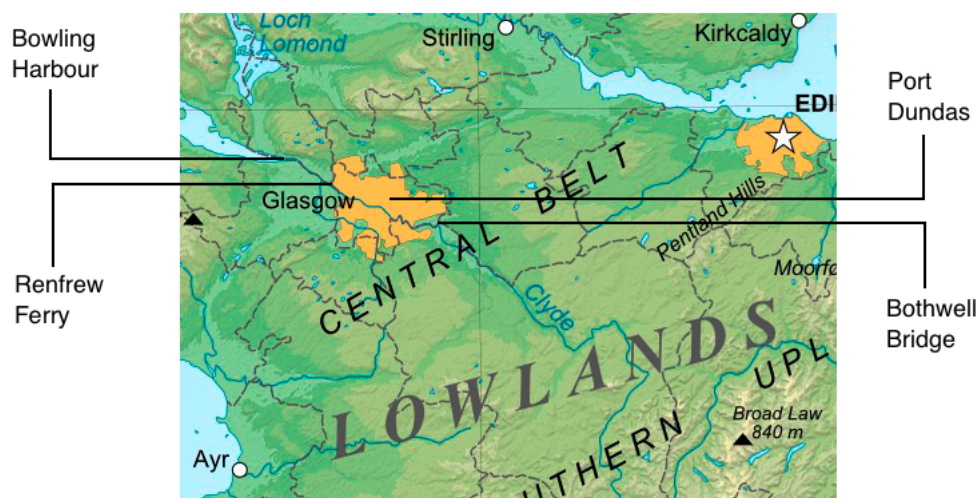


Figure 4.1: Map of the sampling locations in the vicinity of Glasgow, United Kingdom

Table 4.1: GPS coordinates of sampling locations.

Location Name	Sampling Date	GPS Coordinates
Port Dundas	06/02/2012	55°52'20.22"N 4°15'3.60"W
	26/01/2012	55°52'23.21"N 4°14'48.03"W
Renfrew Ferry	30/01/2012	55°53'8.88"N 4°22'57.99"W
Bowling Harbour	30/01/2012	55°55'48.58"N 4°29'1.20"W
Bothwell Bridge	18/01/2012	55°47'42.97"N 4° 3'29.69"W

Properties of the water at each site, including temperature, pH, conductivity, turbidity, total dissolved solids, salinity, and sediment depth were measured using a Horiba U-52G Multiparameter Water Quality Meter (Horiba, Japan). The top 10 – 15 cm of sediment was collected using a stainless steel bucket attached to a 30 m rope. Sediment was stored in plastic bottles and refrigerated at 4°C until further use.

4.2.2.2 Measurement of Total Organic Carbon

Sediment samples were sieved using a wire mesh sieve with an aperture of 2.0 mm. The total organic carbon (TOC) and moisture content of the sediment samples were determined using the American Society for Testing and Materials (ASTM) method D2974 – 07a (ASTM, 2007). Moisture content of each sediment sample was determined by heating the sample in an evaporating dish at 105°C for 16 hours, followed by heating for one hour increments until the weight was stable to the nearest 0.01 g (Equation 4.2). TOC was determined by igniting the oven dried solids at 440°C in a muffle furnace for one hour increments until there was no change in mass to the nearest 0.01 g (Equations 4.3 and 4.4).

$$\text{Moisture Content \%} = [(A - B) \times 100]/A \quad (4.2)$$

Where:

Moisture Content = percentage of total mass

A = mass of as-received test specimen, g

B = mass of oven-dried specimen, g

$$\text{Ash Content \%} = (C \times 100)/B \quad (4.3)$$

Where

C = mass of ash, g

$$\text{Total Organic Content \%} = 100 - D \quad (4.4)$$

Where:

D = ash content, %

pH of the sediment was determined using a 1:1 (w/v) slurry of water and sediment, which was stirred for 30 minutes, then left to stand for one hour before a pH reading was taken using a Mettler Toledo S47 SevenMulti™ pH meter (Mettler Toledo, UK).

4.2.2.3 Trace Elemental Metal Analysis: X-Ray Fluorescence

X-Ray Fluorescence (XRF) was used for elemental analysis of each sediment sample. Sieved (2.0 mm aperture) sediment samples were air dried overnight to remove excessive moisture. A small amount of sediment was placed into the sample container. Sufficient sample was added to fully cover the bottom of the container. XRF was carried out on a handheld Energy Dispersive X-Ray Fluorescence Spectrometer (ED-XRF), Bruker S1 Turbo LE (Bruker, UK). A 10 minute scan was run for each sample.

4.2.2.4 Crystal Lattice Analysis: X-Ray Diffraction

X-Ray diffraction (XRD) was used to determine the crystal lattice structure of each sediment sample. Sieved (2.0 mm wire mesh) sediment samples were air dried overnight to remove excessive moisture. A small amount was placed onto a quartz disc and smoothed over with a metal spatula, with care taken to ensure coarse material had been removed. XRD was carried out on a Bruker D8 Advance XRD (Bruker, UK), with a copper tube with 1.5419 [Å]. Voltage was set to 40 kV, and current at 40 mA. The step time was 0.600 s, 2Theta was run from 15-80 at increments of 0.0255.

4.2.3 Sediment-Water Partition Coefficient, K_d

The K_d values of selected MA waste impurities were measured following the ASTM standard method E1195 – 01 (ASTM, 2008). Sorption of MA, *N*-methylacetamide, P2P, and 2,6-di-tert-butylphenol (2,6-DTBP) was measured by equilibrating them in a mixture of water and sediment at constant temperature ($22^{\circ}\text{C} \pm 2^{\circ}\text{C}$). The amount of chemical added was determined by taking into account its water solubility, predicted adsorption coefficient, and limit of detection of the analytical instrument used to quantify the amount of chemical left in the aqueous phase. An initial estimate of each chemical's adsorption coefficient was determined using Equation 4.5, which predicts K_{OC} to within one order of magnitude (ASTM, 2008).

$$\ln K_{OC} = (-\ln W_S - 0.01(MP - 25) + 15.1621)/1.7288 \quad (4.5)$$

Where:

W_S = water solubility, mg/mL

MP = melting point, °C (for liquids at 25°C, MP = 25)

The water to soil ratios were calculated to achieve chemical adsorption between 20-80%. With a fixed aqueous volume of 10 mL, the water to sediment ratios used were 1:2, 1:3, and 1:5, which corresponds to 5 g, 3.33 g, and 2 g of sediment, respectively. Using 20 mL glass universal bottles fitted with tin foil lined caps, 1.0 mL of 1.0 mg/mL in water of MA, *N*-methylacetamide, and P2P was added to the sediment. The volume was brought to 10 mL using Nanopure water (Barnstead Nanopure, ThermoFisher Scientific, UK), therefore those three chemicals were present at a final concentration of 0.1 mg/mL. The concentration of 2,6-DTBP was lower because of its smaller water solubility. The water solubility of 2,6-DTBP is 2.5 mg/L at 25°C, however one half of that concentration would not completely dissolve in water at 20°C. As per the standard method, the solution was then made up in 10% ACN and 2.0 mL of 1.25 mg/L of 2,6-DTBP was added to the vials, for a final concentration of 0.025 mg/mL.

The vials were mixed on a horizontal shaker for 10 minutes, 20 minutes, 40 minutes, one hour, two hours, or four hours to determine equilibration time. The vials were then centrifuged at 4500 RPM for 10 minutes and a portion of the supernatant filtered using Pasteur pipettes plugged with glass fiber filter paper (GF/F grade, Whatman, UK). The filtered supernatant was added to 2 mL autosampler vials, to which bisphenol A (40 µL of 1.0 mg/mL in methanol) was added as an internal standard. The samples were quantified using HPLC (Dionex UltiMate 3000) with a gradient of acetonitrile (ACN) and water as follows: 20% acetonitrile (ACN), 80% H₂O for one minute, increasing to 40% ACN/60% H₂O over five minutes, and held for nine minutes for a total run time of 15 minutes. The column phase was C₁₈ (Techsphere5ODS, 25 cm x 4.6 mm) and the sample loop volume was 10 µL.

4.2.4 Organic Carbon Partition Coefficient, K_{OC}

The organic carbon partition coefficient can also be referred to as the organic carbon normalized sorption constant. The K_{OC} value factors into account the percentage of organic carbon (%OC) present in the soil or sediment, which can greatly influence the amount of adsorption. K_{OC} as

a function of K_d is given by Equation 4.6.

$$K_{OC} = \left(\frac{K_d}{\%OC} \right) \times 100 \quad (4.6)$$

In the absence of a known K_d value, K_{OW} can be used to estimate K_d using Equation 4.7, which can subsequently be substituted into Equation 4.6 to calculate K_{OC} (Andersen et al., 2005).

$$K_d = 0.39 + 0.67 \times K_{OW} \quad (4.7)$$

4.2.5 K_d and K_{OC} Revisited

After analysing the K_d and K_{OC} results from the above sections, adjustments were made and the experiments repeated with several amendments. One of the challenges with the initial experiment was matrix interference effects from the sediment. In an effort to negate matrix interferences, artificial soils were prepared for the sorption experiments. The chemicals tested were also changed in the second batch of experiments. P2P, MA, and *N*-methylacetamide were repeated, 2,6-DTBP was omitted while phenol and benzaldehyde, oxime were added. One additional amendment to the method was made to account for laboratory equipment malfunctions; a roller mixer was used instead of a horizontal shaker.

4.2.5.1 Artificial Soils

Three different artificial soils were prepared for the sorption experiments to provide a range of organic carbon content and to reduce matrix interferences from polluted site samples. Garden compost with 63% peat content (Verve Multipurpose Compost, B&Q, UK), sand (Portland Builder's sand), and clay (WBB Minerals, UK) were mixed with silt collected from a stream in Calderglen Country Park, Glasgow, UK (55°44'57.48"N, 4° 8'34.40"W). The particle size of sand, silt, and clay as defined by British Standard BS 3882:2007 (British Standards, 2007) is shown in Table 4.2. The collected silt was oven dried at 110°C overnight, ground with a mortar and pestle, and subsequently sieved through sieves with the following aperture sizes: 2 mm, 1.18 mm, 600 µm, 425 µm, 300 µm, 212 µm, 150 µm, and 63 µm. The portion passing through the

63 μm sieve was retained as “silt” and used in the preparation of the artificial soil.

Table 4.2: Particle size of sand, silt, and clay according to British Standard BS 3882:2007 (British Standards, 2007)

Sand	Silt	Clay
2000 μm - 600 μm	60 μm - 2 μm	< 2 μm

The composition of each soil is shown in Table 4.3. Each soil is classified as sandy loam according to BS 3882:2007 (British Standards, 2007). The artificial soils were characterized identically to the collected sediments, as described in Section 4.2.2 on page 132. Characterisation tests included: pH, moisture content, organic carbon content, XRF, and XRD analysis. Additionally, the individual sand, silt, and humus components were subject to particle size distribution. Clay was not subject to particle size distribution analysis as it was commercially purchased to industry standards in order to be classified as “clay”.

Table 4.3: Percentage of soil components in each artificial soil

	Soil #1	Soil #2	Soil #3
Sand	41.56	58.17	78.85
Silt	5.55	7.29	9.41
Clay	2.79	3.65	4.70
Humus	50.10	30.89	7.04

4.2.5.2 Particle Size Distribution

Particle size distribution of the humus, sand, and silt used for the artificial soil mixtures was undertaken in triplicate following British Standard Method BS 11277:2009 (British Standards, 2009). The humus, sand, and silt were dry-sieved using wire mesh sieves with the following apertures: 2 mm, 1.18 mm, 600 μm , 425 μm , 300 μm , 212 μm , 150 μm , and 63 μm . The sieves were stacked on top of each other in order from smallest mesh size at the bottom to the largest mesh size at the top, with a collection plate underneath the 63 μm sieve. 200 g to 250 g of sample was weighed out and placed in the sieve with the largest aperture, 2 mm. A lid covered the top sieve and the stack of sieves was placed on a mechanical shaker and left to shake for 20 minutes. The material in each sieve was weighed and a percentage of the overall mass determined.

The fraction of the “silt” portion passing through the 63 μm sieve was collected for sedimentation tests to determine if it is classified as silt according to BS 3882:2007 (British Standards, 2007). Triplicate sedimentation analysis of the < 63 μm portion was carried out as follows. Ten grams of sample was placed in a 250 mL conical flask along with 30 mL of deionized water and 30 mL of 30% hydrogen peroxide. The mixture was left to stand covered overnight to dissolve organic matter. The following morning, the mixture was gently heated to a boil to bubble off any remaining hydrogen peroxide. Once the bubbling had stopped, the flask was removed from heat and diluted with 100-150 mL of deionized water. The sediment/water mixture was centrifuged (4500 RPM for 20 minutes) in batches until the supernatant was clear. The sediment was mixed with 150 mL of deionized water to rinse out the flasks and transfer the contents to a 250 mL plastic bottle. 25 mL of dispersing agent (33 g sodium hexametaphosphate and 7 g anhydrous sodium carbonate in 1 L of deionized water) was added and mixed on an end-over-end shaker for 18 hours. The contents of the bottle were transferred to a sedimentation tube; in this case a 500 mL glass measuring cylinder was used. The volume in the cylinder was topped up to the 500 mL mark with water. The cylinder was capped with a rubber bung and shaken end over end for two minutes. As soon as the cylinder was placed onto the bench top, a stopwatch was started. Samples were collected at set time points according to the method, as determined by the temperature of the room in which the experiment was being conducted. In this case, the room temperature was 20°C, therefore the time points were as follows: 56s, 4m38s, 51m35s, and 7h44m16s. Those time-points corresponded to particle sizes of 63 μm , 20 μm , 6 μm , and 2 μm , respectively. When samples were collected at each time-point, 10 mL was removed from the glass cylinder using a glass pipette measured to a depth of 10 cm. The collected sample was transferred to a pre-weighed porcelain evaporating dish and placed in the oven at 105°C until evaporated to dryness, as determined by consecutive weighing to the nearest 0.0001 g.

The mass of solid in a 500 mL suspension, for each pipette sampling time is calculated according to Equation 4.8.

$$mf_x = ms_x (500/V_c) \quad (4.8)$$

Where:

mf_x = mass of solid in suspension in 500 mL (g)

ms_x = mass of material from the x^{th} pipette sampling (g)

V_c = calibrated volume of the pipette (mL)

This method assumes that the sample mass is the sum of the constituent fractions, and not the mass of sample used at the beginning (10 g). This method also assumes there are no losses at each stage of sampling, drying, and weighing of each fraction.

4.2.6 Revised K_d

Similar to Section 4.2.3, the K_d values of selected MA waste impurities were measured following the ASTM standard method E1195 – 01 (ASTM, 2008). Sorption of MA, *N*-methylacetamide, phenol, benzaldehyde, oxime, and P2P was measured by equilibrating them in a mixture of water and sediment at constant temperature ($20^{\circ}\text{C} \pm 1^{\circ}\text{C}$) in the dark. The amount of chemical added was determined based on its water solubility, predicted adsorption coefficient, and limit of detection of the analytical instrument used to quantify the aqueous phase. Initial estimates of each chemical's adsorption coefficient was determined using Equation 4.5 on page 136, which predicts K_{OC} to within one order of magnitude (ASTM, 2008).

Water to sediment ratios were calculated to achieve chemical sorption between 20-80%. With a fixed aqueous volume of 10 mL, the water to sediment ratios used were 2:1, 3:1, and 5:1. Using 20 mL glass universal bottles fitted with tin foil lined caps, 1.0 mL of 1.0 mg/mL in water of MA; *N*-methylacetamide; phenol; benzaldehyde, oxime; and P2P was added to the sediment. The volume was brought to 10 mL using Nanopure water (Barnstead Nanopure, ThermoFisher Scientific, UK), for a final concentration of 0.1 mg/mL. The contents of the vials were mixed on a roller shaker for one, two, four, eight, 24, or 48 hours. Vials were centrifuged at 4500 RPM for 10 minutes and the supernatant filtered using a membrane syringe filter (0.45 μm ; Millex MF-Millipore™). The filtrate was added to 2 mL autosampler vials, to which bisphenol A (40 μL of 1.0 mg/mL in methanol) was added as internal standard.

Samples were quantified using HPLC (Dionex UltiMate 3000) with a C18 column (25 cm x 4.6 mm, Techsphere5ODS) and a sample loop volume of 10 μL . The mobile phase was a gradient of acetonitrile (ACN) and water as follows: 20% ACN, 80% H_2O for one minute, increasing to

40% ACN/60% H₂O over five minutes, and held for seven minutes for a total run time of 13 minutes.

4.3 Results and Discussion

4.3.1 Octanol-Water Partition Coefficient

The octanol-water partition coefficient is a measurement of the concentration of a chemical in octanol versus the concentration of the chemical in water in a two-phase system at equilibrium. As octanol mimics the lipid layer, K_{OW} values are often used to estimate lipophilicity which helps to predict water solubility, bioconcentration, biomagnification, and aquatic toxicity (USEPA, 2012b). K_{OW} can be measured by two different methods, firstly by quantifying chemical concentrations in the above mentioned two phase system (OECD “shake-flask method” (OECD, 1995)), or by using HPLC to measure the lipophilicity of a chemical (OECD, 1989). The two different methods cover a different range of log K_{OW} values, with the HPLC method appropriate for compounds with a log K_{OW} ranging from 0 to 6, while the shake-flask method is accurate for compounds with a log K_{OW} ranging from -2 to 4. The HPLC method is less sensitive to impurities in the chemical standards and can be performed much more quickly since the determination is based on retention time only and no quantification is required. Additionally, the HPLC method is fully automatable.

In the HPLC system, the octanol layer is represented by the column, which is comprised of long chain hydrocarbons (C₁₈) bonded to silica. As a chemical moves through the HPLC system and along the column, the compound partitions between the hydrocarbon stationary phase and water mobile phase. Thus the chemicals are retained based on their hydrocarbon-water partition coefficient, with water soluble compounds eluting first, and oil soluble compounds eluting last. Therefore, K_{OW} can be correlated using Equation 4.1 on page 131 based on retention times on a reversed phase column, such as a C₁₈ column.

The HPLC used in this study has a UV detector, therefore the λ max for each compound had to be determined so the detector could be set accordingly. The results of the λ max determination

scans are shown in Tables 4.4 and 4.5 for the reference compounds and MA waste compounds, respectively. Of note, *N*-methylacetamide did not show up in the UV-Vis scan from 190 nm to 400 nm. Therefore, it was presumed *N*-methylacetamide did not have a strong enough chromophore to be seen on the HPLC with a UV detector. However, when *N*-methylacetamide was run on the HPLC as part of a mixture at a wavelength of 220 nm, there was an unexpected peak. An HPLC run of *N*-methylacetamide alone confirmed, based on retention time, that the extra peak was *N*-methylacetamide.

Table 4.4: λ max and chemical structures of reference compounds (190 nm to 400 nm scan).

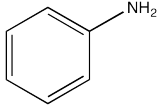
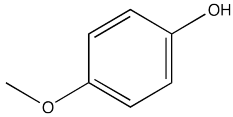
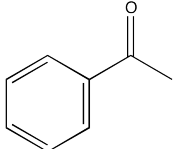
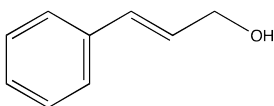
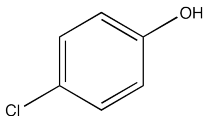
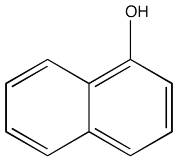
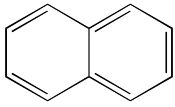
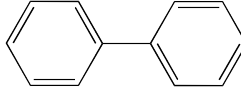
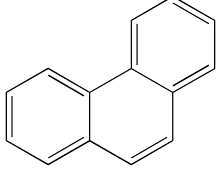
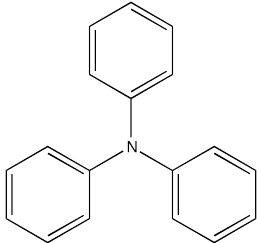
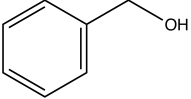
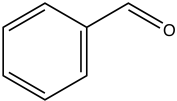
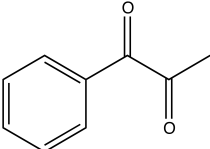
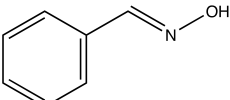
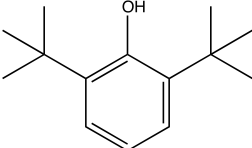
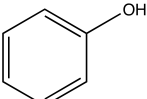
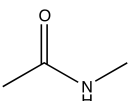
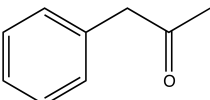
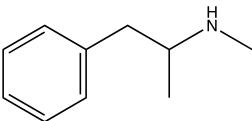
Chemical	Structure	λ max (nm)
Aniline		216
4-methoxyphenol		220
Acetophenone		220
Cinnamyl alcohol		208
4-Chlorophenol		212
1-Naphthol		220
Naphthalene		216
Biphenyl		220
Phenanthrene		220
Triphenylamine		264

Table 4.5: λ max and chemical structures of selected MA waste compounds (190 nm to 400 nm scan).

Chemical	Structure	λ max (nm)
Benzyl alcohol		212
Benzaldehyde		216
1-Phenyl-1,2-propanedione		216
Benzaldehyde, oxime		216
2,6-ditertbutylphenol		212
Phenol		220
<i>N</i> -methylacetamide		-
P2P		208
MA		212

Measured K_{OW} values can range from less than 10^{-4} to 10^{+8} , a span of at least 12 orders of magnitude. Thus K_{OW} values are often presented in their logarithmic form, often referred to as $\log P$ (Meylan and Howard, 1995). The average ($n = 3$) retention times and dead times of each standard are shown in Table 4.6 and each MA waste compound are shown in Table 4.7.

Table 4.6: HPLC dead times and retention times of K_{OW} reference materials

	RT	DT	k	$\log k$	$\log K_{OW}^*$
Aniline	3.345	2.455	2.345	0.370	0.9
4-Methoxyphenol	2.813	2.460	1.813	0.258	1.3
Acetophenone	3.564	2.462	2.564	0.409	1.7
Cinnamyl alcohol	3.280	2.456	2.280	0.358	1.9
4-Chlorophenol	3.333	2.464	2.333	0.368	2.4
1-Naphthol	3.649	2.478	2.649	0.423	2.7
Naphthalene	6.764	2.464	5.764	0.761	3.6
Biphenyl	9.129	2.462	8.129	0.910	4.0
Phenanthrene	13.402	2.462	12.402	1.094	4.5
Triphenylamine	20.357	2.444	19.357	1.287	5.7

* values from OECD (1989)

RT = Retention time (minutes)

DT = Dead time (minutes)

$$k = \frac{RT-DT}{DT}$$

Table 4.7: HPLC dead times and retention times of MA waste components

	RT	DT	k	$\log k$
Benzyl alcohol	2.971	2.456	1.971	0.295
Benzaldehyde	-	-	-	-
1-phenyl-1,2-propanedione	3.304	2.456	2.304	0.363
Benzaldehyde oxime	3.020	2.447	2.020	0.305
2,6-ditertbutylphenol	13.109	2.451	12.109	1.083
Phenol	2.891	2.458	1.891	0.277
<i>N</i> -methylacetamide	1.575	2.455	0.575	-0.240
P2P	3.380	2.453	2.380	0.377
MA	3.733	2.466	2.733	0.437

RT = Retention time (minutes)

DT = Dead time (minutes)

$$k = \frac{RT-DT}{DT}$$

Using the listed $\log K_{OW}$ from the standard method, a calibration graph was constructed plotting $\log k$ versus $\log K_{OW}$, shown in Figure 4.2. The K_{OW} of the MA waste compounds was calculated using $\log k$ and the equation of the line from Figure 4.2. A sample calculation for MA is shown below.

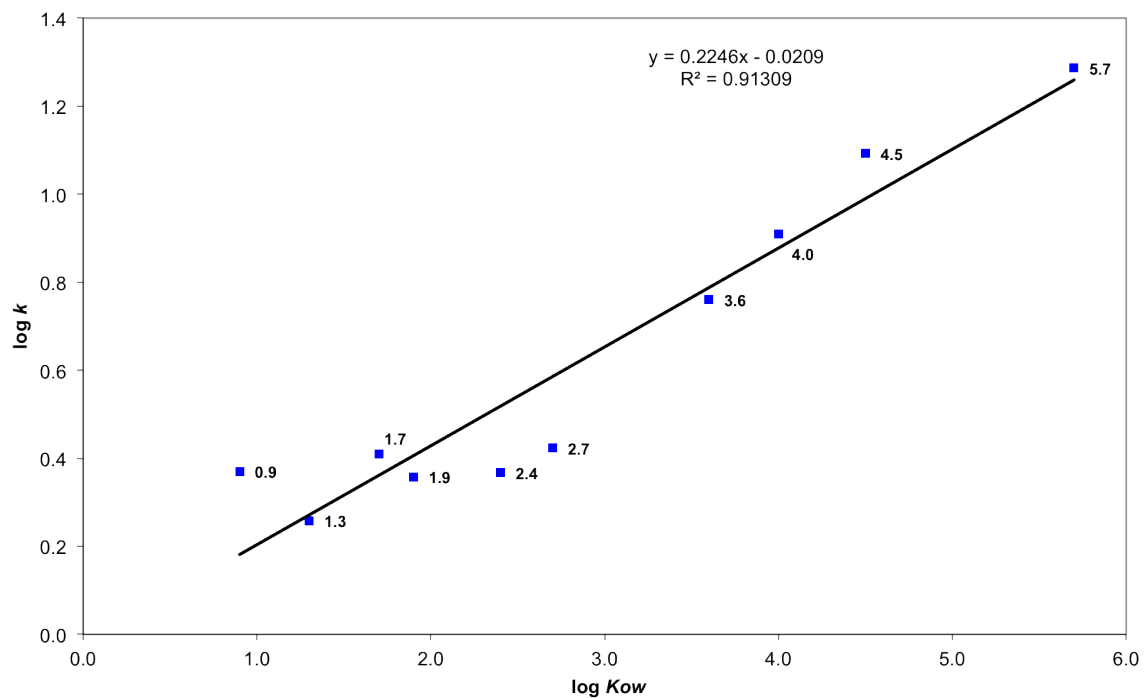


Figure 4.2: Calibration graph of HPLC $\log k$ values versus $\log K_{OW}$ standard values

For MA, $\log k = 0.437$, therefore $\log K_{OW}$ can be calculated using the equation of the line in Figure 4.2 as follows:

$$\begin{aligned}
 y &= 0.2246x - 0.0208 \\
 \log k &= (0.2246 \times \log K_{OW}) - 0.0208 \\
 \log K_{OW} &= \frac{(\log k + 0.0208)}{0.2246} \\
 &= \frac{(0.437 + 0.0208)}{0.2246} \\
 &= 2.04
 \end{aligned}$$

The log K_{OW} values of MA waste that were experimentally determined are compared with EPI Suite™ predicted log K_{OW} values in Table 4.8.

Table 4.8: Log K_{OW} values determined using OECD standard method 117 compared against EPI Suite™ estimated values.

Chemical	Log K_{OW}	
	Experimental	EPI Suite™
Benzyl alcohol	1.40	1.10
Benzaldehyde	-	1.48
1-Phenyl-1,2-propanedione	1.71	1.11
Benzaldehyde, oxime	1.45	1.85
2,6-ditertbutylphenol	4.91	4.92
Phenol	1.32	1.46
<i>N</i> -methylacetamide	-0.98	-0.70
P2P	1.77	1.44
MA	2.04	2.07

In general, small molecules with low K_{OW} values are more likely to be water soluble, whereas larger molecules with high K_{OW} values are more likely to dissolve in lipids and adsorb to solids. High K_{OW} values are also associated with a higher bioconcentration factor, which is linearly related to K_{OW} , as seen previously in Equation 2.6 (page 51). K_{OW} , which is essentially a measurement of polarity, can help to predict the distribution and persistence of a compound in the environment. Hydrophilic compounds tend to be dissolved and distributed throughout surface water, conversely lipophilic compounds tend to become associated with particulate matter, mostly sediments (Walker et al., 1996).

Benzaldehyde was an interesting molecule that resulted in three peaks in the chromatogram (Figure 4.3 on the next page). Standard solutions were re-made in order to ensure there was no contamination, however the triple peak persisted. It was attempted to use the retention time of the middle peak in Equation 4.1, however the retention time of the first peak masked the small negative peak that would indicate the dead time. Therefore, the log K_{OW} of benzaldehyde could not be experimentally determined in this study.

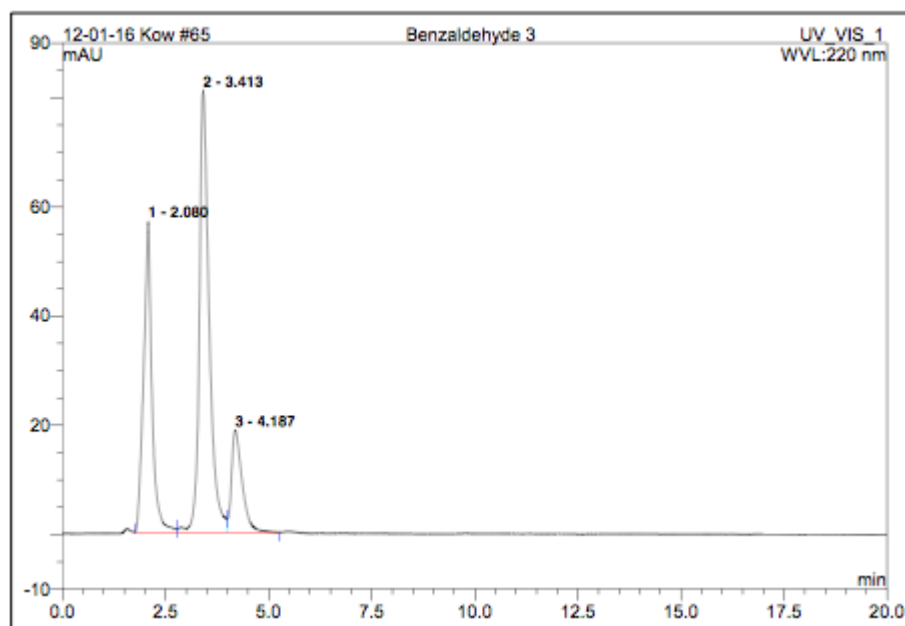


Figure 4.3: HPLC chromatogram of benzaldehyde at 220 nm.

The chemicals examined from MA waste display the following order of lipophilicity, from lowest to highest: *N*-methylacetamide < phenol < benzyl alcohol < benzaldehyde, oxime < 1-phenyl-1,2-propanedione < P2P < MA < 2,6-DTBP. Using the linear relationship between K_{OW} and BCF (Equation 2.6 on page 51), the same order can be applied towards the tendency of these chemicals to accumulate in aquatic organisms.

Comparison of the experimental values with the EPI Suite™ shows no general trend for the accuracy of the predicted values; that is EPI Suite™ does not consistently over or under estimate $\log K_{OW}$ values. Given the large range of K_{OW} values and their reporting on a log scale, the experimental values are remarkably similar to the computer estimated values. The experimental and predicted $\log K_{OW}$ values of 2,6-DTBP were nearly identical, whereas the largest difference in values was for 1-phenyl-1,2-propanedione, with a difference of 0.60.

Even though the $\log K_{OW}$ values are remarkably equivalent over the log scale, the differences become more apparent when the log function is removed, which may affect environmental compartment distribution. The effects of the differences in $\log K_{OW}$ on the environment will be investigated using a fugacity model in Chapter 5.

The EPI Suite™ K_{OW} estimation model is based on the methodology published by Meylan and Howard (1995), which uses a type of QSAR model to calculate K_{OW} values. The EPI Suite™ model is a “fragment constant” method, where a structure is divided into fragments - atoms or functional groups - and a coefficient value assigned to each atom or group. The coefficient values were determined using multiple regression analysis of 2447 reliably measured $\log K_{OW}$ values. By adding together the coefficient values for a compound, an estimate of $\log K_{OW}$ can be calculated. Correction factors may also be applied for more complex atoms which correct for steric interactions, hydrogen bonds, and effects from polar functional groups. Correction factors fall into two categories: factors involving aromatic ring substituent positions, and miscellaneous factors. Correction factor values were derived from the differences between $\log K_{OW}$ estimates from atoms alone and the measured $\log K_{OW}$ values. Equation 4.9 is the general equation derived from successive multiple regressions for the estimation of $\log K_{OW}$ of any organic compounds, as derived by Meylan and Howard (1995).

$$\log K_{OW} = \sum (f_i n_i) + \sum (c_j n_j) + 0.229 \quad (4.9)$$

Where:

f_i = coefficient for each atom/fragment

n_i = the number of times the atom/fragment occurs in the structure

c_j = coefficient for each correction factor

n_j = the number of times the correction factor occurs in the molecule

There are, however, several assumptions of the EPI Suite™ estimation model. Firstly, the molecular weight range for the 2447 training compounds was 18.02 to 719.92, with an average of 199.98. $\log K_{OW}$ estimates may not be as accurate for compounds outside that range, which for this study includes 2,6-DTBP with a molecular weight of 203.32 g/Mol . A more important assumption for the model is that the estimates apply to the non-ionised form of the compound. If a compound is ionisable, its $\log K_{OW}$ value can vary greatly with pH. In general, when compounds exist predominantly in their ionised form, the $\log K_{OW}$ value will be lower than the non-ionised form. Most $\log K_{OW}$ values are measured around pH 7.4, a physiologically important pH for drug discovery. The degree of ionisation would depend on the pH of the substrate and the pK_a of the compound under investigation. A formula can be used to “correct”

$\log K_{OW}$ values for ionisation (Equation 4.10).

$$\log K_{OW}(\text{corrected}) = \log K_{OW}(\text{at pH } 7.4) + \log(1 + 10^{(pKa-7.4)}) \quad (4.10)$$

Unfortunately, pKa values are not available for many compounds. There are computer programmes available that estimate pKa values, however they are still only estimates. The pKa values for three of the compounds identified from the MA waste were found in published material. The pKa values for phenol (9.99) and benzaldehyde (14.90) were obtained from the CRC Handbook of Chemistry and Physics (2010), while the pKa value of MA (9.9) was obtained from Castiglioni et al. (2011). Estimated pKa values using the properties calculator on chemicalize.org from ChemAxon (2013) are shown in Table 4.9.

Table 4.9: Computer estimated pKa values of MA waste components using chemicalize.org (ChemAxon, 2013)

	pKa 1	pKa 2	Ionised at pH 7.4
Benzyl alcohol	15.02	-2.79	no
Benzaldehyde	-7.11		no
1-phenyl-1,2-propanedione	16.92	-8.11	no
Benzaldehyde oxime	8.74	2.85	no
2,6-ditertbutylphenol	11.26	-4.60	no
Phenol	10.02	-5.48	no
<i>N</i> -methylacetamide	16.47	-1.09	no
P2P	15.92	-7.37	no
MA	10.2		yes

Despite the differences between published values and the computer calculated values, the trend of MA waste components is to be in their neutral form at pH 7.4. The only compound tested in this study which will be ionized at pH 7.4 is MA. With a pKa value of 9.9-10.2, MA will remain in its protonated form until the pH reaches 10. While a pH of 7.4 may not always reflect environmental conditions, neither does a pH of 10. Is it unlikely for MA to be found in its neutral form unless it is in a highly polluted area where the pH is very basic. While a correction factor exists to take into account different pH and pKa values, ultimately the $\log K_{OW}$ of MA was measured at a neutral pH, therefore this value is more likely to be a reflection of the behaviour of MA in the environment, rather than a corrected value.

The OECD standard method used in this study for the determination of K_{OW} was carried out under neutral conditions. This may not always reflect environmental conditions, however neither do the extremes of 2 or 10. If the chemical is predominantly in its ionised form in the environment, then its log K_{OW} value may be lower. Under those circumstances, the chemical may be more water soluble and less likely to accumulate in lipids.

An example of how environmental conditions affect log K_{OW} values was investigated by Bangkedphol et al. (2009), who studied the effect of salinity on log K_{OW} values. They used the OECD shake-flask method to measure the K_{OW} value of tributyltin (TBT). In choosing that method, they were able to vary the salinity of the water phase. TBT is an anti-fouling paint formerly used extensively on the hulls of ships before being regulated in 2002. Due to its prevalence in the marine environment, the investigation into the effects of salinity on K_{OW} would be important for accurately predicting the behaviour of TBT in the environment. The researchers determined that an increase in salinity also increased the log K_{OW} of TBT, which would lead to an increase in the accumulation and persistence of TBT in the lipids of aquatic organisms. Thus it is important to consider the environmental conditions where the pollutants are likely to be found.

For the MA waste components examined in this study, the two chemicals of most concern are MA and 2,6-DTBP. MA has been used for many years in pharmaceutical products that have been detected in the environment. Thus MA is a physiologically active compound with a log K_{OW} of 2.04-2.07, which is the second highest of the compounds studied here and may indicate a propensity for MA to accumulate in lipids. 2,6-DTBP has a much higher log K_{OW} value of 4.92, which is predicted to have a much higher aquatic toxicity and bioconcentration factor, potentially being the most harmful component of MA waste (see Section 5.3.4 on page 223).

Organic chemicals, such as 2,6-DTBP, with high log K_{OW} values have a tendency to be adsorbed to sediment, rather than remain dissolved in the water. As such, their accessibility to aquatic organisms may be limited to bottom-dwelling organisms who consume sediment along with the intake of food (Walker et al., 1996). If the sediment was fine enough, it may become disturbed and travel throughout the water compartment as particulate material, which could be consumed by other aquatic organisms. Once the sediment has been consumed by the organism, the desorption

of the chemical into the lipids will depend on the strength of the chemical-sediment bond, the species in question, and may also depend on the temperature, pH, and oxygen content of the ambient water (Walker et al., 1996).

Overall, the OECD standard method for the measurement of K_{OW} by HPLC showed only minor differences with the EPI Suite™ computer estimated values. However, both of those methods calculate K_{OW} under standard, ideal conditions which may not reflect environmental conditions. These predictive models would be a good starting point for assessing the environmental impacts of a new chemical. They would serve as the lower estimate for a chemical's harmfulness, which may prompt further studies which take into account environmental conditions before a chemical is released onto the market. If a new chemical cannot pass the lowest estimate, it would be an indication to halt or re-evaluate further development.

4.3.2 Characterisation of Sediment

4.3.2.1 Sample Site Characteristics

The sampling site data for collected sediments used in the first adsorption experiments are shown in Table 4.10. The measurement of dissolved oxygen (DO) content in the water was producing readings much higher than 100%. It was determined that the DO probe on the field instrument was not properly calibrated prior to use, therefore DO readings were omitted.

Table 4.10: Sampling site data and sediment properties.

	Port Dundas		Renfrew	Bowling	Bothwell
	1	2	Ferry	Harbour	Bridge
Temperature (°C)	8.25	6.82	5.34	5.23	4.89
pH	7.47	7.96	7.58	7.76	8.20
Conductivity (mS/cm)	0.58	0.52	1.14	4.82	0.39
Turbidity (NTU)	17.00	30.70	4.60	4.20	0.00
Total Dissolved Solids (g/L)	0.368	0.331	0.733	3.09	0.256
Salinity (ppt)	0.10	0.10	0.30	1.70	0.10
Depth (m)	1.50	1.10	1.45	0.65	0.25

4.3.2.2 Sediment Properties

The physical properties of the collected sediments and artificial soils are shown in Table 4.11. For organic compounds, adsorption to sediment generally increases with increased organic carbon content. The organic carbon content is also important to measure in order to determine K_{OC} for a site specific model.

Table 4.11: Sediment properties of collected sediments and artificial soils.

	Port Dundas		Renfrew	Bowling	Bothwell	Soil	Soil	Soil
	1	2	Ferry	Harbour	Bridge	#1	#2	#3
pH of sediment	6.97	7.64	7.01	7.52	7.20	5.39	5.50	5.77
Moisture Content (%)	95.04	87.47	70.80	25.43	21.81	13.90	8.75	2.11
TOC (%)	30.63	22.34	9.79	5.17	1.04	7.46	4.37	1.44

4.3.2.3 Elemental Analysis of Soil Using XRF

X-ray fluorescence is a non-destructive technique for the elemental analysis of a variety of different materials, such as metal alloys, plastics, soils, paints, and paper. The XRF used in this study is capable of quantification and qualification of 41 different elements (Bruker, 2013). XRF works on the principle that materials can become ionized when bombarded with short wavelength radiation. When an inner valence electron is ejected from an atom, an electron from an outer shell will drop into the void. This results in the emission of an x-ray photon equal in energy to the energy difference between the two shells. Elements can be identified due to the characteristic transition between specific orbitals in a particular element (Verma, 2007; Wirth and Barth, 2012).

XRF was used to measure the elemental composition of the soils and sediments used in the adsorption studies. XRF data from the three collected sediments is shown in Table 4.12; XRF analysis of the artificial soils is shown in Table 4.13; while the individual components of the artificial soil are shown in Table 4.14.

Table 4.12: Elemental composition of collected sediment samples using XRF (+/- refers to instrument margin of error in ppm)

Element	Bowling		Port Dundas		Bothwell	
	ppm	+/-	ppm	+/-	ppm	+/-
SiO ₂	139,000	25,000	24,000	18,000	558,000	29,000
Ca	4,760	139	9,700	134	2,880	138
Ti	4,050	62	966	37	2,460	59
V	96	44	58	33	0	0
Cr	176	21	92	16	38	21
Mn	635	12	369	9	469	6
Fe	37,000	60	21,000	36	21,000	43
Co	28	1	4	0	1	1
Ni	18	4	18	3	11	4
Cu	61	4	103	4	39	4
Zn	171	3	656	4	72	2
As	15	2	31	2	4	2
Se	8	2	8	1	8	2
Br	372	8	102	8	0	0
Rb	47	2	11	1	22	2
Sr	99	2	68	1	69	2
Zr	130	2	25	2	318	2
Nb	9	2	2	2	2	2
Sn	35	100	0	0	35	113
Ba	391	275	0	0	475	270
Pb	63	4	128	4	17	5
Pd	0	0	0	0	24	5
U	0	0	0	0	0	0
Hf	0	0	0	0	0	0
Ta	0	0	0	0	0	0
W	0	0	0	0	0	0
Bi	0	0	0	0	0	0

Table 4.13: Elemental composition of artificial soil samples using XRF (+/- refers to instrument margin of error in ppm)

Element	Soil #1		Soil #2		Soil #3	
	ppm	+/-	ppm	+/-	ppm	+/-
SiO ₂	325,000	25,000	357,000	27,000	410,000	28,000
Ca	3,050	132	2,930	138	2,640	136
Ti	2,360	54	2,910	60	3,010	60
V	37	37	41	39	49	38
Cr	45	19	29	20	25	20
Mn	422	11	461	12	437	11
Fe	15,000	34	17,000	40	17,000	39
Co	0	0	0	0	0	0
Ni	11	3	10	4	11	4
Cu	49	4	63	4	73	4
Zn	44	4	52	2	52	2
As	6	2	11	2	5	2
Se	8	1	8	2	8	2
Br	26	7	19	7	12	7
Rb	53	2	61	2	59	2
Sr	79	2	98	2	86	2
Zr	165	2	186	2	194	2
Nb	0	0	0	0	0	0
Sn	0	0	0	0	0	0
Ba	339	248	294	270	426	268
Pb	12	4	9	5	16	5
Pd	0	0	0	0	0	0
U	6	3	8	3	7	3
Hf	0	0	0	0	0	0
Ta	0	0	0	0	0	0
W	0	0	0	0	0	0
Bi	0	0	0	0	0	0

Table 4.14: Elemental composition of artificial soil sample components using XRF (+/- refers to instrument margin of error in ppm)

Element	Silt		Sand		Clay	
	ppm	+/-	ppm	+/-	ppm	+/-
SiO ₂	384,000	38,000	498,000	27,000	218,000	26,000
Ca	5,570	169	2,020	127	1,330	129
Ti	11,000	101	1,130	48	4,860	70
V	193	54	55	33	95	45
Cr	228	27	42	19	36	21
Mn	1,760	20	285	10	183	10
Fe	72,000	106	11,000	28	9,610	29
Co	78	1	0	0	0	0
Ni	41	3	0	0	16	4
Cu	414	8	25	4	45	5
Zn	291	4	28	3	48	5
As	9	2	5	2	28	2
Se	8	2	8	2	10	2
Br	80	7	0	0	0	0
Rb	65	2	51	2	176	2
Sr	154	2	75	2	105	2
Zr	522	3	141	2	135	2
Nb	24	3	0	0	0	0
Sn	0	0	0	0	91	90
Ba	810	384	296	241	402	289
Pb	84	6	0	0	64	5
Pd	0	0	0	0	0	0
U	6	4	0	0	73	4
Hf	0	0	0	0	20	6
Ta	0	0	0	0	2	0
W	0	0	0	0	8	3
Bi	0	0	0	0	48	5

For all nine compounds analysed, silica was the most abundant compound, which was to be expected as silica is the backbone of soil colloids.

In all three collected sediments, the element with the next highest abundance is iron, followed by calcium and titanium. The proportions of each varied by location, with Bothwell Bridge having the highest amount of silica, and lowest amount of calcium and iron. Bothwell Bridge

also corresponds to the sediment with the lowest organic carbon content and was a much coarser, sandy sediment compared to the other two sites. Port Dundas, the most polluted site, had a clay-like texture and the lowest silica and highest calcium composition of the three sites. Bowling Harbour, which is still an active harbour, had the highest proportion of iron, likely on account of the high boat traffic in the area.

For the artificial soils, the proportions of the trace elements did not change much, however the difference in silica composition is noticeable and corresponds directly with the manufacture of the soils. Soil #1 had the lowest percentage of sand, whereas soil #3 had the highest. This is reflected in the difference in silica readings from the XRF.

In Table 4.14, the individual soil components, humus is missing. That is because there were not enough trace elements present to register a response on the instrument. Once again, the highest readings after silica were from iron, titanium, and calcium. The iron levels in the collected silt were quite high at 72,000 ppm and is the highest iron reading of all nine samples.

Trace metal contamination in soils and sediments can have an effect on adsorption of other contaminants. Trace metals may form organo-metallic complexes which increase adsorption of negatively charged species. As previously mentioned, the only ionised compound in MA waste at pH 7.4 is MA itself, which is present in its protonated form. Organo-metallic complexes are not predicted to be a significant force of adsorption.

4.3.2.4 Crystal Lattice Analysis Using XRD

The inorganic fraction of soils and sediments is comprised of rocks and minerals of various sizes. These minerals are arranged into different crystal lattice structures depending on their molecular composition, mostly made up of silicates and oxides. It is the finer portion, clay, that exhibits colloidal properties, and thus participates in chemical reactions (Tan, 1998).

The simplest lattice structure is a silica SiO_4 tetrahedron (Figure 4.4), which can combine to form sheets by sharing an oxygen, also shown in Figure 4.4 on the following page (Tan, 1998).

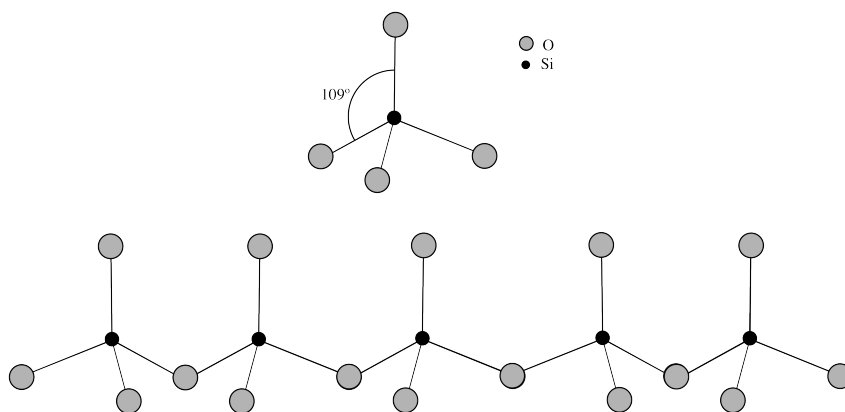


Figure 4.4: Molecular structure of a single silica tetrahedron (top) and silica tetrahedron sheet (bottom) (reproduced from Tan, 1998).

Silica oxides will also form complexes with aluminium oxide octahedrons (Figure 4.5) to form aluminosilicate sheets (Tan, 1998).

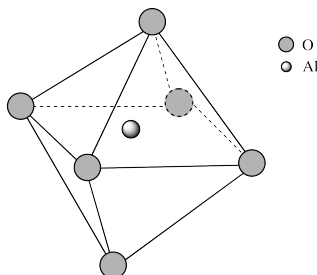


Figure 4.5: Aluminium oxide octahedron (reproduced from Tan, 1998).

In addition to the formation of sheets with different complexes, clays can also be stacked layers. The structure of stacked layers can vary according to how many types of units are stacked together and the order or disorder of the packing (Tan, 1998).

An example of layer clays is kaolinite (Figure 4.6 on the next page) which is a 1:1 layer clay of stacked hydrated aluminosilicates. This crystal is composed of aluminium octahedra sheets stacked above silica tetrahedron sheets, with a chemical composition of $2\text{SiO}_2:\text{Al}_2\text{O}_3:2\text{H}_2\text{O}$. The lattice structure is non-symmetrical with a silica tetrahedra sheet on one side and an aluminium octahedra sheet on the other (Tan, 1998).

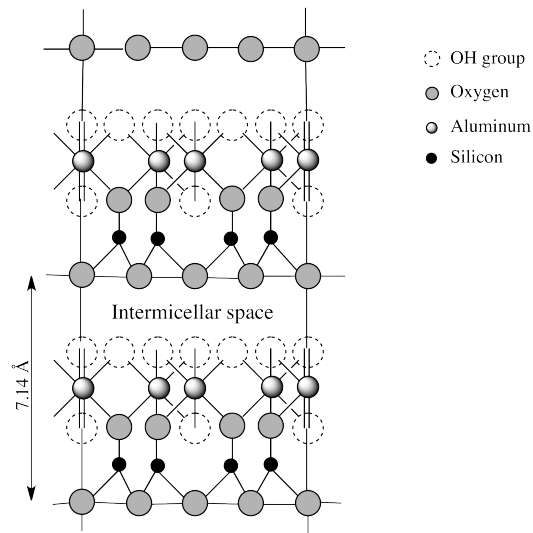


Figure 4.6: Schematic of kaolinite (reproduced from Tan, 1998).

Another 1:1 clay layer is hallocite, which is similar in structure to kaolinite, however the layers are stacked in a more disordered fashion with one or more interlayers of water. In addition to 1:1 layer clays, there are 2:1 layer clays, such as montmorillonite and illite, which have a variable composition (Tan, 1998).

XRD is the most commonly used method to identify clays. Each mineral species has a characteristic arrangement of atoms in the crystal planes. These atomic planes can diffract x-rays which produce characteristic patterns. The short wavelength of x-rays makes them able to penetrate the atomic spacings with similar dimensions. The x-ray diffraction pattern is unique to each crystal plane and thus unknown mineral species can be identified (Tan, 1998).

Using Bragg's law, the spacing between crystal planes can be determined. Bragg's law is defined in Equation 4.11, and illustrated in Figure 4.7 on the following page.

$$n\lambda = 2d \sin \theta \quad (4.11)$$

Where:

n = order of diffraction

λ = wavelength

d = spacings between atomic planes

ϑ = glancing angle of diffraction

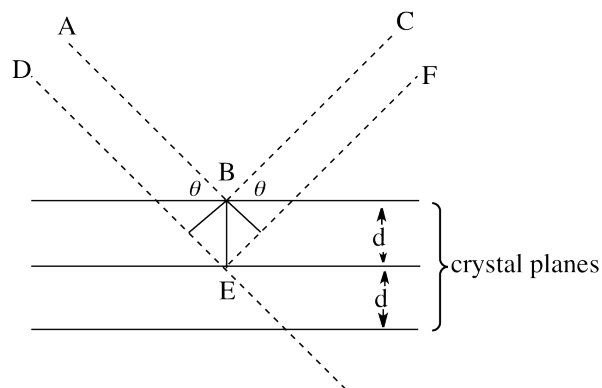


Figure 4.7: Illustration of x-ray beam diffracting from crystal planes following Braag's law (reproduced from Tan, 1998)

XRD is a non-destructive technique, however it is not suitable for the analysis of amorphous or non-crystalline compounds. As a result, the analysis of the humus component yielded a low detector response and few identifiable fragmentation patterns (Figure 4.8).

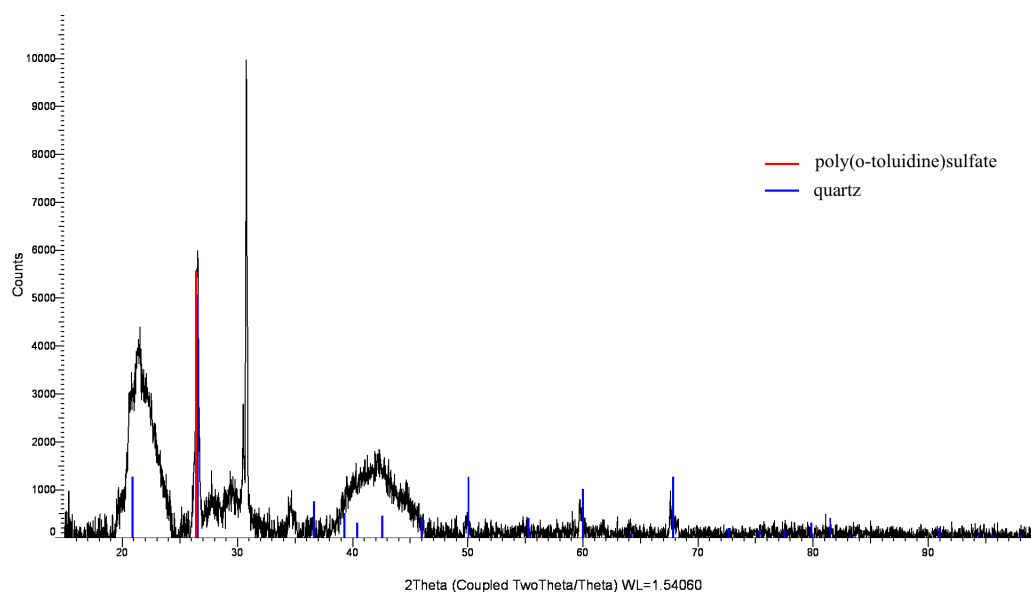


Figure 4.8: XRD spectra of humus component of artificial soils

The minerals identified in the soils tested are: quartz, kaolinite, illite, and montmorillonite.

Quartz was by far the most abundant mineral identified. A summary of the minerals identified in each sample is shown in Table 4.15. The XRD spectra for each sample are presented in Appendix B on page 278.

Table 4.15: Minerals identified in soil and sediment samples from XRD analysis

Sample	Minerals
Port Dundas	quartz, gypsum
Bothwell Bridge	quartz
Bowling Harbour	boron nitride, montmorillonite, quartz
Soil #1	quartz
Soil #2	quartz
Soil #3	quartz
Humus	quartz, poly(o-toluidine)sulfate
Sand	quartz, montmorillonite
Silt	quartz, kaolinite, illite
Clay	dickite, kaolinite, quartz

4.3.2.5 Lattice Spacing and Adsorption

The d-spacing of the crystal lattice can have an influence over the adsorption of a compound as adsorption may increase or decrease depending on the size of the molecule. The d-spacing of minerals identified in the soils samples (Table 4.16) was compared to the van der Waals volume of MA waste components (Table 4.17 on the following page).

Table 4.16: d-spacing of common clay lattice structures detected in XRD analysis of sample soils and sediments (from Tan, 1998)

Structural Arrangement	d-spacing
Kaolinite	7.14 Å
Illite	10 Å
Montmorillonite	12.3 Å
Quartz	4.26 Å

Table 4.17: Molecular size of MA waste components (from ChemAxon, 2013)

Chemical	van der Waals volume
Benzyl alcohol	107.43 Å ³
Benzaldehyde	101.21 Å ³
1-phenyl-1,2-propanedione	137.54 Å ³
Benzaldehyde oxime	112.57 Å ³
2,6-ditertbutylphenol	227.73 Å ³
Phenol	90.52 Å ³
<i>N</i> -methylacetamide	75.84 Å ³
P2P	134.92 Å ³
MA	162.56 Å ³

The volume of space occupied by the MA waste components is considerably larger than the d-spacing in the identified minerals. This indicates that adsorption of those compounds will be reduced due to steric hinderance effects. The waste components may be adsorbed by surface interactions (discussed in further detail in Section 4.3.5), however they are not likely to be incorporated into the lattice structure itself simply because the molecules are too large to fit in the intermicellar spaces.

4.3.2.6 Particle Size Distribution of Artificial Soils

Particle size can affect surface area, which correlates to the number of sorption sites. Additionally, the K_d standard method (ASTM, 2008) recommends conducting particle size distribution. This was only carried out for the second half of the study for sorption onto the artificial soils. Particle size distribution was particularly important to measure for the silt fraction in order to ensure the particle size conforms to the British Standard for top soil requirements (British Standards, 2007). The results of the sieve analysis are shown in Table 4.18 on the next page.

Table 4.18: Percent particle size distribution of components of artificial soils

Sieve Aperture	Humus	Sand	Silt
2.0 mm	71.82	0.05	3.02
1.18 mm	18.09	0.16	8.99
600 μm	9.62	0.86	16.27
425 μm	0.38	2.68	7.89
300 μm	0.05	10.77	7.85
212 μm	0.02	26.12	10.24
150 μm	0.00	19.70	7.53
63 μm	0.01	37.78	24.83

The humus size distribution is not representative of the sample. The commercially purchased humus was hand-sieved through a 2.0 mm aperture. However, with the mechanical shaker, the moist humus clumped together, resulting in the majority of the fraction remaining in the 2.0 mm sieve.

The results of the sedimentation test for size distribution of the silt sample is presented in Table 4.19. The fraction of silt used in the artificial soils was the fraction which passed through the 63 μm sieve.

Table 4.19: Sedimentation test of silt (average of three replicates)

Particle diameter	Percentage of Mass
63 μm	38.10
20 μm	27.06
6 μm	20.15
2 μm	14.69

The sedimentation test on the silt fraction confirmed that the collected material used as “silt” has a particle size consistent with British Standard BS 3882:2007 (British Standards, 2007) classification of silt (63 μm to 2 μm).

4.3.3 Sorption of MA Waste onto Sediment: Part 1

The process of adsorption is characterised as the concentration of materials on the surface. Since adsorption reactions take place on the sediment surface, at the solid-liquid interface, properties of the sediment greatly influence the adsorption of a chemical, and thus its behaviour in the environment (Tan, 1998). Adsorption is related to functional groups on the sediment surface, organic functional groups such as carboxyl groups and phenolic hydroxyl groups, and inorganic functional groups such as siloxane, oxyhydroxy, and silanol. Each functional group will possess a different charge at different pH, which can affect adsorption. Adsorption is also affected by surface area, with the amount of compound adsorbed frequently directly proportional to the surface area.

Due to the intensive nature of sorption experiments, only four compounds were selected for this portion of the study. Those four compounds were: *N*-methylacetamide, 2,6-DTBP, P2P, and MA. P2P and MA were selected as they are both controlled substances in the UK and are good potential markers for an illicit MA dumpsite. MA has been detected in several aqueous environments (Zuccato et al., 2008) and P2P is a component of MA waste synthesised via different routes. *N*-methylacetamide and 2,6-DTBP were selected because they represent the lowest and highest log K_{OW} values, respectively, and are predicted to behave completely differently in the environment. The predicted K_{OC} values for those four compounds, as calculated from Equation 4.5 on page 136, are shown in Table 4.20.

Table 4.20: Calculated $\ln K_{OC}$ values of selected MA waste impurities based on Equation 4.5 on page 136

Compound	CAS Number	Estimated $\ln K_{OC}$	Estimated K_{OC}
2,6-ditertbutylphenol	128-39-2	8.18	3568.85
<i>N</i> -methylacetamide	79-16-3	0.77	2.16
P2P	103-79-7	3.82	45.60
MA	537-46-2	2.42	11.25

However, ultimately the K_{OC} of 2,6-DTBP was not able to be determined using this methodology. According to the standard method, initial chemical concentrations should not exceed one

half of its water solubility. The water solubility of 2,6-DTBP is 2.5 mg/L at 25°C, and one half of that concentration would not dissolve in water at approximately 20°C. As per the standard method, the solution was then made up in 10% ACN. 2 mL of 1.25 mg/L of 2,6-DTBP was added to the sorption experiment vials. Once the first set of samples were analysed using HPLC, 2,6-DTPB was below the detection limits. Given the high calculated K_{OC} value (Table 4.20), this was expected as most of the chemical is predicted to adsorb to the sediment, leaving very little to detect in the aqueous layer. Subsequent preparations for the adsorption experiment omitted 2,6-DTBP.

HPLC analysis of the aqueous layer showed that for each of the five sediments, there are compounds which elute at the same time as MA. Given that the HPLC used has a UV detector, it was not possible to differentiate the peak of the sediment background from the MA peak. Subtraction of a background sample, using the instrument software, resulted in negative peaks, again masking the retention time where MA was expected to elute. Therefore, the K_{OC} value of MA could not be determined following the method used in this study. Figure 4.9 is a chromatogram overlay of all five sediment sample blanks, which shows the matrix interferences at the beginning of the chromatogram.

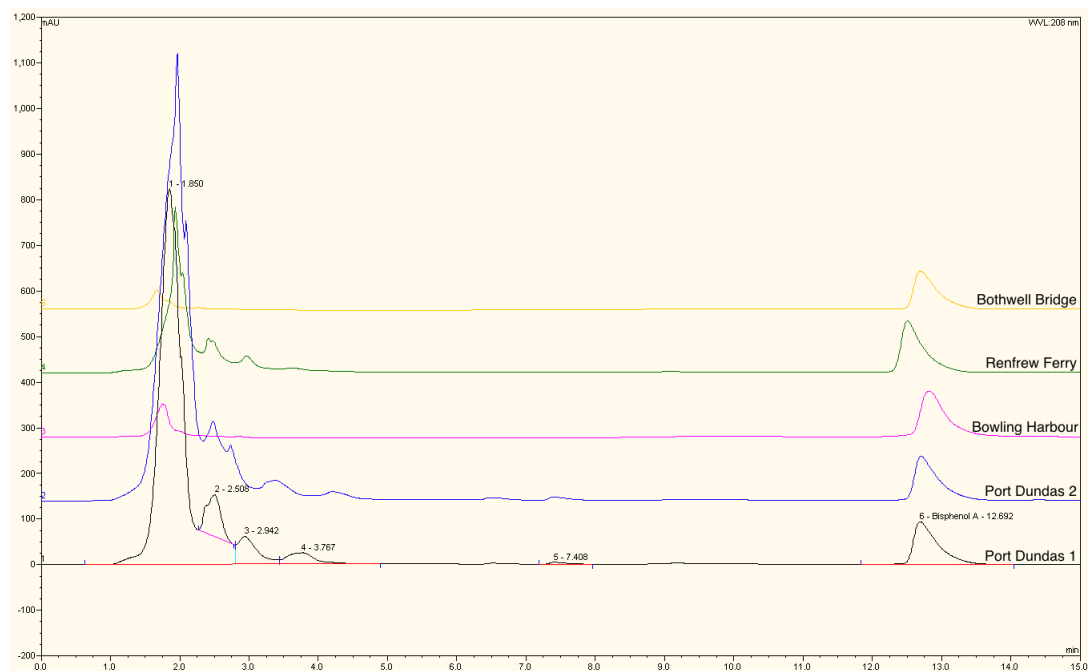


Figure 4.9: Overlay HPLC chromatogram of sediment blank samples at 208 nm.

The wavelength displayed is 208 nm, slightly below the λ max of 212 nm for MA. Samples were analysed at three different wavelengths simultaneously: 208, 212, and 220. Despite the λ max of MA being 212 nm, it displayed strongest absorbance (by peak area) at 208 nm. This is likely because of different calibrations of the different instruments used. The preliminary UV-Vis scan to determine λ max showed MA has a second chromophore at 260 nm, which has a much smaller absorbance than 212 nm. It was then attempted to run the samples at 260 nm, however even at that wavelength the matrix interferences were too strong to be able to quantify MA.

Figure 4.10 is a chromatogram from a calibration sample containing 0.05 mg/mL of MA, *N*-methylacetamide, P2P, and the internal standard, BPA. As it can be seen from the chromatogram, MA has a retention time near 1.5 minutes, which corresponds to the matrix interference seen from the sediment blanks in Figure 4.9.

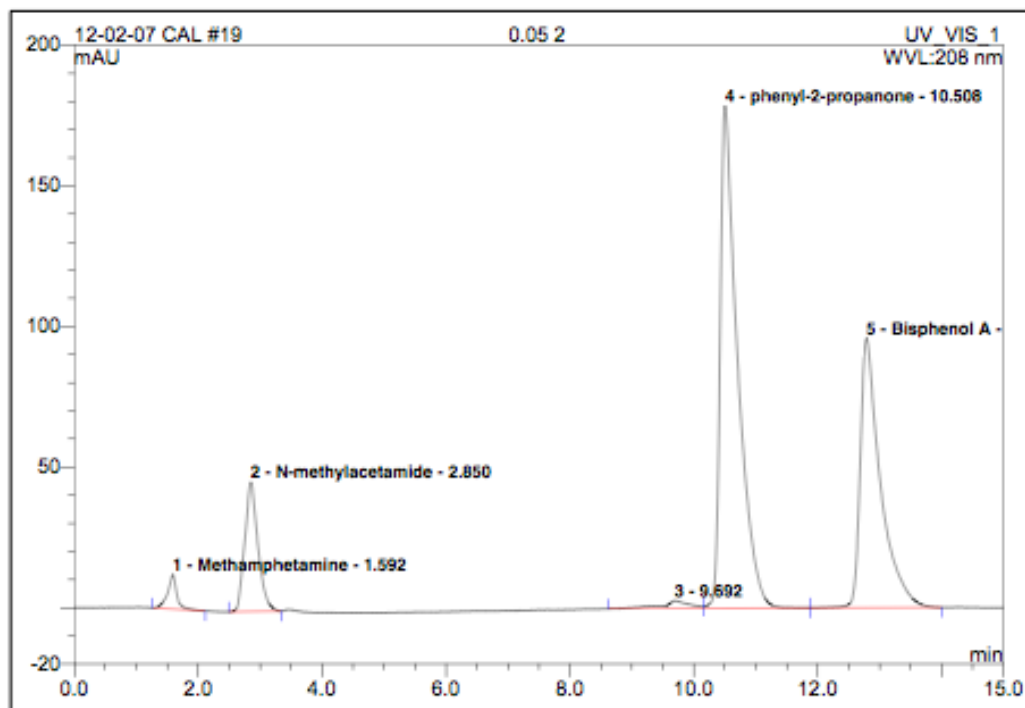


Figure 4.10: HPLC calibration sample (0.05 mg/mL) of MA, *N*-methylacetamide, P2P, and the internal standard, BPA.

Further comparison between the calibration and sediment blank chromatograms shows additional interferences with *N*-methylacetamide and three of the five sediment samples: Port

Dundas 1, Port Dundas 2, and Renfrew Ferry. This meant that reliable quantification for *N*-methylacetamide could only be accomplished in two of the five sites: Bothwell Bridge and Bowling Harbour. Fortunately, P2P eluted much later than the other two compounds and is clear of any matrix effects. Therefore, of the four compounds originally selected for adsorption analysis, only P2P was able to be fully assessed as per the ASTM standard method - which recommends using at least four different sediment samples with different TOC contents.

The measurement of the K_{OC} of P2P was not entirely successful in this study. The main obstacle was the poor condition of the horizontal shaker. The horizontal shaker was not fully functional and was not able to reach high enough rotational speeds to keep the sediment suspended at all times - a key requirement of the standard method. The result was that after the four hours of shaking, the majority of the sediment had settled to the bottom of the vials. Thus there was not enough mixing to ensure adequate surface area for the adsorption of P2P.

The lack of adsorption to the sediment was evident after quantification of the aqueous layer by HPLC. After up to four hours of shaking, many of the samples quantified had chemical concentrations which were higher than the amounts initially added to the vials. This can be accounted for by analytical error and pipette calibration. The problem with having more in the aqueous layer than was added is this gave “negative” amounts of P2P in the sediment. Figures 4.11 to 4.14 are equilibrium plots of P2P aqueous concentration versus time for each water:sediment ratio at each of the four sampling locations.

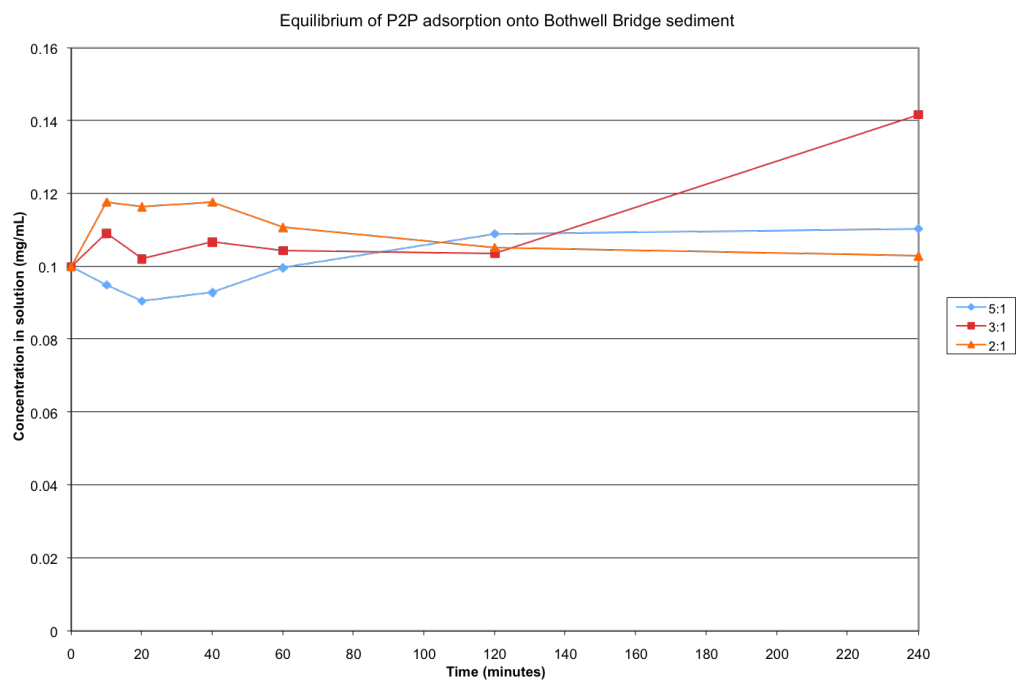


Figure 4.11: Equilibrium graph of P2P adsorption onto Bothwell Bridge sediment at three different water:sediment ratios

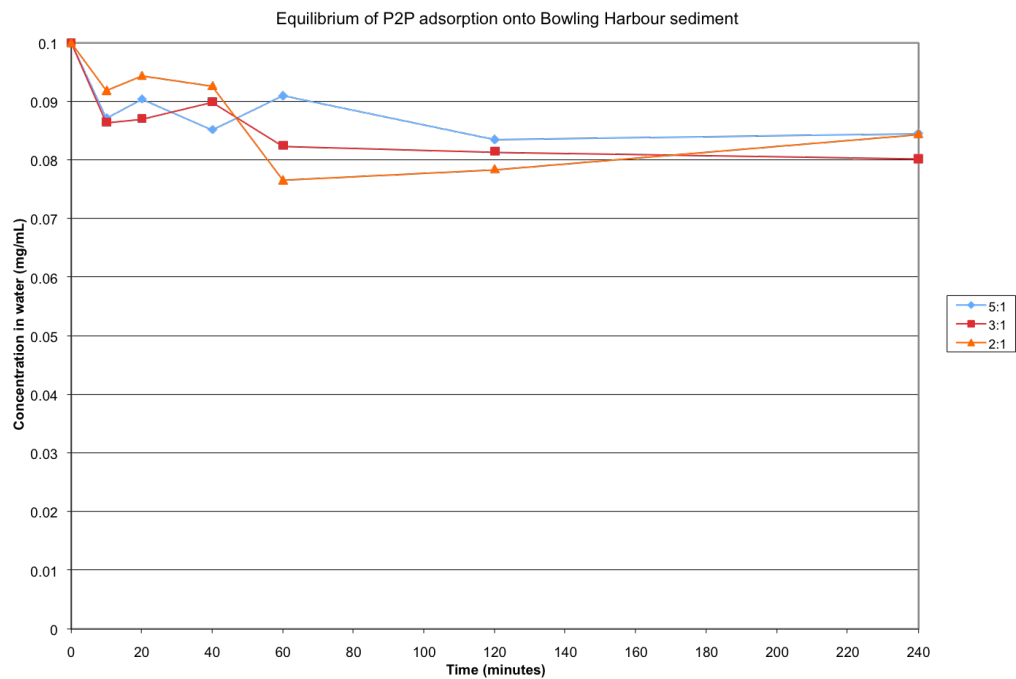


Figure 4.12: Equilibrium graph of P2P adsorption onto Bowling Harbour sediment at three different water:sediment ratios

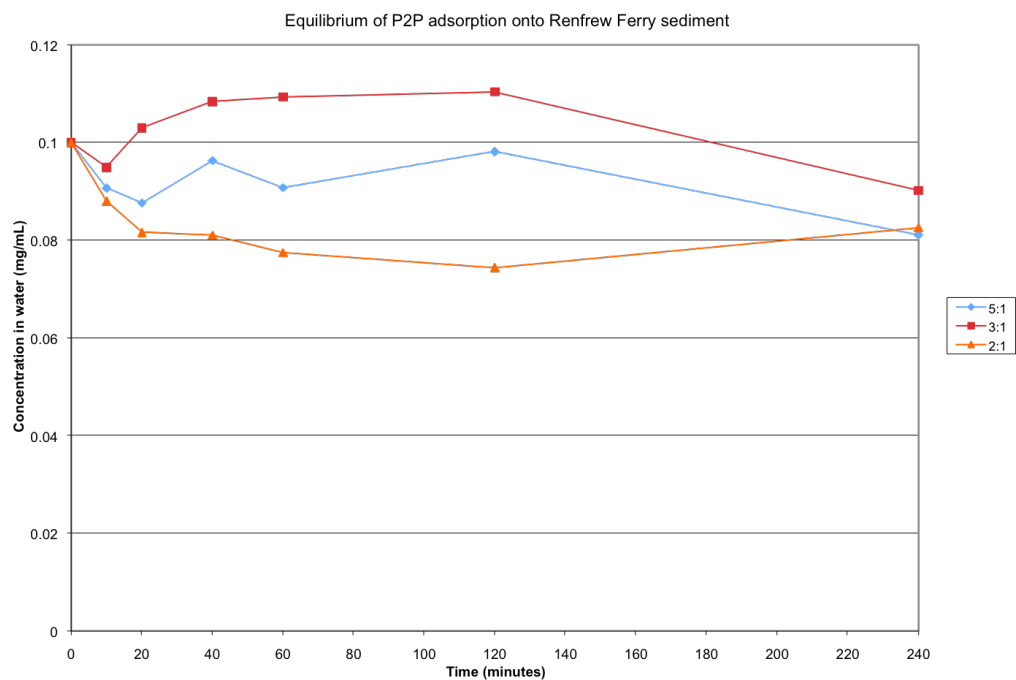


Figure 4.13: Equilibrium graph of P2P adsorption onto Renfrew Ferry sediment at three different water:sediment ratios

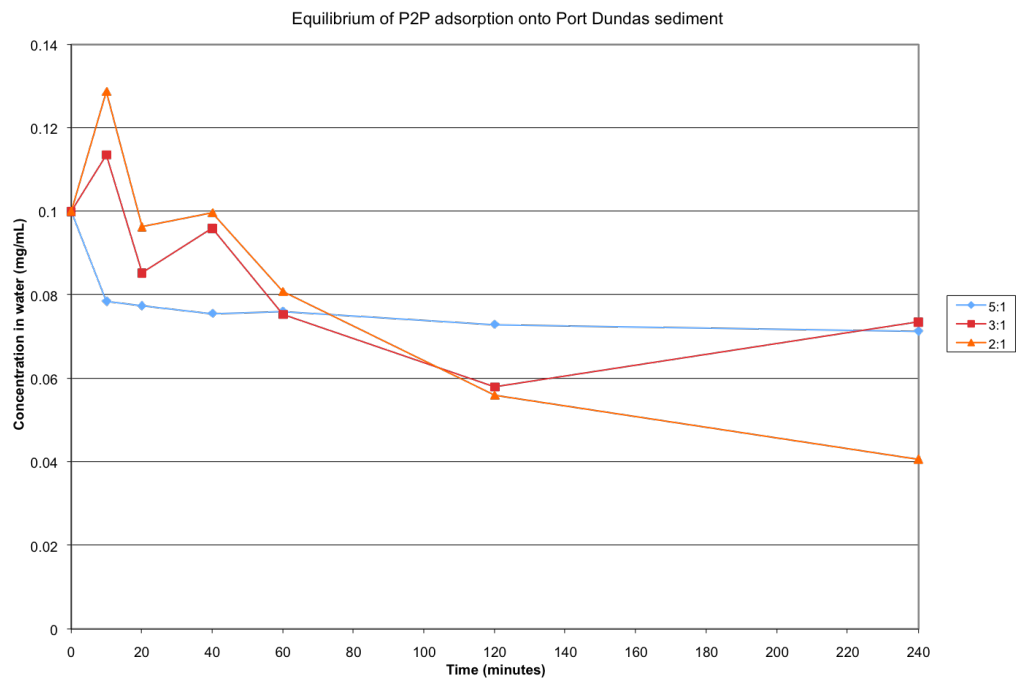


Figure 4.14: Equilibrium graph of P2P adsorption onto Port Dundas sediment at three different water:sediment ratios

As the equilibrium graphs show, an equilibrium point was reached for most sediments and most water:sediments ratios after two hours. A four hour equilibration time was selected based on the chemical structure of the analytes under study and their water solubilities. The increase in P2P concentration in the water phase in some samples was likely caused by desorption from the sediment back into the water phase. Due to the poor mixing, P2P concentrations did not significantly decrease and seemed to desorb from the sediment between two and four hours. A comprehensive desorption study would be required to assess desorption equilibrium times and amounts.

Another potential source of error in this study is the initial amount of chemical added. The initial amount of chemical added was based on preliminary EPI Suite™ estimates for the given organic carbon content of the soil. Early predictions suggested a high proportion of P2P would be adsorbed to the sediment. Thus a level was chosen that was arithmetically simple and would be within the limits of quantification of the HPLC. Unfortunately, it appears this concentration was too high and is much higher than P2P would likely be found in the environment. The effects of multiple concentrations on adsorption were not examined as the ASTM standard method emphasises that varying organic carbon content of the sediment has more of an effect on sorption than concentration effects. The method assumes that sorption isotherms are approximately linear at low solution concentrations. It appears as though for this study the concentration was too high and the sorption isotherm thus would not be linear. Furthermore, the preliminary EPI Suite™ estimates predicted P2P would partition predominantly into the sediment compartment. P2P is in fact predicted to partition mostly into the water compartment, as explored further in the next chapter.

Comparable results can be seen for *N*-methylacetamide in Figures 4.15 to 4.18. For two of the sediments, Renfrew Ferry (Figure 4.17) and Port Dundas (Figure 4.18), the matrix interferences skew the results, artificially increasing the amount of *N*-methylacetamide found in the aqueous phase.

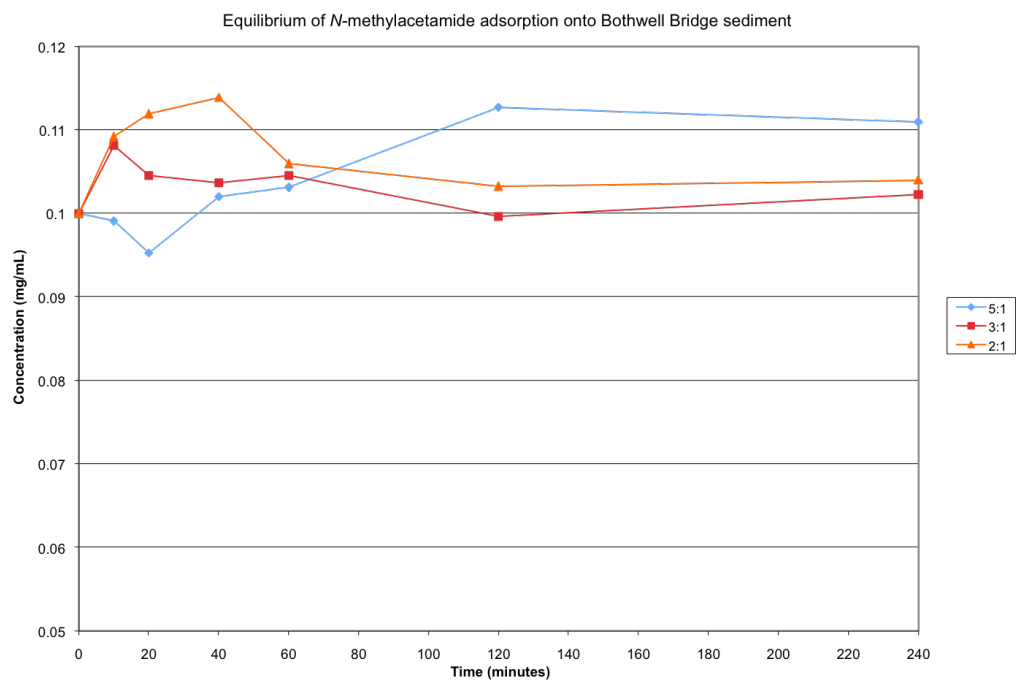


Figure 4.15: Equilibrium graph of *N*-methylacetamide adsorption onto Bothwell Bridge sediment at three different water:sediment ratios

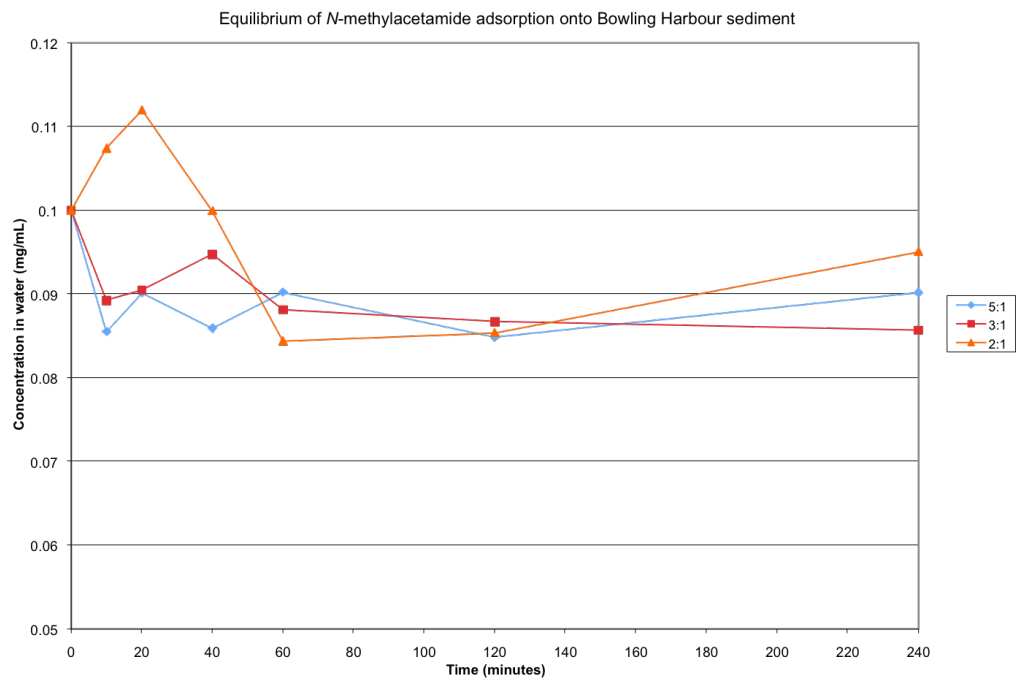


Figure 4.16: Equilibrium graph of *N*-methylacetamide adsorption onto Bowling Harbour sediment at three different water:sediment ratios

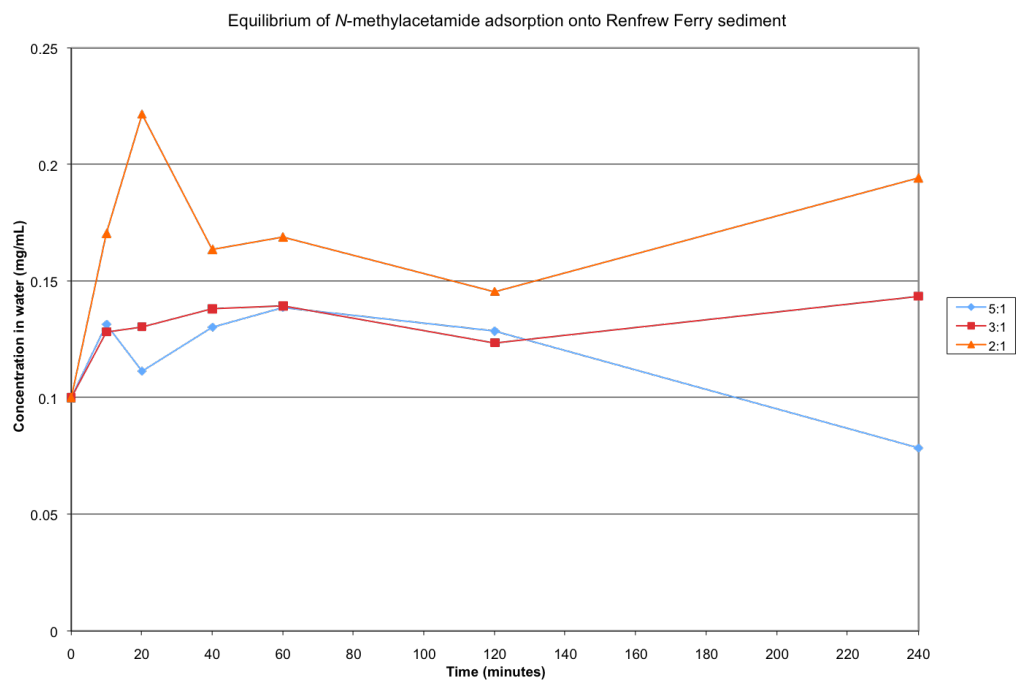


Figure 4.17: Equilibrium graph of *N*-methylacetamide adsorption onto Renfrew Ferry sediment at three different water:sediment ratios

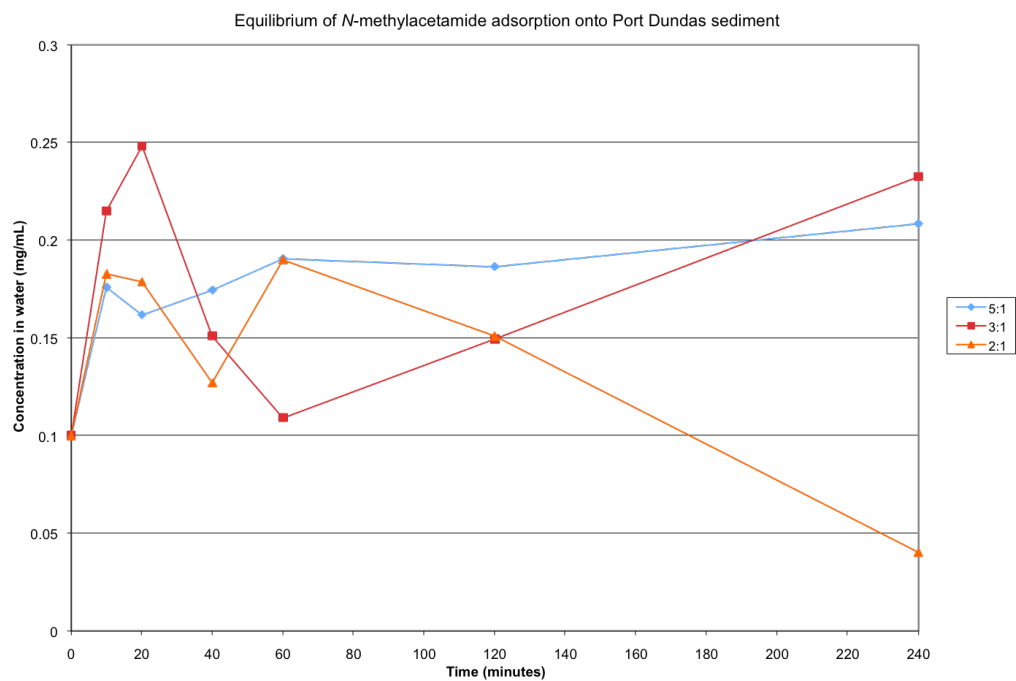


Figure 4.18: Equilibrium graph of *N*-methylacetamide adsorption onto Port Dundas sediment at three different water:sediment ratios

Calculations were carried out to determine the K_{OC} of P2P and *N*-methylacetamide. The sediment concentration at two hours (equilibration time) was used for the calculations. The K_{OC} value for P2P was calculated for all four sediment locations, while that for *N*-methylacetamide was only calculated for the two locations that did not display matrix interferences (Bowling Harbour and Bothwell Bridge). The equations, from ASTM (2008), are as follows:

$$T = W_T \times C_S \quad (4.12)$$

Where:

T = total quantity of chemical left in water, μg

W_T = total quantity of water, mL

C_S = concentration of chemical in water, $\mu\text{g/mL}$

$$G_S = G_A - T \quad (4.13)$$

Where:

G_S = total quantity of chemical sorbed to solids, μg

G_A = total quantity of chemical in control sample, μg

$$K_d = \frac{G_S/B}{C_S} \quad (4.14)$$

Where:

K_d = sorption coefficient

B = oven-dry weight of solids, g

$$K_{OC} = \frac{K_d \times 100}{\%OC} \quad (4.15)$$

Where:

K_{OC} = organic carbon normalised sorption constant

$\%OC$ = percentage of organic carbon in solids

The following sample calculation is for the adsorption of P2P onto sediment collected from Bowling Harbor (%OC = 5.17), with a water:sediment ratio of 2:1, at the equilibrium time of two hours.

$$\begin{aligned}
 T &= 10 \text{ mL} \times 78.42 \text{ } \mu\text{g/mL} \\
 &= 784.2 \text{ } \mu\text{g} \\
 G_S &= 966 \text{ } \mu\text{g} - 784 \text{ } \mu\text{g} \\
 &= 182 \text{ } \mu\text{g} \\
 K_d &= \frac{182 \text{ } \mu\text{g}/5 \text{ g}}{78.42 \text{ } \mu\text{g}} \\
 &= 0.46 \\
 K_{OC} &= \frac{0.46 \times 100}{5.71} \\
 &= 8.90
 \end{aligned}$$

The measured K_{OC} values of P2P and *N*-methylacetamide are shown in Table 4.21, where they are also compared against the calculated estimation of K_{OC} using Equation 4.5, and the EPI Suite™ fugacity model default value. The measured K_{OC} values were calculated using the average water concentration from the three water:sediment ratios. Each water:sediment ratio was run in duplicate and quantified in duplicate by HPLC, therefore $n = 4$.

Table 4.21: Measured K_{OC} values for P2P and *N*-methylacetamide

Sediment	P2P	<i>N</i> -methylacetamide
Port Dundas	42.23	-
Renfrew Ferry	4.88	-
Bowling Harbour	8.10	2.26
Bothwell Bridge	42.50	22.13
Average	24.43	12.19
Estimate, using Equation 4.5	45.60	2.16
EPI Suite™ Default	82.64	2.08

All values vary quite a bit and indicate very different environmental behaviours for the two chemicals. The higher the K_{OC} value, the more likely the chemical is to adsorb to organic carbon, which means it will partition into the sediment or soil compartments rather than the air and water compartments. The K_{OC} is calculated from K_d to be independent of sediment

organic carbon content. Given the range of values, it is difficult to accurately estimate how each chemical will behave in the environment.

4.3.4 Sorption of MA Waste onto Sediment: Part 2

The matrix interferences seen in the K_d measurements in the previous section resulted in the determination of only two K_d values of the four chemicals investigated. In order to mitigate the matrix interferences, artificial soils were prepared to control the percentage unwanted materials in the soil.

While preparing the artificial soils, the individual components (sand, silt, clay, and humus) were run individually on the HPLC to test for interferences. A water:sediment mixture of 2:1 was shaken for one hour, centrifuged, and filtered. The supernatant was run on the HPLC using the same programme as for analysis of the analytes. Chromatographs of sand, silt, clay, and humus are shown in Figures 4.19, 4.20, 4.21, and 4.22, respectively.

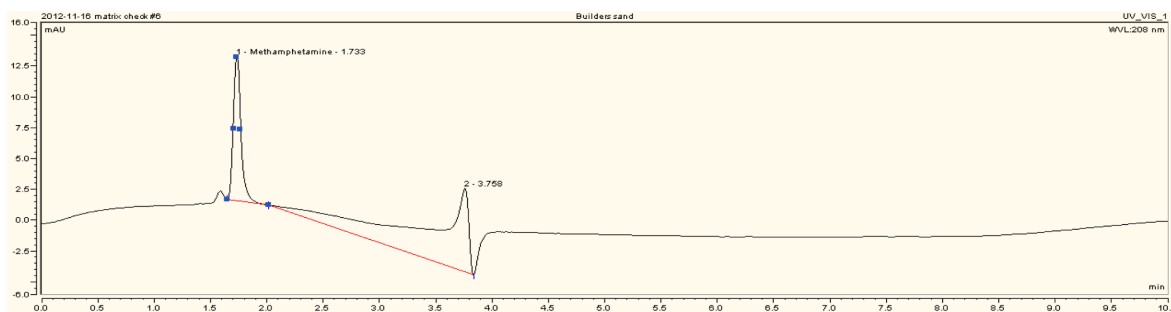


Figure 4.19: HPLC chromatogram of water exposed to sand component

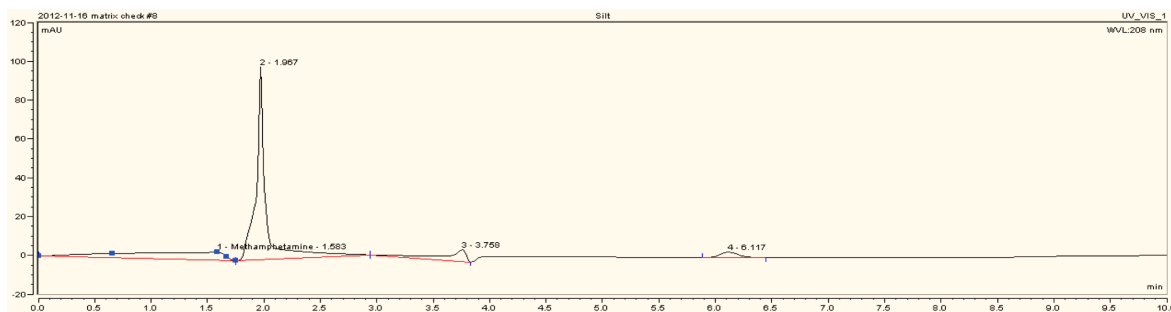


Figure 4.20: HPLC chromatogram of water exposed to silt component

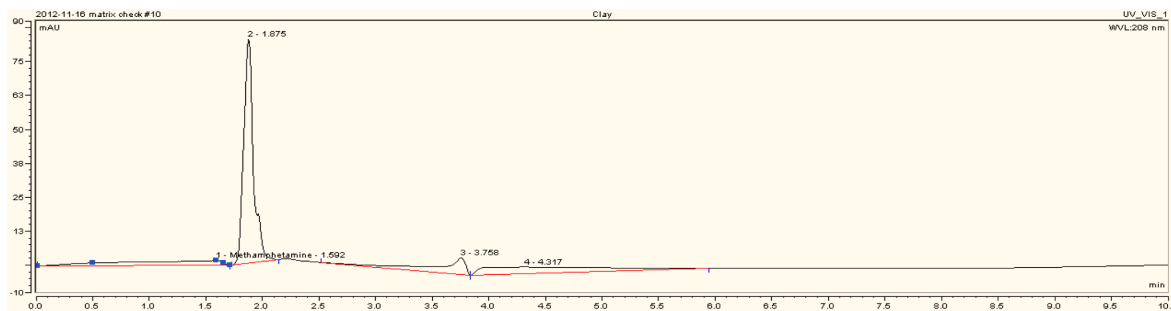


Figure 4.21: HPLC chromatogram of water exposed to clay component

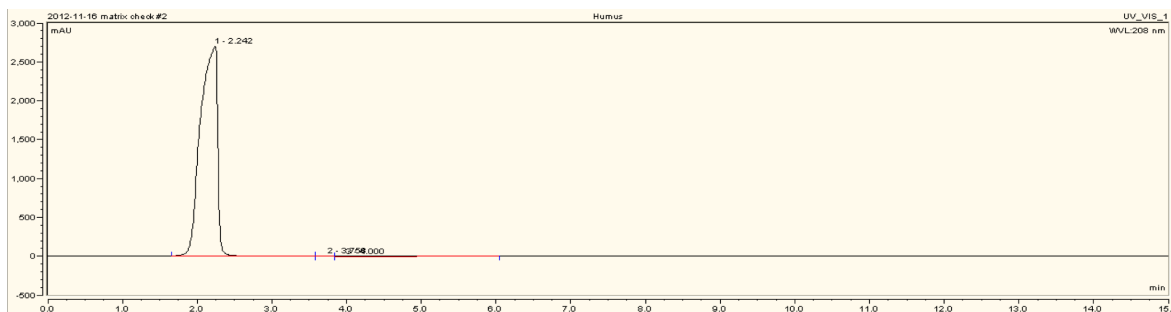


Figure 4.22: HPLC chromatogram of water exposed to humus component

Unfortunately, matrix interferences were still present in the early portions of the chromatograph, which co-elute with MA. The peaks identified as MA in Figures 4.19, 4.20, and 4.21 are not MA as these were matrix blank samples. The Dionex Chromeleon software labelled those peaks as MA according to user-set parameters based on retention time. This clearly indicates the matrix interferences elute at the same time as MA. Therefore, the K_d of MA could ultimately not be measured in this study. In order for the K_d of MA to be measured, a quantification method for MA is required to be developed. That could include using a different instrument, such as LC-MS, where the ions of MA could be targeted. Alternatively, a subsequent clean-up step of the extract could be developed, such as an SPE method. Due to time constraints, further quantification of MA was not pursued in this study.

Since MA could not be measured, that left only *N*-methylacetamide and P2P. In order to gain a more comprehensive understanding of MA waste adsorption, two other chemicals were selected for K_d testing: phenol and benzaldehyde, oxime. Those two chemicals were detected in MA waste as discussed in the previous chapter, and they had elution times that were well clear

of matrix interferences from the artificial soils. Limits of detection (LOD) and quantification (LOQ) for the four chemicals tested are shown in Table 4.22. Limits were calculated using the regression line of the calibration curve as per Miller and Miller (2010). Calculations are shown in Appendix B.

Table 4.22: LOD and LOQ values for HPLC K_{OC} method ($\mu\text{g}/\text{mL}$)

	<i>N</i> -methylacetamide	P2P	Phenol	Benzaldehyde, oxime
LOD	10	2	2	1
LOQ	34	5	5	4

One method for calculating K_d is by using the equation of the line in a Freundlich isotherm, Equation 4.16, where K_d equals the y-intercept. The Freundlich isotherm describes an empirical relationship between sorption of the solute and solid surface area, where adsorption is dependent on the initial concentration.

$$\ln C_a = \log K_d + 1/n \log C_S \quad (4.16)$$

Where:

C_a = chemical adsorbed, oven-dry solids weight, $\mu\text{g}/\text{g}$

K_d = sorption coefficient

C_S = solution concentration at equilibrium, $\mu\text{g}/\text{mL}$

$1/n$ = exponent

Freundlich isotherms were constructed for *N*-methylacetamide, P2P, phenol, and benzaldehyde, oxime and are shown in Figure 4.23 on the following page.

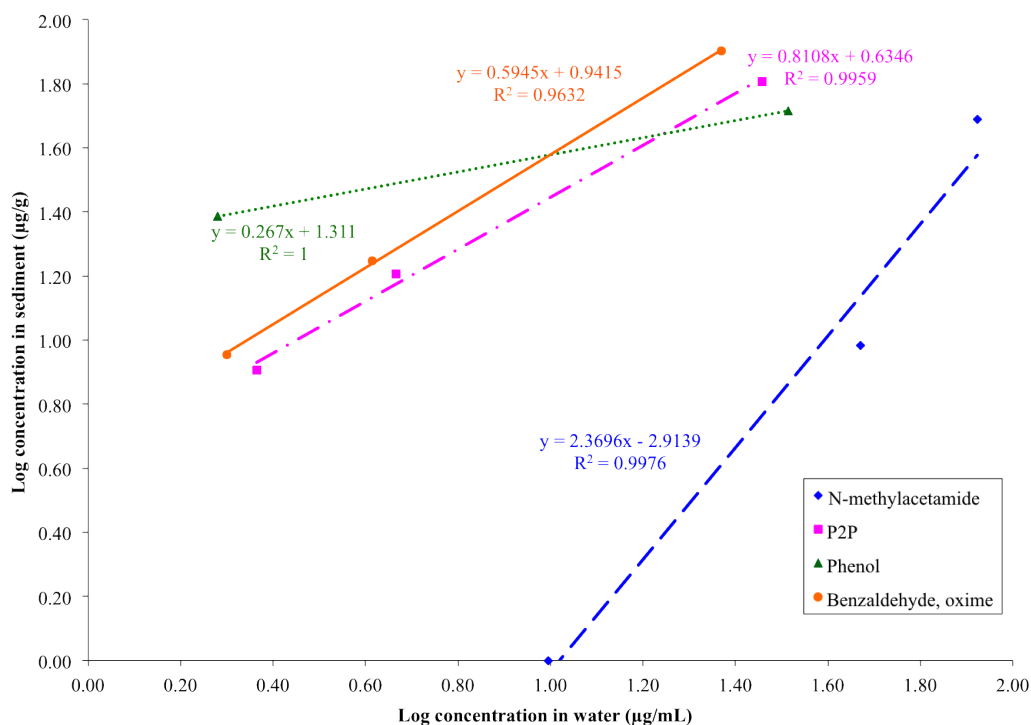


Figure 4.23: Freundlich isotherms for *N*-methylacetamide, P2P, phenol, and benzaldehyde, oxime

In this case, there were not enough data points to be able to accurately determine K_d using the Freundlich isotherm. Values that were below the LOQ were omitted from the graph. In order to properly conduct a Freundlich isotherm, at least four data points over a one hundred fold concentration range are required (ASTM, 2008). However, the ASTM method advocates using three or more soil types rather than focus on solute concentrations. This is because errors from low environmental concentration effects are usually less than the variances between different sediments. Therefore, in this study, a focus was on the number of different soils used rather than the variations in concentration.

Equilibrium graphs of *N*-methylacetamide at each water:sediment ratio, onto each of the three artificial soils are shown in Figures 4.24, 4.25, and 4.26. A full 48 hours was used as the total experiment run time in the second part of the K_d study. This confirmed that four hours is the equilibrium time. It is that time point that was used to ultimately calculate K_{OC} .

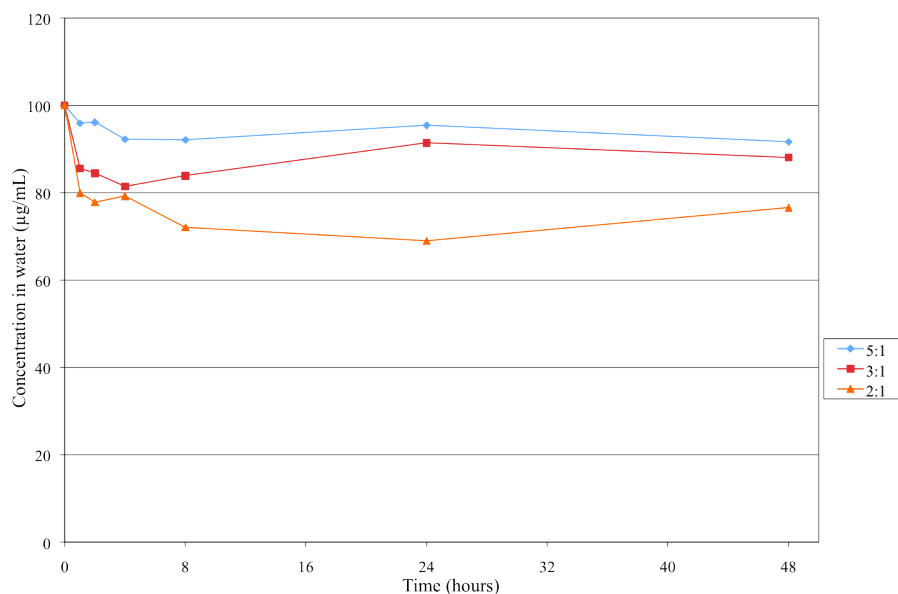


Figure 4.24: Equilibrium graph of *N*-methylacetamide adsorption onto artificial soil #1 at three different water:sediment ratios

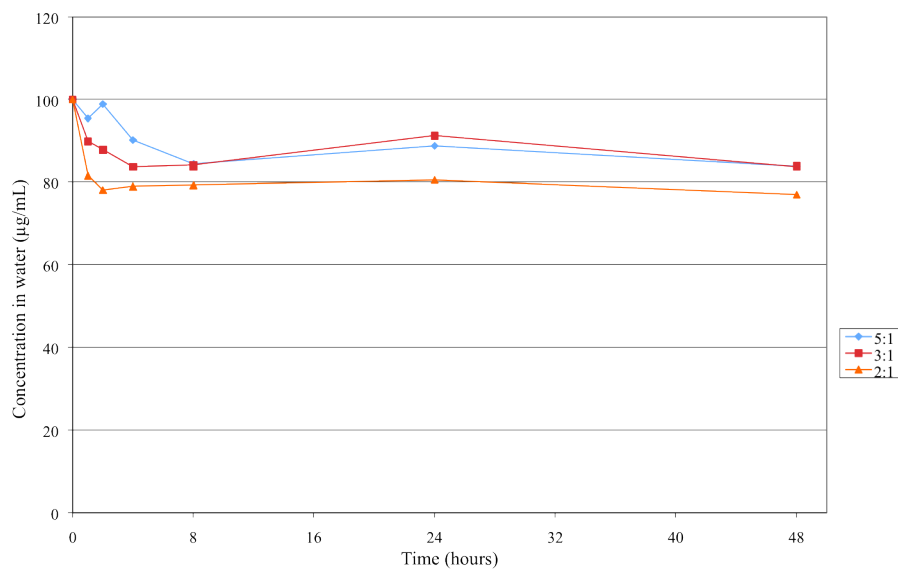


Figure 4.25: Equilibrium graph of *N*-methylacetamide adsorption onto artificial soil #2 at three different water:sediment ratios

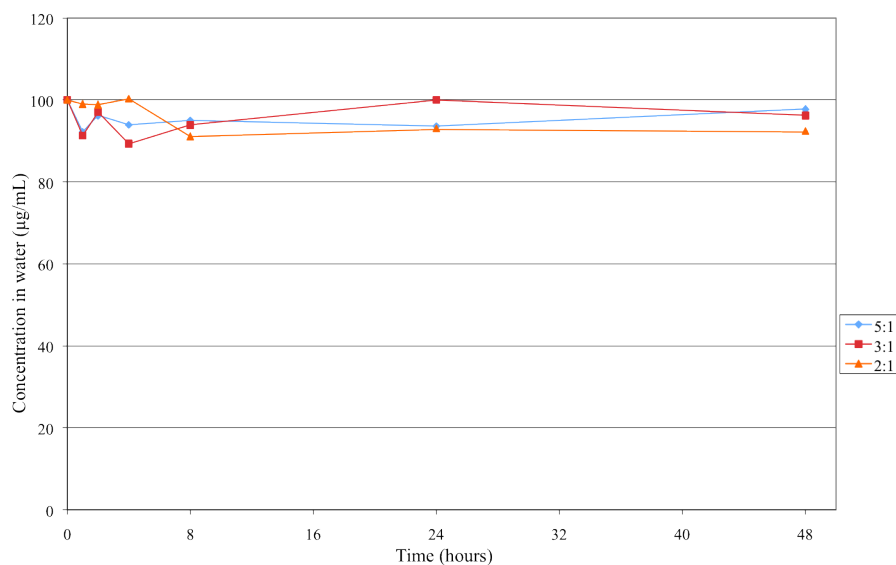


Figure 4.26: Equilibrium graph of *N*-methylacetamide adsorption onto artificial soil #3 at three different water:sediment ratios

The equilibration results in part two are similar to part one whereby the majority of *N*-methylacetamide remained in the water phase. Adsorption decreased slightly as the amount of organic carbon decreased from soil 1 (7.46%) to soil 3 (1.44%).

Equilibrium graphs of P2P at each water:sediment ratio, onto each of the three artificial soils are shown in Figures 4.27, 4.28, and 4.29.

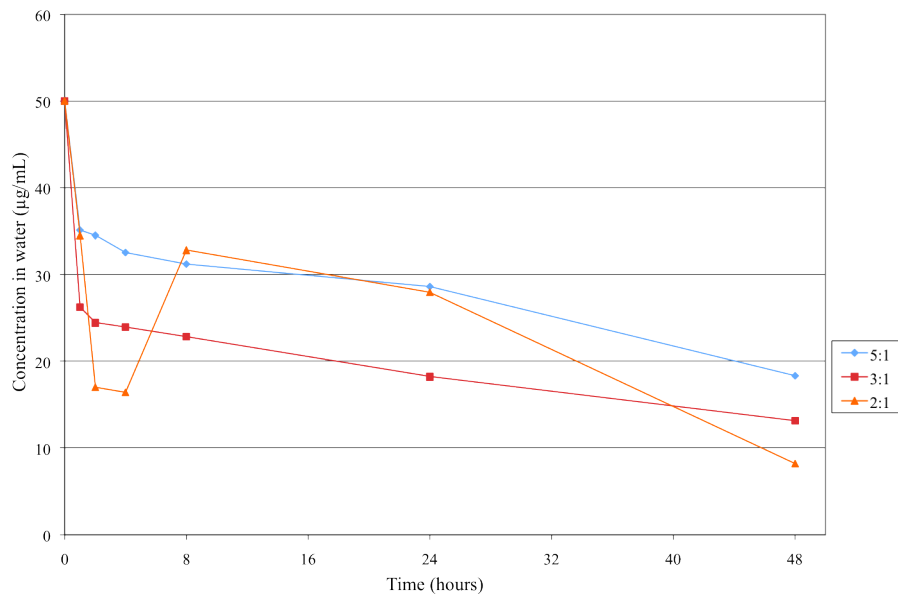


Figure 4.27: Equilibrium graph of P2P adsorption onto artificial soil #1 at three different water:sediment ratios

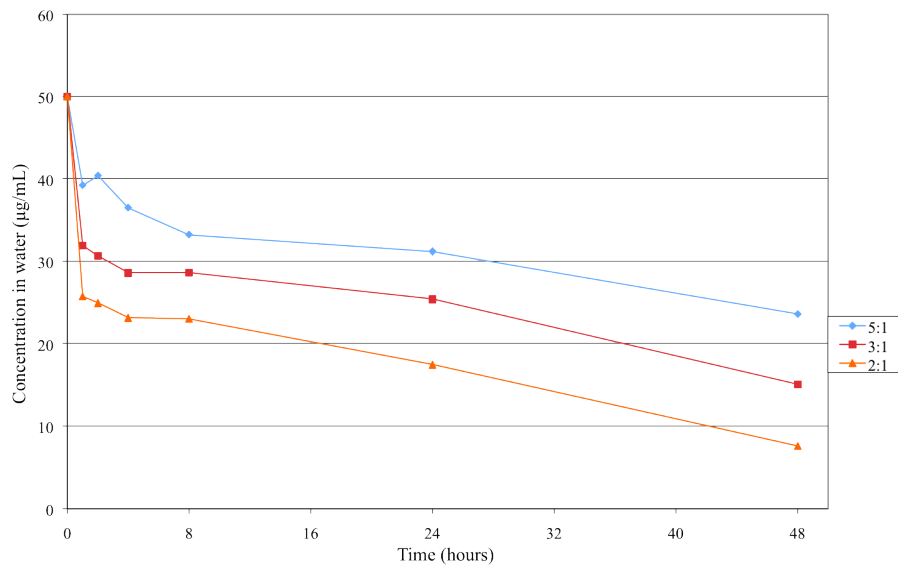


Figure 4.28: Equilibrium graph of P2P adsorption onto artificial soil #2 at three different water:sediment ratios

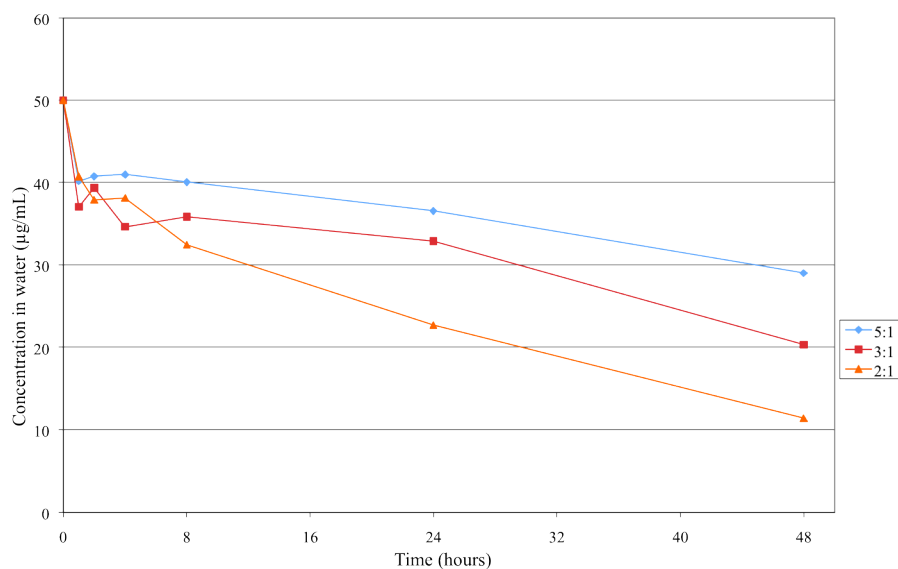


Figure 4.29: Equilibrium graph of P2P adsorption onto artificial soil #3 at three different water:sediment ratios

The equilibrium time of P2P was also confirmed to be four hours. There is evidence of adsorption-desorption cycles taking place after equilibrium is reached, however after 24 hours, there is a sharp decrease in water concentration which could indicate degradation. The positive concentration controls remained constant throughout the 48 hours, therefore losses cannot be attributed to systematic losses.

Equilibrium graphs of phenol at each water:sediment ratio, onto each of the three artificial soils are shown in Figures 4.30, 4.31, and 4.32.

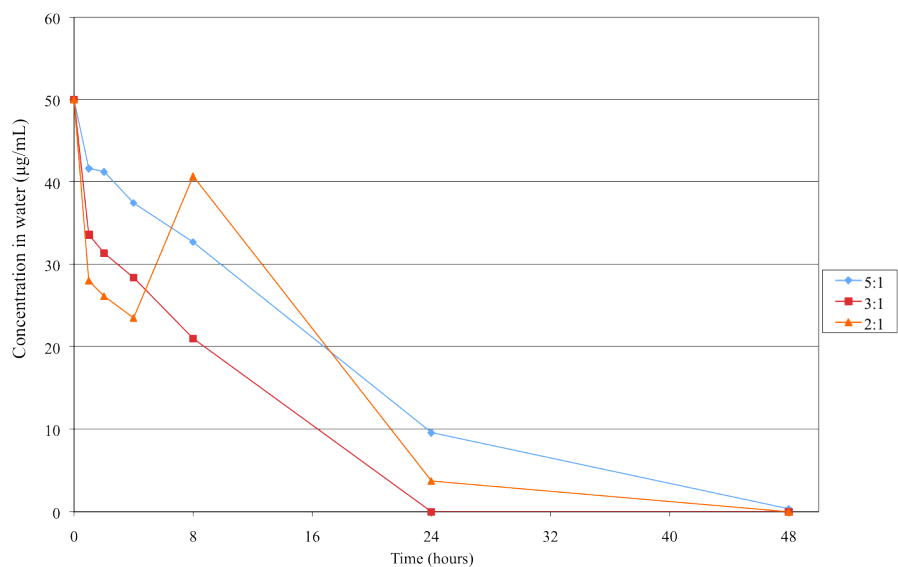


Figure 4.30: Equilibrium graph of phenol adsorption onto artificial soil #1 at three different water:sediment ratios

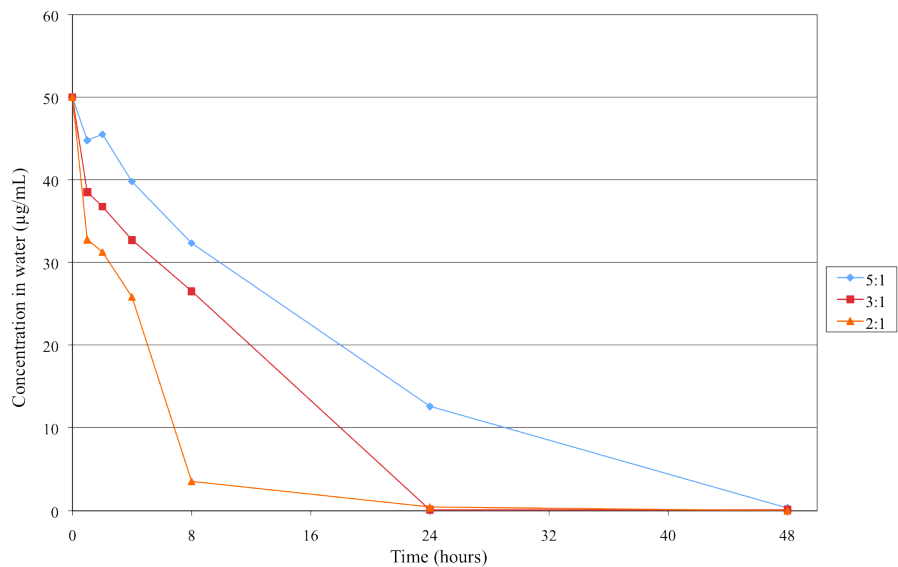


Figure 4.31: Equilibrium graph of phenol adsorption onto artificial soil #2 at three different water:sediment ratios

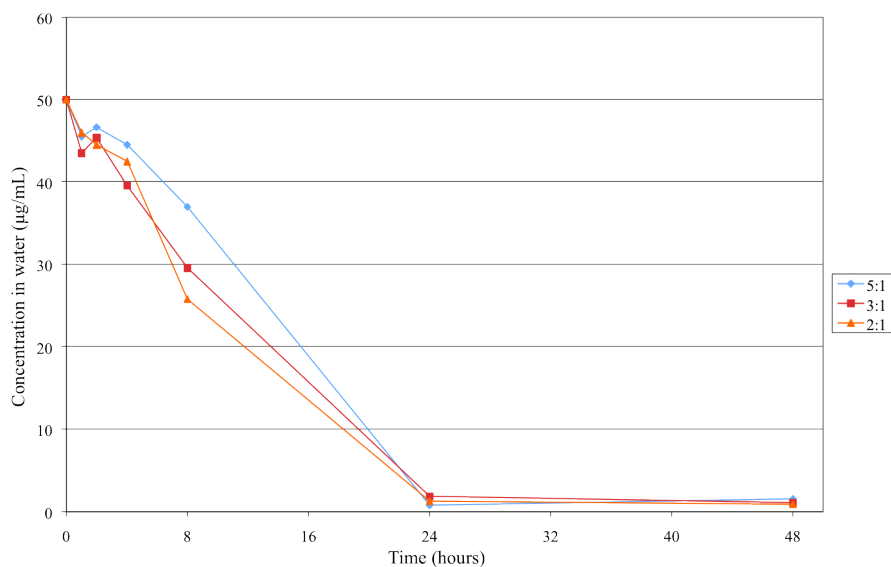


Figure 4.32: Equilibrium graph of phenol adsorption onto artificial soil #3 at three different water:sediment ratios

Phenol shows a sharp decrease in water concentration between eight and 24 hours of mixing. Prior to eight hours, phenol remains predominantly in the water compartment. The water concentration was below the detection limit in many samples, thus considered to be zero. Given the K_{OW} value and calculated estimated K_{OC} value of phenol, it is more likely that a degradation reaction has taken place rather than complete adsorption onto the sediment.

Equilibrium graphs of benzaldehyde, oxime at each water:sediment ratio, onto each of the three artificial soils are shown in Figures 4.33, 4.34, and 4.35.

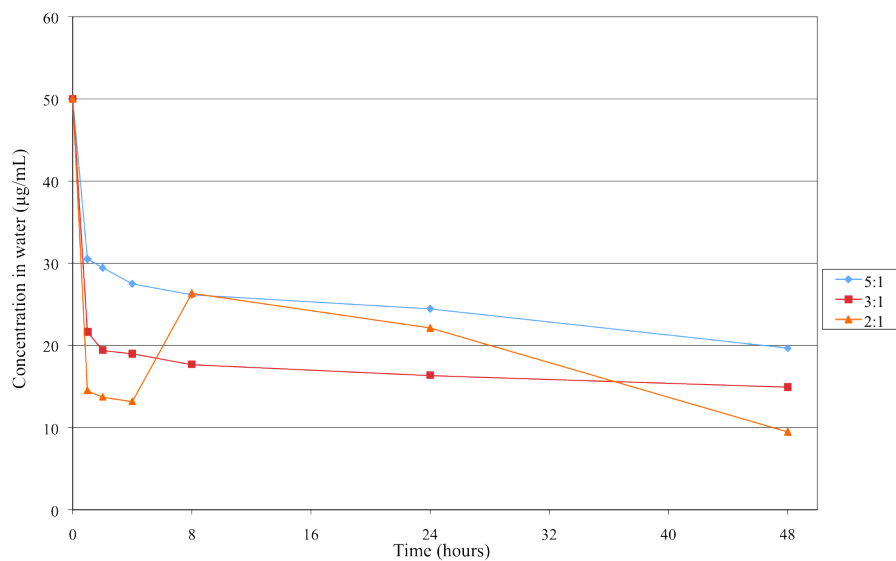


Figure 4.33: Equilibrium graph of benzaldehyde, oxime adsorption onto artificial soil #1 at three different water:sediment ratios

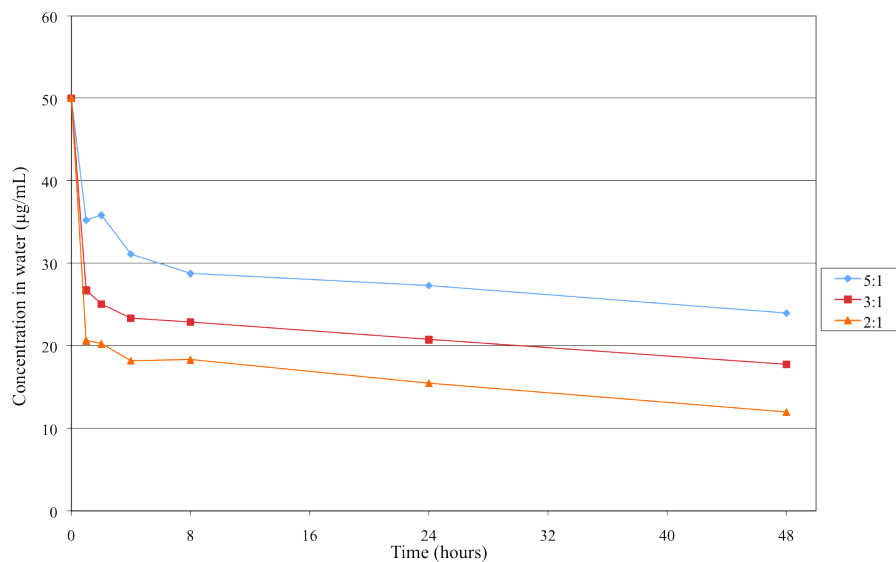


Figure 4.34: Equilibrium graph of benzaldehyde, oxime adsorption onto artificial soil #2 at three different water:sediment ratios

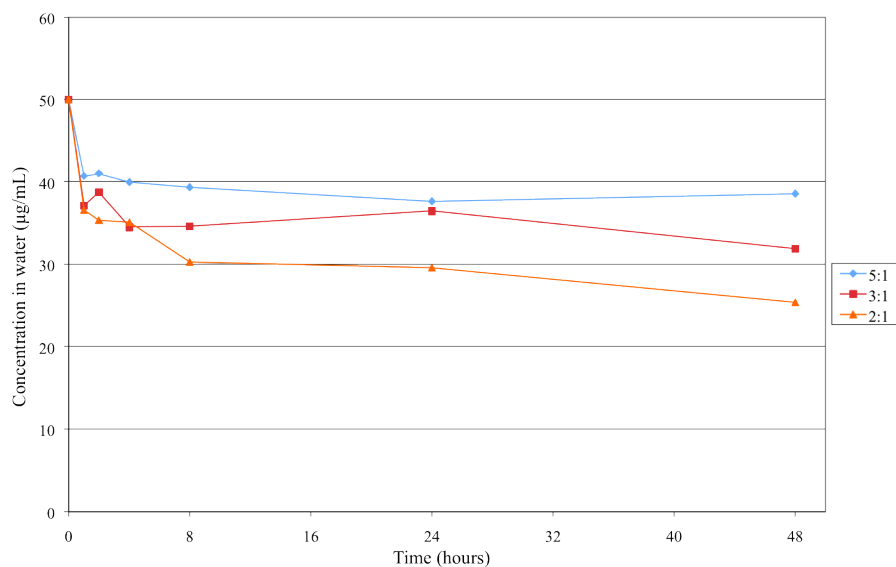


Figure 4.35: Equilibrium graph of benzaldehyde, oxime adsorption onto artificial soil #3 at three different water:sediment ratios

Benzaldehyde, oxime had the lowest water concentration levels after four hours of mixing compared with the other chemicals studied. Adsorption decreased significantly as the amount of organic carbon decreased from soil 1 (7.46%) to soil 3 (1.44%), indicating the adsorption of benzaldehyde, oxime is influenced by the sediment organic carbon content.

4.3.4.1 K_d and K_{OC} Calculations

K_d and K_{OC} were calculated using water/sediment concentrations from the equilibration and concentration studies, using Equations 4.14 and 4.15 on page 174. Sample calculations are the same as in Section 4.3.3 on page 175. The log K_{OC} values were converted to K_{OC} values and both are shown in Table 4.23 on the next page. K_{OC} values are the required format for entering values into the EPI Suite™ environmental model, which will be examined in Chapter 5.

Table 4.23: Experimentally determined log K_{OC} values for MA waste components

	<i>N</i> -methylacetamide	P2P	Phenol	Benzaldehyde, oxime
Soil 1	0.86	1.65	1.44	1.81
Soil 2	1.07	1.69	1.56	1.88
Soil 3	1.20	1.85	1.61	1.90
Average	1.04	1.73	1.54	1.86
K_{OC}	10.96	53.70	34.67	72.44

All of the K_{OC} values measured in this study are within the same order of magnitude, which is in accordance with calculated K_{OC} values using Equation 4.5 on page 136, which estimates K_{OC} values within one order of magnitude. This indicates that the four compounds investigated here have approximately the same propensity to adsorb onto organic carbon. The K_{OC} values ranged from 10.96 for *N*-methylacetamide to 72.44 for benzaldehyde, oxime, indicating *N*-methylacetamide has the lowest affinity for organic carbon, while benzaldehyde, oxime has the highest. Phenol and P2P fit in the middle, with P2P having a slightly higher affinity for organic carbon than phenol.

This ranking is in accordance with the hydrophobic properties of the chemicals, as measured by K_{OW} , with one exception. In the K_{OW} experiments, P2P had a higher K_{OW} than benzaldehyde, oxime, indicating P2P is more hydrophobic and thus more likely to exit the water compartment. However, in the adsorption experiment, more than one method of adsorption may have affected the degree of sorption of each chemical.

The ASTM method makes the assumption that the main factor affecting adsorption for non-polar organic chemicals is the organic carbon content of the sediment. In this study, the chemicals under investigation are fairly polar. In this case, other sediment properties may have greater affect on the adsorption behaviour. Other factors include physical forces, chemical forces, hydrogen bonding, hydrophobic bonding, electrostatic bonding, coordination reactions, and ligand exchanges (Tan, 1998).

4.3.5 Forces of Adsorption

Physical forces mainly include Van der Waals forces, which are the result of short range dipole-dipole interactions. Van der Waals forces dissipate quickly with distance, therefore these forces are more important at close ranges for ions which are in close contact with the colloidal surface. The weaker the force, the smaller the adsorption. Van der Waals forces also influence the adsorption of cations and anions, as well as polar and non-polar ions. Due to Van der Waals forces, adsorption of basic organic compounds can occur when the surface activity is more than two pH units below the pK_a of the compound (Tan, 1998). These forces may increase the adsorption of MA, whose pK_a value is approximately three pH units above the experimental pH.

Chemical forces mainly include protonation forces, which occur at the colloid surface, but may also occur in solution. Protonation forces are important for the adsorption of anions and organic bases in the environment due to the development of positive charges at environmentally neutral pH levels. The protons required for these forces are generated from the dissociation of water in the hydration shell of cations. Protonation of basic organic chemicals may occur on clay sediments saturated with hydrogen and/or aluminium. The positive charge acquired from protonation will be attracted to the negative charge on the clay surface. Protonation of organics at the sediment-water interface is affected by the basicity of the adsorbate, the nature of the exchangeable cation, the negative charges of the clay minerals, the soil water content, and surface acidity, which can be 2-3 pH units below the bulk pH value (Tan, 1998). As with the Van der Waals forces, protonation of the basic compounds in MA waste may increase their adsorption onto sediment under the correct conditions.

Similar to protonation forces, hydrogen bonding occurs when it is a hydrogen atom that acts as the connection linkage. While protonation is a full charge transfer, hydrogen bonding is a partial charge transfer. Organic chemicals with the following functional groups will be expected to be adsorbed through hydrogen bonding with the oxygen at the clay surface: NH, NH₂, OH, and COOH (Tan, 1998). As determined in the Chapter 3, many of the components in MA waste contain NH and OH groups. Thus hydrogen bonding is another adsorption force which is likely to affect the adsorption of MA waste.

Hydrophobic bonding is primarily associated with non-polar compounds that compete with water molecules for binding sites on the sediment, where adsorbed water is expelled by the adsorbate. This process is common for polysaccharides (Tan, 1998). This type of adsorption force is unlikely to have a major influence on MA waste as most of the compounds identified are polar.

Other forces of adsorption that are less likely to affect MA waste are electrostatic bonding, coordination reactions, and ligand bonding. Electrostatic bonding is also similar to protonation forces. Electrostatic bonding is the result of electric charges on the colloid surface and is the reaction for the adsorption of water, cations (cation exchange reactions), and organic compounds. If both organics and clays are negatively charged, the protonation of organics may convert them into positively charged ions. Coordination reactions are covalent bonds that occur when a ligand donates an electron to a metal ion, forming a coordination compound, complex compound, or an organo-metallic complex. An example of coordination reaction is between humic acids and clay, where both species are negatively charged and would naturally repel each other. However the cations on exchange sites on the clay surface are able to form complexes with humic acids in solution. The final adsorption force is ligand exchanges where an adsorbate replaces a ligand. For this to occur, the adsorbate must have a stronger chelation capacity than the ligand (Tan, 1998).

In addition to adsorption forces, the physicochemical properties of organic chemicals will also affect adsorption.

4.3.6 Adsorption and Physicochemical Properties

Adsorption of organic chemicals onto sediment surfaces is influenced by several physicochemical properties of the chemical itself. Examples of those properties include the chemical nature of the adsorbate, water solubility, dissociation capacity, surface charge density, and polarity (Tan, 1998).

What is meant by the chemical nature of an organic compound is the reactivity of its functional groups. The dissociation of functional groups determines whether the molecule will behave as

an acidic, basic, or amphoteric compound. As mentioned above, the occurrence of hydrogen bonding is dependent on the presence of specific dissociation of functional groups, where as coordination bonding requires the functional groups to behave as electron pair donors (Tan, 1998).

Tan (1998) notes that there is conflicting opinions in the literature concerning the relationship between the water solubility of organic compounds and adsorption. While some publications indicate the more soluble the organics, the more they will be adsorbed, others suggest adsorption is inversely related to their water solubility.

The dissociation capacity of organic compounds can be expressed in terms of pK_a values. The pK_a value is an important property since it indicates the ionisation capability of the organics. Organic acids which are capable of dissociating more than one proton per molecule may have more than one pK_a value. Such behaviour, indicating the degree of acidity or basicity, will determine the rate and ease of adsorption by soil minerals (Tan, 1998). As noted in Section 4.3.1, pK_a values will have an effect on K_{OW} values. In the case of MA waste, ionisation of MA will be expected to occur at environmental pHs.

The charge density will also affect a chemical's adsorption onto sediments. In organic substances with lower surface charge densities, the electrostatic charge centers are more widely spaced than in organic compounds possessing higher surface charge densities. The compounds with the more closely spaced charge centers are believed to be adsorbed more readily than those with the widely spaced centers. The effects of charge densities of the identified components of MA waste are unknown. Charge density is more likely to allow chemicals to adsorb into the layers of the sediment structure, penetrating below the surface layer and into the clay platelets (Tan, 1998).

The polarity of organic chemicals determines whether or not it is able to penetrate within the layers of clay platelets to bind to the internal clay surface. The presence of polar functional groups in an organic molecules is thought to increase the separation of the clay sheets (Tan, 1998). Polarity can be related to K_{OW} values, with more polar compounds typically having higher K_{OW} values. Therefore a high polarity can mean two different things. Firstly, the further the chemicals are able to penetrate past the sediment surface, the more likely they are

to persist, meaning they will also be less likely to be accidentally taken up by bottom feeding organisms. Conversely, highly polar compounds with high K_{OW} values are potentially more dangerous to aquatic organisms because of their propensity to bioaccumulate.

Overall, knowledge of a chemical's K_{OW} value provides an enormous amount of information regarding its behaviour in the environment. K_{OW} is related to water solubility and polarity, and can be used to estimate K_{OC} and bioconcentration. Conducting an accurate and reliable K_{OW} measurement is an inexpensive and rapid method to assess the environmental impact of a new or uncommon chemical. This should be a critical step during environmental impact assessments.

4.3.7 Correlation between K_{OW} and K_{OC}

It has long been established that there is a linear relationship between K_{OW} and K_{OC} (USEPA, 1996). In an effort to predict K_{OC} values for chemicals that were not tested, a plot was constructed of $\log K_{OC}$ versus $\log K_{OW}$ (Figure 4.36 on the next page). Three lines are present on the plot: one line from experimental data and two lines from EPI Suite™ estimated values. EPI Suite™ uses two different methods of estimating K_{OC} . One method is based on K_{OW} values (Equation 4.17 on the following page), the other based on molecular connectivity index (MCI, Equation 4.18 on the next page).

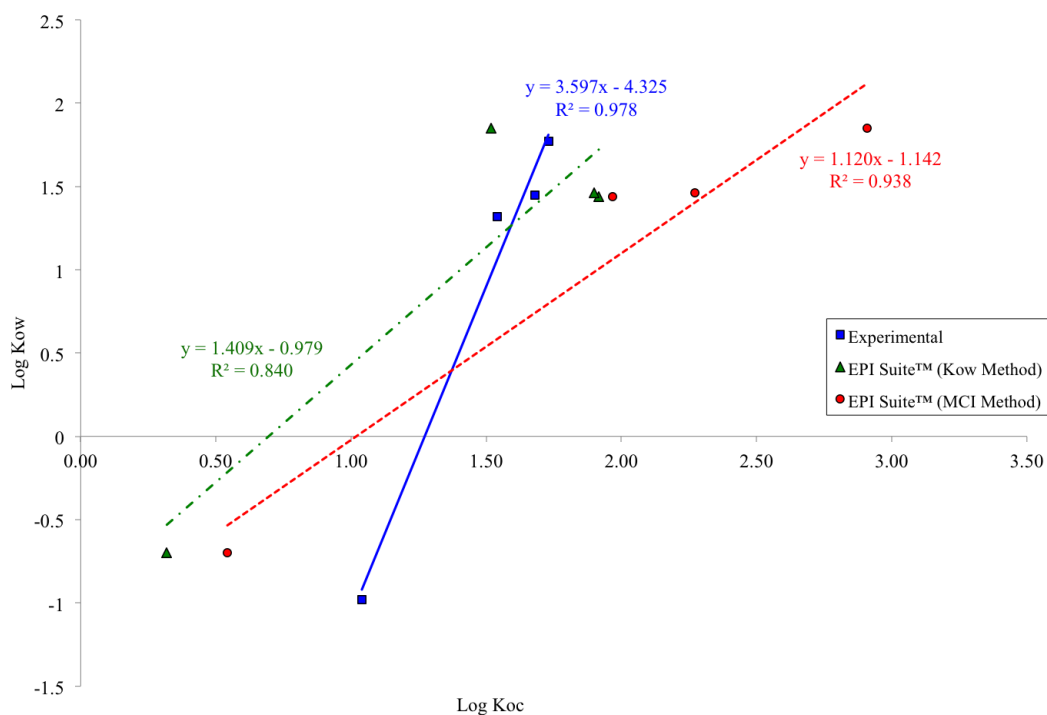


Figure 4.36: Correlation between $\log K_{OW}$ and $\log K_{OC}$

$$\log K_{OC} = 0.8679 \log K_{OW} - 0.0004 \quad (4.17)$$

$$\log K_{OC} = 0.5213 MCI + 0.62 \quad (4.18)$$

Equation of the (blue) line from experimental $\log K_{OW}$ versus experimental $\log K_{OC}$ in Figure 4.36:

$$y = 3.597x - 4.325 \quad (4.19)$$

Looking at the correlation coefficients, the R^2 value from the experimental data is closer to one (0.978) than both EPI Suite™ values (0.938, 0.840), which indicates a stronger linear correlation. The poorest correlation between $\log K_{OC}$ and $\log K_{OW}$ is from the EPI Suite™ method that calculates $\log K_{OC}$ from $\log K_{OW}$. According to the EPI Suite™ methodology guide, $\log K_{OC}$ calculated from $\log K_{OW}$ has an R^2 value of 0.877 ($n = 68$), and an R^2 value of 0.967 ($n = 69$) when calculated using MCI. Using the equation of the line from the experimental data (Equation

4.19), it is possible to calculate K_{OC} values for MA, 2,6-DTBP, 1-phenyl-1,2-propanedione, and benzyl alcohol based on experimentally determined K_{OW} values (Table 4.24). A sample calculation for MA is shown below.

Table 4.24: K_{OC} values calculated using experimental K_{OW} values in Equation 4.19

Chemical	Experimental $\log K_{OW}$	Calculated $\log K_{OC}$	K_{OC}
MA	2.04	1.77	58.82
Benzyl alcohol	1.40	1.59	39.05
2,6-DTBP	4.91	2.57	369.33
1-phenyl-1,2-propanedione	1.71	1.68	47.62

$$\begin{aligned}
 y &= 3.597x - 4.325 \\
 \log K_{OW} &= 3.597 \times \log K_{OC} - 4.325 \\
 \log K_{OC} &= \frac{\log K_{ow} + 4.325}{3.597} \\
 &= \frac{2.04 + 4.325}{3.597} \\
 &= 1.77 \\
 K_{OC} &= 10^{\log K_{OC}} \\
 &= 10^{1.77} \\
 &= 58.82
 \end{aligned}$$

A comparison of Table 4.24 with the ASTM calculation method (Equation 4.5 on page 136), shown below in Table 4.25, shows a few disparities.

Table 4.25: Estimated K_{OC} values of MA waste impurities from K_d part 2 based on Equation 4.5 on page 136

Compound	Estimated $\ln K_{OC}$	Estimated K_{OC}
MA	2.42	11.25
Benzyl alcohol	2.63	13.82
2,6-DTBP	8.18	3577.59
1-phenyl-1,2-propanedione	4.15	63.59

Using the equation of the line, MA and benzyl alcohol have higher K_{OC} values, however they are within the same order of magnitude as the ASTM calculations. 2,6-DTBP is calculated to

be one order of magnitude higher when using the ASTM equation. Overall, calculations using the K_{OW}/K_{OC} correlation are within one order of magnitude of the ASTM calculations which is acceptable according to the standard method. It is likely that there is not necessarily a single definitive K_{OC} value for each chemical, but rather a range of values from which high and low estimates can be obtained. K_{OC} values may heavily influence sorption behaviour, however as with all other sorption factors, sorption is dependent on environmental conditions and a wide range of variables. The effect different K_{OC} values have on environmental partitioning behavior will be examined in Chapter 5 using a fugacity model.

4.4 Conclusions

The octanol-water partition coefficient of eight chemicals identified from MA waste was successfully determined using RPHPLC. The measured values were compared with computer estimated values using the computer modelling programme EPI Suite™ and were shown to be remarkably similar. Given the linear relationship between K_{OW} and bioconcentration, the two most concerning chemicals with the highest K_{OW} values are MA, a physiologically active polar compound, and 2,6-DTPB, a highly polar compound susceptible to sediment adsorption and persistence.

The measurement of K_{OC} of four chemicals (MA, P2P, 2,6-DTBP, and *N*-methylacetamide) identified from MA waste had limited initial success and thus was repeated. One of the biggest factors affecting the first batch of experiments was matrix interferences from the collected sediment samples, which masked the peaks of MA and *N*-methylacetamide. The low solubility of 2,6-DTBP, combined with its high polarity, meant that concentrations in the aqueous layer were below limits of detection, and its K_{OC} could not be determined.

Based on the experimental and derived K_{OC} values, the chemicals examined from MA waste display the following order of lipophilicity, from lowest to highest: *N*-methylacetamide < phenol < benzyl alcohol < benzaldehyde, oxime < 1-phenyl-1,2-propanedione < P2P < MA < 2,6-DTBP. Using the linear relationship between K_{OW} and BCF, the same order can be applied towards the tendency of these chemicals to bioaccumulate in aquatic organisms.

The second batch of experiments attempted to eliminate matrix interference effects by using artificial soils. Using an HPLC with a UV detector, it was still not possible to measure the K_{OC} value of MA due to matrix interferences. However, additional chemicals were added to the sorption experiments, and K_{OC} values were successfully determined for *N*-methylacetamide; P2P; phenol; and benzaldehyde, oxime. The chemicals examined from MA waste display the following order of affinity for organic carbon, from lowest to highest: *N*-methylacetamide < phenol < benzyl alcohol < 1-phenyl-1,2-propanedione < MA < P2P < benzaldehyde, oxime < 2,6-DTBP. This is a different order from the K_{OW} measurements, despite the linear relationship between the two properties. This demonstrates again the importance of laboratory experimentation and the influence of multiple parameters on the behaviour of chemicals in the environment.

K_{OC} values can be difficult to measure experimentally. Adsorption experiments are time consuming, labour intensive, and can suffer from matrix interference effect. However, K_{OW} is an easy parameter to measure in the laboratory. By using the correlation between the two partition coefficients, K_{OC} can reliably be estimated through the measurement of K_{OW} . From the experimental measurement of K_{OC} and K_{OW} , a correlation of $y = 3.597x - 4.325$ ($R^2 = 0.978$) was established. Using the experimentally determined correlation, K_{OC} values for MA waste were determined that were not able to be measured experimentally. It was also determined that experimental K_{OW} values are very similar to computer estimated K_{OW} values, therefore the correlation can be used to estimate K_{OC} values for other waste components as well.

There are many factors that can have an influence on the adsorption of chemicals to soils and sediments. Those factors range from environmental factors, such as pH and salinity, to physicochemical properties, such as K_{OW} and K_{OC} , as well as sediment properties, such as crystal lattice structure, and organic carbon content. It is important to note that the polar nature of the chemicals under investigation suggests that the traditional assumptions of organic carbon partitioning may not apply and other sediment properties may have greater influence on sorption behaviour.

Chapter 5

Environmental Modelling of Methylamphetamine Waste

5.1 Introduction

Environmental modelling is used in order to gain an understanding of the fate and transport of chemicals. This is possible by quantifying their reactions and movement once released into the environment. Modelling is also essential to predict future conditions of potential new contaminants under a variety of scenarios. Using environmental modelling, it is possible to estimate the past, present, or future chemical exposure to aquatic organisms and/or humans. Environmental modelling provides scientists with information regarding degradation rates, fate, transport, and persistence of chemicals in the environment (Schnoor, 1996). Computer modelling is a cost-effective way to learn as much as possible about nearly every chemical, theoretical or in existence (Mackay, 2001).

To aid in the detection and prosecution of an illicit dumpsite, an understanding of the chemical behaviour of the waste components is essential. As such, environmental modelling of organic chemicals is useful in predicting the behaviour of the chemical once released into the environment. While many different environmental models exist, the fugacity model was used in this work. A fugacity model calculates the tendency of a compound to partition into each environmental

compartment. The model uses partition coefficients and mass balance equations to predict the movement of a contaminant across environmental compartments (Mackay, 1979).

An easy to use and freely available fugacity model can be found in the United States Environmental Protection Agency's (US EPA) computer modelling programme EPI (Estimation Programs Interface) Suite™ (USEPA, 2012b). EPI Suite™ uses a Level III fugacity model, meaning it assumes the compartments (air, water, soil and sediment) are homogeneous. A Level III model also assumes steady-state conditions, but not equilibrium. According to Mackay (2001), steady-state implies consistency with time, while equilibrium implies that once equilibrium is reached, concentrations have no tendency for net transfer.

Several of the estimation programmes within the EPI Suite™ package calculate values based on the other programmes. EPI Suite™ also contains a large database of organic chemicals, and experimentally elucidated physical properties may be entered if known. An advantage of using the EPI Suite™ model is the ability to create a site-specific environmental model by easily changing multiple variables. This feature allows the user to enter specific data relating to a sampling location as well as chemical and physical properties of the compounds of interest. For example, it is possible to specify air and water flows, water depth, and wind velocity. In the fugacity model programme, it is possible to alter the amount of chemical being discharged into each compartment, as well as K_{OC} values. In this work, K_{OC} values were changed according to results generated in Chapter 4.

In addition to the environmental partitioning of MA waste, EPI Suite™ may be used to estimate bioconcentration, bioaccumulation, and ecotoxicity using the programme ECOSAR. Toxicological effects can be broadly divided into two categories: acute and chronic. Acute effects are the immediate, short term effects seen from the moment a chemical first enters the environment. Acute effects are not prolonged effects. Chronic effects are the long term, persistent effects that will occur over time, for an extended period of time after a chemical is discharged into the environment. One is not necessarily more harmful than the other, rather acute and chronic effects will affect different aspects of the environment in different ways. Two different approaches were taken in this study: the estimation of ecotoxicity using the EPI Suite™ computer package and the experimental measurement of chemical oxygen demand (COD).

Dissolved oxygen is essential to the health of any body of water as oxygen is essential for metabolic processes of all aerobic aquatic organisms (Canadian Council of Ministers of the Environment, 1999). As a way to estimate the acute environmental impact of the MA waste components, COD can be measured to determine possible oxygen depletion in receiving waters. COD is an indicative value of water and wastewater quality that measures the amount of oxygen consumed by organic pollutants through oxidation.

5.2 Methodology

5.2.1 Estimation of Environmental Fate: Computer Modelling

The long-term environmental fate of MA waste components was estimated using the US EPA's computer modelling programme EPI Suite™, version 4.11 (USEPA, 2012b). EPI Suite™ is freely available from the United States Environmental Protection Agency and has a simple, user-friendly interface (Figure 5.1). The programme also comes with extensive reference material which describes the calculations and theory used in the software applications.

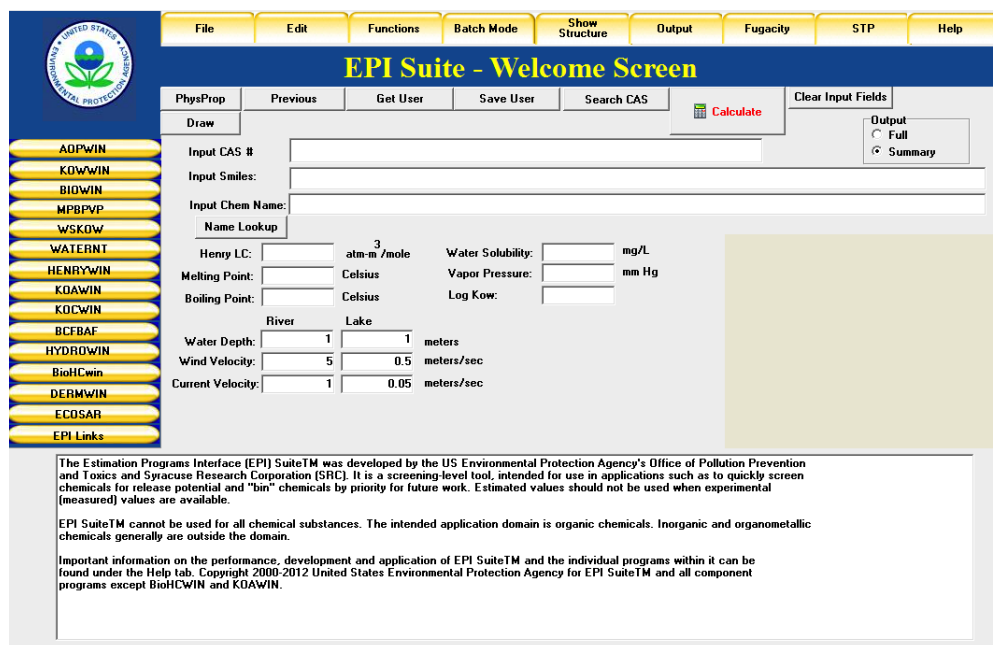


Figure 5.1: EPI Suite™ Homepage (USEPA, 2012b)

The partitioning behaviour of the waste was predicted using the fugacity model function and incorporating experimentally derived K_{OW} and K_{OC} values as determined in the previous chapter.

5.2.2 User-Changed Parameters

It is possible to enter many parameters into the model, from physical chemical properties (i.e. K_{OW} , Henry's Law constant, etc.) to environmental conditions (i.e. water depth, current velocity). In this work, three different parameters were changed and the various models compared with the default model.

5.2.2.1 Log K_{OW} Values

If a log K_{OW} is known, it can be entered on the homepage (Figure 5.2). Log K_{OW} values were determined in the previous chapter for the following eight chemicals: benzyl alcohol; 1-phenyl-1,2-propanedione; benzaldehyde, oxime; 2,6-DTBP; phenol; *N*-methylacetamide; P2P; and MA. The experimental values shown in Table 4.8 on page 148 were entered for use in the model.

The screenshot shows the 'EPI Suite - Welcome Screen' interface. The 'Log Kow' input field is highlighted with a red box. The interface includes a menu bar (File, Edit, Functions, Batch Mode, Show Structure, Output, Fugacity, STP, Help), a toolbar (PhysProp, Previous, Get User, Save User, Search CAS, Calculate, Clear Input Fields), and a sidebar with various model options (ADPWIN, KOWWIN, BIOWIN, etc.). The main form contains input fields for chemical identification and environmental parameters.

Input fields visible in the screenshot:

- Input CAS #
- Input Smiles:
- Input Chem Name:
- Name Lookup
- Henry LC: atm-m³/mole
- Water Solubility: mg/L
- Melting Point: Celsius
- Vapor Pressure: mm Hg
- Boiling Point: Celsius
- Log Kow: (highlighted)
- River/Lake selection
- Water Depth: meters
- Wind Velocity: meters/sec
- Current Velocity: meters/sec

Footer text:

The Estimation Programs Interface (EPI) Suite™ was developed by the US Environmental Protection Agency's Office of Pollution Prevention and Toxics and Syracuse Research Corporation (SRC). It is a screening-level tool, intended for use in applications such as to quickly screen chemicals for release potential and "bin" chemicals by priority for future work. Estimated values should not be used when experimental (measured) values are available.

EPI Suite™ cannot be used for all chemical substances. The intended application domain is organic chemicals. Inorganic and organometallic chemicals generally are outside the domain.

Important information on the performance, development and application of EPI Suite™ and the individual programs within it can be found under the Help tab. Copyright 2000-2012 United States Environmental Protection Agency for EPI Suite™ and all component programs except BioHCWIN and KDAWIN.

Figure 5.2: EPI Suite™ Log K_{OW} entry box

5.2.2.2 Emission Values

In the EPI Suite™ fugacity model, it is possible to alter the emission scenario (Figure 5.3 on the next page). For each model, default and user-changed, the emission values for each environmental compartment were changed. The default emissions values for each compartment (air, water, and soil) are 1,000 kg/hr. The emissions values in this work were changed to simulate a waste discharge scenario directly into either water or soil. A direct release into air was not considered because the chemicals studied are not gases. The emissions were altered as follows: air: 0 kg/hr, water: 1,000 kg/hr, soil: 0 kg/hr for a water-release scenario; or air: 0 kg/hr, water: 0 kg/hr, soil: 1,000 kg/hr for a soil-release scenario.

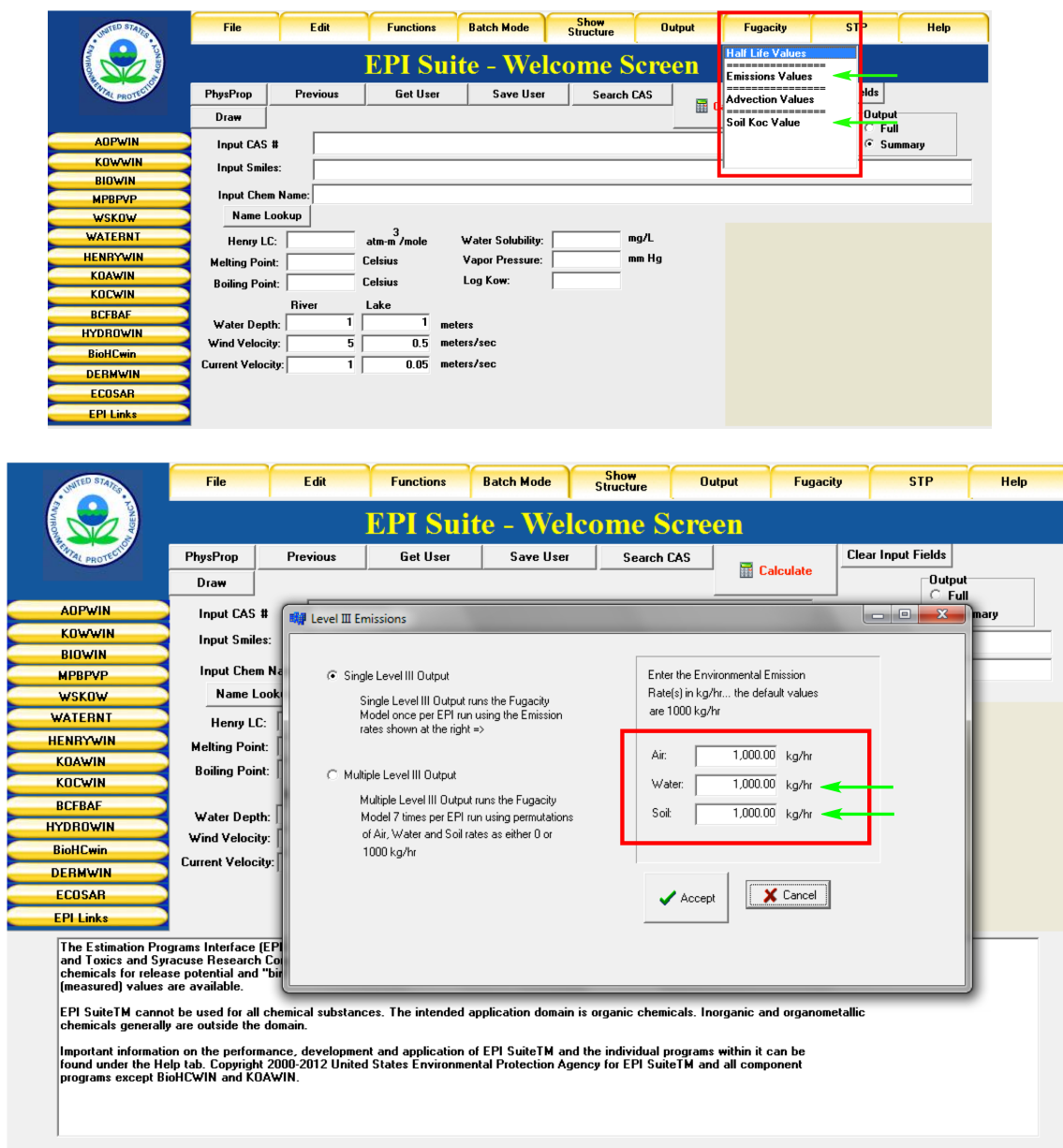


Figure 5.3: EPI Suite™ Fugacity model emissions scenario

5.2.2.3 K_{OC} Values

There are three different options for entering soil K_{OC} values into the fugacity model (Figure 5.4 on the following page). The default mode is to use K_{OC} from a QSAR Molecular Connectivity Index (MCI). The second option is to calculate K_{OC} based on K_{OW} , and the third option is to enter a user-specified K_{OC} value.

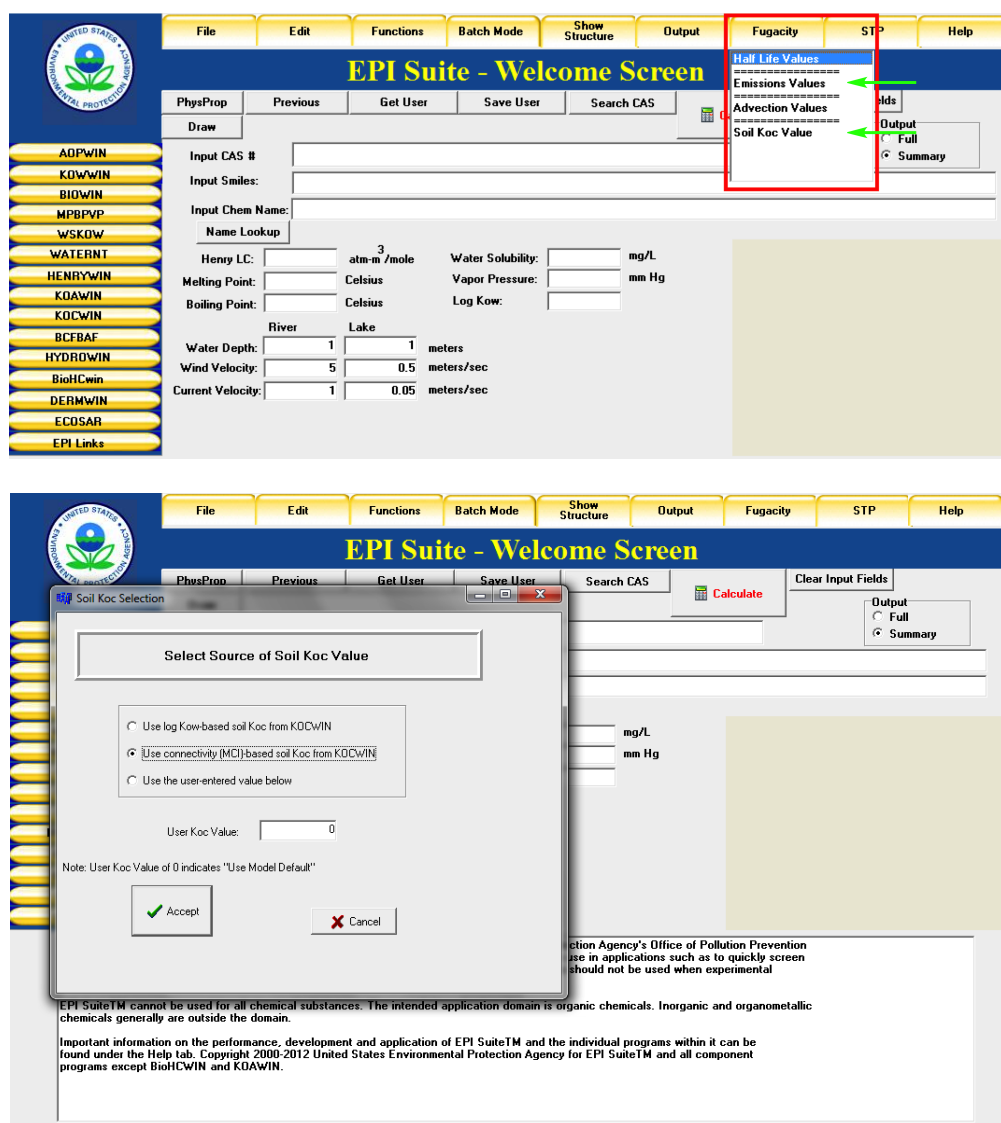


Figure 5.4: EPI Suite™ soil K_{OC} value entry box

The K_{OC} values calculated and measured in Chapter 4 were input to the computer model and compared against the default model values. The experimentally determined K_{OC} values for *N*-methylacetamide; P2P; phenol; and Benzaldehyde, oxime (Table 4.23 on page 188) were used. For MA, benzyl alcohol, 2,6-DTBP, and 1-phenyl-1,2-propanedione, the K_{OC} values calculated from the K_{OC}/K_{OW} correlation (Table 4.24 on page 194) were input.

In Chapter 3 it was determined that *N*-formylmethamphetamine was a key indicator chemical of the manufacture of MA. Without analytical standards, it was not possible to measure either the K_{OC} or K_{OW} . However, given the experimentally determined K_{OW} values were quite similar to the EPI Suite™ K_{OW} values, a K_{OC} value was calculated using the K_{OC}/K_{OW} correlation shown in Section 4.3.7 on page 192. Using a K_{OW} value of 1.68 into Equation 4.19 on page 193, a K_{OC} value of 46.71 was used to run the fugacity model for *N*-formylmethamphetamine.

Benzaldehyde was not included in the fugacity modelling in this chapter, even though it was selected for K_{OW} determination in the previous chapter. As its K_{OW} value could not accurately be determined using the OECD method, an estimate from EPI Suite™ would be required. It was decided that *N*-formylmethamphetamine is more characteristic of an illicit MA laboratory than benzaldehyde, therefore if any chemical was to be included using an estimated K_{OW} value, *N*-formylmethamphetamine would be of greater relevance.

5.2.3 Running the Fugacity Model

Multiple different modelling scenarios were run based on the different K_{OC} values - three or four different modelling scenarios were run for each chemical. The output from the fugacity model is the mass amount distribution of the chemical in each compartment (air, water, soil, and sediment). Each of those values is accompanied by a half life value – the time that is required for half of the chemical to be removed from that compartment. The fugacity model cannot be run without a half-life value. In most cases this is not known, but will be automatically calculated using a different model in the EPI Suite™ package – BIOWIN. The BIOWIN programme calculates aerobic and anaerobic biodegradation. This model assumes that the water:soil:sediment biodegradation ratio is 1:2:9. This ratio is the default model and cannot be changed by the user. If, however, half-life values are known, those can be entered into the fugacity model.

The first scenario executed was using the default settings of the EPI Suite™ programme. Each chemical was entered individually using its name, Chemical Abstract Service (CAS) number or SMILES (Simplified Molecular Input Line Entry System) notation, as summarized in Table 5.1. For the default scenario, no other values were changed apart from the emissions values as outlined above in Section 5.2.2.2. The remaining scenarios were run to allow the input of the

Table 5.1: Name, CAS number and SMILES notation of MA waste components used for entry into EPI Suite™

Name	CAS	SMILES
1,2-Propanedione, 1-phenyl-	579-07-7	<chem>O=C(c(cccc1)c1)C(=O)C</chem>
Phenol, 2,6-bis(1,1-dimethylethyl)-	128-39-2	<chem>Oc(c(ccc1)C(C)(C)C)c1C(C)(C)C</chem>
Benzenemethanol	100-51-6	<chem>OCc(cccc1)c1</chem>
Benzaldehyde, oxime	622-31-1	<chem>N(O)=Cc(cccc1)c1</chem>
<i>N</i> -formylmethamphetamine	42932-20-7	<chem>c1(CC(C)N(C)C(=O))ccccc1</chem>
Acetamide, <i>N</i> -methyl-	79-16-3	<chem>O=C(NC)C</chem>
Methamphetamine	537-46-2	<chem>CNC(C)Cc1ccccc1</chem>
2-Propanone, 1-phenyl-	103-79-7	<chem>O=C(Cc(cccc1)c1)C</chem>
Phenol	108-95-2	<chem>Oc(cccc1)c1</chem>

experimentally determined K_{OW} and K_{OC} values. Since K_{OW} values are much more readily measured experimentally than K_{OC} values, models were run using experimental K_{OW} values and with K_{OC} values calculated using the EPI Suite™ K_{OW} correlation. A summary of the four model scenarios run is presented in Table 5.2. Four model scenarios were run for each chemical for both emission scenarios (soil or water). For *N*-formylmethamphetamine, scenarios one and three are the same given an experimental value for K_{OW} was not determined. Therefore it was only necessary to run three models for *N*-formylmethamphetamine.

Table 5.2: Summary of EPI Suite™ fugacity model scenarios

Scenario	K_{OW} Source	K_{OC} Source
1	Default	Based on K_{OW}
2	Default	MCI
3	Experimental	Based on K_{OW}
4	Experimental	Experimental

5.2.4 Bioconcentration and Bioaccumulation

Another application of K_{OW} values is to estimate the bioconcentration factor (BCF, Equation 2.5 on page 50) and bioaccumulation factor (BAF). High K_{OW} values are associated with high bioconcentration factors as most aquatic organisms will uptake organic pollutants through passive diffusion. BCF and K_{OW} are related by the equation of line, given in Equation 2.6 on page 51, in Chapter 2. BCF and BAF were predicted using the experimentally determined log

K_{OW} values and compared against the EPI Suite™ default values for the water-release emissions scenario.

5.2.5 Ecological Structure Activity Relationships (ECOSAR)

ECOSAR is a stand-alone package in the EPI Suite™ computer programme (Figure 5.5) that can be used to estimate short-term (acute) and long-term (chronic) toxicity to aquatic organisms such as fish, aquatic invertebrates, and aquatic plants by using computerized Quantitative Structure Activity Relationships (QSARs). A discussion on the history and theory of QSARs was presented in Section 2.5.1 on page 49. ECOSAR uses QSARs to predict the aquatic toxicity of untested chemicals based on their structural similarity to chemicals for which aquatic studies are available (USEPA, 2012a). As with running the EPI Suite™ model, each chemical was entered individually using its CAS number, shown in Table 5.1 on the previous page.

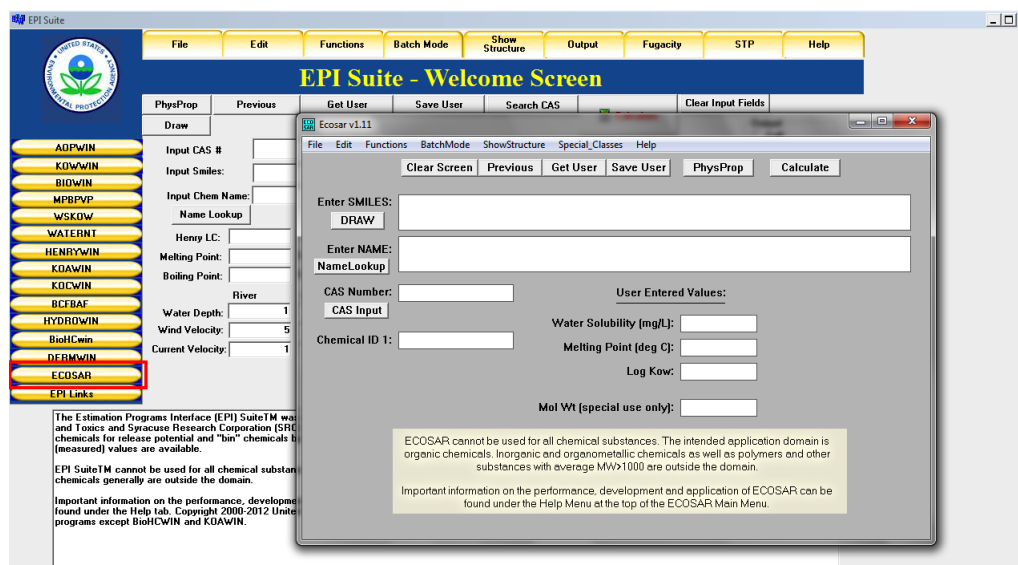


Figure 5.5: ECOSAR Homepage (USEPA, 2012b)

Two ECOSAR scenarios were run for each chemical: one using the default log K_{OW} values, the second using experimental log K_{OW} values. As with the fugacity model, only default log K_{OW} values were used for *N*-formylmethylamphetamine because an experimental log K_{OW} value was not determined in the previous chapter.

5.2.6 Estimation of Acute Environmental Impact: COD

COD was determined using a commercially prepared reactor digestion test tube kit with a range of 0 - 1500 mg/L oxygen (Hach-Lange, UK). Samples were prepared according to the kit instructions, and COD values were measured using a portable colorimeter (DR/850 Hach-Lange, UK). MA; P2P; *N*-methylacetamide; phenol; and benzaldehyde, oxime were tested as individual compounds at concentrations from 1 mg/L to 100 mg/L. Those five compounds were also tested as part of a mixture at concentrations from 0.01 mg/L to 100 mg/L for each chemical. Thus the final chemical concentration in solution ranged from 0.05 mg/L to 500 mg/L. Solutions were made up in Nanopure water (Barnstead Nanopure, ThermoFisher Scientific, UK). The estimated detection limit of the COD method is 30 mg/L (± 16 mg/L).

5.3 Results and Discussion

5.3.1 Environmental Partitioning of MA Waste

The environmental modelling of the waste components was based on compounds in the MA waste mixture identified in the preliminary study (Chapter 3). Many factors influence the environmental partitioning of MA waste; the key factor being the physicochemical properties of the waste itself. After the waste mixture was profiled using GC-MS, prediction of the environmental partitioning behaviour was feasible using the US EPA's EPI Suite™ fugacity model (USEPA, 2012b). Using EPI Suite™, it was possible to generate an estimated fugacity model for nine of the chemicals identified in MA waste. The fugacity model serves as a good indication of how the chemicals are likely to partition between environmental compartments. A discussion on the theory of fugacity modelling was presented in Section 2.5.2 on page 51.

One of the biggest factors that affects partitioning behaviour is the K_{OC} value. As seen in the previous chapter, it is a difficult parameter to measure. Fugacity models were run using different sources of K_{OC} values in order to compare the different model scenarios. There are four different sources of K_{OC} values that were used in the fugacity modelling in this study. The

four different derivations of K_{OC} values are presented in Table 5.3.

Table 5.3: K_{OC} values calculated using different parameters

Source of K_{OC}	Default Log K_{OW}	MCI	Exp. Log K_{OW}	Exp.
Model Scenario	1	2	3	4
2,6-DTBP	6506	9194	6424	369.33
1-phenyl-1,2-propanedione	12.04	10	25.85	47.62
Phenol	79.34	187.2	66.39	34.67
Benzaldehyde, oxime	32.99	813.1	18.12	72.44
Benzyl alcohol	13.25	21.46	19.41	39.05
<i>N</i> -methylacetamide	2.08	3.49	2.28	10.96
P2P	82.64	92.6	125.8	53.70
MA	106.3	892.5	102.3	58.82
<i>N</i> -formylmethylamphetamine	35.15	66.18	-	46.71

Exp. = Experimental

A comparison of the four different K_{OC} values illustrates the importance of compiling as much data as possible and taking the time to interpret the computer model. The K_{OC} values calculated using the MCI do not change based on K_{OW} values. Therefore, this would be a poor derivation to choose if the effects of K_{OW} on partitioning behaviour were being studied.

With a few exceptions, MCI returns the highest K_{OC} value. The exceptions are 1-phenyl-1,2-propanedione; benzyl alcohol; and *N*-methylacetamide, where the highest K_{OC} value was the experimental value. Again with a few exception, all K_{OC} values are within the same order of magnitude. The largest difference is for 2,6-DTBP which had an experimental K_{OC} value of 369 and an MCI K_{OC} value of 9194. The MCI produced K_{OC} values which are one order of magnitude higher for phenol; benzaldehyde, oxime; and MA. For P2P, the highest K_{OC} value was derived from the experimental log K_{OW} value. The experimental K_{OC} values are the highest for 1-phenyl-1,2-propanedione; benzyl alcohol; and *N*-methylacetamide.

In general, there are no trends as to which method produces a higher or lower K_{OC} value. Without extensive experimentation, it would not be possible to determine which value is “correct”. Therefore a range can be taken to produce higher and lower estimates of partitioning behaviour.

The lower the K_{OC} value, the lower the propensity for a chemical to partition into the sediment compartment. Typically, as the organic carbon content of the sediment increases, organic molecules will partition more heavily into that compartment, binding to the organic carbon.

5.3.1.1 Water Discharge Scenario

The first series of fugacity models was created by changing the emissions scenario to emulate a direct discharge of MA waste directly into surface waters. A graphical representation of the fugacity models was created to compare the different K_{OC} and K_{OW} input parameters. By changing one parameter at a time, K_{OC} or K_{OW} , the compartment distribution of each chemical changes slightly. The compound with the largest discrepancies between the default K_{OC} value and the calculated values was 2,6-DTBP. The fugacity model of 2,6-DTBP is shown in Figure 5.6.

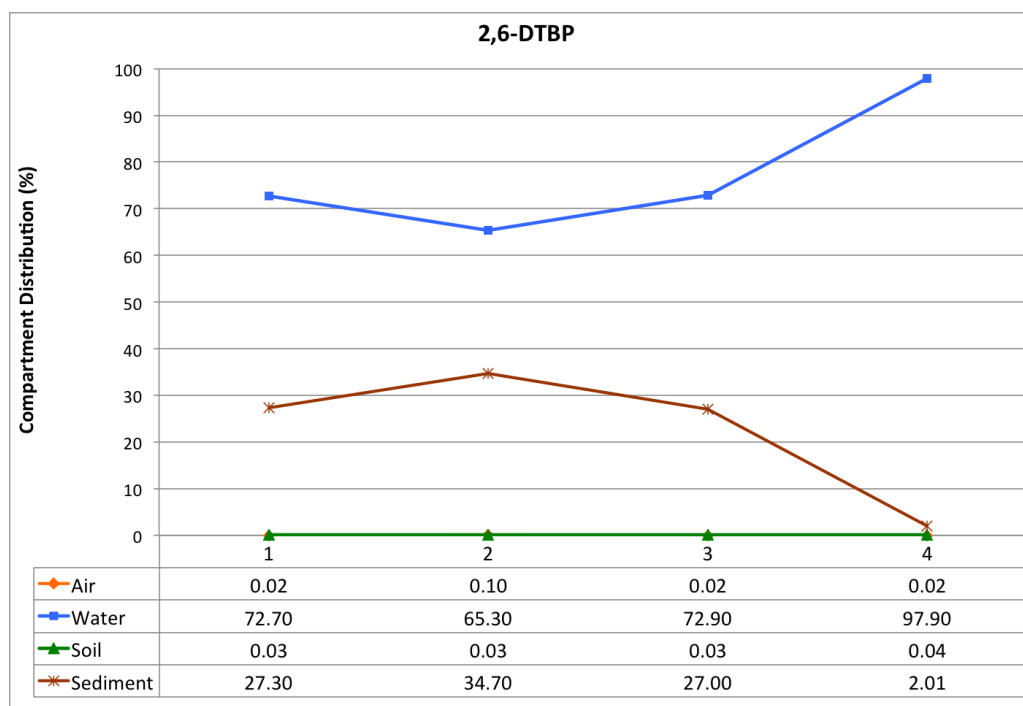


Figure 5.6: Water discharge scenario fugacity model of 2,6-DTBP, from EPI Suite™. (X-axis = model scenario corresponding to Table 5.2 on page 205)

The differences between the default and experiment fugacity models are important, because 2,6-DTBP displays a large variance in partitioning behaviour. In the MCI model (Model 2), 65.3%

of 2,6-DTBP is estimated to partition into the water compartment, whereas in the experimental model (Model 4), 97.9% is estimated to partition into the water, with the remainder partitioning into the sediment compartment. Model scenarios one and three have nearly identical results, which is to be expected because they are both calculated using K_{OC} values based on $\log K_{OW}$ values. The EPI Suite™ default $\log K_{OW}$ of 2,6-DTBP is 4.92, compared to an experimental value of 4.91.

As more mass partitions into the sediment compartment, it needs to be subtracted from another compartment in order to maintain a mass balance. In these model scenarios, the mass is being transferred from the water compartment. Consequently, as the mass amount in the sediment compartment decreases, the mass amount in the water compartment increases. This corresponds with the decrease in K_{OC} values - model scenario four has the lowest K_{OC} value as well as the lowest amount of 2,6-DTBP partitioning into the sediment compartment. Conversely, the MCI K_{OC} value is the highest and model scenario two has the higher proportion of 2,6-DTBP estimated to partition into the sediment compartment.

The difference in the distribution behaviour between the MCI model and the experimental models has implications for sample collection. If only the MCI model was taken into account, samples may be collected from an inappropriate compartment. The MCI model indicates that samples should be collected from the sediment compartment, while the remaining three models indicate samples should be collected from the water compartment. This difference highlights the importance of generating site-specific models, even if they are only estimates.

The behaviour of *N*-methylacetamide (Figure 5.7) was the opposite to that of 2,6-DTBP. *N*-methylacetamide is estimated to partition overwhelmingly (99.80%) into the water compartment, which is in accordance with its low $\log K_{OW}$ and K_{OC} values. The different K_{OC} values did not result in a change in the compartment distribution. This was to be expected given the small variances between the different K_{OC} values shown in Table 5.3 on page 208. Of the compounds positively identified in the MA waste, *N*-methylacetamide is the only one that does not have an aromatic ring, meaning it is not as stable and predicted to be more water soluble than the rest of the waste.

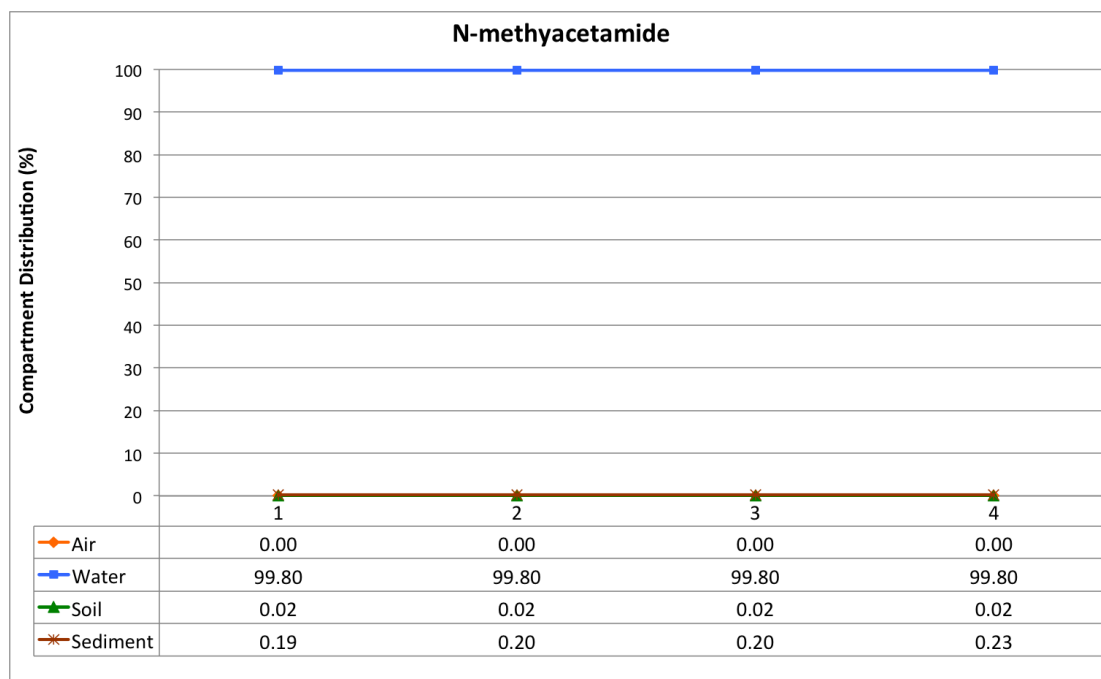


Figure 5.7: Water discharge scenario fugacity model of *N*-methylacetamide, from EPI Suite™. (X-axis = model scenario corresponding to Table 5.2 on page 205)

The remaining seven chemicals that were modelled exhibit similar trends as seen for MA, P2P, and *N*-formylmethylamphetamine in Figures 5.8, 5.9, and 5.10, respectively. The fugacity models for 1-phenyl-1,2-propanedione; benzaldehyde, oxime; benzyl alcohol; and phenol are shown in Appendix C, Figures C.1 on page 289 to C.4 on page 290.

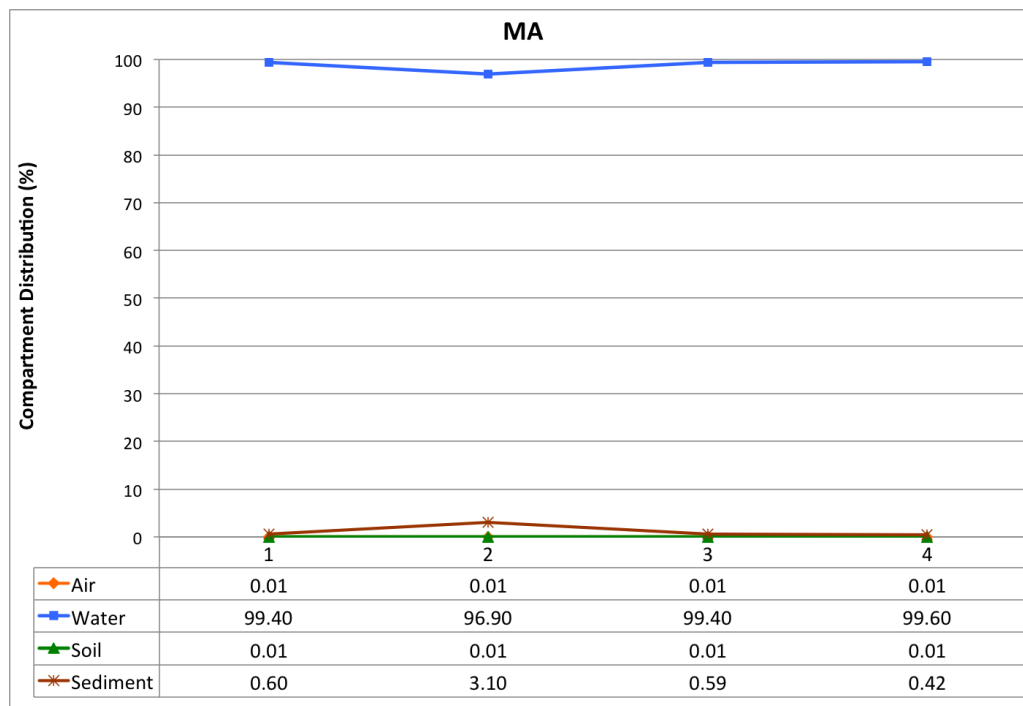


Figure 5.8: Water discharge scenario fugacity model of MA, from EPI Suite™. (X-axis = model scenario corresponding to Table 5.2 on page 205)

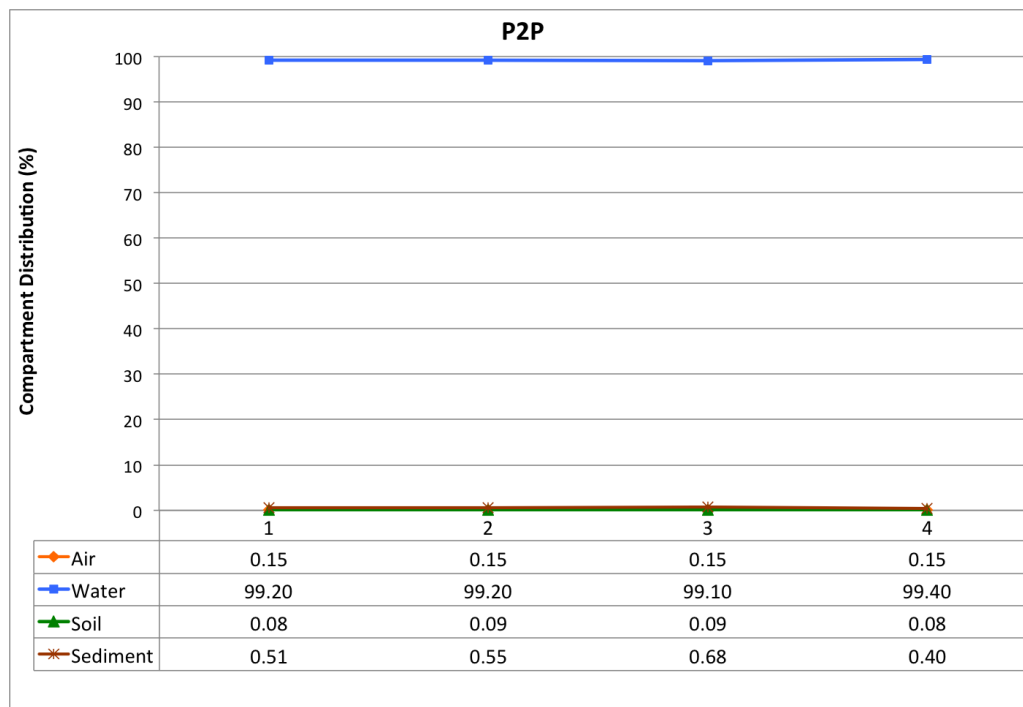


Figure 5.9: Water discharge scenario fugacity model of P2P, from EPI Suite™. (X-axis = model scenario corresponding to Table 5.2 on page 205)

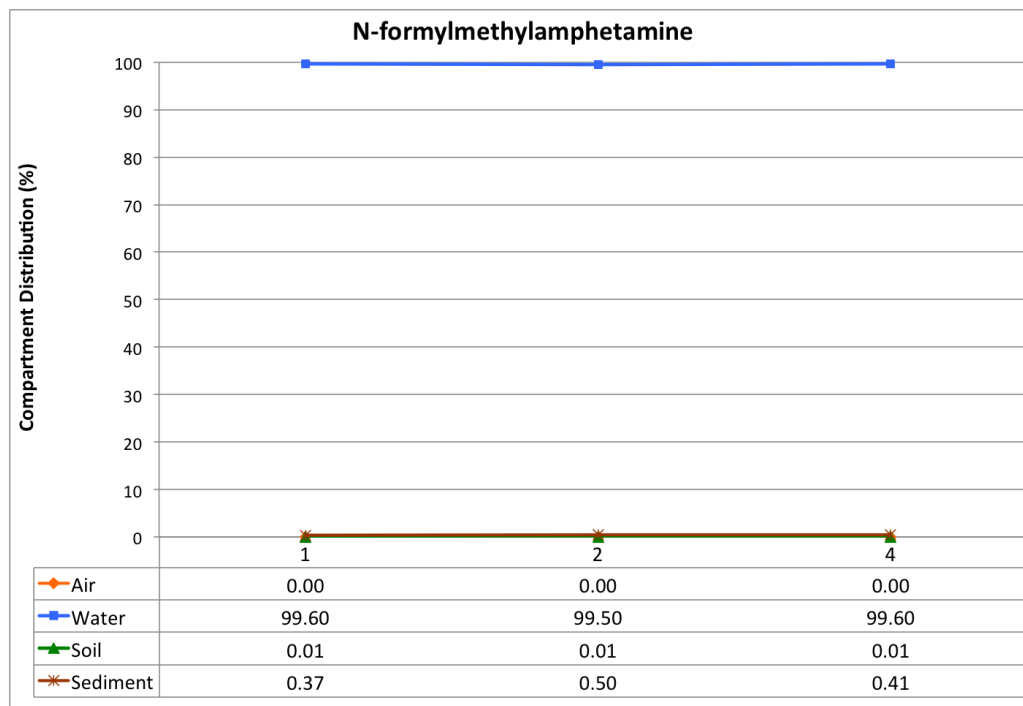


Figure 5.10: Water discharge scenario fugacity model of *N*-formylmethamphetamine, from EPI Suite™. (X-axis = model scenario corresponding to Table 5.2 on page 205)

The general trend is that the chemicals will remain in the water compartment once discharged directly into surface waters. For each of the chemicals, all four models predict that over 99% will remain in the water compartment. The only exception is MA when modelled using the MCI-based K_{OC} value. In this scenario, a small amount (3.10%) is estimated to partition into the sediment compartment.

The similar behaviour of MA, P2P, and *N*-formylmethamphetamine may be attributed to their similar chemical structures, notably the benzene ring with a branched alkane containing an oxygen (P2P) or nitrogen (MA) functional group, or both (*N*-formylmethamphetamine). With the exception of 2,6-DTBP, the majority of the mass of MA waste discharged into surface waters will remain in the water compartment.

In all four of the model scenarios, and for all nine of the chemicals, there is very little partitioning behaviour into the air and soil compartments. Of all model scenarios conducted, the default model predicts the greatest amount of partitioning into the air. Even for that scenario,

the highest mass amount found in the air is 0.15% for P2P. Soil is not a significant factor as the model was specified to be a chemical release directly into water and the water does not interface directly with the soil compartment.

The half lives of each chemical do not change with each model scenario (Table 5.4). The compartment with the lowest mass amount, the sediment compartment, is the compartment with the slowest predicted degradation. Therefore, even though chemicals are present in small amounts, they are likely to still be present in the sediment after nearly 20 months. This may aide in the investigation of a suspected dumpsite as it increases the chances of detecting marker chemicals. However, detection may be difficult given the low partitioning into the sediment compartment. The exception is 2,6-DTBP, which is estimated to partition moderately into the sediment compartment. Given the long half life of 2,6-DTBP in the sediment compartment, it is likely to remain present after nearly 20 months in sufficient quantities to allow for detection. Its persistence in the sediment may also pose an ecotoxicological hazard to the surrounding environment.

Table 5.4: EPI Suite™ estimated half life values, in hours, of MA waste in the environment

Compound	Air	Water	Soil	Sediment
1-phenyl-1,2-propanedione	137	360	720	3240
2,6-DTBP	5.23	900	1800	8100
Benzaldehyde oxime	39.1	360	720	3240
Benzyl alcohol	11.2	360	720	3240
MA	2.77	360	720	3240
<i>N</i> -formylmethylamphetamine	5.75	900	1800	8100
<i>N</i> -methylacetamide	49.4	360	720	3240
P2P	45.5	360	720	3240
Phenol	9.76	360	720	3240

For the other chemicals modelled, whose partitioning will be predominantly into the water compartment, half life values range from 360 hours (15 days) to 900 hours (37.5 days). A persistence time of two weeks may seem like a short time to complete a criminal investigation into environmental pollution, however many clandestine MA laboratories are often only operational for a short period of time before being dismantled and relocated in order to avoid detection. If

MA waste is detected in sufficient quantities, it is likely that the laboratory is still operational and further police intelligence may aid in the detection and dismantling of the laboratory.

The key MA waste marker, *N*-formylmethylamphetamine, has a half life value of more than one month - which is more than double that of MA, P2P, and the other waste components. The detection of *N*-formylmethylamphetamine in the environment would be a good indicator of a clandestine MA dumpsite as it is not manufactured commercially and is predicted to remain in the aqueous phase for over one month. *N*-formylmethylamphetamine is unlikely to be present on its own as other waste components are likely to be present as well and it is the combination of several compounds that would indicate a MA dumpsite.

5.3.1.2 Soil Discharge Scenario

The second series of fugacity models was run identical to the first set, however the emissions scenario was changed to emulate a discharge of MA waste directly into soil. The soil emissions fugacity model of 2,6-DTBP is shown in Figure 5.11.

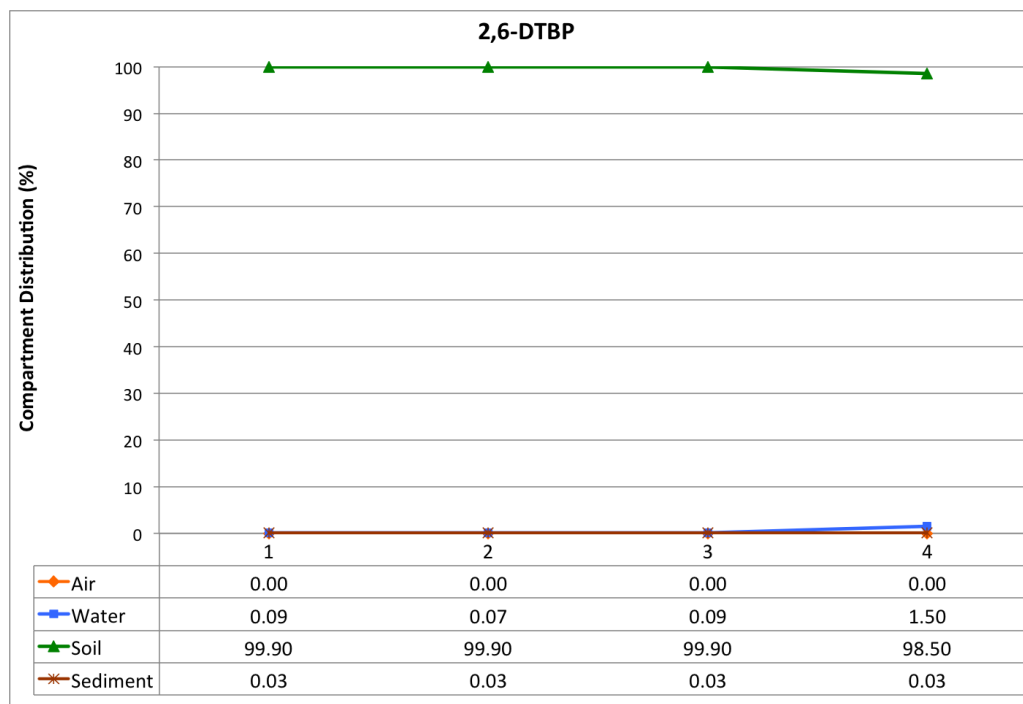


Figure 5.11: Soil discharge scenario fugacity model of 2,6-DTBP, from EPI Suite™. (X-axis = model scenario corresponding to Table 5.2 on page 205)

In the soil emissions scenario, 2,6-DTBP is estimated to remain overwhelmingly in the soil compartment. Models one, two, and three estimate that 99.9% of 2,6-DTBP will remain in the soil compartment, while the experimental values (model four) estimates that only 1.5% of 2,6-DTBP will partition into the water compartment. Based on the log K_{OW} and K_{OC} values, 2,6-DTBP is a hydrophobic chemical with a low water solubility. Therefore it is to be expected to tightly bind to organic matter in the soil. In a scenario where MA waste was dumped into soil, 2,6-DTBP would not migrate to the water table, which would limit its migration and spread in the environment.

N-methylacetamide behaved completely differently from 2,6-DTBP in the water discharge scenario. For the soil discharge scenario (Figure 5.12), the lowest estimated amount of *N*-methylacetamide in the water compartment is from the experimental scenario at 13.2%. The highest water partitioning levels are estimated to be 19.7% from the default model.

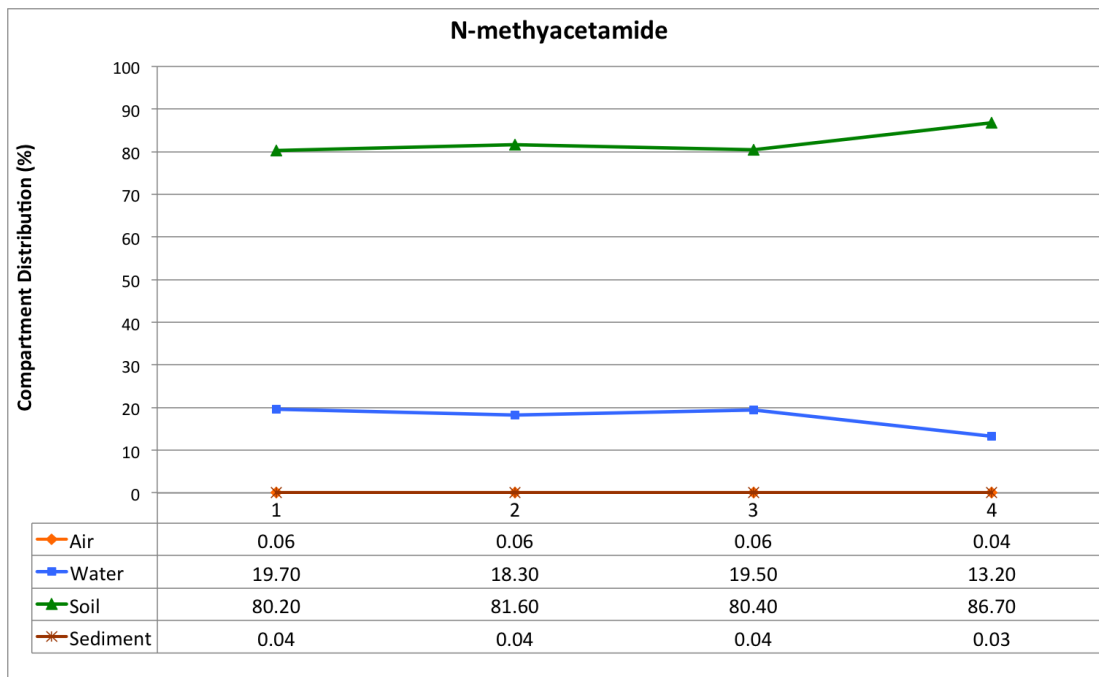


Figure 5.12: Soil discharge scenario fugacity model of *N*-methylacetamide, from EPI Suite™. (X-axis = model scenario corresponding to Table 5.2 on page 205)

MA, P2P, and *N*-formylmethylamphetamine, will exhibit some migration into the water compartment, varying from 0.39% to 10.4%. The soil emissions fugacity models of MA, P2P, and

N-formylmethylamphetamine are shown in Figures 5.13, 5.14, and 5.15, respectively. The soil discharge fugacity models for 1-phenyl-1,2-propanedione, benzaldehyde oxime, benzyl alcohol, and phenol are shown in Appendix C, Figures C.5 on page 291 to C.8 on page 292.

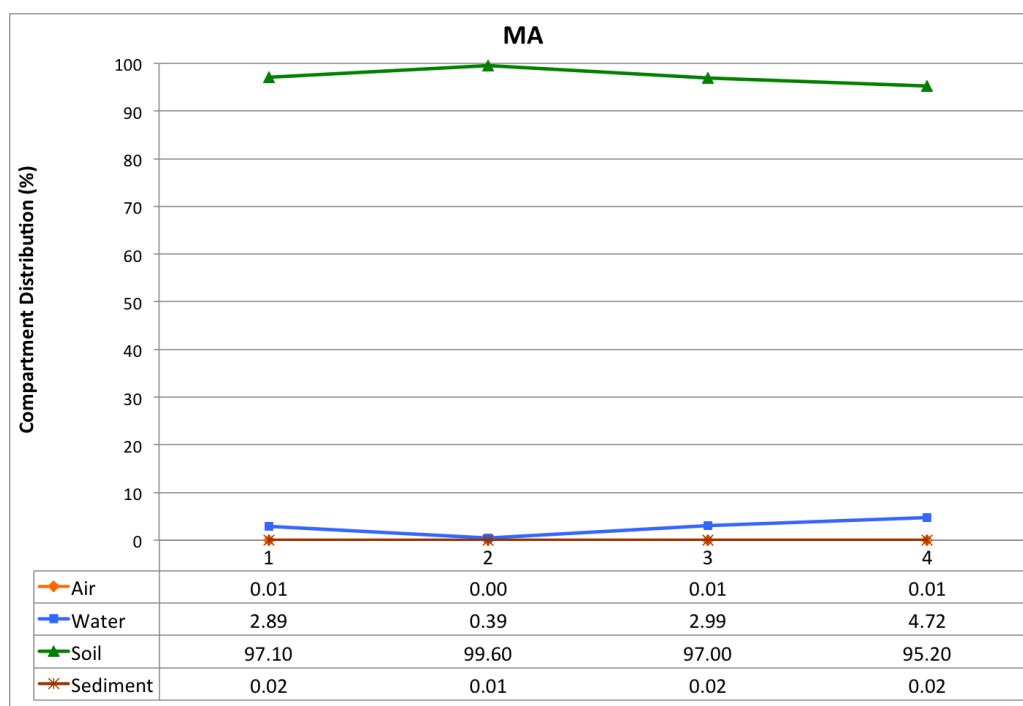


Figure 5.13: Soil discharge scenario fugacity model of MA, from EPI Suite™. (X-axis = model scenario corresponding to Table 5.2 on page 205)

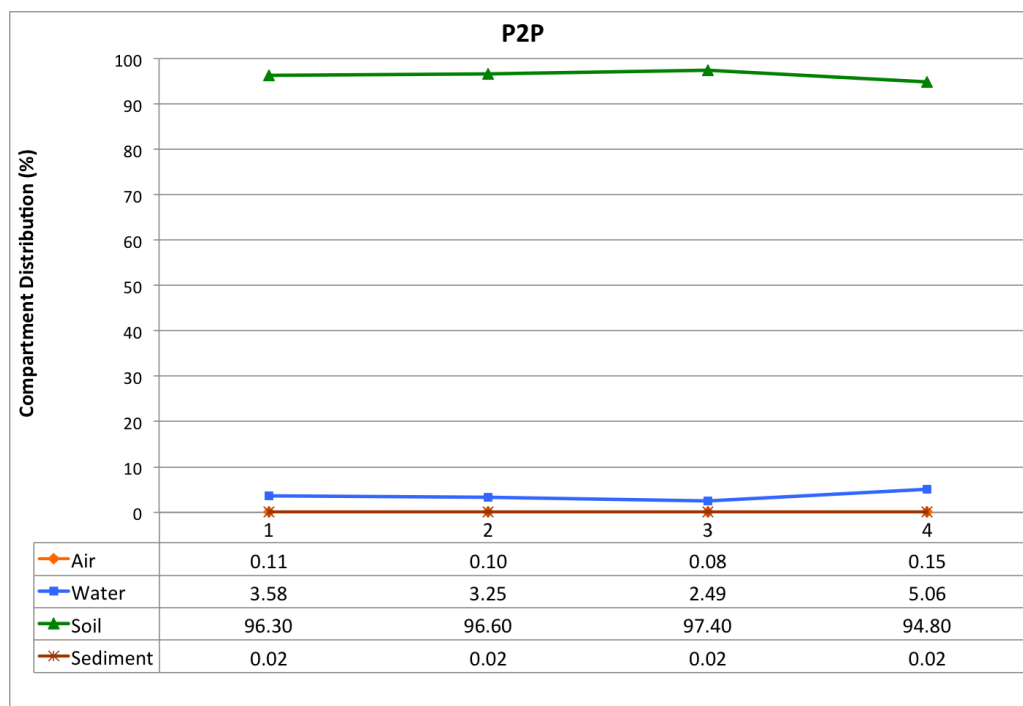


Figure 5.14: Soil discharge scenario fugacity model of P2P, from EPI Suite™. (X-axis = model scenario corresponding to Table 5.2 on page 205)

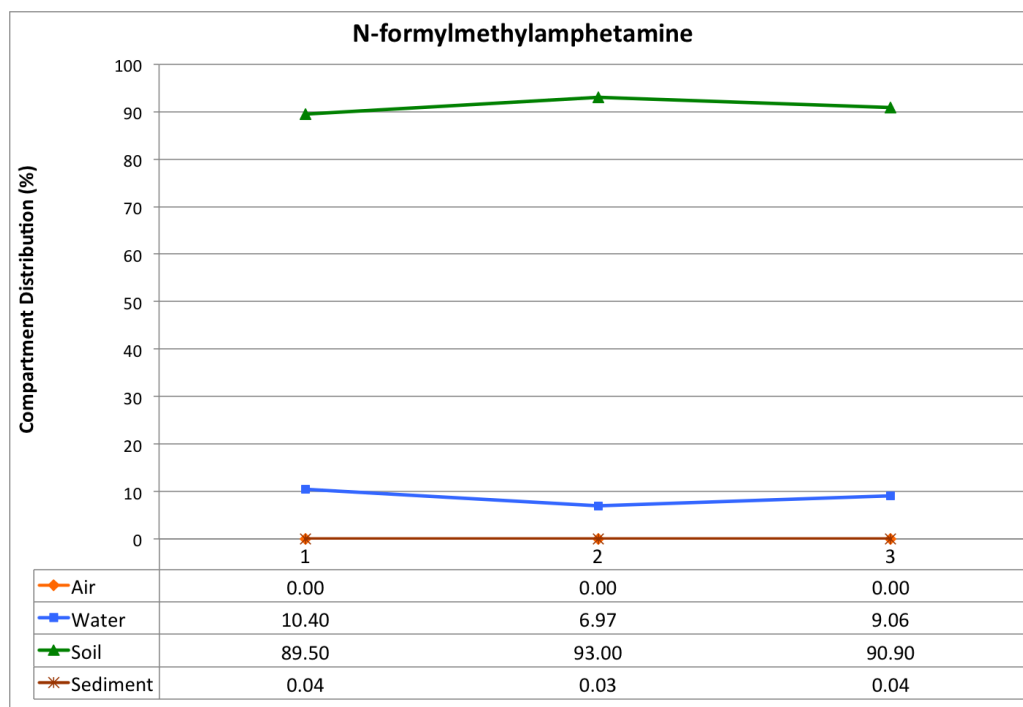


Figure 5.15: Soil discharge scenario fugacity model of *N*-formylmethamphetamine, from EPI Suite™. (X-axis = model scenario corresponding to Table 5.2 on page 205)

As with the water discharge scenario, the general trend is that the chemicals will remain in the soil compartment once discharged directly into soil. For each of the chemicals, all four models predict that 80-99% will remain in the soil compartment. A small amount of migration to water will occur, but for the most part the chemicals will remain in the soil and will not be subject to migration or spreading via the water table. In this scenario, MA waste may be more harmful to plants that may uptake the contaminants along with soil nutrients.

There is once again very little partitioning into the air compartment. In this scenario, the sediment compartment is the one which does not directly interface with the soil compartment, and there is very little partitioning taking place into the sediment.

The half lives of each chemical do not change with the soil discharge scenario (Table 5.4 on page 214). This is more encouraging for sample collection because in the soil discharge scenario, the compartment with the highest mass amount is the compartment with the slowest predicted degradation. Therefore there is a greater chance of detecting MA waste in the soil over a longer period of time. Conversely, the persistence in the soil could create a greater ecological hazard.

Compartment distribution, half life values, and police intelligence all form part of an investigation into a clandestine waste dumpsite. Police intelligence may lead investigators to a location and indicate how much time has elapsed since the disposal of waste has occurred. Knowledge of the compartment distribution and half life values will allow for a targeted sampling approach, to ensure the correct samples are collected. From the fugacity model, it is recommended to collect both water and sediment samples as most of the waste components will partition into the water phase, with the exception of 2,6-DTPB, which is a distinct chemical whose commercial applications are limited. 2,6-DTBP has legitimate commercial uses as an intermediate compound in the synthesis for the production of higher molecular weight phenolic antioxidants. It is also used as an oxidation inhibitor and stabilizer mainly for fuel, oil, and gasoline (UNEP Publications, 2013). Combined with the half life values, the persistence of the chemicals in the sediment compartment may detect compounds which have already migrated from the water compartment.

5.3.2 Effects of K_{OW} Measurements

In Section 4.2.3 it was determined that there was very little difference between experimentally measured $\log K_{OW}$ values and the EPI Suite™ predicted values. However, it was not known whether or not insignificant differences in $\log K_{OW}$ measurements would affect the compartment distribution. Model scenarios one and three (Table 5.2 on page 205) are the same fugacity model, but with different K_{OW} values. Model one uses the EPI Suite™ default value, while model three uses the experimental K_{OW} value. Looking at all the graphs of the fugacity models and comparing model one to model three, there is never more than a 3.5% difference (1-phenyl-1,2-propanedione, soil discharge scenario, Figure C.5 on page 291) in compartment distribution between the two different methods. A 3.5% difference in percent distribution would be difficult to reliably quantify for a suspected dumpsite, depending on limits of quantification, the extraction recovery rate, and extraction reproducibility. A 3.5% difference may be within experimental error.

Where the different partitioning behaviour may have the largest affect is the toxicity to aquatic organisms, such as fish. As the measured $\log K_{OW}$ and K_{OC} values predicts more 2,6-DTBP to partition into the water compartment, it may be more bioavailable to fish. Given the high $\log K_{OW}$ value of 2,6-DTBP, it is likely that it will be taken up by the fish through passive diffusion through the gills. In contrast to the default model, where more partitioning is expected to occur in the sediment compartment, uptake of 2,6-DTBP by fish may occur as the fish feed and accidentally ingest the sediment simultaneously. The toxicity of 2,6-DTBP on aquatic organisms would depend on the route of uptake and biological processes of the individual organism. While one organism may be more affected by passive diffusion from the water phase, a different organism may be more affected by ingestion of the sediment. In the absence of further laboratory experimentation, it is difficult to speculate further on potential toxicity effects. Additional estimation into the toxicity of 2,6-DTBP and other MA waste chemicals can be conducted using a bioconcentration model and ECOSAR evaluation.

5.3.3 Assumptions and Limitations of the EPI Suite™ Fugacity Model

EPI Suite™ has several assumptions and limitations that must be taken into account when interpreting the results. The model is designed to be a screening tool and should not be used if measured values are available. EPI Suite™ uses a Level III Fugacity model which has several assumptions of its own. The Level III model assumes steady state conditions, but not equilibrium conditions. This means the model assumes that chemical concentrations in each compartment will approach zero over time. The Level III model does not assume that each phase is in equilibrium, meaning that if a chemical is released into one compartment it can partition into the other compartments. In the Level III model, a chemical is continuously discharged at a constant rate and achieves a steady state condition when input and output rates are equal (CCEMC, 2002; USEPA, 2012b).

Chemical losses occur through two methods: reaction and advection. Reactions include biotic or abiotic degradation of the chemical in each of the four compartments. Advection is the removal of a chemical from a compartment through losses other than degradation, such as bulk media transport via river currents. Advection processes are not considered for the soil compartment. Additional assumptions of the Level III model are that there are no direct emissions into the sediment compartment and it cannot model ionizing or speciating chemicals (CCEMC, 2002; USEPA, 2012b).

There are several parameters that can be changed by the user in EPI Suite™ in order to create a chemical and site specific model; however, there are also numerous parameters that cannot be changed. For example, a fixed temperature of 25°C is assumed. That temperature will not reflect many countries mean annual temperatures, nor will it take into account daytime and seasonal variations. A full list of set and variable parameters are presented in Table 5.5 (USEPA, 2012b).

Table 5.5: Set and variable parameters of the EPI Suite™ fugacity model

Set Parameters	Variable Parameters
Temperature	Henry's law constant
Salinity	Melting point
pH	Boiling point
Biodegradation ratio	Water solubility
Rain rate	Vapour pressure
Aerosol deposition	Log K_{OW}
Soil water runoff	Water depth
Diffusion mass transfer coefficients	Wind velocity
Compartment dimensions	Current velocity
Volume fractions of media	Advection values
Density of media	Soil K_{OC} values
Lipid concentrations	Emission values
Organic carbon concentrations	Half-life values

Each of the above parameters will affect fugacity and compartment distribution. While a site specific model can be approximated, the limitations in setting parameters will prevent a truly site specific model from being designed. This once again reinforces the need for laboratory experimentation, particularly in environments that vary considerably from the model default values. An additional limitation of the model is that mixtures cannot be evaluated. After understanding the assumptions and limitations of the EPI Suite™ fugacity model, its advantages are also important to note. Compared to other environmental models, such as a mass balance model, the fugacity model is easy to understand and it does not rely on units, but rather it is based on ratios therefore the units cancel out. In order to properly use a mass balance model, it is required to have estimated input concentrations of the chemicals. For this study, concentrations of MA waste have never been measured or studied in a large scale, real-life scenario. Another advantage to using the EPI Suite™ modelling programme is that it provides the probability of rapid degradation as well as the removal rate in wastewater treatment plants, which can indicate the amount of chemical discharged into receiving waters. There is a wealth of information provided by EPI Suite™ that is not available in models that consider only one environmental effect at a time.

5.3.4 Accumulation of MA Waste in Biota

Bioaccumulation and bioconcentration are two terms which help describe the accumulation of chemical contaminants in biota. Bioaccumulation is the net accumulation of a contaminant in an organism from all sources - water, air, soil, sediment, food, and suspended particles. Bioconcentration is the net accumulation of a contaminant in an organism from the water compartment only. Contaminants will affect target organs or tissues in biota, and it is important to be able to predict the accumulation of a contaminant in the food chain. As contaminants move up the trophic levels of the food chain, contaminants may become more concentrated, known as biomagnification. Therefore organisms at higher trophic levels, such as humans, may be more susceptible to the toxic effects of certain contaminants that were initially ingested by lower trophic levels, such as fish. The extent to which a chemical will bioaccumulate or bioconcentrate in an organism will be dependent on three processes: uptake, biotransformation, and elimination (Newman and Unger, 2003).

Contaminant uptake can occur through three general routes: lipids, aqueous, and endocytotic routes. In the lipid route, lipophilic (high K_{OW}) contaminants pass through the bilayer of lipid membranes by diffusion. In an aquatic system, small, uncharged polar contaminants which are dissolved in the water phase may readily diffuse across the lipid bilayer as water passes through the gills of a fish. Contaminant uptake via the aqueous route occurs using membrane transport proteins, while in endocytotic routes, the contaminant is released into the organism once it has been incorporated into a vesicle that is subsequently lysed. This route of uptake is common for metals, such as iron (Newman and Unger, 2003).

In order for a contaminant to be taken up by an organism, it must first come into contact with a surface of the organisms through sorption or adsorption. Once the contaminant has made contact with the organism, uptake may occur through several mechanisms: adsorption, passive diffusion, active transport, facilitated diffusion or transport, exchange diffusion, and endocytosis. Diffusion is the movement of a contaminant down an electrochemical gradient (i.e. concentration, activity, or electrical gradient), while facilitated and exchange diffusion require transport proteins. Active transport is the reverse of diffusion - transport up a gradient which requires energy (Newman and Unger, 2003).

Once an organism has taken up a contaminant, it may undergo biotransformation (metabolism) where it is transformed from one compound to another. The transformed product may be less harmful than the parent contaminant and enhance the elimination of the contaminant by, for example, converting the chemical into a more hydrophilic form. The contaminant may also undergo biotransformation to form a more harmful product than the parent contaminant, termed activation, where a non-toxic contaminant is converted into a product with harmful bioactivity (Newman and Unger, 2003).

After biotransformation, the contaminant may be excreted, decreasing the amount remaining in the organism. For compounds with $\log K_{OW}$ values less than three (most of the MA waste components), elimination may occur rapidly by diffusion through the gills. For compounds with a higher lipophilicity (2,6-DTBP), diffusion may take a longer time, or the compound may be eliminated through the liver, into bile and lost in feces. Using kinetic and pharmacokinetic modeling, it is possible to estimate the excretion of a contaminant, and to estimate the persistence time in the organism (Newman and Unger, 2003). Bioaccumulation, biotransformation, and elimination half lives can be calculated using $\log K_{OW}$ values as part of the EPI Suite™ package.

The bioaccumulation factor (BAF) and bioconcentration factor (BCF) were estimated using the EPI Suite™ model (Table 5.6). As the estimates are dependent on K_{OW} values, the BAF and BCF were calculated using both the default K_{OW} values and the experimental K_{OW} values. BCF and BAF values are expressed in L/Kg wet-weight of fish, which enables comparison between different species by normalising for lipid content. If the percent lipid of the organism is known, this can be accomplished by dividing the wet weight (L/Kg) by percent lipid, resulting

in a value with units of L/Kg lipid weight.

Table 5.6: Estimated bioaccumulation and bioconcentration factor based on default and experimental log K_{OW} values.

Chemical	Default log K_{OW}		Experimental log K_{OW}	
	BAF	BCF	BAF	BCF
	(L/Kg wet-wt)		(L/Kg wet-wt)	
2,6-DTBP	631.5	639.0	542.8	546.0
1-phenyl-1,2-propanedione	1.952	1.952	6.337	6.337
Phenol	2.419	2.419	2.419	2.419
Benzaldehyde, oxime	3.681	3.681	2.738	2.738
Benzyl alcohol	1.549	1.549	2.777	2.777
<i>N</i> -methylacetamide	0.8951	0.8951	0.8997	0.8997
P2P	2.803	2.803	5.908	5.908
MA	11.84	11.84	12.86	12.86
<i>N</i> -formylmethylamphetamine	2.896	2.896	-	-

Recalling the linear relationship between log K_{OW} and BAF and BCF, it was expected that BAF and BCF based on the estimated and experimental log K_{OW} values would display minimal differences, as seen in Table 5.6. This behaviour was expected due to the insignificant difference between the two log K_{OW} values, as described in Section 4.3.1. Two chemicals, 1-phenyl-1,2-propanedione and P2P, exhibited notable increases in BAF and BCF when calculated using the experimental log K_{OW} , which corresponds to an increase in the potential harm these chemicals will have towards fish. BAF and BCF values of 1-phenyl-1,2-propanedione increased by over three-fold, from 1.952 to 6.337, when calculated using the experimental log K_{OW} value compared to the estimated log K_{OW} value. The BAF and BCF values of P2P also increased when they were calculated based on the experimental log K_{OW} compared to the estimated log K_{OW} , displaying a two-fold increase from 2.803 to 5.908.

The most harmful chemical from MA waste was determined to be 2,6-DTBP, having BAF and BCF values from 542 to 639 L/Kg wet-wt in upper trophic level fish. The BAF and BCF values decreased slightly when calculations were based on the experimental log K_{OW} value, which is in accordance with the experimental value (4.91) being quite similar to the estimated value (4.92). The least harmful component of the MA waste that was tested is predicted to be

N-methylacetamide, with BAF and BCF values ranging from 0.8951 to 0.8997 L/Kg wet-wt. This is consistent with the low log K_{OW} values of *N*-methylacetamide (-0.70 estimated, -0.98 experimental). BCF and BAF are only an estimate of potential harmfulness. Their effects are more likely to be seen over the long term and may affect the species as a whole population, rather than individuals. For example, BCF may affect the reproductive systems of organisms, affecting the population of the next generation. BAF may affect the reproductive systems of organisms higher up the food chain, or may have acute effects on the organisms that ingest food which has accumulated a high amount of a toxic substance.

MA itself was predicted to have the second highest BCF/BAF values of all the components of the MA waste. This is particularly concerning due to the biological activity of MA. If MA were to bioaccumulate in the lipid layers of fish, it would be unlikely to enter into the blood stream of the organism, meaning MA would not cross the blood-brain barrier and would not have the same physiological effects as an organism who ingested the drug directly. However, if environmental stresses were to occur, the organism may experience rapid weight loss, causing the MA (along with any other contaminants) to be released from the lipid layer and become bioavailable. When the MA becomes mobilised in the blood stream, its physiologically active nature may result in potentially toxic and fatal effects towards the organism.

Of the nine chemicals examined, 2,6-DTBP was the only one to have different BAF and BCF values, a distinction which is related to the distribution patterns of the chemicals. Of the compounds modelled, 2,6-DTBP is the only chemical which is predicted to have any significant partitioning into the sediment compartment (2-34%) in the water-discharge scenario. For the other compounds, 97-99% of the chemical is predicted to remain in the water compartment. This affects the BAF and BCF values because BAF is the accumulation of a contaminant from all of the compartments, whereas BCF is the net accumulation solely from the water compartment. If the chemicals will not be partitioning outside of the water compartment, the contribution to BAF from other compartments will be negligible, resulting in BAF being equal to BCF.

EPI Suite™ has a programme which estimates the biotransformation rate in fish, generating half life values for the residence time of organic chemicals in fish. In EPI Suite™, biotransforma-

tion is defined as “the change of the parent substance to another molecule or a conjugated form of the parent substance” (USEPA, 2012b). The model assumes first order kinetics and does not take into account metabolic products, only the parent compound. If metabolic products are known, they would have to entered into a separate model. The estimated biotransformation half life values for the identified MA waste components are shown in Table 5.7.

Table 5.7: Estimated biotransformation half lives of fish based on default and experimental K_{OW} values.

Chemical	Default log K_{OW}	Experimental log K_{OW}
	Half Life (days)	Half Life (days)
2,6-DTBP	1.653	1.445
1-phenyl-1,2-propanedione	0.09339	0.1532
Phenol	0.03152	0.03152
Benzaldehyde, oxime	0.03374	0.02971
Benzyl alcohol	0.02671	0.0362
<i>N</i> -methylacetamide	0.007043	0.009414
P2P	0.05875	0.07908
MA	0.367	0.3775
<i>N</i> -formylmethylamphetamine	0.02354	-

As seen with the BAF and BCF results, it is 2,6-DTBP, with the highest log K_{OW} value, which is predicted to cause the have the greatest affect on aquatic organisms. 2,6-DTBP has the longest half life values in fish, predicted to require 1.4-1.6 days for a fish to metabolise half the amount of chemical taken up. This is the only compound with a half life time over one day. Conversely, *N*-methylacetamide with the lowest log K_{OW} value, is predicted to have the shortest half life time, undergoing biotransformation in less than one hour. A longer half life value will increase the chances of another organism, such as humans, consuming the contaminant along with the fish, increasing the biomagnification potential of the contaminant. A longer persistence time will also provide a wider window of opportunity to discover the presence of the contaminant in the fish to provide supporting evidence of an illicit MA waste dumpsite.

For example, there was a clandestine laboratory located near a stream in the province of British Columbia, Canada. The laboratory was discovered and seized after the discovery of dead fish in

the stream, however no criminal charges arose relating to pollution of the environment (Hugel, 2010). If the fish were analysed as part of the criminal investigation, they may have been able to test tissue samples for the presence of contaminants related to the clandestine laboratory. When testing for contaminants, care must be taken when selecting which contaminants to test for.

A compound such as *N*-formylmethylamphetamine is a highly specific indicator of an illicit clandestine MA laboratory, however it has a relatively short half life time of approximately half an hour. MA has a longer half life (approximately 9 hours), however it has been detected in surface waters as a residual product from WWTPs (Zuccato et al., 2008), therefore other potential sources must be taken into consideration. A compound such as 2,6-DTBP, with a high affinity for lipids and sediment, and with a long half life, may be an excellent indicator of an illicit MA dumpsite, however the legitimate sources of 2,6-DTBP are limited. *N*-methylacetamide would be a poor choice for a marker compound due to its high water solubility, low $\log K_{OW}$, and short biotransformation half life.

The modelling performed in this study did not take into account that the waste components will be released into the environment as part of mixtures. As such, the toxicity of the mixture may vary from that of the individual compounds. The compounds may exhibit additive toxicity where the toxic effects of the mixture are greater than the sum of the toxic effects of the individual compounds. It may also be possible that when the waste is released into the environment, the components of the waste will react with one another to produce less toxic compounds. Current mathematical models are unable to model mixtures of compounds, therefore the ideal method to investigate the effects of mixtures is through laboratory experimentation.

5.3.5 Estimation of Ecotoxicity

The US EPA has been using QSARs to estimate ecotoxicity for over 25 years. QSARs are a cost effective way to estimate the physicochemical properties and ecotoxicity of new chemicals before they become available commercially. Importers and manufacturers submit over 2000 applications for new chemicals each year, and only approximately 35% have any experimental data. According to US legislation, the US EPA has the burden of proof to demonstrate whether or

not a new chemical “may present” an unreasonable risk to human health or the environment. As such, they have developed programmes such as ECOSAR to rapidly assess over 150 attributes of new chemicals in a short amount of time. ECOSAR is used to assess aquatic hazards to aid in making regulatory decisions for new chemicals based on potential risks (Mayo-Bean et al., 2012).

The relationship between $\log K_{OW}$ and LC_{50} (median lethal concentration) and EC_{50} (median effective concentration) is used to estimate LC_{50} or EC_{50} values in order to determine acute ecotoxicological effects. Chronic effects are determined using the mean value between no observed effect concentration (NOEC) and the lowest observed effect concentration (LOEC). ECOSAR estimates toxicity to three aquatic surrogate species to predict the effects on the general aquatic community. The three aquatic species are: fish (freshwater), daphnid (planktonic crustaceans), and green algae. For fish and daphnids, an LC_{50} level is estimated, while for green algae an EC_{50} value is estimated. Chronic values are calculated for the same three aquatic species. For some chemicals, estimates of chronic values for earthworms are also provided (Mayo-Bean et al., 2012). LC_{50} and EC_{50} values for acute and chronic toxicity using the default $\log K_{OW}$ values are shown in Table 5.8 and Table 5.9 on the next page, respectively. LC_{50} and EC_{50} values for acute and chronic toxicity using experimental $\log K_{OW}$ values are shown in Table 5.10 and Table 5.11 on page 231, respectively.

Table 5.8: ECOSAR predicted acute ecotoxicity using default log K_{OW} values (mg/L)

Chemical	ECOSAR Class	Fish (96 Hr)	Daphnid (48 Hr)	Green Algae (96 Hr)
1-phenyl-1,2-propanedione	Neutral Organics	766	400	212
2,6-DTBP	Phenols	0.47	0.42	1.53
Benzyl alcohol	Benzyl Alcohols	214	158	48
Benzaldehyde, oxime	Aliphatic Amines	28	3	3
MA	Aliphatic Amines	20	2	2
<i>N</i> -Formylmethamphetamine	Amides	89	114	3
<i>N</i> -Methylacetamide	Amides	1850	7056	32
P2P	Neutral Organics	328	177	108
Phenol	Phenols	38	9	45

Table 5.9: ECOSAR predicted chronic ecotoxicity using default log K_{OW} values (mg/L)

Chemical	ECOSAR Class	Fish	Daphnid	Green Algae	Earthworm (14 day)
1-phenyl-1,2-propanedione	Neutral Organics	68	31	46	318
2,6-DTBP	Phenols	0.07	0.08	0.70	18 *
Benzyl alcohol	Benzyl Alcohols	15	20	19	-
Benzaldehyde, oxime	Aliphatic Amines	2	0.27	0.93	-
MA	Aliphatic Amines	1	0.21	0.66	-
<i>N</i> -Formylmethamphetamine	Amides	0.13	5	2	
<i>N</i> -Methylacetamide	Amides	0.64	67	10	
P2P	Neutral Organics	30	15	25	264
Phenol	Phenol	4	2	21	138

* Chemical may not be soluble enough to measure this predicted effect. If the effect level exceeds the water solubility by 10X, typically no effects at saturation are reported.

Table 5.10: ECOSAR predicted acute ecotoxicity using experimental log K_{OW} values (mg/L)

Chemical	ECOSAR Class	Fish (96 Hr)	Daphnid (48 Hr)	Green Algae (96 Hr)
1-phenyl-1,2-propanedione	Neutral Organics	222	123	82
2,6-DTBP	Phenols	0.22	0.24	0.84
Benzyl alcohol	Benzyl Alcohols	111	84	29
Benzaldehyde, oxime	Aliphatic Amines	53	6	6
MA	Aliphatic Amines	27	3	3
<i>N</i> -Methylacetamide	Amides	2952	12831	49
P2P	Neutral Organics	177	99	67
Phenol	Phenols	54	12	59

Table 5.11: ECOSAR predicted chronic ecotoxicity using experimental log K_{OW} values (mg/L)

Chemical	ECOSAR Class	Fish	Daphnid	Green Algae	Earthworm (14 day)
1-phenyl-1,2-propanedione	Neutral Organics	21	11	20	279
2,6-DTBP	Phenols	0.03	0.05	0.38	12*
Benzyl alcohol	Benzyl Alcohols	7	12	12	-
Benzaldehyde, oxime	Aliphatic Amines	4	0.46	2	-
MA	Aliphatic Amines	1.55	0.27	0.88	-
<i>N</i> -Methylacetamide	Amides	0.86	100	13	-
P2P	Neutral Organics	17	9	17	246
Phenol	Phenol	5	2	28	166

* Chemical may not be soluble enough to measure this predicted effect. If the effect level exceeds the water solubility by 10X, typically no effects at saturation are reported.

The ECOSAR estimates of ecotoxicity give the concentration of chemical (mg/L) that will be fatal to half of the species population. The lower the value in the tables shown above, the less chemical is required to elicit a negative response, therefore the more toxic the chemical is.

The acute and chronic values vary dramatically. Acute values are an estimate of the chemical concentration that will cause immediate effects to the species and are one to two orders of magnitude higher than the chronic values. A low chemical concentration over a long period of time is what typically results in chronic effects. Neither acute nor chronic effects are necessarily worse than the other, they are just different and require a second examination of the chemicals

under study. Once a chemical is discharged into the environment it will likely remain there for an extended period of time. A chemical that is not harmful in the short term may cause great harm in the long term. Therefore it is important to consider both scenarios.

It is clear that the most ecologically harmful chemical studied in this research is 2,6-DTBP. It has the highest log K_{OW} value, the highest calculated log K_{OC} value, and the lowest LC₅₀ values (0.03 to 18 mg/L). Across all four model scenarios, 2,6-DTBP consistently had the lowest LC₅₀ value, with the one exception being if the chronic/default model (Table 5.9) for green algae, where it ranked second behind MA.

An overall ranking for the ecotoxicity of MA waste components can be estimated as follows based on the ECOSAR results: *N*-methylamphetamine \leq 1-phenyl-1,2-propanedione < P2P < *N*-formylmethylamphetamine \leq phenol \leq benzyl alcohol < benzaldehyde, oxime < MA < 2,6-DTBP. This order deviates from the lipophilicity of the chemicals, which was determined in Chapter 4 to be as follows: *N*-methylacetamide < phenol < benzyl alcohol < benzaldehyde, oxime < 1-phenyl-1,2-propanedione < P2P < MA < 2,6-DTBP. Based on the linear relationship between BCF/BAF and log K_{OW} , it is a logical extrapolation that ecotoxicity would exhibit a similar relationship. However, the ESOCAR ecotoxicity estimates show P2P and 1-phenyl-1,2-propanedione are less harmful than anticipated based solely on log K_{OW} values, while phenol and benzaldehyde, oxime are estimated to be more harmful in terms of the rankings of the chemicals. An attempt to measure LC₅₀ values experimentally was conducted and is outlined in Chapter 6.

The rankings change slightly depending on the aquatic species being examined. For example, when looking at *N*-formylmethylamphetamine and phenol in Table 5.8, phenol is the most harmful to daphnid at 9 mg/L, while it takes a higher concentration *N*-formylmethylamphetamine to elicit the same response (114 mg/L). Conversely, *N*-formylmethylamphetamine is more harmful towards green algae (3 mg/L) than phenol (45 mg/L). Generally, green algae was the most susceptible species, requiring the lowest chemical concentration to reach EC₅₀. The fish species is estimated to be the most resilient, generally requiring the highest concentration to reach LC₅₀. A notable exception is *N*-methylamphetamine, which had higher LC₅₀ values for daphnid.

The ecotoxicity estimates are based on the relationship between $\log K_{OW}$ and LC_{50}/EC_{50} . Therefore, differences in LC_{50}/EC_{50} are to be expected between the different models using default $\log K_{OW}$ values versus models using experimental $\log K_{OW}$ values from Section 4.3.1 on page 142. There is no general trend as to whether or not experimental $\log K_{OW}$ values increased or decreased LC_{50}/EC_{50} concentrations. There are variances between species and chemicals, but overall the general ranking does not change. There are small differences in the rankings of the middle chemicals (i.e. P2P, phenol, benzyl alcohol), however the three most harmful chemicals remain 2,6-DTBP, MA, and benzaldehyde, oxime. The two least harmful chemicals remain *N*-methylacetamide and 1-phenyl-1,2-propanedione.

One limitation of the ECOSAR model is that specific species information has not been provided. The user manual does not specify which species of fish or green algae or daphnid is being used in the model. The information thus must be used in a comparative mannerr and not as absolute values. The lack of species information would make it impossible to compare with laboratory experimental results.

5.3.6 Acute Environmental Impact of MA Waste

In order to compliment the information on acute effects gathered using the computer model ECOSAR, COD of individual waste components and mixtures was measured. COD can be used as an evaluative tool on the immediate impact of chemical waste in the environment. COD is an indirect measurement of oxygen consumption by organic and inorganic chemicals in water (USEPA, 2009a). The addition of oxidisable contaminants into water systems can result in the depletion of dissolved oxygen (DO) concentration (Harrison, 2007), which potentially harms aquatic species. Results of the COD tests on MA waste are shown in Table 5.12 on the following page and Table 5.13 on the next page. The results are defined as amount (mg) oxygen consumed per litre of sample.

Table 5.12: COD of individual MA waste chemicals (mg/L COD; n = 2)

[Chemical] (mg/L)	MA	P2P	<i>N</i> -methylacetamide	Phenol	BOX	COD Sum
1	BDL	BDL	BDL	BDL	BDL	BDL
50	106 ± 5	141 ± 3	190 ± 38	127 ± 8	137 ± 10	701
100	201 ± 8	252 ± 6	119 ± 2	235 ± 1	249 ± 5	1056

BDL = below detection limit (30 mg/L (±16 mg/L))

Table 5.13: COD of five MA waste chemicals in a mixture (mg/L COD; n = 2)

Individual [Chemical] (mg/L)	Total [Chemical] (mg/L)	COD
0.01	0.05	35 ± 35
0.1	0.5	BDL
1	5	BDL
10	50	130 ± 4
100	500	1081 ± 25

BDL = below detection limit (30 mg/L (±16 mg/L))

The European Union legislated value for COD levels of chemical discharge into the environment is 125 mg/L (Council of European Union Communities, 1991). For individual waste components (Table 5.12), this threshold is reached at concentrations of 50 mg/L or 100 mg/L. For the mixture of the five chemicals (Table 5.13), the legislated threshold is exceeded at a relatively low concentration of 10 mg/L. Comparing results from the individual chemicals to the results of the mixture, MA waste is not more harmful as a mixture than its individual components. At a chemical concentration of 100 mg/L, the summation of COD from the individual components (1056 mg/L COD) is comparable to the COD values of the mixture (1081 mg/L COD). The difference is more pronounced at lower chemical concentrations: at 50 mg/L the sum of the individual components (701 mg/L COD) is over five times higher than the COD results from the mixture (130 mg/L COD). This result suggests that the mixture is less harmful than the individual components. With the exception of phenol, these chemicals have few legitimate uses and are more likely to be found in the environment as part of a mixture. The mixture is a better indication of a real-life dumpsite scenario.

While concentrations of MA waste in the environment have not been explored through case study, concentrations of 10 to 100 mg/L are exceedingly low for environmental dumping. On many occasions, clandestine MA manufacturers will stock pile waste before disposing of it. In such circumstances, several tons of waste may be discharged in one location over a short period of time. The COD results indicate that such an event has the potential to cause depletion in the amount of DO to such an extent that it would become harmful to aquatic organisms. In one case study in Canada, a clandestine drug laboratory was seized based on the discovery of dead fish in a nearby stream (Hugel, 2010). While it is probable that several factors likely contributed to the death of the fish, the COD results from this experiment indicate oxygen depletion is certainly a potential contributor.

There are two major sources of DO in water: atmospheric oxygen and photosynthesis by aquatic vegetation. At standard atmospheric pressure, the solubility of oxygen in freshwater at 5°C is 12.77 mg/L. Several factors affect oxygen solubility, such as atmospheric pressure, water turbulence and currents, temperature, salinity, ice cover, and biological processes. DO concentrations in water range from undetectable to 18.4 mg/L (Canadian Council of Ministers of the Environment, 1999).

Oxygen levels can become depleted due to oxidation at the sediment-water interface where bacterial activity and organic matter are concentrated. DO is also reduced by respiration from bacteria, plants, and animals. Additionally, oxygen depletion can occur by direct chemical oxidation of dissolved organic matter. Reduced oxygen levels can have lethal and behavioural effects on various organisms, with fish being especially sensitive, and younger fish being more sensitive than older fish. Low DO concentrations (< 3 mg/L DO) can result in delayed embryo development and reduced hatching success in salmonids. If DO concentrations remain low during embryonic development, a number of deformities can occur. For largemouth bass embryos exposed to DO levels of 1 mg/mL, locked lower jaws have been observed, which resulted in the fish being unable to feed. Steelhead trout eggs exposed to DO levels of 2.6 mg/L showed significant deformities, such as deformed tails and spines, and abnormal nervous systems and brain development. Behavioural changes in chum salmon have been observed in their migrating patterns. Chum salmon avoid migrating in areas with DO levels of 3.5 - 5 mg/L. Juvenile chum

salmon have been observed avoiding waters up to 10 Km away from a pulp mill, where severely depleted DO conditions were detected in an inlet (Canadian Council of Ministers of the Environment, 1999).

Environment Canada's guidelines for DO levels for fish in warm freshwater are 6 mg/L for early life stages, and 5.5 mg/L for other life stages. For cold water, the DO requirements are higher: 9.5 mg/L for early life stages and 6.5 mg/L for other life stages (Canadian Council of Ministers of the Environment, 1999). Deleterious effects begin to be observed at 3 mg/L, a difference of 2.5 mg/L from the guideline values. These observations show the sensitivity fish and their embryos have to depleted DO environments and indicate that small quantities of pollutants which can effectively remove oxygen may have acute effects on the immediate environment. Specific DO requirements for several different saltwater species are shown in Figure 5.16.

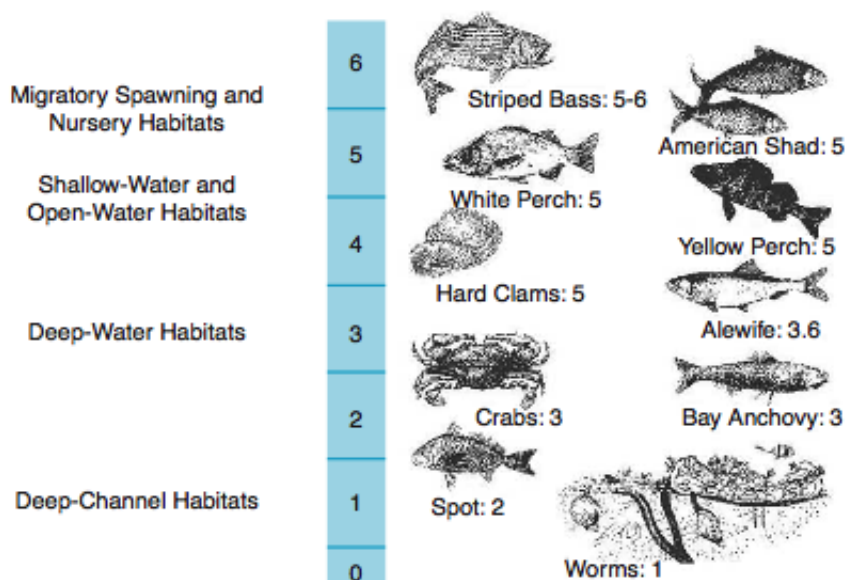


Figure 5.16: Required DO concentrations (mg/L) of different saltwater species (Reproduced from USEPA, 2003.)

By comparing experimental values with regulated COD values, it is clear MA waste is likely to pose a risk to the environment, even at low concentrations. In Section 5.3.5, MA waste was demonstrated to be highly toxic. As stressed previously, computer models limit user input and are therefore essentially default models. More importantly, the ECOSAR model cannot deter-

mine toxicity of mixtures. While there are likely to be some interactions between compounds in the mixture, there is no statistically significant difference between COD measurements of the mixtures and the sum of the COD measurements for the single compound solutions. Further research exploring the chemical interactions between waste constituents would be helpful as part of determining their environmental fate in site specific conditions.

Turning to the literature to investigate ecotoxicity of MA waste, there has been one study into the toxicity of illicit laboratories in the environment. Work conducted by Australian researchers (Pal et al., 2008) used enzyme assays in an attempt to calculate EC_{10} for 18 illicit drug-related compounds in three different local soils. The compounds studied included amphetamine type stimulants, pre-cursors, by-products, and intermediates (no waste chemicals). Toxicity was determined by measuring potential nitrification rate, dehydrogenase activity (a measure of total microbial activity); and the enzyme activity of enzymes associated with certain nutrient cycles: nitrate reductase (nitrogen cycle), sulphatase (sulphur cycle), and phosphatase (phosphate cycle). Table 5.14 on the following page is a reproduction of the EC_{10} and EC_{50} results for six chemicals. To put the chemicals into context, they have the following uses:

- Benzaldehyde: pre-cursor material
- 4-methyl-5-phenylpyrimidine: intermediate chemical
- Nitroethane: pre-cursor material
- 2-nitro-1-phenylpropene: pre-cursor material
- Piperonal: pre-cursor material
- Safrole: pre-cursor material

Table 5.14: EC₁₀ and EC₅₀ values for the dehydrogenase activity of 3 test soils. (Reproduced from Pal et al., 2008)

Compound	Soil	EC ₁₀ (mg/Kg)	EC ₅₀ (mg/Kg)
Benzaldehyde	1	383	1660
	2	2200	3280
	3	1170	1960
4-methyl-5-phenylpyrimidine	1	26	127
	2	57	440
	3	58	88
Nitroethane	1	331	696
	2	375	1660
	3	283	603
2-nitro-1-phenylpropene	1	6	67
	2	135	1690
	3	283	604
Piperonal	1	2160	3590
	2	86	734
	3	339	648
Safrole	1	5190	8090
	2	3350	8390
	3	1010	8490

The researchers found that very little toxicity was exhibited, and in fact nitroethane (a pre-cursor to MA and AMP) increased nitrification rate, suggesting an increase in biological activity. Only six of the 18 compounds tested exhibited a decrease in dehydrogenase activity. Pal et al. (2008) concluded that disruption to regular soil biological activity is only likely to occur at high concentrations of the test compounds - concentrations that may not be reflective of environmental levels typically exhibited for contaminants. A study following the methodology of the Pal et al. (2008) study would be useful in comparing the results between MA intermediates, pre-cursors, and the waste. While this method determines LC₅₀ values, they are not readily comparable to ECOSAR values as ECOSAR estimates LC₅₀ values for aquatic species, while Pal et al. studies soil and soil bacteria.

5.4 Conclusions

By using a combination of laboratory experimentation and computer modelling, the environmental fate of MA waste components was estimated. Considering the long-term implications for a water discharge of MA waste, the waste is estimated to remain in the water compartment and has a half-life ranging from 15 to 37.5 days. The partitioning indicates that for suspected water dumpsites of MA waste, water samples should be collected within two weeks. The analysis of sediment samples is not predicted to contain evidence of clandestine MA waste. For a soil dumpsite of MA waste, the chemicals are predicted to remain predominantly in the soil compartment with half-lives remaining the same, from 15 to 37.5 days. The trend for all chemicals is that they are estimated to remain in the compartment into which they were discharged.

In the case of MA waste being disposed of directly into surface waters, the fugacity models indicate that most of the chemicals will remain in the water compartment, meaning the majority of the chemicals will be water soluble and susceptible to dispersion following water currents. In this phase they are also available to be taken up by aquatic organisms, such as fish, and partition into the lipid layer, which may bioaccumulate and persist for several days. The behaviour of the waste components in the environment is strongly linked to their K_{OW} values, which is related to water solubility, BAF, BCF, and biotransformation rates. Knowledge of an accurate K_{OW} value is essential in generating a reliable environmental model for contaminant behaviour. It was found that the similarities between estimated K_{OW} values using EPI Suite™ and measured K_{OW} values do not exhibit a difference in the fugacity model, nor significant differences in predicting BAF, BCF, and biotransformation. Therefore in the absence of experimental K_{OW} values, the EPI Suite™ estimate is acceptable for modelling purposes and can be used to deduce K_{OC} values based on the correlation determined in the previous chapter. When entering the source of soil K_{OC} value into the fugacity model, it is important to understand the three different options as each value is calculated in different ways. While it may not be practically feasible to experimentally determine the “correct” K_{OC} value for each chemical, the various EPI Suite™ models can be used, with discretion, as higher and lower estimates of a chemical’s partitioning behaviour.

LC₅₀ and EC₅₀ values for MA waste components were estimated using ECOSAR. The chemicals can be ranked based on their estimated harmfulness to the aquatic species studied (fish, daphnid, green algae). *N*-methylacetamide is estimated to be the least harmful, both in the short term and long term scenarios. The most harmful chemical is predicted to be 2,6-DTBP. In general, the chemicals can be ranked as follows: *N*-methylacetamide \leq 1-phenyl-1,2-propanedione $<$ P2P $<$ *N*-formylmethylamphetamine \leq phenol \leq benzyl alcohol $<$ benzaldehyde, oxime $<$ MA $<$ 2,6-DTBP.

The acute environmental impacts of MA waste were estimated using COD. In the immediate term, the waste is likely to be harmful to aquatic organisms based on the amount of oxygen consumed through the oxidation reactions of the compounds. MA waste generated COD values which were higher than legislated levels allowed for the discharge of chemicals into the environment. A mixture of the individual waste components was found to consume less or equal amounts of oxygen than the individual chemicals. This result suggests that MA waste poses a greater threat to the environment as individual components than as a mixture, which is more reflective of a practical scenario.

The results obtained from COD experiment must be taken into context with the fugacity model. The fugacity models in Chapter 5 estimate that MA waste components will remain in the environment from 15 to 37.5 days. During that time, the waste will continue to oxidise and therefore will continue to cause oxygen depletion in the surrounding waters. The impacts of dumping MA waste are not just immediate but can last for several weeks, thus adversely affecting all aquatic life.

While useful, EPI Suite™ is essentially a default model. By changing the K_{OC} value, it is possible to create a site-specific model. The more values that can be experimentally determined, the more accurate the model is likely to be. This has important implications for the investigation of suspected MA waste dumpsites. Knowledge of how the chemicals are partitioning will allow a targeted sampling approach. From the fugacity model, it is recommended to collect both water and sediment samples as most of the waste components will partition into the water phase, with the exception of 2,6-DTPB, which is a hydrophobic chemical whose commercial applications are limited.

The fugacity modelling of compounds based on chemical and physical properties has been shown to be a useful tool. However, it can be concluded that computer modelling should not be a replacement for laboratory experimentation.

Chapter 6

Conclusions and Recommendations

6.1 Summary Conclusions

This research represents the first environmental assessment of waste from clandestine MA manufacture. For the first time, a full chemical profile of MA waste was determined for three different synthetic routes. The environmental fate of the waste was estimated using a combination of laboratory experimentation and computer modelling.

The organic chemical profile of waste produced from illicit MA manufacture was successfully determined for three different synthetic routes: Leuckart, Moscow, and Hypophosphorous. Key chemical markers of the waste include MA, P2P, 1-phenyl-2-propanol, 1-phenyl-1,2-propanedione, and *N*-formylmethamphetamine. Other, less specific, components of the waste include xylene, phenol, and benzaldehyde. It was possible to use previously published methods to extract MA, P2P, and *N*-formylmethamphetamine from sediment and water, though recoveries were low (13% to 18%) and variabilities were acceptable (1.16 to 4.3 %RSD).

Chemical profiling of the waste was accomplished using well established methods for the profiling of illicit MA. The LLE methods were originally designed for the extraction of powdered illicit drugs, however the methods were able to extract impurities from liquid MA waste. Although the extraction efficiency of d5-MA was low, these methods were designed to extract impurities and

by-products, not MA itself. Future work should include measuring the extraction efficiencies of the impurities in order to estimate how much exists in the environment of a suspected dumpsite.

The SPE methods used for the extraction of diluted Leuckart waste were only able to recover three MA waste compounds: phenol, MA, and *N*-formylmethylamphetamine. The absence of a profile corresponding to the crude waste is disappointing, however the methods appear to hold promise based on the extraction of the key MA by-product *N*-formylmethylamphetamine. The SPE concentration factors of MA ranged from 160 to 333. Without an analytical standard of *N*-formylmethylamphetamine, the concentration factor was not determined. The method used for the extraction of MA from sediment had a low recovery rate, from 12-23%, and also had high variability, from 4 to 49 %RSD. The extraction efficiency and %RSD were highly variable between the three synthetic routes. Further research is required to produce a more suitable extraction method for MA waste from sediment.

The benefits of adapting accepted, published, and validated methods provides a reliable starting point for the acceptance of waste profiling methods in a court of law. Additionally, by using methods already familiar to the forensic science community, supplemental staff training would be minimal. The difficulty in profiling MA waste is the high variability between samples since clandestinely manufactured MA, and subsequently its waste, varies widely from batch to batch. Even the waste considered in this study, manufactured under closely monitored conditions, varied widely. An additional consideration to take into account is the practice of stock-piling waste prior to disposal. This would greatly change the waste profile, especially if more than one synthetic route was used in a single clandestine laboratory.

In order to assess the environmental effects of MA waste, physicochemical properties were measured: K_{OW} and K_{OC} . The octanol-water partition coefficient of eight chemicals identified from MA waste was successfully determined following standard methods using RP-HPLC. The measured values were compared with computer estimated values using the computer modelling programme EPI Suite™ and were shown to be remarkably similar. Given the linear relationship between K_{OW} and bioconcentration, the two most concerning chemicals with the highest K_{OW} values are MA, a physiologically active polar compound, and 2,6-DTPB, a highly polar compound susceptible to sediment adsorption and persistence. The chemicals examined from MA

waste display the following order of lipophilicity, from lowest to highest: *N*-methylacetamide < phenol < benzyl alcohol < benzaldehyde, oxime < 1-phenyl-1,2-propanedione < P2P < MA < 2,6-DTBP. Using the linear relationship between K_{OW} and BCF, the same order can be applied towards the tendency of these chemicals to bioaccumulate in aquatic organisms.

The measurement of K_{OC} of four chemicals (MA, P2P, 2,6-DTBP, and *N*-methylacetamide) identified from MA waste had limited initial success and thus was repeated. One of the biggest factors affecting the first batch of experiments was matrix interferences from the collected sediment samples, which masked the peaks of MA and *N*-methylacetamide. The low solubility of 2,6-DTBP, combined with its high polarity, meant that concentrations in the aqueous layer were below limits of detection, and its K_{OC} could not be determined.

The second batch of experiments attempted to eliminate matrix interference effects by using artificial soils. Using an HPLC with a UV detector, it was still not possible to measure the K_{OC} value of MA due to matrix interferences. However, additional chemicals were added to the sorption experiments, and K_{OC} values were successfully determined for *N*-methylacetamide, P2P, phenol, and benzaldehyde, oxime.

K_{OC} values can be difficult to measure experimentally. Adsorption experiments are time consuming, labour intensive, and can suffer from matrix interference effect. However, K_{OW} is an easy parameter to measure in the laboratory. By using the correlation between the two partition coefficients, K_{OC} can reliably be estimated through the measurement of K_{OW} . From the experimental measurement of K_{OC} and K_{OW} , a correlation of $y = 3.597x - 4.325$ ($R^2 = 0.978$) was established. Using the experimentally determined correlation, K_{OC} values for MA waste components were determined that were not able to be measured experimentally. It was also determined that experimental K_{OW} values are very similar to computer estimate K_{OW} values, therefore the correlation can be used to estimate K_{OC} values for other waste components as well. A comparison of K_{OC} values from different sources is found in Table 5.3 on page 208.

The chemicals examined from MA waste display the following order of affinity for organic carbon, from lowest to highest: *N*-methylacetamide < phenol < benzyl alcohol < 1-phenyl-1,2-propanedione < MA < P2P < benzaldehyde, oxime < 2,6-DTBP. This is a different order

from the K_{OW} measurements, despite the linear relationship between the two properties. This demonstrates again the importance of laboratory experimentation and the influence of multiple parameters on the behaviour of chemicals in the environment.

There are many factors that can have an influence on the adsorption of chemicals to soils and sediments. Those factors range from environmental factors, such as pH and salinity, to physicochemical properties, such as K_{OW} and K_{OC} , as well as sediment properties, such as CEC, crystal lattice structure, and organic carbon content. It is important to note that the polar nature of the chemicals under investigation suggests that the traditional assumptions of organic carbon partitioning may not apply and other sediment properties may have greater influence on sorption behaviour.

The measured partition coefficients were combined with computer modelling to create a chemical-specific fugacity model in order to estimate the environmental impact of MA waste.

Considering long-term implications, for a water discharge of MA waste, the waste is estimated to remain in the water compartment and has a half-life of 15 to 37.5 days. The partitioning indicates that for suspected water dumpsites of MA waste, water samples should be collected within two weeks. The analysis of sediment samples is not predicted to contain significant evidence of clandestine MA waste. For a soil dumpsite of MA waste, the chemicals are predicted to remain predominantly in the soil compartment with half-lives remaining the same, at 15 to 37.5 days. The trend for all chemicals is that they are estimated to remain in the compartment into which they were discharged.

In the case of MA waste being disposed of directly into surface waters, the fugacity models indicate that most of the chemicals will remain in the water compartment, meaning the majority of the chemicals will be water soluble and susceptible to dispersion following water currents. In this phase they are also available to be taken up by aquatic organisms, such as fish, and partition into the lipid layer, which may bioaccumulate and persist for several days. The behaviour of the waste components in the environment is strongly linked to their K_{OW} values, which is related to water solubility, BAF, BCF, and biotransformation rates. Knowledge of an accurate K_{OW} value is essential in generating a reliable environmental model for contaminant behaviour. It

was found that the similarities between estimated K_{OW} values using EPI Suite™ and measured K_{OW} values do not exhibit a difference in the fugacity model, nor significant differences in predicting BAF, BCF, and biotransformation. Therefore in the absence of experimental K_{OW} values, the EPI Suite™ estimate is acceptable for modelling purposes and can be used to deduce K_{OC} values based on the correlation determined in Chapter 4. When entering the source of soil K_{OC} value into the EPI Suite™ fugacity model, it is important to understand the three different options as each value is calculated in different ways. While it may not be practically feasible to experimentally determine the “correct” K_{OC} value for each chemical, the various EPI Suite™ models can be used, with discretion, as higher and lower estimates of a chemical’s partitioning behaviour.

LC₅₀ and EC₅₀ values for MA waste components were estimated using the computer model, ECOSAR. The chemicals can be ranked based on their estimated harmfulness to the aquatic species studied (fish, daphnid, green algae). *N*-methylacetamide is estimated to be the least harmful, both in the short term and long term scenarios. The most harmful chemical is predicted to be 2,6-DTBP. In general, the chemicals can be ranked as follows: *N*-methylamphetamine ≤ 1-phenyl-1,2-propanedione < P2P < *N*-formylmethylamphetamine ≤ phenol ≤ benzyl alcohol < benzaldehyde, oxime < MA < 2,6-DTBP.

While useful, EPI Suite™ is essentially a default model. By changing the K_{OC} value, it is possible to create a site-specific model. The more values that can be experimentally determined, the more accurate the model is likely to be. This has important implications for the investigation of suspected MA waste dumpsites. Knowledge of how the chemicals are partitioning will allow a targeted sampling approach. From the fugacity model, it is recommended to collect both water and sediment samples as most of the waste components will partition into the water phase, with the exception of 2,6-DTPB, which is a hydrophobic chemical whose commercial applications are limited.

The fugacity modelling of compounds based on chemical and physical properties has been shown to be a useful tool. However, it can be concluded that computer modelling should not be a replacement for laboratory experimentation.

The acute environmental impacts of MA waste were estimated using COD. In the immediate term, the waste is likely to be harmful to aquatic organisms based on the amount of oxygen consumed through the oxidation reactions of the compounds. MA waste generated COD values which were higher than legislated levels allowed for the discharge of chemicals into the environment. A mixture of the individual waste components was found to consume less or equal amounts of oxygen than the individual chemicals. This result suggests that MA waste poses a greater threat to the environment as individual components than as a mixture, which is more reflective of a practical scenario.

The results obtained from COD experiment must be taken into context with the fugacity model. The fugacity models in Chapter 5 estimate that MA waste components will remain in the environment from 15 to 37.5 days. During that time, the waste will continue to oxidise oxygen and therefore will continue to cause oxygen depletion in the surrounding waters. The impacts of dumping MA waste are not just immediate but can last for several weeks, thus adversely affecting all aquatic life.

This study encompasses research into the waste produced from the illicit manufacture of MA. Several marker compounds were discovered through the chemical profiling of the waste, such as *N*-formylmethylamphetamine, 2,6-di-*tert*-butylphenol, MA, and P2P. It is anticipated these marker compounds may assist in the discovery of clandestine waste dumpsites and aid in the enforcement of environmental protection laws against people involved in the clandestine synthesis of MA. Chemical profiling and environmental modelling of waste from clandestine drug manufacture are the first steps to fully understanding the environmental impacts of clandestine drug laboratories. As more evidence on the harmful nature of these laboratories is obtained, the more feasible it will become to prosecute clandestine drug manufacturers for polluting the environment. By using both drug manufacturing legislation and environmental protection legislation, it will be possible to prosecute clandestine drug manufacturers to the fullest extent of the law.

6.2 Recommendations for future work

Although the aim and objectives for this work were achieved, further research into waste from clandestine methylamphetamine laboratories is essential to facilitate the enforcement of environmental protection laws. Future suggested works include:

- Chemical profiling of waste from the remaining synthetic routes that were not profiled in this study, which are: reductive amination, Nagai, Birch/Nazi, Rosenmund, and Emde. It would also be an interesting project to combine waste from different synthetic routes, to produce a mixture for chemical profiling.
- This project examined the organic impurities of the waste using GC-MS. Further chemical profiling of the inorganic components of the waste, such as iodine, phosphorous, and aluminum, is possible using other analytical techniques, such ICP-MS.
- In this study, *N*-formylmethylamphetamine was found to be a key marker of MA waste. It was unfortunate that a standard was unavailable for purchase in order to conduct K_{OW} and K_{OC} experiments. If a standard becomes available in the future, or if *N*-formylmethylamphetamine can be synthesised in-house, those experiments should be completed.
- Improvement of the extraction procedures to remove waste components from sediment and water samples. A method to consider is pressurised liquid extraction for the extraction of waste from sediment samples.
- More accurate environmental profiling of the waste would be made possible with reliable K_{OC} values for as many of the components as is practically feasible. Further experimentation to determine accurate K_{OC} values for the waste components is strongly recommended. However, the costs and extensive time commitment of the experiments must be taken into consideration.
- In order to accurately determine K_{OC} values, it is important to eliminate matrix interference effects. This may be accomplished using a different analytical instrument, such as LC-MS, or by introducing an additional clean-up step in the method, such as SPE.

- Assessment of waste degradation and transformation products can be examined in the laboratory using a simulated environment, such as microcosms. Microcosms may also be used to measure fugacity of the waste, which may then be compared to the EPI Suite™ models.
- An investigation into the toxicity of the waste on the environment would be beneficial to successful criminal proceedings. If chemicals are dumped illegally into the environment, it would be advantageous to prove that they are causing harm in order to facilitate prosecution for harming the environment. The toxicity of the waste should be investigated as individual components as well as a mixture to test for any additive and synergistic effects.
- As the components of the waste identified in the profiling study are only present in small quantities, the effects of dumping several litres of MA contaminated solvents into the environment need to be fully understood as well. It may be that the most harm from clandestine drug dumpsites is primarily from the dumping of bulk solvents and acids, rather than the individual components. However, it is the individual components which will indicate the dumpsite is from illicit methylamphetamine manufacture rather than another source.
- The methods outlined in this study are still in early developmental stages. It is essential to be able to apply the profiling of waste to suspected dumpsites in the real world. The analysis of samples from seized or suspected clandestine laboratories or dumpsites would be an excellent collaborative project with law enforcement personnel.

References

- Aalberg, L., Andersson, K., Bertle, C., Cole, M. D., Finnon, Y., Huizer, H., Jalava, K., Kaa, E., Lock, E., Lopes, A., Poortman-van de Meer, A., Sippola, E., Dahlén, J., 2005a. Development of a harmonised method for the profiling of amphetamines II. Stability of impurities in organic solvents. *Forensic Science International* 149, 231–241.
- Aalberg, L., Andersson, K., Bertler, C., Borén, H., Cole, M. D., Dahlén, J., Finnon, Y., Huizer, H., Jalava, K., Kaa, E., Lock, E., Lopes, A., Poortman-van de Meer, A., Sippola, E., 2005b. Development of a harmonised method for the profiling of amphetamines I. Synthesis of standards and compilation of analytical data. *Forensic Science International* 149, 219–229.
- Abdullah, A. L., Miskelly, G. M., 2010. Recoveries of trace pseudoephedrine and methamphetamine residues from impermeable household surfaces: Implications for sampling methods used during remediation of clandestine methamphetamine laboratories. *Talanta* 81, 455–461.
- ACMD, November 2005. Methylamphetamine review. Tech. rep., Advisory Council on the Misuse of Drugs.
URL <http://www.homeoffice.gov.uk/publications/alcohol-drugs/drugs/acmd1/ACMD-meth-report-November-2005?view=Binary>
- Andersen, H. R., Hansen, M., Kjølholt, J., Stuer-Lauridsen, F., Ternes, T., Halling-Sørensen, B., 2005. Assessment of the importance of sorption for steroid estrogens removal during activated sludge treatment. *Chemosphere* 61, 139.
- Andersson, K., Jalava, K., Lock, E., Finnon, Y., Huizer, H., Kaa, E., Lopes, A., Poortman-van de Meer, A., Cole, M., Dahlén, J., Sippola, E., 2007a. Development of a harmonised method for the profiling of amphetamines III. Development of the gas chromatographic methods. *Forensic Science International* 169, 50–63.

- Andersson, K., Jalava, K., Lock, E., Huizer, H., Kaa, E., Lopes, A., Poortman-van der Meer, A., Cole, M., Dahlén, J., Sippola, E., 2007b. Development of a harmonised method for the profiling of amphetamines IV. Optimisation of sample preparation. *Forensic Science International* 169, 64–76.
- Andersson, K., Lock, E., Jalava, K., Huizer, H., Jonson, S., Kaa, E., Lopes, A., Poortman-van de Meer, A., Sippola, E., Dujourdy, L., Dahlén, J., 2007c. Development of a harmonised method for the profiling of amphetamines VI. Evaluation of methods for comparison of amphetamine. *Forensic Science International* 169, 86–99.
- ASTM, 2007. Standard Test Method for Moisture, Ash, and Organic Matter of Peat and Other Organic Soils (Designation: D2974 - 07a).
- ASTM, 2008. Standard Test Method for Determining a Sorption Constant (K_{oc}) for an Organic Chemical in Soil and Sediments (Designation: E1195-01).
- Australian Government, 2011. Guidelines for Environment Investigations, Remediation and Validation of former Clandestine Drug Laboratory Sites. Tech. rep., Australian Government. URL http://www.ag.gov.au/Documents/2109%20Remediation%20Guidelines_WEB.PDF
- Australian/New Zealand Standard, October 2002. Handling and destruction of drugs.
- Bangedphol, S., Keenan, H., Davidson, C., Sakultanimetha, A., Songsasen, A., 2009. The partition behavior of tributyltin and prediction of environmental fate, persistence and toxicity in aquatic environments. *Chemosphere* 77 (10), 1326–1332.
- Boles, T. H., Wells, M. J., 2010. Analysis of amphetamine and methamphetamine as emerging pollutants in wastewater and wastewater-impacted streams. *Journal of Chromatography A* 1217, 2561–2568.
- British Standards, 2007. BS 3882:2007 Specification for topsoil and requirements for use.
- British Standards, September 2009. BS 11277:2009 Soil quality - Determination of particle size distribution in mineral soil material - Method by sieving and sedimentation.
- Bruker, 2013. XRF Basics. URL <http://www.bruker.com/products/x-ray-diffraction-and-elemental-analysis/handheld-xrf/handheld-xrf-basics.html>

- Buchanan, H. A. S., 2009. An evaluation of isotope ratio mass spectrometry for the profiling of 3,4-methylenedioxyamphetamine. Ph.D. thesis, University of Strathclyde.
- Canadian Council of Ministers of the Environment, 1999. Canadian water quality guidelines for the protection of aquatic life: Dissolved oxygen (freshwater). Tech. rep., Environment Canada.
- Castiglioni, S., Zuccato, E., Crisci, E., Chiabrando, C., Fanelli, R., Bagnati, R., 2006. Identification and measurement of illicit drugs and their metabolites in urban wastewater by liquid chromatography-tandem mass spectrometry. *Analytical Chemistry* 78 (24), 8421–8429.
- Castiglioni, S., Zuccato, E., Fanelli, R., 2011. Illicit drugs in the environment: occurrence, analysis, and fate using mass spectrometry. John Wiley & Sons.
- CCEMC, March 2002. Level iii model.
URL <http://www.trentu.ca/academic/aminss/envmodel/models/VBL3.html>
- ChemAxon, 2013. Properties viewer.
URL <http://www.chemicalize.org/>
- Chemical Abstract Service, 2012. By the numbers.
URL <http://www.cas.org/infographic2/index.html>
- Chiou, C. T., 2002. Partition and Adsorption of Organic Contaminants in Environmental Systems. John Wiley & Sons, New York, NY.
- Collins, M., Huttunen, J., Evans, I., Robertson, J., June 2007. Illicit drug profiling: the Australian experience. *Australian Journal of Forensic Sciences* 39 (1), 25–32.
- Council of European Union Communities, 1991. Directive 91/271/EEC. Tech. rep., Official Journal of the European Communities.
- Cruickshank, C. C., Dyer, K. R., 2009. A review of the clinical pharmacology of methamphetamine. *Addiction* 104, 1085–1099.
- Draber, W., Fujita, T. (Eds.), 1992. Rational Approaches to Structure, Activity, and Ecotoxicology of Agrochemicals. CRC Press, Boca Raton, FL.
- Drillia, P., Stamatelatou, K., Lyberatos, G., 2005. Fate and mobility of pharmaceuticals in solid matrices. *Chemosphere* 60, 1034–1044.

- Dujourdy, L., Dufey, V., Besacier, F., Miano, N., Marquis, R., Lock, E., Aalberg, L., Dieckmann, S., Zrcek, F., Bozenko Jr., J., 2008. Drug intelligence based on organic impurities in illicit MA samples. *Forensic Science International* 177, 153–161.
- European Parliament, 2004. Directive 2004/35/CE of the European Parliament and of the Council.
- URL <http://eur-lex.europa.eu/LexUriServ/LexUriServ.do?uri=OJ:L:2004:143:0056:0075:EN:PDF>
- Finnon, Y., Waddell, R., Nic Daéid, N., Carter, K., 2001. Preliminary investigation of the toxicity levels of amphetamine impurities (poster). *Science & Justice* 41 (3), 229–230.
- Glassmeyer, S. T., Furlong, E. T., Kolpin, D. W., Cahill, J. D., Zaugg, S. D., Werner, S. L., Meyer, M. T., Kryak, D. D., 2005. Transport of chemical and microbial compounds from known wastewater discharges: Potential for use as indicators of human fecal contamination. *Environmental Science & Technology* 39 (14), 5157–5169.
- Hansch, C., Hoekman, D., Leo, A., Zhang, L., Li, P., 1995. The expanding role of quantitative structure-activity relationships (QSAR) in toxicology. *Toxicology Letters* 79, 45–53.
- Hargreaves, G., April 2000. Clandestine Drug Labs: Chemical Time Bombs. *FBI Law Enforcement Bulletin* 69 (4 (April 2000)), 1–6.
- URL <http://www.fbi.gov/stats-services/publications/law-enforcement-bulletin/2000-pdfs/apr001eb.pdf>
- Harrison, R. M., 2007. *Principles of Environmental Chemistry*. Royal Society of Chemistry, Cambridge, UK.
- Hayes, T. B., Anderson, L. L., Beasley, V. R., de Solla, S. R., Iguchi, T., Ingraham, H., Kestemont, P., Kniewald, J., Kniewald, Z., Langlois, V. S., Luque, E. H., McCoy, K. A., de Toro, M. M., Oka, T., Oliveira, C. A., Orton, F., Ruby, S., Suzawa, M., Tavera-Mendoza, L. E., Trudeau, V. L., Victor-Costa, A. B., Willingham, E., 2011. Demasculinization and feminization of male gonads by atrazine: Consistent effects across vertebrate classes. *The Journal of Steroid Biochemistry and Molecular Biology* 127, 64–73.
- Hayes, W. (Ed.), 2010. *CRC Handbook of Chemical and Physics*, 91st Edition. CRC Press.

- Heberer, T., 2002. Occurrence, fate, and removal of pharmaceutical residues in the aquatic environment: a review of recent research. *Toxicology Letters* 131, 5–17.
- Hiromatsu, K., Yakabe, Y., Katagiri, K., Nishihara, T., 2000. Prediction for the biodegradability of chemicals by empirical flowchart. *Chemosphere* 41, 1749–1754.
- Home Office, March 2011. Regulation of Precursor Chemicals in the United Kingdom.
URL <http://www.homeoffice.gov.uk/publications/alcohol-drugs/drugs/drug-licences/precursor-chemicals-wallchart?view=Binary>
- House of Commons, 2005. Forensic Science on Trial: Seventh Report of Session 2004-2005. Tech. rep., Science and Technology Committee.
URL <http://www.publications.parliament.uk/pa/cm200405/cmsselect/cmsctech/96/96i.pdf>
- Huerta-Fontela, M., Galceran, M. T., Martin-Alonso, J., Ventura, F., 2008. Occurrence of psychoactive stimulatory drugs in wastewaters in north-eastern Spain. *Science of the Total Environment* 397, 31–40.
- Hugel, J., October 2010. Personal communication, Forensic Services Group, NSW Police Force.
- Hunt, D., Kuck, S., Truitt, L., 2005. Methamphetamine Use: Lessons Learned. Tech. rep., United States Department of Justice.
URL www.ncjrs.gov/pdffiles1/nij/grants/209730.pdf
- Inoue, H., Kanamori, T., Iwata, Y. T., Ohmae, Y., Tsujikawa, K., Saitoh, S., Kishi, T., 2003. Methamphetamine impurity profiling using a 0.32 mm i.d. nonpolar capillary column. *Forensic Science International* 135, 42–47.
- Interpol, 2009. Strategic Plan 2009-2010.
URL <http://www.interpol.int/Public/EnvironmentalCrime/Manual/strategicplan.pdf>
- Janusz, A., Kirkbride, K., Scott, T., Naidu, R., Perkins, M., Megharaj, M., 2003. Microbial degradation of illicit drugs, their precursors, and manufacturing by-products: implications for clandestine drug laboratory investigation and environmental assessment. *Forensic Science International* 134, 62–71.

- Jayaram, S. K., 2012. A comprehensive chemical examination of methylamphetamine produced from pseudoephedrine extracted from cold medication. Ph.D. thesis, University of Strathclyde.
- Jensen, F., 2007. Introduction to Computational Chemistry. John Wiley & Sons, Oxford, UK.
- Kasprzyk-Hordern, B., Dinsdale, R., Guwy, A., 2007. Multi-residue method for the determination of basic/neutral pharmaceuticals and illicit drugs in surface water by solid-phase extraction and ultra performance liquid chromatography-positive electrospray ionisation tandem mass spectrometry. *Journal of Chromatography A* 1161, 132–145.
- Kasprzyk-Hordern, B., Dinsdale, R. M., Guwy, A. J., 2009. Illicit drugs and pharmaceuticals in the environment - Forensic applications of environmental data. Part 1: Estimation of the usage of drugs in local communities. *Environmental Pollution* 157 (6), 1773–1777.
- Kealey, D., Haines, P., 2002. Instant Notes in Analytical Chemistry. Taylor & Francis.
- Keenan, H., Sakultanimetha, A., Bangkedphol, S., 2008. Environmental fate and partition coefficient of oestrogenic compounds in sewage treatment process. *Environmental Research* 106, 313–318.
- King, L., 2009. Forensic Chemistry of Substance Misuse: A Guide to Drug Control. The Royal Society of Chemistry, Cambridge, UK.
- Kirkbride, P., July 2010. Personal communication, Australian Federal Police.
- Ko, B. J., Suh, S. I., Suh, Y. J., In, M. K., Kim, S.-H., 2007. The impurity characteristics of methamphetamine synthesized by Emde and Nagai method. *Forensic Science International* 170, 142–147.
- Kunalan, V., 2010. An investigation into the ability of three analytical techniques to discriminate batches of methylamphetamine prepared by seven synthetic routes. Ph.D. thesis, University of Strathclyde.
- Kunalan, V., Nic Daéid, N., Kerr, W. J., Buchanan, H. A., McPherson, A. R., 2009. Characterization of route specific impurities found in methamphetamine synthesized by the Leuckart and reductive amination methods. *Analytical Chemistry* 81 (17), 7342–7348.

- Lee, J. S., Han, E. Y., Lee, S. Y., Kim, E. M., Park, Y. H., Lim, M. A., Chung, H. S., Park, J. H., 2006. Analysis of the impurities in the methamphetamine synthesized by three different methods from ephedrine and pseudoephedrine. *Forensic Science International* 161 (2-3), 209–215.
- Lock, E., Aalberg, L., Andersson, K., Dahlén, J., Cole, M., Finnon, Y., Huizer, H., Jalava, K., Kaa, E., Lopes, A., Poortman-van de Meer, A., Sippola, E., 2007. Development of a harmonised method for the profiling of amphetamines V. Determination of the variability of the optimised methods. *Forensic Science International* 169, 77–85.
- Mackay, D., 1979. Finding fugacity feasible. *Environmental Science & Technology* 13, 1218–1223.
- Mackay, D., 2001. *Multimedia Environmental Models: The Fugacity Approach*, 2nd Edition. Lewis Publishers, Boca Raton, FL.
- Mackay, D., Paterson, S., Shiu, W. Y., 1992. Generic models for evaluating the regional fate of chemicals. *Chemosphere* 24, 695–717.
- Makino, Y., Urano, Y., Nagano, T., 2005. Investigation of the origin of ephedrine and methamphetamine by stable isotope ratio mass spectrometry: a japanese experience. *Bulletin on Narcotics LVII* (1 and 2), 63–78.
- Man, G., Stoeber, B., Walus, K., 2009. An assessment of sensing technologies for the detection of clandestine methamphetamine drug laboratories. *Forensic Science International* 189, 1–13.
- Marnell, T., 2001. *Drug Identification Bible*. Amera-Chem, Inc., Grand Junction, CO.
- Martyny, J. W., Arbuckle, S. L., McCammon Jr., C. S., Esswein, E. J., Erb, N., Van Dyke, M., 2007. Chemical concentrations and contamination associated with clandestine methamphetamine laboratories. *Journal of Chemical Health & Safety* July/August, 40–52.
- Maxwell, J. C., Rutkowski, B. A., 2008. The prevalence of methamphetamine and amphetamine abuse in North America: a review of the indicators, 1992-2007. *Drug and Alcohol Review* 23, 229.
- Mayo-Bean, K., Moran, K., Meylan, B., Ranslow, P., 2012. Methodology Document for the ECOlogical Structure-Activity Relationship Model (ECOSAR) Class Program. Tech. rep., Office of Pollution Prevention and Toxics U.S. Environmental Protection Agency.

- Meylan, W. M., Howard, P. H., 1995. Atom/fragment contribution method for estimating octanol-water partition coefficients. *Journal of Pharmaceutical Sciences* 84 (1), 83–92.
- Miller, J. N., Miller, J. C., 2010. *Statistics and chemometrics for analytical chemistry*, 6th Edition. Pearson Education.
- Morrison, R. D., 2000. *Environmental Forensics: principles and applications*. CRC Press LLC, Boca Raton, FL.
- New Zealand Ministry of Health, August 2010. *Guidelines for the Remediation of Clandestine Methamphetamine Laboratory Sites*, 168.
URL <http://www.health.govt.nz/publications>
- Newman, M. C., Unger, M. A., 2003. *Fundamentals of Ecotoxicology*, 2nd Edition. Lewis Publishers.
- NIST, 2008. NIST 08 MS Library and MA Search Program v.2.0f. National Institute of Standards and Technology, v.2.0f Edition.
- OECD, March 1989. Partition coefficient (n-octanol/water), high performance liquid chromatography (HPLC) method.
URL <http://www.oecd.org/dataoecd/17/36/1948177.pdf>
- OECD, July 1995. Partition coefficient (n-octanol/water): Shake flask method.
URL <http://browse.oecdbookshop.org/oecd/pdfs/free/9710701e.pdf>
- Pal, R., Mallavarapu, M., Naidu, R., Kirkbride, P., 2008. *Illicit Drug Laboratories and the Environment*. Tech. rep., National Drug Law Enforcement Research Fund, Australia.
- Pal, R., Megharaj, M., Kirkbride, K. P., Heinrich, T., Naidu, R., 2011. Biotic and abiotic degradation of illicit drugs, their precursor, and by-products in soil. *Chemosphere* 85 (6), 1002–1009.
- Pal, R., Megharaj, M., Kirkbride, K. P., Naidu, R., 2012. Fate of 1-(1',4'-cyclohexadienyl)-2-methylaminopropane (CMP) in soil: Route-specific by-product in the clandestine manufacture of methamphetamine. *Science of the Total Environment* 416, 394–399.
- Patrick, G. L., 2005. *An Introduction to Medicinal Chemistry*, 3rd Edition. Oxford University Press, Oxford, UK.

- Pomati, F., Castiglioni, S., Zuccato, E., Fanelli, R., Vigetti, D., Rossetti, C., Calamari, D., 2006. Effects of a complex mixture of therapeutic drugs at environmental levels on human embryonic cells. *Environmental Science & Technology* 40 (7), 2442–2447.
- Qi, Y., Evans, I., McCluskey, A., 2007. New impurity profiles of recent Australian imported ice: Methamphetamine impurity profiling and the identification of (pseudo)ephedrine and Leuckart specific marker compounds. *Forensic Science International* 169, 173–180.
- Remberg, B., Stead, A., 1999. Drug characterization/impurity profiling, with special focus on methamphetamine: recent work of the United Nations International Drug Control Programme. *Bulletin on Narcotics* LI (1-2), 97–118.
- Robinson, J. W., Frame, E. M. S., Frame, G. M., 2004. Undergraduate instrumental analysis, 6th Edition. Marcel Dekker Inc.
- Rosenmund, K. W., Karg, E., 1942. Über die Darstellung von β -Aryl-alkylaminen (Concerning the preparation of beta-Aryl-Alkylamines). *Berichte* 75 (12), 50–59.
- Samiullah, Y., 1990. Prediction of the environmental fate of chemicals. Elsevier Applied Science.
- Schnoor, J. L., 1996. Environmental Modeling: Fate and transport of pollutants in water, air, and soil. *Environmental Science and Technology: A Wiley-Interscience Series of Texts and Monographs*. John Wiley & Sons, New York, NY.
- Scott, M. S., Dedel, K., 2006. Clandestine Methamphetamine Labs. Tech. rep., Community Oriented Policing Services, United States Department of Justice.
URL <http://www.cops.usdoj.gov/files/RIC/Publications/e07063402.pdf>
- Shulgin, A., Shulgin, A., 1991. PiHKAL: A chemical love story. Transform Press.
- Skinner, H., 1990. Methamphetamine synthesis via hydriodic acid/red phosphorus reduction of ephedrine. *Forensic Science International* 48, 123.
- Strömberg, L., 1975. Comparative gas chromatographic analysis of narcotics II. Amphetamine sulphate. *Journal of Chromatography A* 106, 335–342.
- Sumpter, J. P., Johnson, A. C., 2005. Lessons from endocrine disruption and their application to other issues concerning trace organics in the aquatic environment. *Environmental Science & Technology* 39 (12), 4321–4332.

- Tan, K. H., 1998. Principles of Soil Chemistry, 3rd Edition. Marcel Dekker, Inc.
- Uncle Fester, 2005. Secrets of Methamphetamine Manufacture, 7th Edition. Loomponics Un-
limited, Port Townsend, WA.
- Uncle Fester, 2009. Secrets of Methamphetamine Manufacture, 8th Edition. Festering Publica-
tions, Green Bay, WI.
- UNEP Publications, 2013. 2,6-Di-tert-butylphenol Cas No: 128-39-2 (Screening Information
Dataset). Tech. rep., OECD.
URL <http://www.chem.unep.ch/irptc/sids/OECDSEIDS/128392.pdf>
- United States Supreme Court, 1993. Daubert v. Merrell Dow Pharmaceuticals (92-102), 509
U.S. 579 (1993).
- UNODC, 2009. World Drug Report 2009. Tech. rep., United Nations Office on Drugs and Crime.
URL <http://www.unodc.org/unodc/en/data-and-analysis/WDR-2009.html>
- UNODC, 2011. World Drug Report 2011. Tech. rep., United Nations Office on Drugs and Crime.
URL <http://www.unodc.org/unodc/en/data-and-analysis/WDR-2011.html>
- UNODC, 2012. World Drug Report 2012. Tech. rep., United Nations Office on Drugs and Crime.
URL <http://www.unodc.org/unodc/en/data-and-analysis/WDR-2012.html>
- USDEA, 2005. Guidelines for law enforcement for the cleanup of clandestine drug laboratories.
Tech. rep., United States Drug Enforcement Administration.
- USEPA, 1996. Soil Screening Guidance: Technical Background Document, Part 5: Chemical-
Specific Parameters. Tech. rep., United States Environmental Protection Agency.
URL <http://www.epa.gov/superfund/health/conmedia/soil/toc.htm#p5>
- USEPA, April 2003. Ambient Water Quality Criteria for Dissolved Oxygen, Water Clarity and
Chlorophyll a for the Chesapeake Bay and Its Tidal Tributaries. Tech. rep., United States
Environmental Protection Agency.
- USEPA, 2005. RCRA Hazardous Waste Identification of Methamphetamine Production Process
By-products. Report to congress, United States Environmental Protection Agency.
URL <http://www.epa.gov/osw/hazard/wastetypes/wasteid/downloads/rtc-meth.pdf>

- USEPA, 2009a. Drinking Water Glossary: A Dictionary of Technical and Legal Terms Related to Drinking Water. Tech. rep., Office of Water/Office of Ground Water and Drinking Water.
- USEPA, 2009b. Voluntary guidelines for methamphetamine laboratory cleanup. Tech. rep., United States Environmental Protection Agency.
- USEPA, August 2010. TSCA 5(e) Exposure-Based Policy: Testing.
URL <http://www.epa.gov/oppt/newchemicals/pubs/expbasedtesting.htm>
- USEPA, June 2012a. Ecological Structure Activity Relationships (ECOSAR).
URL <http://www.epa.gov/oppt/newchemicals/tools/21ecosar.htm>
- USEPA, November 2012b. Estimation Programs Interface Suite for Microsoft Windows, v 4.11. United States Environmental Protection Agency.
URL <http://www.epa.gov/oppt/exposure/pubs/episuite.htm>
- USEPA, March 2012c. New chemicals program.
URL <http://www.epa.gov/oppt/newchemicals/index.htm>
- Verma, H., 2007. Atomic and Nuclear Analytical Methods: XRF, Mössbauer, XPS, NAA and B63Ion-Beam Spectroscopic Techniques. Springer Berlin Heidelberg.
- Walker, C. H., Hopkin, S. P., Sibly, R. M., Peakall, D. B., 1996. Principles of Ecotoxicology. Taylor & Francis, Bristol, UK.
- Wang, Z., Stout, S. A., 2007. Oil spill environmental forensics: fingerprinting and source identification. Elsevier/Academic Press.
- White, M., 2004. FSS Report on Methylamphetamine: Chemistry, seizure statistics, analysis, synthetic routes and history of illicit manufacture in the UK and the USA. Tech. rep., Forensic Science Service.
- Widstrand, C., Bergström, S., Wihlborg, A.-K., Trinh, A., 2008. The extraction of amphetamine and related drugs using molecularly imprinted polymer spe. Reporter US 26.1.
- Wirth, K., Barth, A., November 2012. X-Ray Fluorescence (XRF).
URL http://serc.carleton.edu/research_education/geochemsheets/techniques/XRF.html

Wise, A., O'Brien, K., Woodruff, T., 2011. Are oral contraceptives a significant contributor to the estrogenicity of drinking water? *Environmental Science & Technology* 45 (1), 51–60.

Zuccato, E., Castiglioni, S., Bagnati, R., Chiabrando, C., Grassi, P., Fanelli, R., 2008. Illicit drugs, a novel group of environmental contaminants. *Water Research* 42 (4-5), 961–968.

Zuccato, E., Chiabrando, C., Castiglioni, S., Calamari, D., Bagnati, R., Schiarea, S., Fanelli, R., 2005. Cocaine in surface waters: a new evidence-based tool to monitor community drug use. *Environmental Health* 4 (14).

URL <http://www.ehjournal.net/content/4/1/14>

Appendix A

A.1 Calculation of d5-MA extraction efficiency for LLE

Table A.1: Calculation data of extraction efficiency for d5-MA from phosphate buffer LLE of Moscow waste #1, six replicate extractions

	[d5-MA]* (mg/mL)	mg d5-MA in 0.500 mL waste	amount d5-MA added (mg)	% recovery
		<i>A</i>	<i>B</i>	$(A/B) \times 100$
Moscow 1.1	0.008	0.004	0.025	16.586
Moscow 1.2	0.008	0.004	0.025	16.906
Moscow 1.3	0.009	0.004	0.025	17.113
Moscow 1.4	0.008	0.004	0.025	16.758
Moscow 1.5	0.008	0.004	0.025	17.056
Moscow 1.6	0.008	0.004	0.025	16.805
			Average	16.871
			Standard Deviation	0.196
			% RSD	1.163

* Equation of MA regression line: $y = 126.837x - 0.6286$

Table A.2: Average d5-MA percent recoveries from phosphate buffer LLE of each synthetic route

	[d5-MA]* (mg/mL)	mg d5-MA in 0.500 mL waste	Amount d5-MA added (mg)	% recovery
		<i>A</i>	<i>B</i>	$(A/B) \times 100$
Moscow 1	0.008	0.004	0.025	16.871
Moscow 2	0.008	0.004	0.025	16.762
Leuckart 1	0.007	0.003	0.025	13.534
Leuckart 2	0.007	0.003	0.025	13.889
Hypo	0.009	0.005	0.025	18.91
			Average	16.262
			Standard Deviation	2.414
			% RSD	14.847

* Equation of MA regression line: $y = 126.837x - 0.6286$

A.2 Calculation of LOD for MA determined by GC-MS

LOD was calculated using y -residuals of the calibration curve regression line equation, as per Miller and Miller (2010).

Table A.3: Calculation data of LOD for MA determined by GC-MS

Concentration (mg/mL)	Peak Area/IS Area y_i	Signal from line $[\hat{y}]$ $[\hat{y}] = 126.837x - 0.6286$	y-residuals $[y_i - \hat{y}]^2$
0.005	0.2284	0.0056	0.0497
0.01	0.6255	0.6397	0.0002
0.05	5.3155	5.7132	0.1582
0.1	12.2442	12.0551	0.0358

$$LOD\ Signal = a + 3S_{\frac{y}{x}}$$

Where:

$a = \text{intercept of regression line}$

$$S_{\frac{y}{x}} = \sqrt{\frac{\sum (y_i - \hat{y})^2}{n-2}}, n = 4$$

Therefore:

$$LOD\ Signal = -0.6286 + 3(0.3492)$$

$$LOD\ Signal = 0.4189$$

Using the equation from the regression line: $y = 126.837x - 0.6286$

Whereby:

$$y = LOD\ Signal$$

$$x = LOD$$

Therefore:

$$LOD = 0.008\ mg/mL$$

A.3 Tables of compounds identified from LLE of crude MA waste

Table A.4: Complete list of compounds identified in the waste extract of MA synthesised from the Leuckart route (#1)

Peak No	RT (min)	Compound	Peak m/z	R. Match
1	3.78	<i>p/m-Xylene</i>	91, 106, 105, 77	948
2	4.19	<i>o-Xylene</i>	91, 106, 105, 77	936
3	4.33	Styrene	104, 103, 78, 77	920
4	4.36	Acetamide, <i>N</i> -methyl-	73, 58, 74, 54	909
5	5.01	1-Ethyl-2-methylbenzene	117, 118, 115, 91	874
6	5.86	Phenol	94, 66, 65, 63	955
7	6.11	Benzaldehyde	105, 106, 77, 51	912
8	6.43	Benzene, 2-propenyl	117, 118, 115, 91	949
9	6.63	Benzonitrile	103, 76, 104, 75	913
10	7.07	Benzylidenemethylamine	118, 119, 77, 107	882
11	7.12	Benzyl alcohol	108, 107, 79, 77	922
12	7.41	Phenol, 4-methyl-	107, 108, 77, 79	923
13	7.80	Acetophenone	105, 77, 120, 51	868
14	7.94	Benzoic acid, methyl ester	105, 77, 136, 51	907
15	8.25	Amphetamine	91, 65, 92, 63	920
16	8.47	1-Phenyl-2-propanol	92, 91, 65, 93	894
17	8.75	1-Phenyl-2-propanone	88, 58, 91, 134	
SUR	8.83	D5-Methylamphetamine	62, 92, 63, 66	N/A
18	8.88	Methylamphetamine	58, 91, 56, 65	931
19	9.00	1-Methylbutylbenzene	105, 103, 104, 77	809
20	9.24	Benzaldehyde, oxime	103, 121, 104, 77	907
21	9.32	1-Phenyl-1,2-propanedione	105, 77, 51, 106	886
22	9.65	Dimethylamphetamine	72, 91, 70, 73	875
23	10.14	3-Buten-2-one, 3-phenyl-	103, 146, 77, 104	857
IS	10.19	Tetradecane	71, 57, 85, 70	940
24	10.82	Acetophenone, oxime	135, 77, 104, 103	874
25	11.04	2-Propanone, 1-phenyl-, oxime	149, 91, 116, 65	940
26	11.12	3-Methylbenzyl cyanide	91, 131, 116, 130	740
27	11.48	Pentadecane	71, 57, 85, 70, 212	901
28	12.56	Benzamide	105, 77, 121, 51	892
29	13.04	Benzamide, <i>N</i> -methyl-	105, 77, 134, 135	903
30	13.21	Unknown	149, 105, 77, 148	

continued on next page

Peak No	RT (min)	Compound	Peak m/z	R. Match
31	13.66	Unknown	58, 147, 106, 107	
32	13.73	Benzeneacetamide, <i>N</i> -methyl	92, 91, 58, 105	925
33	14.21	Unknown	104, 147, 105, 103	
34	14.61	<i>N</i> -Formylamphetamine	72, 118, 91, 117, 163	932
35	15.17	<i>N</i> -Formylmethamphetamine	86, 58, 91, 118, 177	960
36	15.34	<i>N</i> -Acetylmethylamphetamine	68, 58, 100, 91, 191	715
37	16.29	Unknown	148, 118, 117, 115	
38	16.40	Unknown	102, 187, 103, 76	
39	16.48	Unknown	179, 180, 178, 165, 117	
40	16.98	Unknown	132, 105, 104, 133	
41	17.16	Ethanone, 1,2-diphenyl-	105, 77, 106, 199	918
42	17.40	Unknown	117, 132, 91, 189	
43	17.55	Unknown	203, 126, 105, 188	
44	17.63	Benzylamphetamine	148, 91, 149, 65	907
45	17.69	Unknown	105, 175, 77, 99	
46	18.01	4-Aminophthalimide	162, 91, 119, 70, 163	779
47	18.07	4-Aminophthalimide	162, 91, 119, 163, 70	766
48	18.46	Unknown	200, 102, 134, 91	
49	18.64	Unknown	118, 202, 77, 115	
50	19.23	Unknown	188, 102, 103, 203	
51	19.30	Unknown	176, 91, 58, 119	
52	19.36	Unknown	176, 91, 58, 119	
53	19.79	Unknown	91, 161, 118, 143	
54	20.46	Unknown	187, 158, 104, 102	
55	21.29	2,6 Di- <i>p</i> -tolylpyridine	259, 258, 260, 115	835
56	21.40	2,6 Di- <i>p</i> -tolylpyridine	259, 258, 260, 243	829
57	21.54	Unknown	144, 185, 104, 117	
58	21.79	3-Ethyl-2,6-diphenylpyridine	258, 259, 243, 244	874
59	21.93	Unknown	272, 273, 258, 257	
60	22.34	Unknown	272, 273, 263, 182	
61	22.50	Unknown	262, 277, 200, 56	
62	22.88	Unknown	260, 261, 259, 215	
63	23.11	Unknown	273, 257, 274, 272	
64	23.30	Unknown	291, 200, 143, 128	
65	23.69	Unknown	273, 274, 257, 272	
66	23.83	Unknown	247, 246, 218, 203	
67	23.87	Unknown	143, 202, 287, 128	
68	23.95	Unknown	273, 274, 91, 335	
69	24.04	Unknown	264, 279, 202, 201	

continued on next page

Peak No	RT (min)	Compound	Peak m/z	R. Match
70	24.75	Unknown	162, 134, 143, 234	
71	25.28	Unknown	274, 275, 198, 276	
72	25.94	Unknown	334, 335, 258, 336	
73	26.34	Unknown	287, 105, 288, 210	
74	26.42	Unknown	264, 181, 265, 57	
75	26.60	Unknown	334, 335, 320, 336	
76	27.17	Unknown	234, 191, 338, 233	
77	27.33	Unknown	349, 350, 333, 348	
78	27.61	Unknown	200, 172, 201, 157	
79	28.06	Unknown	334, 335, 256, 258	
80	29.03	Unknown	250, 207, 105, 251	
81	32.57	Unknown	363, 105, 364, 77	

end

Table A.5: Complete list of compounds identified in the waste extract of MA synthesised from the Leuckart route (#2)

Peak No	RT (min)	Compound	Peak m/z	R. Match
1	3.77	<i>p/m-Xylene</i>	91, 106, 105, 77	948
2	4.18	<i>o-Xylene</i>	91, 106, 105, 77	947
3	4.32	Styrene	104, 103, 78, 77	919
4	5.85	Phenol	94, 66, 65, 95	959
5	6.09	Benzaldehyde	105, 106, 77, 51	909
6	6.41	Benzene, 2-propenyl-	117, 118, 115, 91	942
7	6.62	Benzonitrile	103, 76, 104, 75	928
8	7.05	Unknown	108, 107, 118, 77	
9	7.11	Benzyl alcohol	108, 107, 79, 77	926
10	7.39	Phenol, 4-methyl-	107, 108, 79, 77	924
11	7.78	Acetophenone	105, 77, 120, 51	885
12	7.93	Benzoic acid, methyl ester	105, 77, 136, 106	905
13	8.24	Amphetamine	91, 65, 120, 92	915
14	8.45	1-Phenyl-2-propanol	92, 91, 65, 93	879
15	8.73	1-Phenyl-2-propanone	91, 88, 134, 92	799
SUR	8.82	d5-Methylamphetamine	62, 92, 63, 66	N/A
16	8.87	Methylamphetamine	58, 91, 56, 65	934
17	8.99	1-Methylbutylbenzene	105, 103, 104, 77	840
18	9.17	1-Phenyl-1-propanone	105, 77, 134, 106	858

continued on next page

Peak No	RT (min)	Compound	Peak m/z	R. Match
19	9.23	Benzaldehyde, oxime	121, 103, 104, 77	916
20	9.30	1-Phenyl-1,2-propanedione	105, 77, 106, 51, 148	932
21	9.64	Dimethylamphetamine	72, 91, 73, 70	879
22	10.13	3-Buten-2-one, 3-phenyl-	103, 146, 77, 104	853
IS	10.17	Tetradecane	71, 57, 85, 70	962
23	10.82	Acetophenone, oxime	135, 77, 104, 103	886
24	11.04	2-Propanone, 1-phenyl-, oxime	149, 91, 116, 92	934
25	11.12	3-Methylbenzyl cyanide	91, 131, 116, 92	746
26	11.48	Pentadecane	71, 57, 85, 70, 212	907
27	12.24	Benzalacetone	103, 145, 131, 146	846
28	12.55	Benzamide	105, 121, 77, 51	866
29	13.04	<i>Benzamide, N-methyl-</i>	105, 77, 134, 135	902
30	13.20	<i>Unknown</i>	149, 105, 91, 148	
31	13.64	Unknown	58, 147, 106, 91	
32	13.72	Benzeneacetamide, N-methyl	92, 91, 58, 105	935
33	14.61	N-Formylamphetamine	72, 118, 91, 117	929
34	15.17	N-Formylmethamphetamine	86, 58, 118, 91	960
35	15.34	N-Acetylmethylamphetamine	58, 100, 86, 91	923
36	16.28	Unknown	148, 118, 115, 203	
37	16.39	Unknown	102, 187, 103, 76	
38	16.46	Unknown	179, 180, 178, 165	
39	16.94	Unknown	132, 105, 91, 133	
40	17.14	Ethanone, 1,2-diphenyl-	105, 77, 106, 199	943
41	17.38	Unknown	117, 91, 132, 189	
42	17.54	Unknown	203, 126, 188, 105	
43	17.61	Benzylamphetamine	148, 91, 149, 65	905
44	17.67	Unknown	105, 175, 77, 99	
45	18.00	4-Aminophthalimide	162, 91, 119, 163	771
47	18.06	4-Aminophthalimide	162, 91, 119, 163	772
48	18.29	Unknown	179, 222, 152, 164	
49	18.44	Unknown	91, 134, 117, 104	
50	18.62	Unknown	202, 118, 115, 217	
51	19.21	Unknown	188, 102, 103, 203	
52	19.29	Unknown	176, 91, 58, 119	
53	19.35	Unknown	176, 91, 58, 119	
54	19.77	Unknown	161, 91, 118, 143	
55	20.45	Unknown	187, 158, 104, 186	
56	21.28	2,6 Di-p-tolylpyridine	259, 258, 260, 115	834
57	21.39	2,6 Di-p-tolylpyridine	259, 258, 260, 115	834

continued on next page

Peak No	RT (min)	Compound	Peak m/z	R. Match
58	21.51	Unknown	144, 185, 117, 104	
59	21.78	3-Ethyl-2,6-diphenylpyridine	258, 259, 244, 243	870
60	21.92	Unknown	272, 273, 258, 274	
61	22.33	Unknown	272, 273, 182, 263	
62	22.49	Unknown	262, 277, 200, 56	
63	22.87	Unknown	260, 259, 261, 215	
64	23.11	Unknown	273, 274, 257, 272	
65	23.29	Unknown	291, 200, 143, 128	
66	23.68	Unknown	273, 274, 257, 272	
67	23.83	Unknown	247, 246, 218, 203	
68	23.86	Unknown	143, 202, 287, 60	
69	23.94	Unknown	273, 274, 279, 264	
70	24.03	Unknown	264, 279, 202, 115	
71	24.75	Unknown	162, 134, 143, 234	
72	25.28	Unknown	274, 275, 198, 276	
73	25.94	Unknown	334, 335, 258, 336	
74	26.32	Unknown	287, 105, 288, 210	
75	26.41	Unknown	264, 181, 265, 91	
76	26.58	Unknown	334, 335, 320, 257	
77	27.15	Unknown	234, 191, 338, 235	
78	27.31	Unknown	349, 350, 333, 348	
79	27.60	Unknown	200, 172, 201, 157	
80	28.04	Unknown	334, 335, 258, 256	
81	28.48	Unknown	161, 105, 77, 265	
82	29.01	Unknown	250, 207, 105, 251	
83	32.71	Unknown	363, 105, 364, 77	

end

Table A.6: Complete list of compounds identified in the waste extract of MA synthesised from the Leuckart route (#3)

Peak No	RT (min)	Compound	Peak m/z	R. Match
1	4.14	<i>p/m-Xylene</i>	91, 106, 105, 103	898
2	4.31	Acetamide, <i>N</i> -methyl-	73, 58, 74, 54	970
3	5.80	Phenol	94, 66, 65, 63	931
4	6.04	Benzaldehyde	105, 106, 77, 51	874
5	7.01	<i>N</i> -Methylbenzaldimine	118, 119, 77, 91	883

continued on next page

Peak No	RT (min)	Compound	Peak m/z	R. Match
6	7.06	Benzyl alcohol	108, 107, 79, 77	874
7	8.40	1-Phenyl-2-propanol	92, 91, 65, 93	857
8	8.66	Unknown	88, 58, 57, 59	
9	8.82	Methylamphetamine	58, 91, 56, 65	939
10	9.17	Benzaldehyde oxime	103, 104, 121, 105	848
IS	10.13	Tetradecane (old)	57, 71, 85, 99, 198	927
11	10.97	1-Phenyl-2-propanone oxime	149, 91, 116, 65	932
12	13.60	Unknown	147, 91, 162, 148	
13	16.90	Phenyl[(1-phenyl-2-propanyl)amino]acetonitrile	132, 105, 133, 91	860
14	17.57	Unknown	148, 91, 149, 70	
15	17.67	Unknown	149, 150, 57, 56	
16	17.94	4-Aminophthalimide	162, 91, 119, 163	780
17	18.01	4-Aminophthalimide	162, 91, 119, 163	817
18	19.23	Unknown	176, 91, 58, 119	
19	19.30	Unknown	176, 91, 58, 119	
20	20.57	Unknown	98, 99, 107, 77	
21	20.65	Unknown	248, 233, 247, 77	
22	20.86	Unknown	259, 258, 191, 181	
23	21.22	Unknown	258, 259, 260, 243	
24	21.33	Unknown	259, 258, 260, 261	
25	21.72	Unknown	258, 259, 243, 244	
26	21.76	Unknown	247, 246, 202, 248	
27	21.86	Unknown	272, 273, 258, 243	
28	22.26	Unknown	272, 273, 182, 258	
29	22.43	Unknown	262, 277, 200, 56	
30	23.03	Unknown	273, 257, 274, 272	
31	23.22	Unknown	291, 200, 143, 128	
32	23.62	Unknown	273, 274, 272, 257	
33	25.19	Unknown	274, 275, 276, 198	
34	25.87	Unknown	334, 335, 258, 336	
35	26.35	Unknown	264, 181, 265, 91	
36	26.50	Unknown	334, 335, 320, 257	
36	27.23	Unknown	349, 350, 333, 70	

end

Table A.7: Complete list of compounds identified in the waste extract of MA synthesised from the Leuckart route (#4)

Peak No	RT (min)	Compound	Peak m/z	R. Match
1	4.14	<i>p/m-Xylene</i>	91, 106, 105, 77	906
2	4.30	Acetamide, <i>N</i> -methyl-	73, 58, 74, 54	959
3	5.80	Phenol	94, 66, 65, 63	930
4	6.04	Benzaldehyde	105, 106, 77, 51, 78, 107	901
5	6.36	Benzene, 2-propenyl-	117, 118, 115, 91	883
6	7.01	<i>N</i> -Methylbenzalimine	118, 119, 77, 91	896
7	7.06	Benzyl alcohol	108, 107, 79, 77	891
8	7.34	Phenol, 4-methyl-	107, 108, 77, 79	917
9	8.40	1-Phenyl-2-propanol	92, 91, 65, 93	839
10	8.66	Unknown	88, 69, 57, 87	
11	8.82	Methylamphetamine	58, 91, 56, 65	937
12	9.17	Benzaldehyde oxime	103, 104, 121, 105	868
13	9.60	Dimethylamphetamine	72, 91, 56, 73	859
IS	10.13	Tetradecane (old)	71, 57, 85, 70, 198	936
14	10.79	<i>Unknown</i>	135, 77, 104, 103	
15	10.97	1-Phenyl-2-propanone oxime	149, 91, 116, 65	943
16	11.06	Unknown	91, 131, 116, 92	
17	13.60	Unknown	147, 91, 162, 119	
18	15.10	<i>N</i> -Formylmethamphetamine	86, 58, 91, 118	948
19	15.28	Unknown	100, 58, 101, 115	
20	16.90	Unknown	132, 105, 91, 70	
21	17.95	Unknown	162, 91, 119, 163	
22	18.01	Unknown	162, 91, 119, 163	
23	19.24	Unknown	176, 91, 58, 119	
24	19.30	Unknown	176, 91, 58, 119	
25	21.22	Unknown	259, 258, 260, 243	810
26	21.33	Unknown	259, 258, 269, 184	788
27	21.72	Unknown	258, 259, 243, 260	
28	21.76	Unknown	247, 246, 202, 248	
29	21.87	Unknown	272, 273, 258, 257	
30	22.27	Unknown	272, 273, 182, 181	
31	22.43	Unknown	262, 277, 200, 56	
32	22.81	Unknown	260, 261, 259, 215	
33	23.04	Unknown	273, 274, 257, 272	
34	23.23	Unknown	291, 200, 143, 292	
35	23.62	Unknown	273, 274, 257, 272	

continued on next page

Peak No	RT (min)	Compound	Peak m/z	R. Match
36	23.80	Unknown	143, 202, 287, 128	
37	23.88	Unknown	273, 274, 91, 180	
38	24.68	Unknown	162, 134, 143, 105	
39	25.20	Unknown	274, 275, 258, 198	
40	25.87	Unknown	334, 335, 258, 336	

end

Table A.8: Complete list of compounds identified in the waste extract of MA synthesised from the Leuckart route (#5)

Peak No	RT (min)	Compound	Peak m/z	R. Match
1	4.14	<i>p/m-Xylene</i>	91, 106, 105, 103	928
2	4.31	Acetamide, <i>N</i> -methyl-	73, 58, 74, 54	915
3	5.82	Phenol	94, 66, 65, 63	951
4	6.04	Benzaldehyde	105, 106, 77, 51	903
5	6.36	Benzene, 2-propenyl-	117, 118, 115, 91	896
6	7.01	<i>N</i> -Methylbenzaldimine	118, 119, 77, 91	869
7	7.06	Benzyl alcohol	108, 107, 79, 77	902
8	7.40	Phenol, 4-methyl-	107, 108, 79, 77	916
9	8.19	Amphetamine	91, 65, 120, 63	917
10	8.40	1-Phenyl-2-propanol	92, 91, 65, 93	901
11	8.69	Unknown	88, 58, 91, 134	
12	8.82	Methylamphetamine	58, 91, 56, 65	943
13	9.61	Dimethylamphetamine	72, 91, 70, 73	871
IS	10.13	Tetradecane (old)	71, 57, 85, 70	880
14	10.97	1-Phenyl-2-propanone oxime	149, 91, 116, 92	922
15	11.42	<i>Unknown</i>	151, 109, 57, 69	
16	13.60	Unknown	147, 162, 91, 119	
17	14.20	Unknown	56, 91, 117, 118	
18	15.10	<i>N</i> -Formylmethamphetamine	86, 58, 91, 118	961
19	16.90	Phenyl[(1-phenyl-2-propanyl)amino]acetonitrile	132, 105, 91, 133	906
20	17.94	Unknown	162, 91, 119, 163	
21	18.00	Unknown	162, 91, 119, 163	
22	19.23	Unknown	176, 91, 58, 119	
23	19.29	Unknown	176, 91, 58, 119	
24	21.22	Unknown	259, 258, 260, 173	

continued on next page

Peak No	RT (min)	Compound	Peak m/z	R. Match
25	21.33	Unknown	258, 259, 261, 184	
26	21.72	Unknown	258, 259, 243, 260	
27	21.78	Unknown	247, 273, 258, 257	
28	21.86	Unknown	272, 273, 258, 257	
29	22.14	Unknown	188, 221, 147, 189	
30	22.27	Unknown	272, 273, 182, 181	
31	22.43	Unknown	262, 277, 258, 200	
32	22.80	Unknown	260, 261, 259, 215	
33	23.04	Unknown	273, 274, 257, 272	
34	23.22	Unknown	291, 200, 261, 143	
35	23.62	Unknown	273, 274, 257, 272	
36	23.80	Unknown	143, 202, 287, 128	
37	23.88	Unknown	273, 274, 180, 91	
38	24.68	Unknown	162, 134, 143, 234	
39	25.19	Unknown	274, 275, 198, 276	
40	25.87	Unknown	334, 335, 258, 336	
41	26.35	Unknown	264, 181, 265, 91	
42	26.50	Unknown	334, 257, 348, 179	
43	27.23	Unknown	349, 350, 333, 160	
44	27.50	Unknown	200, 172, 201, 157	
45	27.95	Unknown	334, 335, 258, 256	
46	28.04	Unknown	292, 290, 349, 198	

end

Table A.9: Complete list of compounds identified in the waste extract of MA synthesised from the Moscow route (#2)

Peak No	RT (min)	Compound	Peak m/z	R. Match
1	3.71	Ethylbenzene	91, 106, 65, 105	934
2	3.80	<i>p/m-Xylene</i>	91, 106, 105, 103	921
3	4.19	<i>o-Xylene</i>	91, 106, 105, 103	893
4	4.33	Unknown	56, 98, 55, 83	
5	4.45	Unknown	81, 97, 96, 55	
6	4.66	4-methoxy-4-methyl-2-pentanone	73, 100, 115, 55	889
7	4.91	Unknown	184, 141, 127, 169	
8	6.06	Benzaldehyde	105, 106, 77, 51	919
9	6.59	Benzyl chloride	91, 126, 65, 92	898

continued on next page

Peak No	RT (min)	Compound	Peak m/z	R. Match
10	7.07	Benzyl alcohol	108, 107, 79, 77	927
11	7.44	Unknown	69, 70, 55, 56	
12	8.69	1-Phenyl-2-propanone	91, 134, 92, 65	920
13	8.82	Methylamphetamine	58, 91, 56, 65	919
14	9.12	1-Phenyl-1-propanone	105, 77, 134, 51	840
15	9.18	Unknown	170, 135, 91, 172	
16	9.25	1,2-Propanedione, 1-phenyl-	105, 77, 51, 106	912
IS	10.21	Tetradecane (old)	71, 57, 85, 70, 198	
17	10.76	Unknown	95, 67, 81, 96	
18	11.79	Unknown	91, 65, 119, 168	
19	12.19	Unknown	103, 156, 131, 146	
20	12.74	Long chain alkene or alcohol	69, 97, 55, 70	
21	12.97	2,6-Di-tert-butylphenol	191, 206, 192, 57	940
22	15.03	Long chain alkene or alcohol	97, 69, 55, 83	
23	15.51	Unknown	317, 332, 57, 318	
24	15.81	Benzophenone	105, 77, 182, 51	889
25	17.11	Long chain alkene or alcohol	97, 69, 83, 55	
26	17.38	Unknown	147, 221, 236, 163	
27	17.99	Unknown	299, 243, 300, 314	
28	18.13	Benzenepropanoic acid, 3,5-bis-(1,1-dimethylethyl)-4-hydroxy-, methyl ester	277, 147, 292, 219	862
29	18.67	Long chain alkene or alcohol	69, 97, 83, 55	
30	19.01	Fatty acid methyl ester	74, 69, 97, 87	
31	20.09	Unknown PAH	232, 217, 215, 202	
32	20.61	Unknown PAH	232, 217, 215, 202	
33	22.89	Unknown	58, 190, 91, 105	
34	23.39	Unknown benzenedicarboxylic acid ester	149, 167, 70, 71	
35	24.06	Unknown	105, 91, 190, 119	
36	24.28	Unknown	131, 188, 103, 102	
37	34.65	Unknown	219, 57, 147, 203	

end

Table A.10: Complete list of compounds identified in the waste extract of MA synthesised from the Moscow route (#3)

Peak No	RT (min)	Compound	Peak m/z	R. Match
1	3.71	Ethylbenzene	91, 106, 105, 65	929
2	3.80	<i>p/m-Xylene</i>	91, 106, 105, 103	930
3	4.33	Unknown	56, 98, 55, 83	
4	4.45	Unknown	81, 97, 96, 55	
5	4.91	Unknown	184, 141, 91, 127	
6	4.98	Unknown	95, 110, 67, 69	
7	5.07	Benzene, 1-ethyl- β -methyl-	105, 68, 95, 120	
8	5.19	Benzene, 1-ethyl- β -methyl-	105, 120, 91, 106	
9	5.41	Benzene, 1-ethyl- β -methyl-	105, 120, 103, 92	
10	5.61	Benzene, 1-ethyl- β -methyl-	105, 120, 91, 106	
11	6.06	Benzaldehyde	105, 106, 77, 51	902
12	6.26	Unknown	99, 81, 67, 110	
13	6.59	Benzyl chloride	91, 126, 65, 63	906
14	7.07	Benzyl alcohol	108, 107, 79, 77	829
15	7.59	Unknown	70, 91, 57, 55	
16	8.18	Long chain alkane	71, 57, 85, 70	
17	8.69	1-Phenyl-2-propanone	91, 134, 65, 92	906
18	8.84	Methylamphetamine	58, 56, 91, 65	936
19	8.99	Benzyl acetate	108, 150, 91, 107	922
20	9.25	1,2-Propanedione, 1-phenyl-	105, 77, 106, 51	889
21	9.57	Toluene	91, 92, 65, 63	926
IS	10.21	Tetradecane (old)	71, 57, 85, 70, 198	
22	10.98	Long chain alkane	71, 57, 85, 99	
23	12.16	Unknown	191, 103, 131, 145	
24	12.74	Long chain alkene or alcohol	69, 97, 55, 70	
25	12.96	2,6-Di-tert-butylphenol	191, 206, 192, 57	941
26	15.03	Long chain alkene or alcohol	69, 97, 83, 55	
27	16.22	Long chain alkene or alcohol	71, 57, 85, 99	
28	16.80	Dimethoxynaphthalene	145, 188, 173, 102	876
29	17.11	Long chain alkene or alcohol	97, 69, 83, 57	
30	17.70	Hexadecanoic acid, ethyl ester	101, 88, 157, 70	882
31	17.99	Unknown	147, 235, 250, 163	
32	18.09	Unknown	317, 289, 316, 332	
33	18.67	Unknown	291, 147, 306, 219	
34	18.76	Dibutyl phthalate	149, 150, 223, 205	918
35	19.01	Long chain alkene or alcohol	97, 69, 70, 55	

continued on next page

Peak No	RT (min)	Compound	Peak m/z	R. Match
36	19.56	Octadecanoic acid, ethyl ester	101, 88, 157, 312	850
37	19.71	Acetic acid, octadecyl ester	69, 97, 83, 57	929
38	20.09	Unknown PAH	232, 217, 215, 202	
39	20.61	Unknown PAH	232, 217, 215, 202	
40	22.31	Unknown	355, 101, 356, 57	
41	22.89	Unknown	58, 190, 91, 105	
42	23.39	Unknown benzenedicarboxylic acid ester	149, 167, 279, 71	
43	23.86	Unknown	383, 101, 384, 129	
44	24.28	Unknown phenyl ketone	131, 188, 103, 77	
45	25.60	Unknown	57, 231, 232, 147	
46	27.44	Long chain alkene or alcohol	97, 69, 83, 57	
47	34.64	Unknown	219, 57, 147, 203	

end

A.4 Calculation of d5-MA extraction efficiency for sediment extraction

Table A.11: Average d5-MA percent recoveries from sediment extraction of each synthetic route

	[d5-MA]* (mg/mL)	mg d5-MA in 0.500 mL waste <i>A</i>	Amount d5-MA added (mg) <i>B</i>	% recovery $(A/B) \times 100$	% RSD
Moscow	0.006	0.004	0.050	12.06	4.36
Leuckart	0.011	0.003	0.050	21.48	44.48
Hypo	0.011	0.005	0.050	22.83	49.08
			Average	16.262	
			Standard Deviation	2.414	
			% RSD	14.847	

* Equation of MA regression line: $y = -1.037x + 251.713$

Appendix B

B.1 X-Ray Diffraction Spectra

X-Ray diffraction was used to determine the crystal lattice structure of each sediment sample. Sieved (2.0 mm wire mesh) sediment samples were air dried overnight to remove excessive moisture. A small amount was placed onto a quartz disc and smoothed over with a metal spatula, with care taken to ensure coarse material had been removed. XRD was carried out on a Bruker D8 Advance with DaVinci XRD (Bruker, UK), with a copper tube with 1.5419 \AA . Voltage was set to 40 kV, and current at 40 mA. The step time was 0.600 s, 2Theta was run from 15-80 at increments of 0.0255.

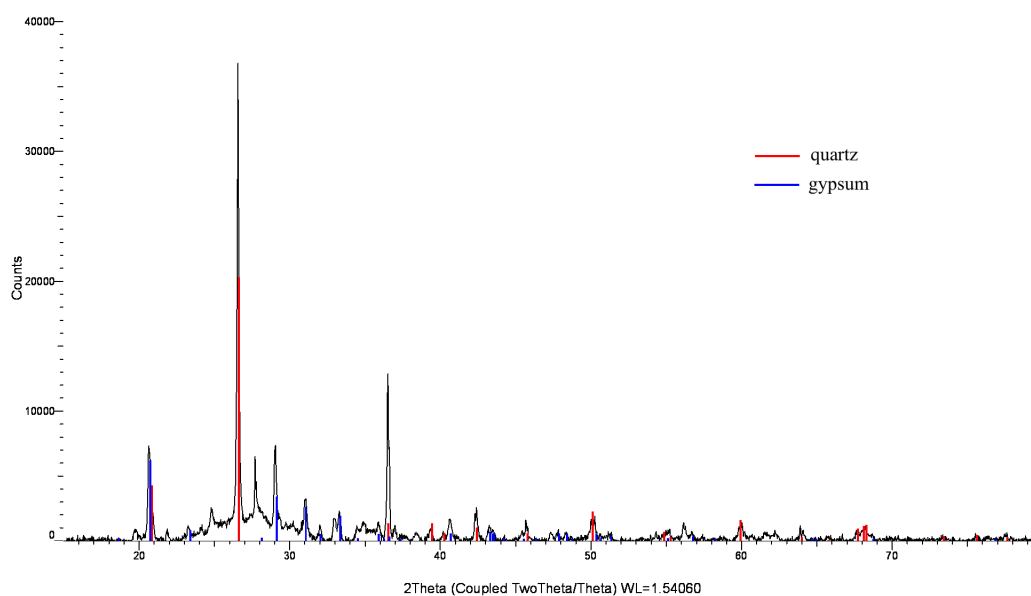


Figure B.1: XRD spectra of Port Dundas sediment sample

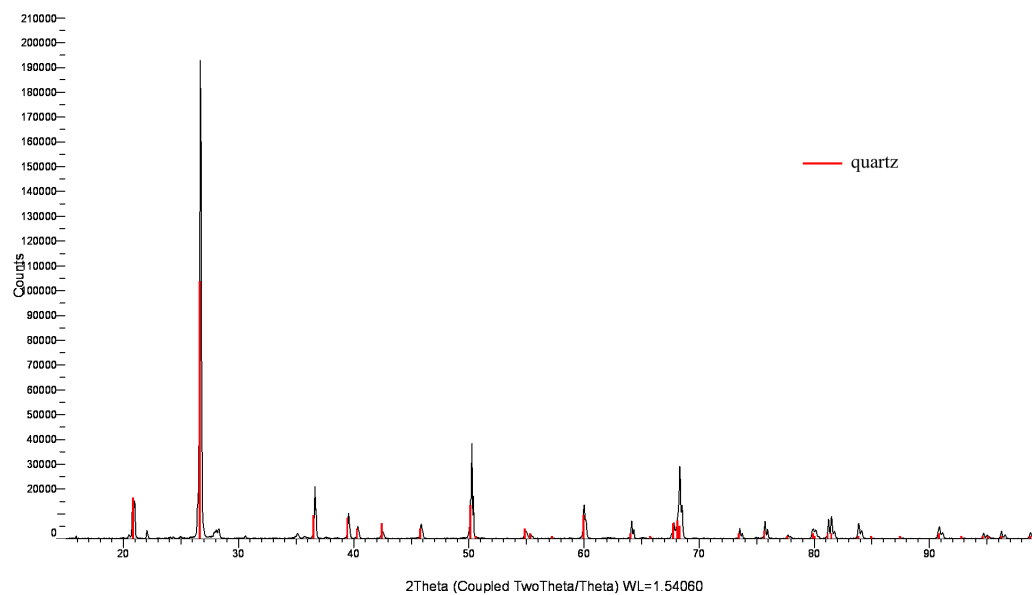


Figure B.2: XRD spectra of Bothwell Bridge sediment sample

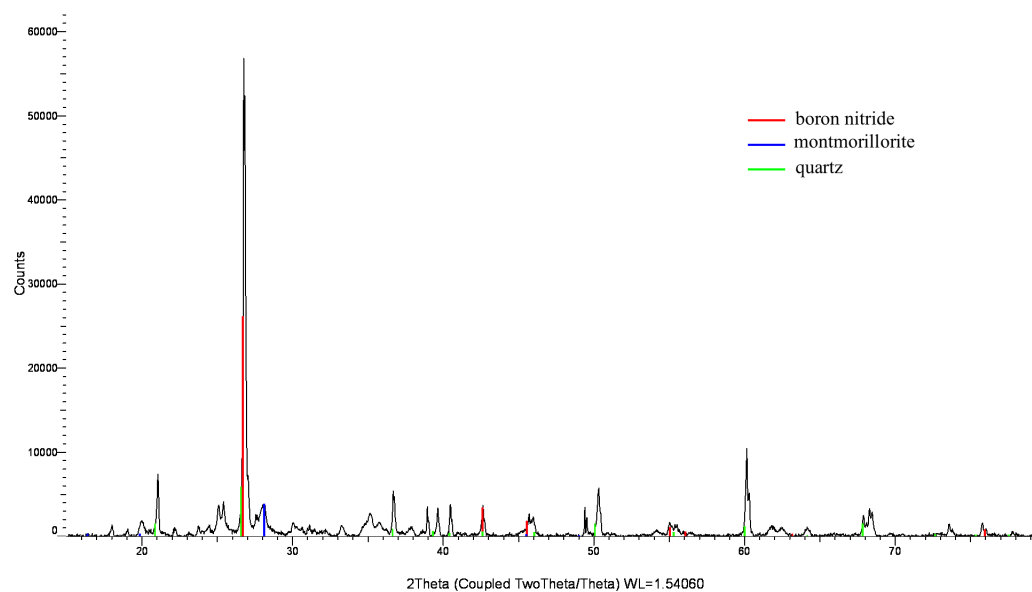


Figure B.3: XRD spectra of Bowling Harbour sediment sample

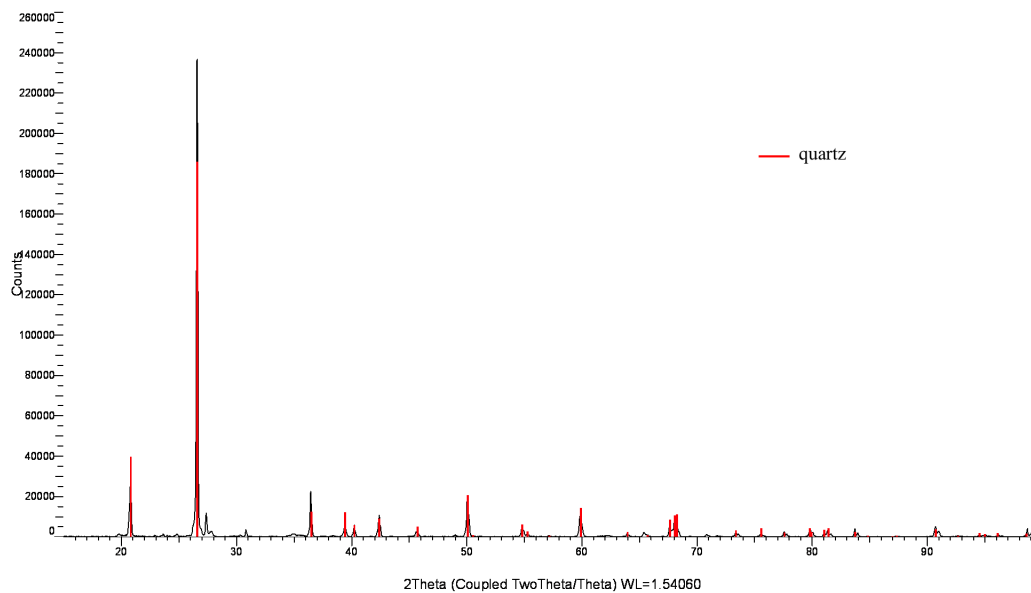


Figure B.4: XRD spectra of Soil #1

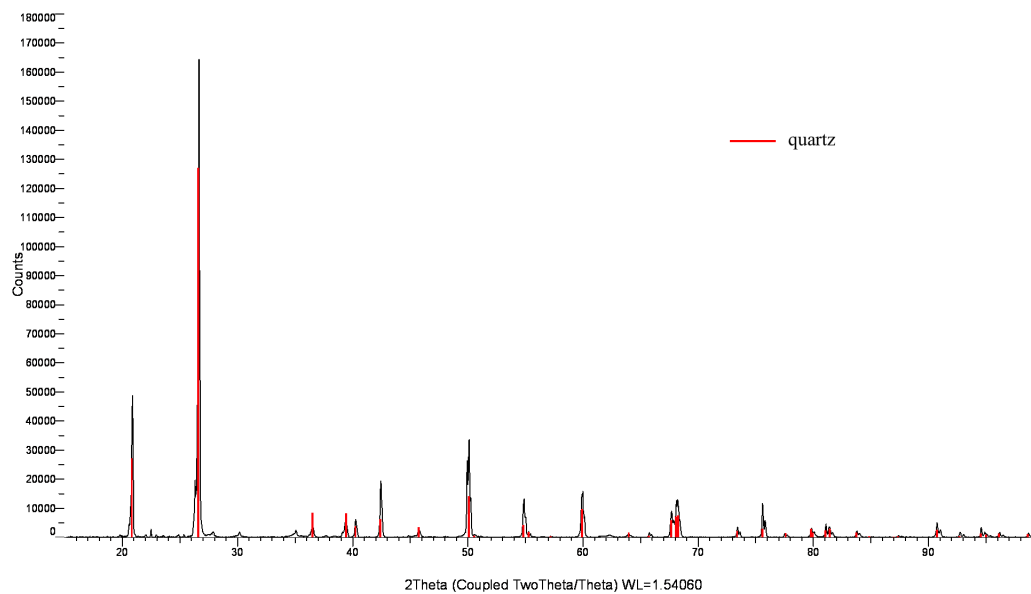


Figure B.5: XRD spectra of Soil #2

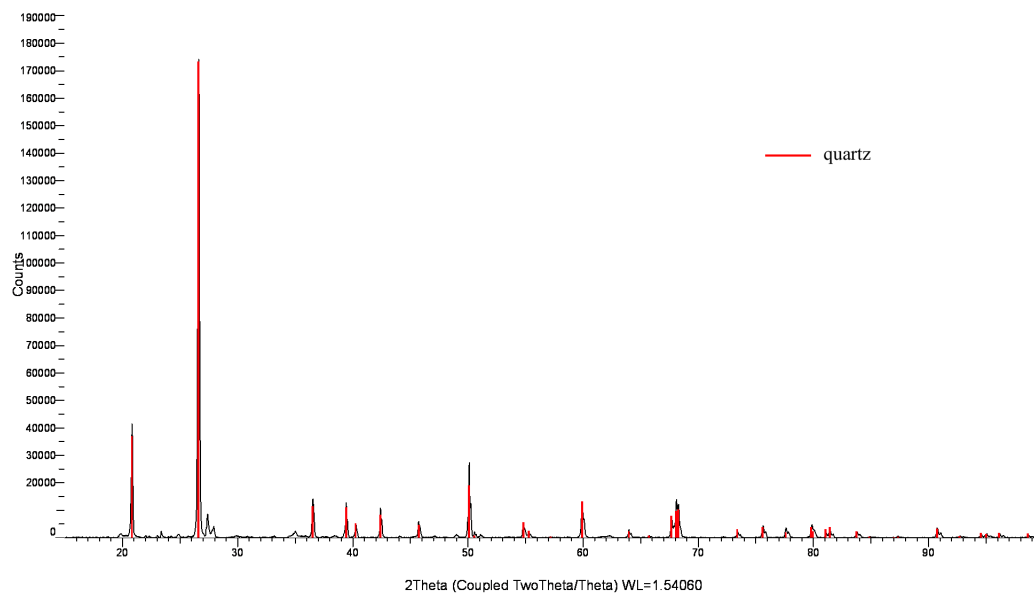


Figure B.6: XRD spectra of Soil #3

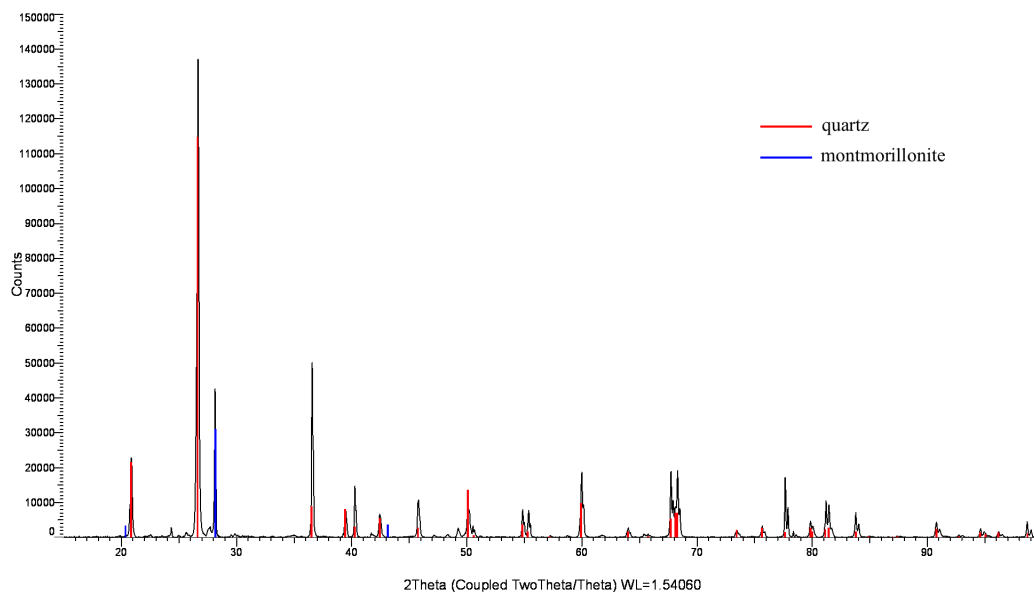


Figure B.7: XRD spectra of sand component of artificial soils

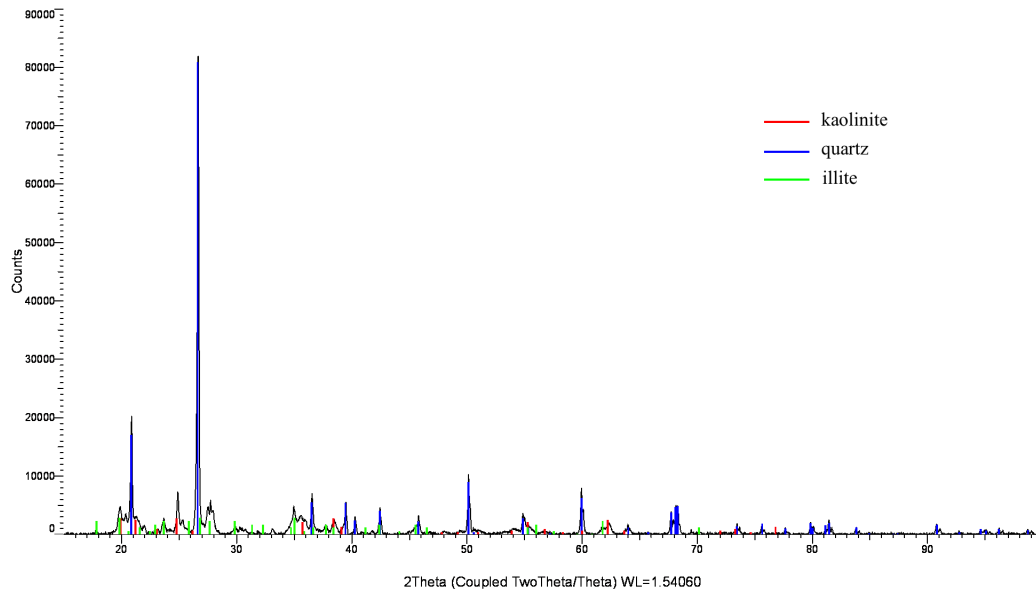


Figure B.8: XRD spectra of silt component of artificial soils

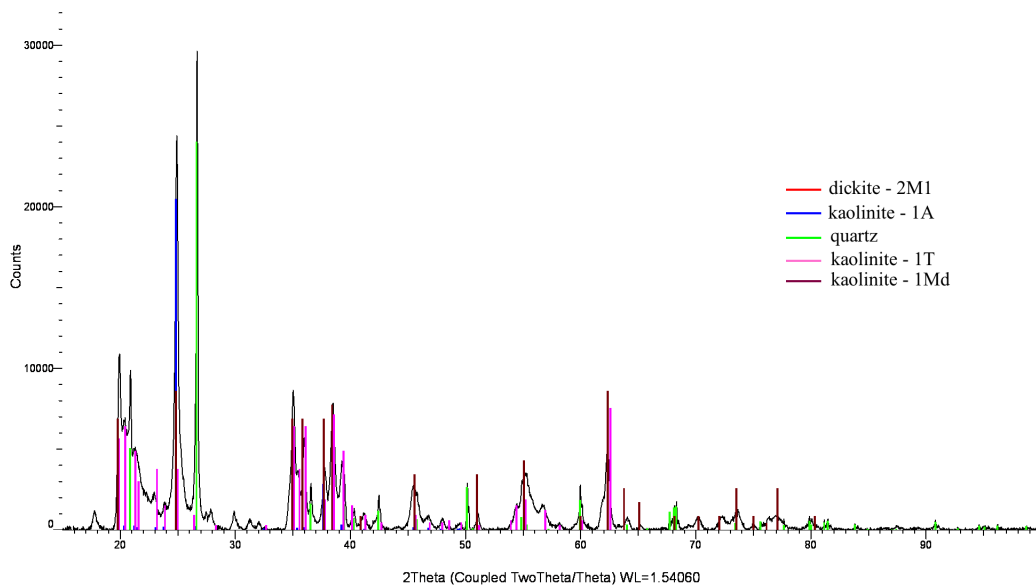


Figure B.9: XRD spectra of clay component of artificial soils

B.2 Calculation of LOD from HPLC Analysis

LOD was calculated using y -residuals of the calibration curve regression line equation, as per Miller and Miller (2010). The calibration curves for P2P, N-methylacetamide, phenol, and benzaldehyde, oxime are shown in Figure B.10. LOD calculations for each of the four compounds are shown on the subsequent four pages.

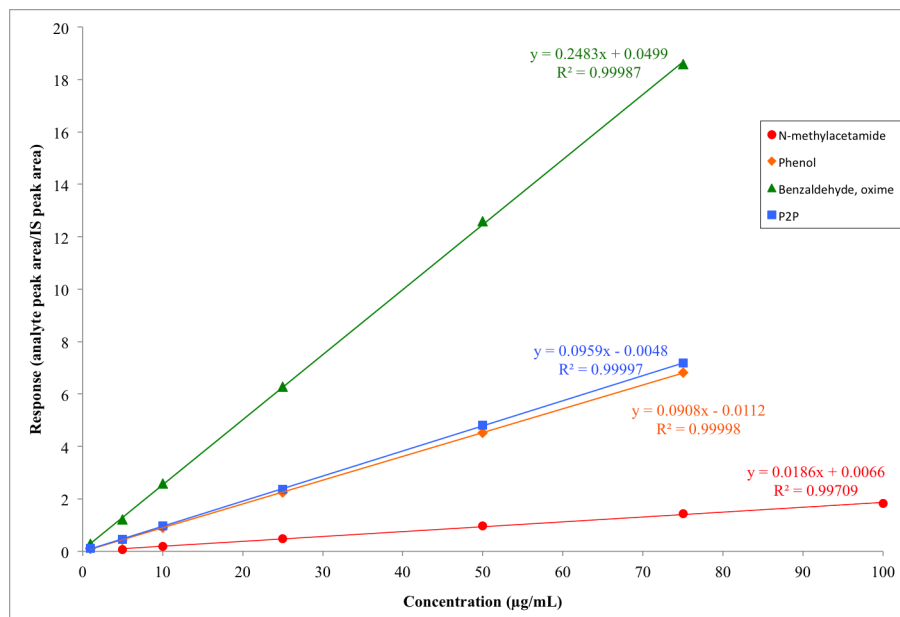


Figure B.10: HPLC calibration curves

Table B.1: Calculation data of LOD for P2P determined by HPLC

Concentration ($\mu\text{g/mL}$)	Peak Area/IS Area y_i	Signal from line $[\hat{y}]$ $[\hat{y}] = 0.095x - 0.004$	y-residuals $[y_i - \hat{y}]^2$
1	0.101255	0.091	0.000105
5	0.457348	0.471	0.000186
10	0.967543	0.946	0.000464
25	2.373157	2.371	4.65681E-06
50	4.807643	4.746	0.003799
75	7.177270	7.121	0.003166
		Sum	0.007727

$$LOD\ Signal = a + 3S_{\frac{y}{x}}$$

Where:

$a = \text{intercept of regression line}$

$$S_{\frac{y}{x}} = \sqrt{\frac{\sum (y_i - \hat{y})^2}{n-2}}, n = 6$$

Therefore:

$$LOD\ Signal = -0.004 + 3(0.044)$$

$$LOD\ Signal = 0.330$$

Using the equation from the regression line: $y = 0.095x - 0.004$

Whereby:

$$y = LOD\ Signal$$

$$x = LOD$$

Therefore:

$$LOD = \frac{0.330 + 0.004}{0.095}$$

$$LOD = 1.472\ \mu\text{g/mL}$$

Table B.2: Calculation data of LOD for *N*-methylacetamide determined by HPLC

Concentration ($\mu\text{g/mL}$)	Peak Area/IS Area y_i	Signal from line $[\hat{y}]$ $[\hat{y}] = 0.018x - 0.006$	y-residuals $[y_i - \hat{y}]^2$
5	0.059158	0.096	0.001357
10	0.194799	0.186	7.74332E-05
25	0.484388	0.456	0.000805
50	0.974873	0.906	0.004743
75	1.445874	1.356	0.008077
100	1.821053	1.806	0.000226
		Sum	0.0152

$$LOD\ Signal = a + 3S_{\frac{y}{x}}$$

Where:

$a = \text{intercept of regression line}$

$$S_{\frac{y}{x}} = \sqrt{\frac{\sum (y_i - \hat{y})^2}{n-2}}, n = 6$$

Therefore:

$$LOD\ Signal = -0.006 + 3(0.015)$$

$$LOD\ Signal = 0.191$$

Using the equation from the regression line: $y = 0.018x - 0.006$

Whereby:

$$y = LOD\ Signal$$

$$x = LOD$$

Therefore:

$$LOD = \frac{0.191 + 0.006}{0.018}$$

$$LOD = 10.304\ \mu\text{g/mL}$$

Table B.3: Calculation data of LOD for phenol determined by HPLC

Concentration ($\mu\text{g/mL}$)	Peak Area/IS Area y_i	Signal from line $[\hat{y}]$ $[\hat{y}] = 0.090x - 0.011$	y-residuals $[y_i - \hat{y}]^2$
1	0.093696	0.079	0.000215
5	0.428212	0.439	0.000116
10	0.905814	0.889	0.000282
25	2.250846	2.239	0.000140
50	4.520556	4.489	0.000995
75	6.806833	6.739	0.004601
		Sum	0.006

$$LOD\ Signal = a + 3S_{\frac{y}{x}}$$

Where:

$a = \text{intercept of regression line}$

$$S_{\frac{y}{x}} = \sqrt{\frac{\sum (y_i - \hat{y})^2}{n-2}}, n = 6$$

Therefore:

$$LOD\ Signal = -0.011 + 3(0.040)$$

$$LOD\ Signal = 0.130$$

Using the equation from the regression line: $y = 0.090x - 0.011$

Whereby:

$$y = LOD\ Signal$$

$$x = LOD$$

Therefore:

$$LOD = \frac{0.130 + 0.011}{0.090}$$

$$LOD = 1.573\ \mu\text{g/mL}$$

Table B.4: Calculation data of LOD for benzaldehyde, oxime determined by HPLC

Concentration ($\mu\text{g}/\text{mL}$)	Peak Area/IS Area y_i	Signal from line $[\hat{y}]$ $[\hat{y}] = 0.248x + 0.049$	y-residuals $[y_i - \hat{y}]^2$
1	0.272506	0.297	0.000599
5	1.213029	1.289	0.005771
10	2.578562	2.529	0.002456
25	6.280800	6.249	0.001011
50	12.590770	12.449	0.020098
75	18.576630	18.649	0.005237
		Sum	0.035

$$LOD \text{ Signal} = a + 3S_{\frac{y}{x}}$$

Where:

$a = \text{intercept of regression line}$

$$S_{\frac{y}{x}} = \sqrt{\frac{\sum (y_i - \hat{y})^2}{n-2}}, n = 6$$

Therefore:

$$LOD \text{ Signal} = 0.049 + 3(0.094)$$

$$LOD \text{ Signal} = 0.330$$

Using the equation from the regression line: $y = 0.248x + 0.049$

Whereby:

$$y = LOD \text{ Signal}$$

$$x = LOD$$

Therefore:

$$LOD = \frac{0.330 - 0.049}{0.248}$$

$$LOD = 1.134 \mu\text{g}/\text{mL}$$

Appendix C

C.1 Fugacity models of additional MA waste components

C.1.1 Water Emissions Scenario

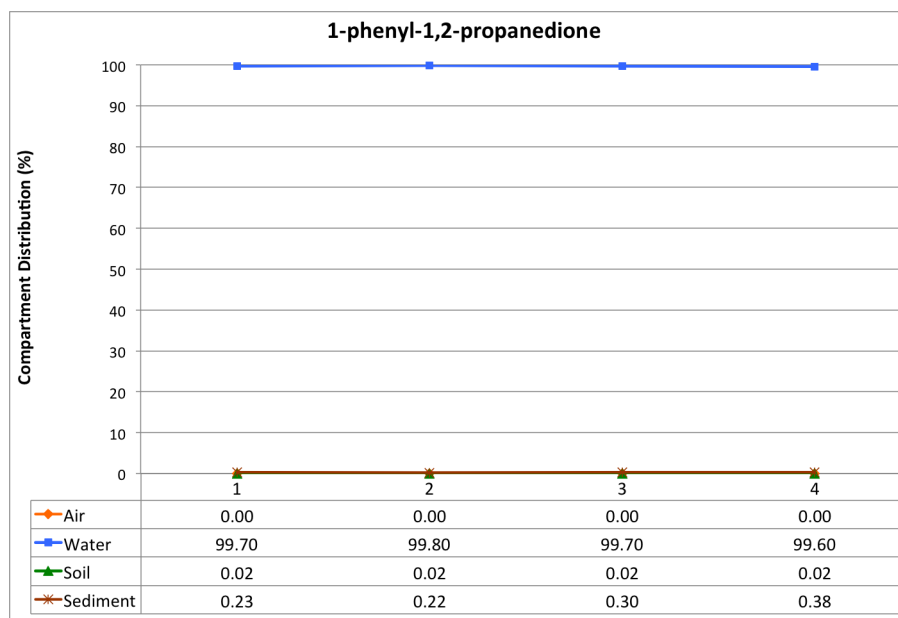


Figure C.1: Water discharge scenario fugacity model of 1-phenyl-1,2-propanedione, from EPI Suite™. (X-axis = model scenario corresponding to Table 5.2 on page 205)

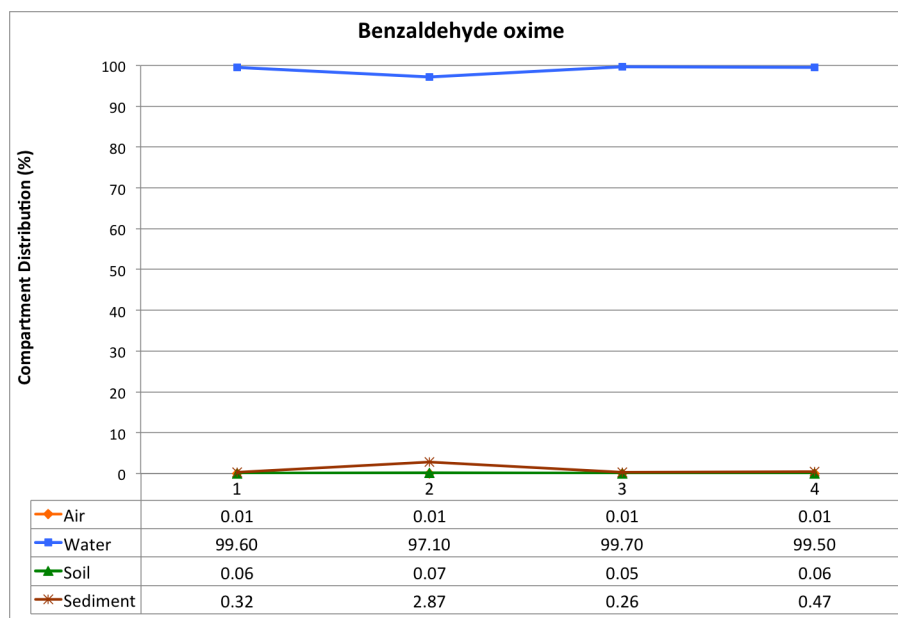


Figure C.2: Water discharge scenario fugacity model of benzaldehyde oxime, from EPI Suite™. (X-axis = model scenario corresponding to Table 5.2)



Figure C.3: Water discharge scenario fugacity model of benzyl alcohol, from EPI Suite™. (X-axis = model scenario corresponding to Table 5.2)

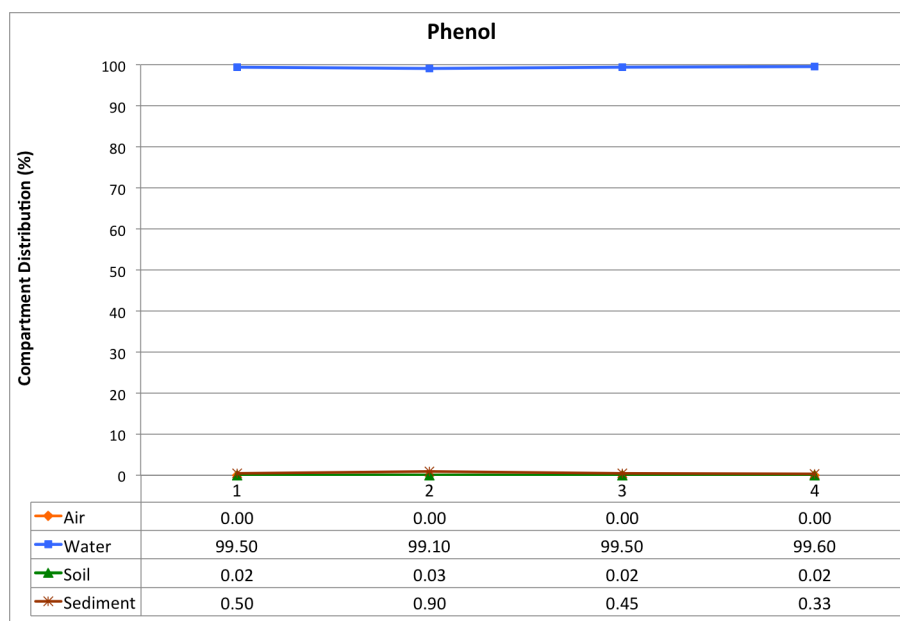


Figure C.4: Water discharge scenario fugacity model of phenol, from EPI Suite™. (X-axis = model scenario corresponding to Table 5.2)

C.1.2 Soil Emissions Scenario

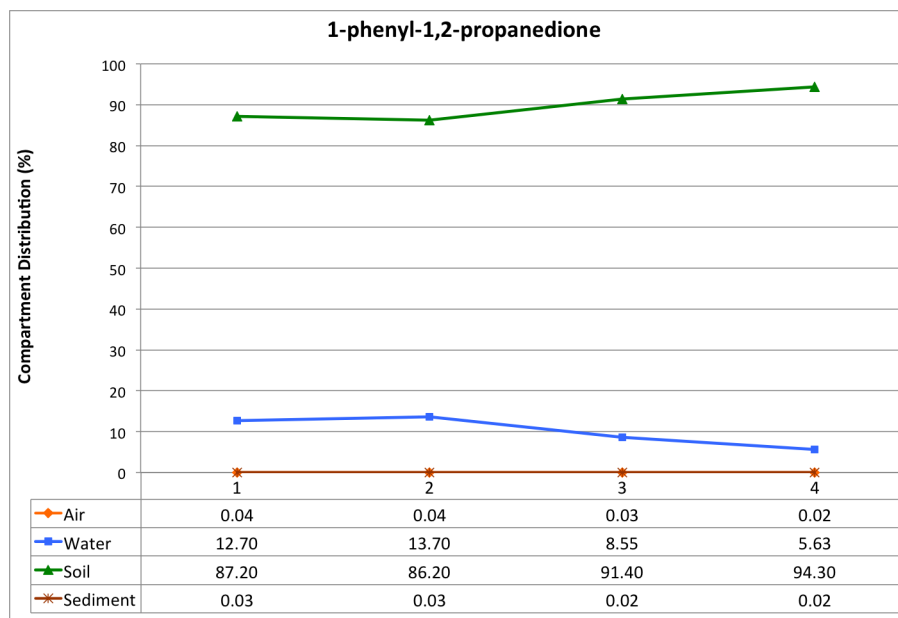


Figure C.5: Soil discharge scenario fugacity model of 1-phenyl-1,2-propanedione, from EPI Suite™. (X-axis = model scenario corresponding to Table 5.2 on page 205)

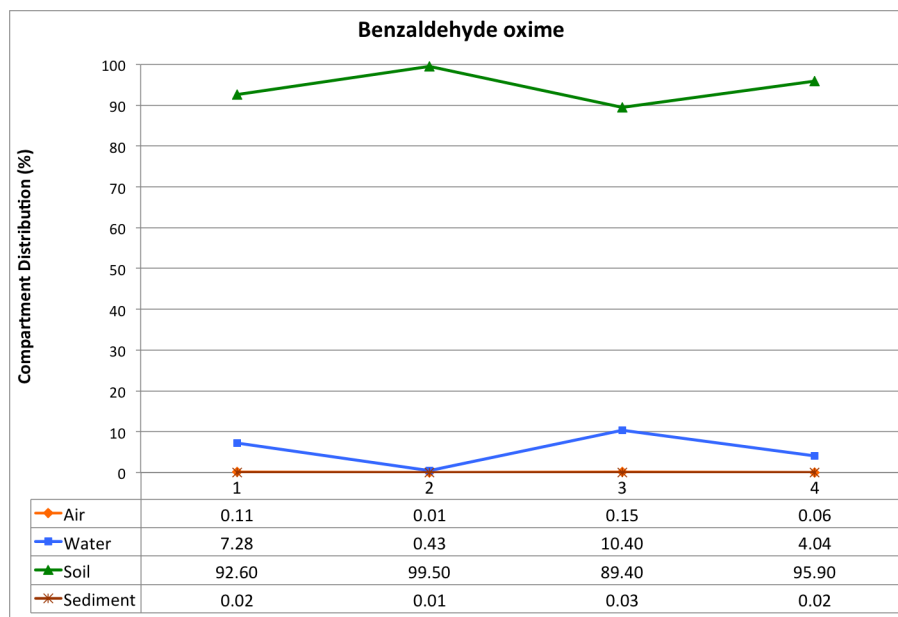


Figure C.6: Soil discharge scenario fugacity model of benzaldehyde oxime, from EPI Suite™. (X-axis = model scenario corresponding to Table 5.2)

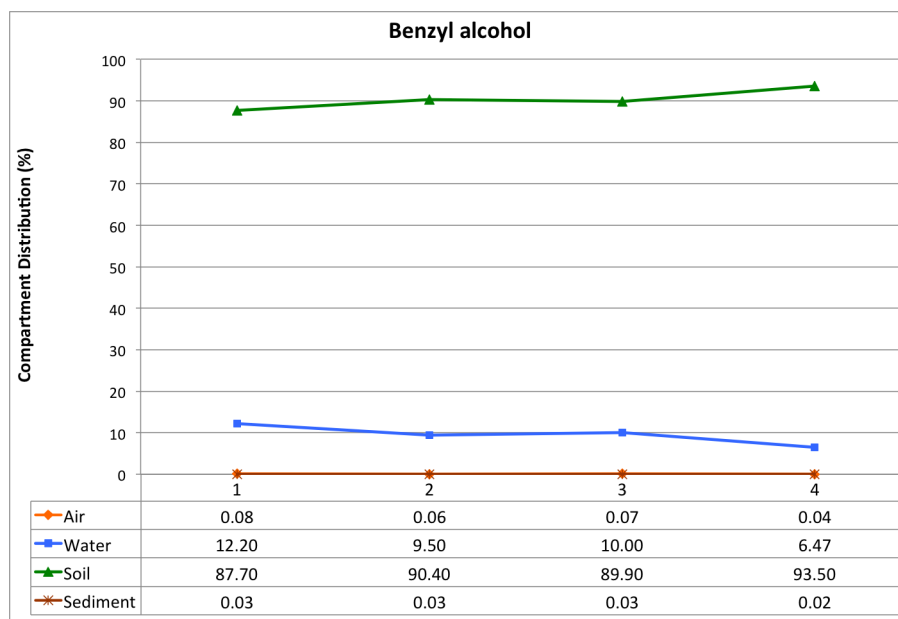


Figure C.7: Soil discharge scenario fugacity model of benzyl alcohol, from EPI Suite™. (X-axis = model scenario corresponding to Table 5.2)

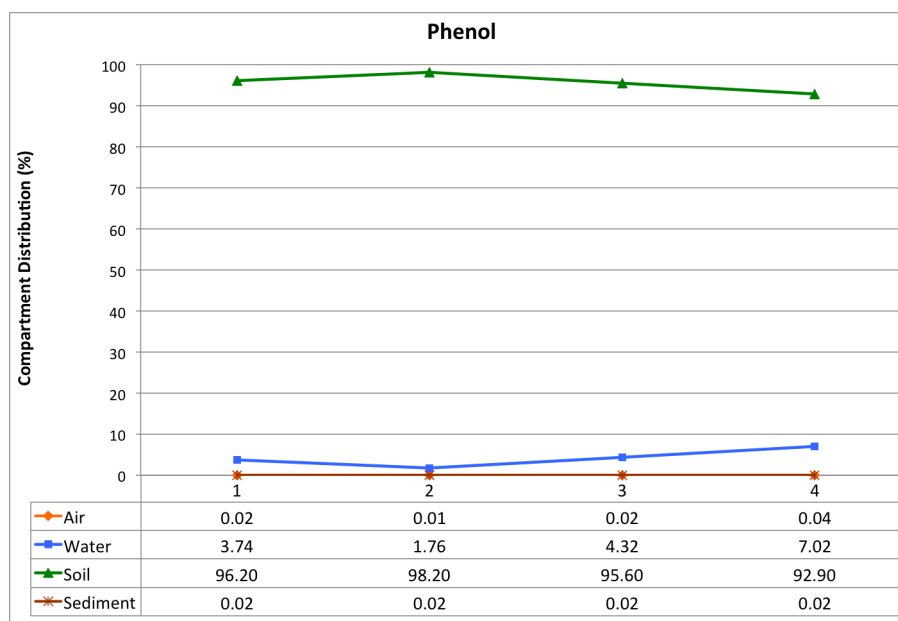


Figure C.8: Soil discharge scenario fugacity model of phenol, from EPI Suite™. (X-axis = model scenario corresponding to Table 5.2)

Appendix D:
Peer-Reviewed Conference Paper

PREDICTION OF THE ENVIRONMENTAL FATE OF METHYLAMPHETAMINE WASTE

Lisa N. Kates,¹ Caroline Gauchotte,¹ Niamh Nic Daéid,² Robert M. Kalin,¹ Charles W. Knapp¹ and Helen E. Keenan¹

¹ Department of Civil Engineering, University of Strathclyde, John Anderson Building, Glasgow G4 0NG, UK

² Centre for Forensic Science, University of Strathclyde, Royal College, Glasgow G1 1XW, UK

1 INTRODUCTION

The abuse of illicit drugs is cause for concern throughout the world. The United Nations Office on Drugs and Crime (UNODC) estimates that 3.3% to 6.1% of the population aged 15 - 64 (149 - 272 million people) consumed illicit drugs in 2009.¹ The most widely abused drug globally is cannabis, followed by amphetamine-type stimulants (ATS). ATS are synthetic drugs first manufactured in the late 1800s and early 1900s to treat asthma and for use as decongestants.^{1,2} The synthetic nature of these drugs means they can be manufactured anywhere; unlike crop-dependent drugs such as cocaine and heroin, ATS are not confined to any particular region of the globe. Throughout the years, illicit ATS manufacture has been detected in over 60 countries.¹ In 2009, a total of 10,598 illicit ATS laboratories were reported; 10,195 of those were reported as methylamphetamine laboratories.¹

Methylamphetamine (also known as methamphetamine or metamfetamine, Figure 1) is the most commonly produced ATS worldwide. Methylamphetamine (MA) is typically manufactured in clandestine laboratories close to the consumer; inter-regional trafficking is uncommon.¹

MA is controlled in the United Kingdom under the Misuse of Drugs Act 1971. MA is currently a Class A substance, meaning the maximum penalties are life imprisonment and/or an unlimited fine for supply, trafficking or production and seven years imprisonment and/or an unlimited fine for possession.^{2,3} As of 2009 (the most recent year for which data is available), there are an estimated 14 - 53 million amphetamine-group users worldwide (0.3 - 1.3% of the population aged 15 - 64), making amphetamine-group substances more widely abused than cocaine and heroin combined, and second only to

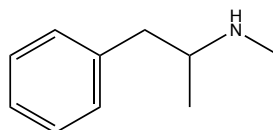


Figure 1 Chemical structure of methylamphetamine

cannabis. It is estimated MA users account for 54-59% of amphetamines-group users.¹

There are many different pathways used to synthesise MA, and recipes are readily available on the Internet, in publically accessible journal articles, and in published books.² Its synthesis is relatively simple and requires an assortment of household chemicals. As such, it is no surprise that over 90% of those arrested for clandestine MA manufacture are not trained chemists.⁴ Ultimately, the route chosen by the clandestine manufacturer is dictated by the availability of precursor materials and the skill level of the “chemist”.⁵

The illicit manufacture of MA produces a large amount of harmful waste that is often dumped illegally, creating a potential source of pollution. One kilogram of MA produces five to seven kilograms of waste that includes many volatile, flammable, and corrosive chemicals, as well as heavy metals.⁵ Common routes of disposal include poured down indoor plumbing, direct discharge into surface waters, or the waste being burned and/or buried.⁶ Illicit drug manufacturers are often not prosecuted for crimes relating to polluting the environment due to the costs associated with prosecution and lack of research in this area.

To aid in the detection and prosecution of an illicit dumpsite, an understanding of the chemical behaviour of the waste components is essential. As such, environmental modelling of organic chemicals is useful in predicting the behaviour of the chemical once released into the environment. While many different environmental models exist, the fugacity model was used in this work. A fugacity model calculates the tendency of a compound to partition into each environmental compartment. The model uses partition coefficients and mass balance equations to predict the movement of a contaminant across environmental compartments.⁷

An easy to use and freely available fugacity model can be found in the United States Environmental Protection Agency’s (US EPA) computer modelling programme EPI (Estimation Programs Interface) Suite™.⁸ EPI Suite™ uses a Level III fugacity model, meaning it assumes the compartments (air, water, soil and sediment) are homogeneous. A Level III model also assumes steady-state conditions, but not equilibrium. According to Mackay,⁹ steady-state implies consistency with time, while equilibrium implies that once equilibrium is reached, concentrations have no tendency for net transfer.

An advantage of using the EPI Suite™ model is the ability to create a site-specific environmental model by easily changing multiple variables. This feature allows the user to enter specific data relating to a sampling location as well as chemical and physical properties of the compounds of interest.

It is important to determine the chemical composition of the waste in order to identify potential markers of a MA dumpsite. To facilitate the prosecution of clandestine drug chemists for polluting the environment, it is equally important to understand what happens to the waste once it enters the environment. The environmental partitioning of MA and its waste products can be predicted using environmental modelling.

2 EXPERIMENTAL METHODS

2.1 Methylamphetamine Synthesis

MA was synthesised and its waste products collected. MA synthesis was conducted in-house following two different routes that require different precursor materials. The Leuckart route (Figure 2) uses 1-phenyl-2-propanone (P2P or benzylmethyl ketone, BMK) as the starting material, and the Moscow route (Figure 3) uses pseudoephedrine as starting material. The Leuckart synthesis was taken only to the methylamphetamine base stage

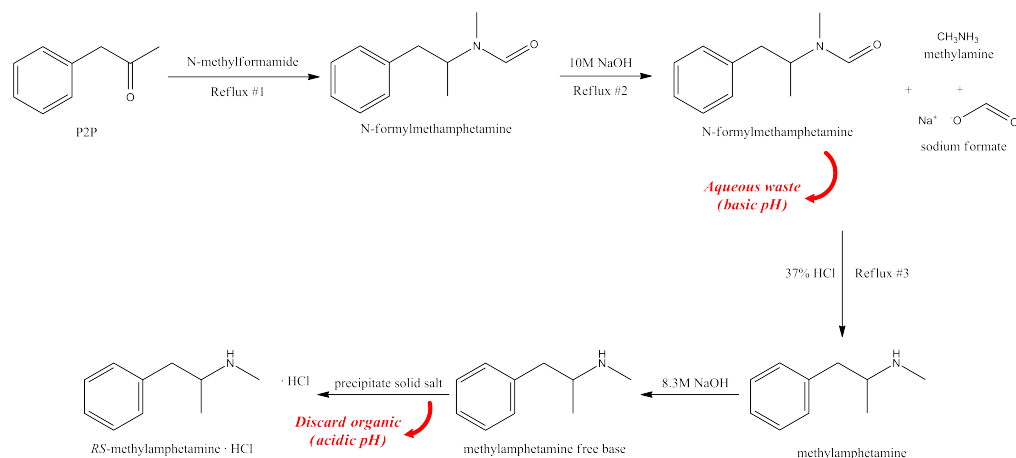


Figure 2 Methylamphetamine synthesis using the Leuckart route (aqueous waste collected)

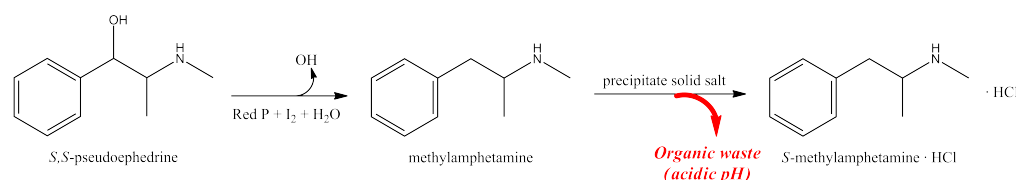


Figure 3 Methylamphetamine synthesis using the Moscow route (organic waste collected)

and was not converted to its hydrochloride salt. The Moscow route was converted to the hydrochloride salt (the form in which is it most commonly sold).

In the Leuckart synthesis, the aqueous phase was collected from the mid-point of the synthesis (Figure 2). In the Moscow synthesis, the toluene waste was collected from the salting out step. The waste was collected and stored in glass bottles at 4°C until further analysis.

2.2 Profiling of Methylamphetamine Waste

Profiling of the MA waste was carried out using a liquid-liquid extraction method, followed by identification of the organic components using gas chromatography-mass spectrometry (GC-MS). These methods were derived from validated methods used to profile MA for organic impurities.^{10,11,12}

2.2.1 Extraction Method. Various liquid-liquid extractions devised for the profiling of MA solids were investigated for the suitability of profiling MA waste.^{10,11,12} Three different buffers were examined: acetate buffer, pH 6; phosphate buffer, pH 10.5 and Tris(hydroxymethyl)aminomethane (TRIS) buffer, pH 8.1. The buffer with the best performance was the phosphate buffer, and thus was selected for further applications. The phosphate buffer was able to extract all of the impurities found using both the acetate and TRIS buffers.

The following extraction methodology was determined to yield the best results of those tested.¹² 0.5 mL of the waste was added to 2.0 mL of the 0.1 M phosphate buffer (pH 10.5 with 10% Na₂CO₃). The mixture was sonicated for 5 minutes, followed by 2 minutes of vortex mixing. 200 µL of ethyl acetate was added, along with an internal standard – in this case 5µL of 1.0 mg/mL C20. This was centrifuged for 5 minutes and the organic layer removed for analysis using GC-MS. Extracts were analysed within 48 hours.

2.2.2 GC-MS Method. Analysis was performed on a Thermo Trace Ultra GC coupled with a DSQII mass spectrometer, fitted with a DB35-MS capillary column (30 m x 0.32 mm ID x 0.25 µm film thickness, J & W). Initial oven temperature was 50°C, held for 1 minute, increased to 300°C at 10°C/minute and held for 10 minutes. Helium was the carrier gas at 1 mL/min; inlet temperature 220°C; transfer line 320°C.

2.3 Sediment Characterisation

Several sediment samples were collected from the River Clyde in Glasgow, United Kingdom. The sampling locations were selected to represent different chemical properties of the sediment. Total organic carbon content of the sediment was measured in order to create a site-specific model in the computer modelling programme (Section 2.4).

2.3.1 Sample Collection. Sediment samples were collected from three different locations along the River Clyde in the vicinity of Glasgow, United Kingdom (Figure 4). Sample 1 was taken from Bothwell Bridge (55°47'42.99"N, 4°3'29.70"W), to the east of Glasgow before the river enters the city. Sample 2 was taken from the Renfrew Ferry terminal (55°53'9.95"N, 4°22'57.91"W), in the west end of Glasgow after the river has passed through the city centre, two waste water treatment plants and one hospital. The third sample was collected from Bowling Harbour (55°55'48.57"N, 4°29'1.17"W), to the west of Glasgow, where the Forth and Clyde Canal meets the Clyde River estuary. The top 10 – 15 cm of sediment was collected using a stainless steel bucket attached to a 30 m rope. Sediment was stored in plastic bottles and refrigerated at 4°C until further use.

2.3.2 Measuring Total Organic Carbon. Sediment samples were sieved using a wire mesh sieve with a particle size of 3.5 mm. The total organic carbon (TOC) content in the sediment samples was determined using the American Society for Testing and Materials (ASTM) method D2974 – 07a.¹³ Briefly, moisture content of each sediment sample was first determined by heating the sample in an evaporating dish at 105°C for 16 hours, followed by one hour increments until the weight was stable to the nearest 0.01 g. TOC

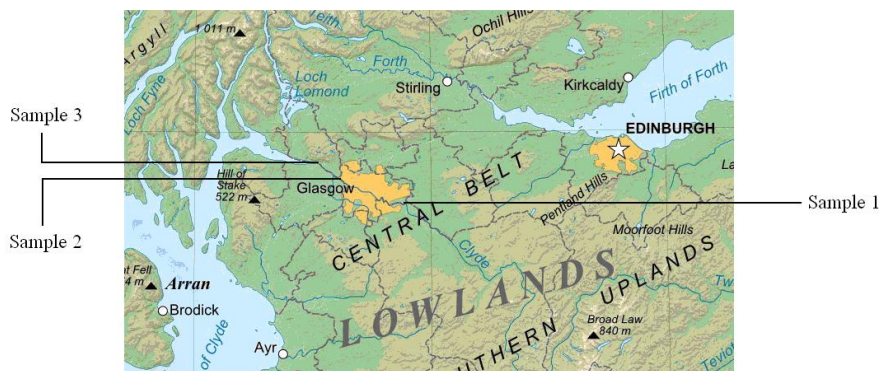


Figure 4 Map of the sampling locations in the vicinity of Glasgow, United Kingdom

was determined by igniting the oven dried solids at 440°C in a muffle furnace for one hour increments until there was no change in mass to the nearest 0.01 g.

2.4 Environmental Modelling

The environmental partitioning of the waste components was predicted using the US EPA's computer modelling programme EPI Suite™, version 4.10.⁸ The partitioning behaviour of the waste was predicted using the fugacity model.

2.4.1 Organic Carbon Partition Coefficient (K_{oc}). The TOC values measured in section 2.3 were input into the computer model and compared against the default values. As there is no function that permits the input of TOC directly, the measured TOC values were used to calculate K_{oc} using the following equations:

$$K_d = 0.39 + 0.67 \times K_{ow} \quad (1)^{14}$$

$$K_{oc} = \frac{K_d \times 100}{\%TOC} \quad (2)^{13}$$

where

K_d	=	sediment-water partition coefficient
K_{ow}	=	octanol-water partition coefficient
K_{oc}	=	organic carbon partition coefficient
%TOC	=	percent total organic carbon

Note that a K_d value is also required to calculate K_{oc} . K_d values are dependant on the properties of the chemical and can be correlated using K_{ow} , as shown in equation (1). In this work, K_{ow} values were taken from the EPI Suite™ KOWWIN v. 1.68 estimation programme. K_{oc} values need to be calculated for each chemical and for each sediment type, giving three different K_{oc} values per chemical.

2.4.2 Emission Values. In the EPI Suite™ model, it is possible to alter the emission scenario. The emission values for each environmental compartment were changed in order to create a model that simulates the dumping of chemicals directly into a body of water. The default emissions values for each compartment (air, water, and soil) are 1,000 kg/hr. The emissions values in this work were changed as follows: air: 0 kg/hr, water: 1,000 kg/hr, soil: 0 kg/hr.

2.4.3 Running the Model. A total of four different environmental modelling scenarios were run. The output of interest from the fugacity model is the mass amount of the chemical in each compartment (air, water, soil and sediment). Each of those values is accompanied by a half life – the time that is required for half of the chemical to be removed from that compartment.

The fugacity model cannot be run without a half-life value. In most cases this is not known, but may be automatically calculated using a different model in the EPI Suite™ package – BIOWIN. The BIOWIN programme calculates aerobic and anaerobic biodegradation. This model assumes that the water:soil:sediment biodegradation ratio is 1:2:9. This ratio is the default model and cannot be changed by the user. If, however, half-life values are known, those can be entered into the fugacity model.

The first scenario executed was using the default settings of the EPI Suite™ programme. Each chemical was entered individually using its Chemical Abstract Service (CAS) number. The name and SMILES (Simplified Molecular Input Line Entry System) were retrieved using the EPI Suite™ database to ensure the correct CAS number was

entered and that the database entry was the correct chemical. For the default scenario, no other values were changed apart from the emissions values as outlined in section 2.4.2.

The remaining three scenarios were run to allow the input of the calculated K_{oc} values. The K_{oc} value in the model was changed to correspond with the calculated K_{oc} value from each chemical and for each sediment type. Therefore four models were run per chemical: one for the default model and three for each calculated K_{oc} value based on the three sediment samples.

3 RESULTS

3.1 Profiling of Methylamphetamine Waste

A chemical profile of the organic components of MA waste was determined using GC-MS. The compounds were identified using mass spectrometry. Positive identification was accomplished, where possible, using a literature search and a NIST library search. Data on the identification of the waste components for the Leuckart and Moscow synthetic routes is shown in Tables 1 and 2, respectively.

3.2 Sediment Characterisation

Two characteristics of the sediment samples were measured in order to ascertain site-specific information for input into the EPI Suite™ environmental modelling programme. The moisture content and TOC of the sediment samples were experimentally determined. The measured values for each sediment sample are presented in Table 3.

Table 1 *Compounds identified in MA waste synthesised using the Leuckart route*

Compound	Retention Time (minutes)	Major Ions
N-methylacetamide	4.06	73, 40, 43, 58
Phenol	5.55	94, 66
Methylamphetamine	8.63	58, 91, 65
Benzaldehyde, oxime	8.99	121, 78, 77, 94
N,2-dimethyl-1-phenylpropan-2-amine	9.42	72, 41, 71, 91
1-Phenyl-2-propanone oxime	10.85	91, 149, 116
N-Formylmethamphetamine	15.10	86, 58, 91

Table 2 Compounds identified in MA waste synthesised using the Moscow route

Compound	Retention Time (minutes)	Major Ions
Benzaldehyde	5.81	105, 106, 77, 51
Phenylmethanol	6.85	79, 108, 107, 77
1-phenyl-2-propanone	8.50	91, 43, 134, 92
Methylamphetamine	8.65	58, 91, 65
1-phenyl-1,2-propanedione	9.09	105, 77, 51
2,6-di-tert-butylphenol	12.94	191, 206, 192, 57
Methyl 3-(3,5-di-tert-butyl-4-hydroxyphenyl)propanoate	18.26	277, 147, 292

Table 3 Properties of sediment from three sampling sites

Sample	Moisture Content (%)	TOC (%)
1) Bothwell Bridge	21.53	0.55
2) Renfrew Ferry	59.56	2.01
3) Bowling Harbour	72.74	2.32

3.3 EPI Suite™ Fugacity Modelling

The environmental modelling of the waste constituents was based on the compounds identified in the MA waste mixture; however, not all of the compounds identified in Tables 1 and 2 were available to purchase as analytical standards - only nine (out of thirteen) were commercially available. Only those compounds that were available for purchase were tested in the fugacity model. The nine compounds to undergo environmental modelling in this work are as follows: benzaldehyde, benzyl alcohol, 1-phenyl-2-propanone, N-methylacetamide, phenol, methylamphetamine, 1-phenylpropane-1,2-dione, benzaldehyde oxime, and 2,6-di-tert-butylphenol.

A total of 36 modelling scenarios were run. Each of the nine chemicals was modelled four times (default model conditions and for each sediment K_{oc} value). A fugacity model using the default K_{oc} values is shown in Table 4. Fugacity models using K_{oc} values calculated from the sediment TOC values of 0.46%, 2.01% and 2.32% are shown Tables 5, 6 and 7, respectively.

4 DISCUSSION

Many factors influence the environmental partitioning of MA waste; the key factor being the chemical properties of the waste itself. Once the waste mixture was profiled using GC-MS, prediction of the partitioning behaviour was feasible using the US EPA's EPI Suite™ fugacity model.

Table 4 *EPI Suite™ fugacity model using the default settings*

	Benzaldehyde	Benzyl alcohol	1-phenyl-2-propanone	N-methyl-acetamide	Phenol	Methyl-amphetamine	1-phenylpropane-1,2-dione	Benzaldehyde oxime	2,6-di-tert-butylphenol
K_{oc}	33	13	83	2	79	106	12	33	6506
Compartment	% $t_{1/2}$	% $t_{1/2}$	% $t_{1/2}$	% $t_{1/2}$	% $t_{1/2}$	% $t_{1/2}$	% $t_{1/2}$	% $t_{1/2}$	% $t_{1/2}$
Air	0.54 20	0.00 11	0.15 45	0.00 49	0.00 10	0.01 3	0.00 137	0.0 39	0.01 5
Water	99.20 360	99.70 360	99.20 360	99.80 360	99.10 360	96.90 360	99.80 360	97.10 360	65.30 900
Soil	0.03 720	0.02 720	0.09 720	0.02 720	0.03 720	0.01 720	0.02 720	0.07 720	0.03 1800
Sediment	0.23 3240	0.27 3240	0.55 3240	0.20 3240	0.90 3240	3.10 3240	0.23 3240	2.87 3240	34.70 8100

% = percent of chemical mass in specified compartment; $t_{1/2}$ = half life, hours

Table 5 *EPI Suite™ fugacity model using conditions represented at Bothwell Bridge (%TOC=0.46)*

	Benzaldehyde	Benzyl alcohol	1-phenyl-2-propanone	N-methyl-acetamide	Phenol	Methyl-amphetamine	1-phenylpropane-1,2-dione	Benzaldehyde oxime	2,6-di-tert-butylphenol
K_{oc}	755472	183591	438328	11384	479799	2425703	196115	1088213	439871011
Compartment	% $t_{1/2}$	% $t_{1/2}$	% $t_{1/2}$	% $t_{1/2}$	% $t_{1/2}$	% $t_{1/2}$	% $t_{1/2}$	% $t_{1/2}$	% $t_{1/2}$
Air	0.02 20	0.00 11	0.01 45	0.00 49	0.00 10	0.00 3	0.00 137	0.00 39	0.00 5
Water	8.72 360	19.00 360	11.30 360	74.70 360	10.80 360	6.08 360	18.20 360	7.57 360	2.45 900
Soil	0.00 720	0.00 720	0.01 720	0.02 720	0.00 720	0.00 720	0.00 720	0.00 720	0.00 1800
Sediment	91.30 3240	81.00 3240	88.60 3240	25.30 3240	89.20 3240	93.90 3240	81.80 3240	92.40 3240	97.50 8100

% = percent of chemical mass in specified compartment; $t_{1/2}$ = half life, hours

Table 6 *EPI Suite™ fugacity model using conditions represented at Ferry Terminal (TOC = 2.01%)*

	Benzaldehyde	Benzyl alcohol	1-phenyl-2-propanone	N-methyl-acetamide	Phenol	Methyl-amphetamine	1-phenylpropane-1,2-dione	Benzaldehyde oxime	2,6-di-tert-butylphenol
K_{oc}	172894	42016	100314	2605	109805	555136	44882	249044	100666998
Compartment	% t _{1/2}	% t _{1/2}	% t _{1/2}	% t _{1/2}	% t _{1/2}	% t _{1/2}	% t _{1/2}	% t _{1/2}	% t _{1/2}
Air	0.09 20	0.00 11	0.04 45	0.00 49	0.00 10	0.00 3	0.00 137	0.00 39	0.00 5
Water	19.70 360	46.00 360	27.90 360	92.30 360	26.40 360	10.00 360	44.50 360	15.70 360	2.47 900
Soil	0.01 720	0.01 720	0.02 720	0.03 720	0.01 720	0.00 720	0.01 720	0.01 720	0.00 1800
Sediment	80.20 3240	54.00 3240	72.00 3240	7.70 3240	73.60 3240	90.00 3240	55.50 3240	84.30 3240	97.50 8100

% = percent of chemical mass in specified compartment; t_{1/2} = half life, hours

Table 7 *EPI Suite™ fugacity model using conditions represented at Bowling Harbour (TOC = 2.32%)*

	Benzaldehyde	Benzyl alcohol	1-phenyl-2-propanone	N-methyl-acetamide	Phenol	Methyl-amphetamine	1-phenylpropane-1,2-dione	Benzaldehyde oxime	2,6-di-tert-butylphenol
K_{oc}	149792	36402	86910	2257	95133	480958	38885	215766	87215804
Compartment	% t _{1/2}	% t _{1/2}	% t _{1/2}	% t _{1/2}	% t _{1/2}	% t _{1/2}	% t _{1/2}	% t _{1/2}	% t _{1/2}
Air	0.10 20	0.00 11	0.04 45	0.00 49	0.00 10	0.00 3	0.00 137	0.00 39	0.00 5
Water	21.60 360	49.30 360	30.50 360	93.20 360	28.80 360	10.80 360	47.80 360	17.20 360	2.47 900
Soil	0.01 720	0.01 720	0.03 720	0.03 720	0.01 720	0.00 720	0.01 720	0.01 720	0.00 1800
Sediment	78.30 3240	50.70 3240	69.40 3240	6.81 3240	71.10 3240	89.20 3240	52.20 3240	82.80 3240	97.50 8100

% = percent of chemical mass in specified compartment; t_{1/2} = half life, hours

4.1 Profile of Methylamphetamine Waste

The waste products identified from clandestine MA manufacture contain mostly aromatic compounds. This is in accord with the structures of both the starting materials and end product (see Figures 1 and 2). In each of the two synthetic routes examined, there was no precursor material found in the waste products. (In the Leuckart route, there is no P2P present in the waste, and similarly for the Moscow route there is no pseudoephedrine present in the waste.) This is an indication that the synthesis went to completion. Additionally, MA was the only compound identified in both sets of waste.

Of note, P2P was identified in the waste from the Moscow route. This was expected as P2P is a well-known reaction impurity found in MA synthesised using pseudoephedrine.¹⁵ Therefore, the presence of P2P in the environment can mean two different things: 1) P2P was used in the clandestine laboratory as a starting material, or 2) P2P was produced as a reaction impurity. Given the difficulty of obtaining P2P on the black market, the disposal of pure P2P seems unlikely unless the clandestine “chemist” was trying to dispose of evidence. Further research into the ratios of P2P and other waste marker compounds may give an indication as to the origin of P2P at a dumpsite. This would have implications to law enforcement personnel to determine the synthetic route used at a clandestine MA laboratory. Information on synthetic routes is often useful for intelligence purposes and calculations can be made to determine the manufacturing capacity of a clandestine laboratory.

4.2 Environmental Partitioning of Methylamphetamine Waste

Using EPI Suite™, it was possible to generate an estimated fugacity model for each of the nine chemicals identified in MA waste. The fugacity model serves as a good indication of how the chemicals may partition between environmental compartments.

A comparison of the default fugacity model in Table 4 to the site-specific fugacity models in Tables 5-7 illustrates several significant disparities. Firstly, the K_{oc} values between the default model and each of the site-specific models vary by three to four orders of magnitude. As the K_{oc} values in the experimental models were calculated using the total organic carbon content of the sediment, the influence of organic carbon content becomes clear.

As the %TOC decreases, the calculated K_{oc} increases. A decrease in %TOC corresponds to greater partitioning of the chemicals into the sediment compartment (Table 5 compared to Table 7). This is a trend exhibited by all nine of the chemicals tested. Across all four models, the lower the K_{oc} value, the lower the mass amount will be in the sediment compartment. This is not a common partitioning trend for organic chemicals. Typically, as the organic carbon content of the sediment increases, organic molecules will partition more heavily into that compartment, binding tightly to the organic carbon. In this instance, the opposite effect is being predicted by the fugacity model and can be attributed to the polar nature of the MA waste components.

As more mass partitions into the sediment compartment, it needs to be subtracted from another compartment in order to maintain a mass balance. In these model scenarios, the mass is being transferred from the water compartment. Consequently, as the mass amount in the sediment compartment decreases, the mass amount in the water compartment increases. This corresponds with a decrease in K_{oc} values. Thus, with increasing organic carbon content in the sediment, the chemicals are more likely to partition into the water compartment at steady-state.

The largest disparity between the default model and the experimental models is the partitioning behaviour between the water and sediment compartments. In the default model (Table 4), the compartment with the majority of the mass amount of each chemical is the water compartment (65.30% - 99.80%). By comparison to Tables 5-7, the majority of the mass amount is in the sediment compartment (50.70% - 97.50%). An exception to that trend is N-methylacetamide. In all four modelling scenarios, the majority of N-methylacetamide (74.70% - 92.30%) is predicted to be found in the water compartment. It does, however, follow the previous trend of greater partitioning into the water compartment with an increase in %TOC. The different behaviour of this chemical may be attributed to its chemical structure. Of the compounds positively identified in the MA waste, N-methylacetamide is the only one that does not have an aromatic ring, meaning it is not as stable and more water soluble.

In all four of the model scenarios, and for all nine of the chemicals, there is very little partitioning behaviour into the air and soil compartments. Of all four model scenarios, the default model predicts the greatest amount of partitioning into the air. Even for that scenario, the highest mass amount found in the air is 0.54% for benzaldehyde. Soil is not a significant factor as the model was specified to be a chemical release directly into water. The water compartment only interfaces directly with the sediment and air compartments.

The half lives of each chemical do not change with each model scenario. The predicted persistence in the sediment compartment is far greater than any other compartment. The compartment with the largest mass amount is also the compartment with the slowest predicted degradation. Chemicals are likely to still be persistent in the sediment after nearly 20 months. This is encouraging information for the investigation of a suspected dumpsite as it increases the chances of detecting marker chemicals.

5 CONCLUSIONS

Using the EPI Suite™ computer modelling program, the environmental fate of MA waste was estimated. A fugacity model was used to predict the partitioning of the waste components into each environmental compartment. Waste from illicit MA manufacture that is dumped into the water compartment will overwhelmingly partition into the sediment compartment. However, the higher the %TOC of the site, the more likely the contaminants are to partition into the water compartment. Normally, a higher %TOC causes organic chemicals to partition into the sediment compartment. In this work, the opposite is being observed, which can be attributed to the polarity of the waste components.

The fugacity models indicate that the chemicals relating to the illicit manufacture of MA will mostly be found in the sediment compartment. This means the majority of the chemicals will be tightly bound to the organic carbon in the soil, making them inaccessible to microorganisms and biota. Furthermore, strong bonding to the organic carbon means that the chemicals will not be highly mobile. Once they are adsorbed to the sediment, there is little potential for dispersion.

While useful, EPI Suite™ is essentially a default model. By changing the %TOC it is possible to create a site-specific model. The more values that can be experimentally determined, the more accurate the model is likely to be. This has important implications for the investigation of suspected MA waste dumpsites. Knowledge of how the chemicals are partitioning will allow a targeted sampling approach.

The fugacity modelling of compounds based on chemical and physical properties has been shown to be a useful tool. However, it can be concluded that computer modelling should not be a replacement for laboratory experimentation.

Acknowledgments

Many thanks to Mr. Saravana Jayaram from the Centre for Forensic Science at the University of Strathclyde for providing samples of methylamphetamine waste from the Moscow route.

References

- 1 United Nations Office on Drugs and Crime, *2011 World Drug Report*. 2011. Available from: <http://www.unodc.org/unodc/en/data-and-analysis/WDR-2011.html>
- 2 Advisory Council on the Misuse of Drugs, *Methylamphetamine Review*, Home Office, United Kingdom, 2005. Available from: <http://www.homeoffice.gov.uk/publications/alcohol-drugs/drugs/acmd1/ACMD-meth-report-November-2005>
- 3 L. King, *Forensic Chemistry of Substance Misuse: A Guide to Drug Control*, RSC Publishing, Cambridge, UK, 2009.
- 4 G. Hargreaves, *Clandestine Drug Lags: Chemical Time Bombs*, FBI Law Enforcement Bulletin, April 2000, 69, 4, pp1-6. Available from: <http://www.fbi.gov/stats-services/publications/law-enforcement-bulletin/2000-pdfs/apr00leb.pdf>
- 5 M. White, *FSS Report on Methylamphetamine: Chemistry, seizure statistics, analysis, synthetic routes and history of illicit manufacture in the UK and the USA*, Forensic Science Service, 2004. Available from: <http://www.homeoffice.gov.uk/publications/alcohol-drugs/drugs/acmd1/ACMD-meth-annex-November-2005?view=Binary>
- 6 United States Environmental Protection Agency, *RCRA Hazardous Waste Identification of Methamphetamine Production Process By-products*, 2005. Available from: <http://www.epa.gov/osw/hazard/wastetypes/wasteid/downloads/rtc-meth.pdf>
- 7 D. Mackay, *Environ. Sci. Technol.*, 1979, **13**, 1218
- 8 US EPA, 2011. Estimation Programs Interface Suite™ for Microsoft® Windows, v 4.10. United States Environmental Protection Agency, Washington, DC, USA
- 9 D. Mackay. *Multimedia Environmental Models: The Fugacity Approach*, Lewis Publishers, Boca Raton, U.S.A., 2001.
- 10 K. Andersson, K. Jalava, E. Lock, et al., *Forensic Sci. Int.*, 2007, **169**, 64.
- 11 L. Dujourdy, V. Dufey, F. Besacier, et al., *Forensic Sci. Int.*, 2008, **177**, 153.
- 12 V. Kunalan, N. Nic Daéid, W.J. Kerr, et al., *Anal. Chem.*, 2009, **81**, 7342
- 13 ASTM International, *Standard Test Method for Moisture, Ash, and Organic Matter of Peat and Other Organic Soils (Designation: D2974 – 07a)*, 2007.
- 14 H.R. Andersen, M. Hansen, J. Kjolholt, et al., *Chemosphere*, 2005, **61**, 139.
- 15 H.F. Skinner, *Forensic Sci. Int.*, 1990, **48**, 123